TECHNISCHE UNIVERSITÄT MÜNCHEN

Institut für Tierphysiologie und Immunologie

Effects of Perilla frutescens on enzymatic activity and cell physiology – Method development and critical assessment

Christine Martina Kaufmann

Vollständiger Abdruck der von der Fakultät Wissenschaftszentrum Weihenstephan für Ernährung, Landnutzung und Umwelt der Technischen Universität München zur Erlangung des akademischen Grades eines

Doktors der Naturwissenschaften

genehmigten Dissertation.

Vorsitzender: Prof. Dr. Dieter Langosch
Prüfer der Dissertation: 1. Priv.-Doz. Dr. Thomas Letzel
2. apl. Prof. Dr. Michael W. Pfaffl
3. Prof. Dr. Wilfried Schwab

Die Dissertation wurde am 20.03.2017 bei der Technischen Universität München eingereicht und durch die Fakultät Wissenschaftszentrum Weihenstephan für Ernährung, Landnutzung und Umwelt am 11.07.2017 angenommen.

Contents

Abbreviations

67LR	67 kDa laminin receptor
ACE	Acetone
AChE	Acetylcholine esterase
ACN	Acetonitrile
Ado	Adenosine
ADP	Adenosine diphosphate
AMP	Adenosine monophosphate
ATP	Adenosine triphosphate
CDNB	2,4-dinitrochlorobenzene
ECIS	Electric cell-substrate impedance sensing
ESI	Electrospray ionization
EtOH	Ethanol
FAc	Formic acid
FBS	Foetal bovine serum
GSH	Glutathione
GST	Glutathione S-transferase
HILIC	Hydrophilic interaction liquid chromatography
HTS	High-throughput screening
iAP	Intestinal alkaline phosphatase
IPA	isopropyl alcohol
K_M	Michaelis-Menten constant
LC-MS	Liquid chromatography-mass spectrometry
LDH	Lactate dehydrogenase
logD	Distribution-coefficient
logP	Partition-coefficient
LPS	Lipopolysaccharide
MeOH	Methanol
MS	Mass spectrometry
NED	N-(1-naphthyl)ethylendiamine

PBS	Phosphate buffer saline
PF	Perilla frutescens
PFP	Pentaflourophenyl
Pi / PPi	Inorganic phosphate / inorganic pyrophosphate
RA	Rosmarinic acid
ROS	Reactive oxygen species
RP	Reversed phase
RT	Retention time
RT-qPCR	Quantitative reverse transcription
SPE	Solid-phase extraction
Tof-MS	Time-of-flight mass spectrometer
V_{max}	Maximum reaction velocity
XOD	Xanthine oxidase

Abstract

The exploration of natural sources for the extraction of promising remedies has gained increasing acceptance and interest in recent years. Hence this study focused on the establishment of suitable methods for the investigation of enzymatic activity and regulation as well as for the detection of proliferation and gene expression changes of a porcine jejunal epithelial cell line in the presence of *Perilla frutescens* (PF) extracts. The first main part encompassed (bio-)analytical methods used for the comparative characterization of PF extracts in terms of molecular composition, total reducing potential and extraction yield. Furthermore several analytical techniques were employed for the investigation of PF extract effects on three health-related enzymes, namely intestinal alkaline phosphatase (iAP), xanthine oxidase (XOD) and glutathione-S-transferase (GST). Enzymatic activity was comparatively assessed using photometric and mass spectrometric (MS) detection, either without or in the presence of individual regulatory compounds or PF extracts. The process of bioanalytical method establishment was approached in detail, in this manner highlighting advantages and disadvantages of the employed setups. The power of MS for the detection of enzymatic regulation was eventually depicted by means of coupling a chromatographic separation with a biochemical assay in the form of an online coupled continuous flow mixing system. Comprehensive control experiments were performed, which included the injection of known enzymatic inhibitors as well as alternative substrates. The observation of the system´s response to the presence of known enzyme-regulatory molecules allowed the distinction between MS signal suppression and actual inhibitory events after the injection of PF to the system. In this regard, an inhibition could be identified after introducing chromatographically separated PF extract to the enzymatic assays of iAP and XOD.

The second main part of this study included the assessment of PF effects on cell proliferation of a porcine jejunal epithelial cell line as well as the detection of gene expression regulation of a panel of cell cycle and cancer-related genes. Cell proliferation was found to be inhibited by physiologically relevant PF extract concentrations. Administered extracts exerted their effects to various degrees but with a good correlation to their respective total reducing potential. Additional experiments to assess gene expression changes revealed a downregulation of cell cycle and cancer related genes, thus being in agreement with the

detected cell growth alterations. In order to verify the results comprehensive controls were established to assess artificial effects, which may arise with *in vitro* experiments. In this regard H_2O_2 generation was investigated, but was found negligible at low PF extract concentration. Furthermore PF extract addition to cell culture medium revealed an impaired stability for a variety of different PF compounds. The observed immediate response of cell proliferation and gene expression to the presence of PF extracts however still suggested their potential to affect cell physiology at the onset of the experiments.

Zusammenfassung

Die vorliegende Arbeit beleuchtet detailliert die Etablierung und Anwendung verschiedener Methoden, um die Wirkung von Perilla frutescens (PF) Extrakten auf die Aktivität gesundheitsrelevanter Enzyme und auf die Physiologie einer Zelllinie aus dem Epithel des porzinen Jejunums zu untersuchen.

Neben der Extraktionsausbeute wurden die PF Extrakte bezüglich ihres Gehalts an reduzierenden Verbindungen und ihrer molekularen Zusammensetzung charakterisiert. Dies ermöglichte die Korrelation der analysierten Extrakteigenschaften mit detektierten Enzymaktivitäts-, Zellproliferations- oder Genexpressionsänderungen.

(Bio-)analytische Untersuchungen umfassten die photometrische und massen-spektrometrische (MS) Detektion der enzymatischen Aktivitäten von intestinaler alkalischer Phosphatase (iAP), Xanthinoxidase (XOD) und Glutathion-S-Transferase (GST) in Gegenwart von PF Extrakten oder auch bekannten enzymregulatorischen Verbindungen. Hierbei wurden sowohl Vor- als auch Nachteile der angewendeten Techniken herausgestellt und notwendige Schritte im Rahmen der Assayetablierungen diskutiert. Für die MS Untersuchung der Enzymreaktionen und –regulationen fanden zwei verschiedene methodische Ansätze Verwendung: Eine direkte Injektion der Assays (continuous flow assay) und ein System, das die kontinuierliche Onlinekopplung einer chromatographischen Trennung mit einem biochemischen Assay erlaubte (online coupled continuous flow mixing system). Für die Untersuchung der Effekte von PF Extrakten auf die Aktivität von iAP, XOD und GST wurde im Vorfeld eine mit dem Online-Kopplungssystem und den Enzymen kompatible chromatographische Trennung etabliert. Zusätzliche Kontrollexperimente beinhalteten die Injektion bekannter Enzyminhibitoren und alternativer Enzymsubstrate. Dies erlaubte schlussendlich eine umfassende Verifikation der im XOD und iAP Assay in Gegenwart von chromatographisch getrenntem PF Extrakt detektierten Inhibitionen.

Neben der Etablierung (bio)analytischer Experimente zum Zwecke der Extrakt-charakterisierung und der Detektion von Enzymreaktionen, wurde der Effekt von PF auf die Proliferation und Genexpression der Zelllinie IPEC-J2 untersucht. Dabei konnte eine Inhibition der Proliferation durch physiologisch relevante PF Konzentrationen festgestellt werden. Die Regulation variierte bezüglich ihrer Ausprägung abhängig vom eingesetzten PF

Extrakt und offenbarte eine gute Korrelation mit dem jeweils festgestellten Gehalt an reduzierenden Verbindungen. Die Untersuchung der Genexpression in Gegenwart von PF Extrakt zeigte außerdem, in Übereinstimmung mit der detektierten Inhibition der Zellproliferation, die Herunterregulierung einiger zellzyklus- und krebsassoziierter Gene.

Um die Ergebnisse der Zellproliferations- und Genexpressionsstudie zu verifizieren wurden zusätzlich umfassende Kontrollexperimente durchgeführt. Diese dienten zum einen der Beurteilung einer möglichen H_2O_2-Bildung *in vitro* und zum anderen der Erfassung der PF Extraktstabilität in Zellkulturmedium. In Gegenwart physiologisch relevanter PF Extraktkonzentrationen konnte keine signifikante und potentiell regulative Konzentration von H_2O_2 nachgewiesen werden. Im Gegensatz dazu wurde eine Beinträchtigung der Stabilität einiger PF Extraktkomponenten festgestellt. Nichtsdestotrotz konnten die unmittelbar auf die Zellproliferation und Genexpression festgestellten Effekte von PF zum Zeitpunkt 0h auf das Vorhandensein regulativer Verbindungen zurückgeführt werden.

1. Introduction

The *in vitro* investigation of enzyme kinetics and cell physiological processes is a common approach in a plethora of different studies to investigate the impact of e.g. pharmaceuticals, toxins, natural compounds or complex mixtures like plant extracts on the activity of health- and disease-related enzymes, cell proliferation or gene expression, respectively. These studies support the finding of new and promising compounds, which may also exert beneficial effects *in vivo*, thus eventually contributing to the successful development of drugs for the treatment and alleviation of a variety of diseases. In this regard Perilla frutescens (PF) extracts were investigated on their activity towards health-related enzymes as well as on their effects on cell proliferation and gene expression of a porcine jejunal epithelial cell line.

1.1. Investigation of enzyme kinetics and enzymatic regulation

The understanding of enzymatic catalysis is essential not only for gaining a comprehensive picture of physiological processes. To benefit from the unique specificity of enzymes their activity has to be analyzed in detail. For this purpose many researchers rely on spectroscopic method like photometry or fluorescence-based detection. Those techniques allow the study of enzyme kinetics as well as the finding of new substrates or the identification of molecules, which may inhibit or activate an enzyme. However, enzymatic reactions are often complex, involving e.g. multiple intermediates. Their detection is usually disregarded with spectroscopic techniques, unless further downstream identification steps are included. In contrast, by applying MS detection the course of enzymatic substrate degradation, possible intermediate and product formation can be comprehensively investigated in one single run [1].

Back more than two decades, first enzymatic assays, measured with low accuracy mass spectrometers, consisted of immobilized proteases and the detection of their peptide products for the purpose of protein sequencing [2, 3]. Thereafter MS enzymatic assay detection has been employed in a plethora of different studies, e.g. for the investigation of further protease catalyzed reactions [4], for the assessment of enzymatic activity in organic solvents [5], for the elucidation of multiple reaction intermediates during hydrolysis of oligosaccharide substrates [1, 6, 7] or of stepwise nucleotide dephosphorylation (Appendix

9

I), for the elucidation of catalytic mechanisms [8-10] and for the determination of enzyme-substrate and enzyme-product complexes [6, 8, 11]. Basically two different general setups are utilized for the determination of enzymatic reactions with MS. They are either captured continuously [1, 6, 7, 12] or by measuring substrate degradation and product generation at defined time points. For a non-continuous determination, the assay is usually quenched, followed by the introduction of the mixture to the MS source either via direct infusion [13, 14] or chromatographically separated [15]. However, several studies also employ rapid mixing devices to determine the assay composition at defined time points by means of different flow rates or capillary length variation [16, 17].

Besides the straightforward assessment of enzymatic activity towards its substrate, MS detection has also been employed for the comprehensive determination of enzymatic inhibition kinetics [8, 9, 13, 14] and the screening of libraries for their inhibitory potential [18-22]. However, screening of large libraries is still usually conducted by means of well-established and fast photometric assays, which is the most common method for finding effective enzymatic regulators. This led to an increasing number of nowadays approved therapeutic substances stemming from natural sources [23]. Compared to the established and fast library screenings of small, chemically synthesized molecules, the identification of new regulatory compounds from natural sources struggles to meet demands in terms of speed, efficiency and quantity [24]. Due to the overall procedure of initially testing the crude natural extract on its activity, followed by chromatographic fractionation to eventually isolate an active compound, it is more elaborate and therefore cost-intensive. Nevertheless the potential to find promising compounds for the alleviation and cure of diseases is still enormous due the structural and chemical diversity present in nature. The development of effective screening methods is therefore required for the successful discovery of new substances from natural sources in a preferably fast, easy and low-cost manner.

The need for reliable and efficient methods for the assessment of potentially regulatory compounds resulted in the development of online coupled continuous flow methods, which allow the consecutive injection of individual compounds to a continuously delivered biochemical assay. The feasibility of the setup for the study of enzymatic inhibition has already been shown for various enzymes, amongst others cytochrome P450, acetylcholine esterase, GST, several proteases and XOD [25-30]. The detection is usually either based on

UV, fluorescence, MS or a combination of them. Furthermore, the online coupling of chromatographically separated natural extracts with an enzymatic assay enables the finding and identification of new inhibitors. This approach is comprehensively described in several reviews [31-33]. The functionality of the concept has already been proven with regard to different natural extracts as well as enzymatic assays by several researchers. De Jong et al. and Ingkaninan et al. observed an inhibition of acetylcholine esterase after the injection of a narcissus extracts to the system [27, 34], whereas de Boer et al. investigated the effect of a red clover extract on the activity of cathepsin [35]. Furthermore the coupling of chromatographically separated Chinese herb extracts, MS, UV detection and α-glucosidase assay allowed Zhao et al. the identification of several inhibitory compounds [36].

The enzymes investigated in this work were selected due to their physiological functions, association with diseases, inflammatory processes, involvement in oxidative stress and detoxification processes. They furthermore differ in terms of their photometric as well as MS detectability, which allows the comparative assessment of the utilized methodologies.

1.1.1. Intestinal alkaline phosphatase

Intestinal alkaline phosphatase (iAP) is an extracellular enzyme of the brush border of enterocytes, which has multiple roles with regard to the maintenance and protection of intestinal homeostasis [37, 38]. This includes the regulation of local surface pH to protect the mucosa against acid injury [39, 40]. iAP activity is distinctly dependent on pH with a suppressed substrate degradation at low pH and vice versa [41], which is the key aspect of its ability to adjust the intestinal pH value. At normal conditions iAP dephosphorylates ATP to adenosine in a stepwise manner [42] (see Appendix I) . Acidic pH however results in the local accumulation of ATP in the intestine, which binds its specific purinergic receptor. Hereby ATP stimulates the secretion of bicarbonate from enterocytes and therewith the increase of pH. Consequently iAP activity increases and ATP is again degraded to adenosine. Associated with iAPs ability to regulate intestinal pH might be its contribution to the regulation and maintenance of normal intestinal microbial homeostasis, which was reported by Malo et al. [43]. A further aspect of iAPs protective effects is its ability to dephosphorylate pro-inflammatory extracellular nucleotides [44-47] or gram-negative bacterial endotoxin lipopolysaccharides (LPS) [48-50], thus attenuating inflammatory responses. In fact

inflammatory bowel disease (IBD), a misregulated response towards bacterial components, has been observed to be associated with decreased iAP levels in areas of inflamed tissue [51]. Administration of iAP has been shown to attenuate LPS induced inflammatory processes [48, 52], to reduce inflammation-associated intestinal epithelial damage [53], to downregulate pro-inflammatory cytokines [54] as well as to suppress the recruitment of inflammatory cells [51]. iAP activity in inflammatory control manifests itself also in regulatory processes, which prevent transmucosal passage of luminal bacteria into the body [48, 55].

iAP expression has been shown in animal studies to be affected by various dietary components including proteins [56], carbohydrates [57, 58] and vitamins [59]. Fasting or a fat-free diet were found to distinctly reduce iAP activity, which results in susceptibility to LPS-induced inflammation [60, 61]. Moreover, the absence of iAP activity in knock-out mice revealed enhanced fat absorption, which suggests an important role of iAP in the regulation of intestinal lipid processing [62, 63].

1.1.2. Xanthine oxidase

Xanthine oxidase (XOD) is one of two interconvertible forms of the enzyme xanthine oxidoreductase, which catalyzes the degradation of hypoxanthine to xanthine to uric acid, the end product of purine metabolism. *In vivo* most xanthine oxidoreductases exist in the form of xanthine dehydrogenase, which can be reversibly or irreversibly transformed into xanthine oxidase by proteolytic cleavage depending on conditions such as oxygen availability [64-66]. In contrast to xanthine dehydrogenase, XOD generates superoxide and other reactive oxygen species (ROS) as by-products of substrate degradation [67]. The enzymatic product uric acid is primarily excreted via the kidneys with the remainder being degraded by intestinal bacteria [68]. Uric acid serum level is highly dependent on the food intake, with the intake of ethanol or fructose potentially increasing its level, either by reducing renal excretion or by stimulation of uric acid production [69-71]. The accumulation of excessive quantities of uric acid results in hyperuricemia, which is widely discussed to be associated with a variety of health risk factors such as hypertension, increased occurrence of cardiovascular diseases, metabolic syndrome and kidney diseases [72-74]. Moreover high uric acid levels can result in the development of gout, which is characterized by the

occurrence of an acute inflammatory reaction in response to the formation of urate crystals [75]. Nevertheless uric acid has also been described as one of the most important natural antioxidant compounds. On the one hand uric acid is capable of scavenging various ROS, but also acting as potent iron chelator, which prevents the generation of ROS through metal-catalyzed Fenton reaction [76, 77]. However uric acid possesses contradictory properties, since various studies also reported an induced ROS generation [74, 78, 79], which is related with its ability to form free radicals [80]. Besides uric acids potential pro-oxidative properties, XOD activity is a major source for the generation of adverse ROS, which are associated with oxidative damage of tissue and dysregulated inflammation [81, 82]. In fact, Liu et al. observed an overactivation of XOD accompanied by high levels of ROS in complications associated with diabetes mellitus, which caused injury to renal cells and eventually the induction of inflammatory processes [83]. Consequently, the administration of XOD inhibitor allopurinol has been proven to have positive effects on various conditions like ischemia, reperfusion injury, chronic heart failure and inflammatory diseases such as IBD or gout [84-87].

1.1.3. Glutathione S-transferase

Glutathione S-transferases (GST) are a large superfamily of soluble or membrane-bound mitochondrial, cytosolic and microsomal enzymes, which are part of biotransformation phase II processes [88]. Whereas phase I biotransformation involves the oxidation of xenobiotics by cytochrome P-450s, phase II is usually associated with a conjugation reaction catalyzed by a variety of enzymes including GSTs [89, 90]. In this regard reduced glutathione (GSH) is added to non-polar substrates containing an electrophilic carbon, nitrogen or sulfur atom [91]. The conjugation with GSH usually results in the metabolic inactivation and in an increase of the compounds polarity and thus facilitates its removal from the cell [92]. In general this cell defense mechanism results in the detoxification of endogenous and exogenous substrates or their metabolic products, which include amongst others adverse oxidative stress derived molecules like quinones, epoxides, α,β-unsaturated aldehydes and DNA or lipid hydroperoxides, but also environmental pollutants and chemical carcinogens [93]. For instance GST-dependent reduction of hydroperoxides prevents the generation of highly reactive and unstable peroxyl radicals and thus the chain reaction mechanism of free

radical propagation and progressive lipid peroxidation [94, 95]. Consequently GST transcriptional induction is regulated by the occurrence of ROS and by a variety of different (prooxidant) xenobiotic chemicals [89, 96, 97].

Apart from their capability to detoxify compounds by means of GSH-conjugation, GSTs are involved in intracellular transport processes of hormones, drugs, some xenobiotics and various cellular metabolites [98]. GSTs are also able to act as a peroxidase towards hydroperoxides, which prevents ROS induced cell damage [89]. Furthermore, however not considered as detoxification reaction, but rather as part of the normal metabolism, GSTs are involved in the synthesis of prostaglandins and leukotrienes [97, 99, 100], which makes them an interesting target for the treatment of inflammation associated diseases.

1.2. Investigation of cell physiology and phytoconstituents

Natural sources are widely and extensively investigated in order to find amelioration for a plethora of different health threats. Desired effects range from antioxidant, anti-allergic, anti-inflammatory, antimicrobial, antiviral, and anti-carcinogenic to the prevention and treatment of obesity and diabetes, to the improvement of wound healing processes, to anti-toxic effects e.g. in case of snake or scorpion bites and eventually to the alleviation of mental disorders and stress. Historically, plants have been the most important source for natural drugs, which led to the development of traditional medicinal treatments administered either by ingestion, topical application or subcutaneous injection. In former times, due to the lack of physiological and biochemical knowledge, therapies were necessarily approached by applying herbal medicines and observing the outcome, which then may have resulted in coincidental findings of effective plants. The development of diagnostic investigation and the increase of scientific understanding of matters connected to the body however led to more specific and targeted searches. In this regard, cell culture studies are widely used for the finding of natural extracts with proliferation-inhibiting properties, in order to identify new possibilities for the treatment of cancer. In this context, various extracts of botanical origin have been reported with inhibitory effects on cell growth and cell survival [101-104], including traditional Asian medicines like Masson pine pollen extracts [105], Ginkgo [106, 107], Ginger [108, 109], Perilla [110-112] or Ginseng [113-115] but also common herbs like Sage [116] and a variety of berries and fruits like blackberries, cherries, apples and plums

[117]. The effect of extracts can be detected by means of various methods. This includes the direct observation of tumor size and number of tumor incidents [113, 118], the assessment of cell cycle and apoptosis related gene expression [105, 110], the continuous long-term observation of cell growth [105], the determination of proliferating or apoptotic cells at specific time-points after treatment [116] or the detection of specific metabolic activities within the cells [101, 110-112] or in the medium, which are e.g. due to apoptotic events [119, 120].

1.2.1. Cell line IPEC-J2

The fate of secondary plant metabolites like polyphenols within the body is widely investigated due to their potential health-promoting effects with regard to the alleviation of a plethora of diseases ranging from cancer to cardiovascular diseases and inflammation-related disorders such as IBD or allergic reactions. Nevertheless the abundance of their intact forms in the plasma, i.e. their bioavailability, has been found to be low. Since most polyphenols are poorly absorbable in their glycosylated form, compounds demonstrated to enter the systemic circulation underwent preceding metabolic conversion by the gastrointestinal microbiota or by endogenous deglycosylating enzymes [121-123]. They are absorbed in the form of aglycones or microbial metabolites and can undergo further bioconversion to form e.g. glucuronic acids, glucuronide or sulfate conjugates, before exerting biological activity and being eventually excreted in the urine or transported back into the small intestine. The conversion of a particular compound is dependent on a variety of factors, including its chemical structure but also on the composition of the gastrointestinal tract microbiota. Although some compounds are likely to lose their ability to exert positive effects after the generation of conjugates or their metabolic conversion to smaller molecules like phenolic acids, some of them have been found to partly retain their biological activity, whereas others possessed even more beneficial potential [122, 124, 125].

In order to determine the fate of natural compounds as unambiguously as possible, *in vivo* animal or human intervention studies are considered the method of choice. It is however still not feasible to factor in all aspects of bioconversion due to the complexity of the system and individual microbial diversity. For these reasons initial screenings for the finding of active compounds or natural extracts are usually performed using well-established, fast and

more economical *in vitro* experiments. Although most studies rely on the utilization of cancer cell lines, non-transformed and non-tumorigenic cell lines may serve as *in vitro* model to mimic physiological conditions more precisely as it would be possible with transformed cell lines, which are likely to respond differently to external stimuli. One of only few non-transformed small intestinal cell lines is IPEC-J2, which is derived from the porcine jejunum. IPEC-J2 cell line has been employed in a variety of different studies, including the detection of interactions between intestinal cells and microbial pathogens or probiotic microorganisms [126-128]. Moreover the cell line was employed for the assessment of mycotoxin [120, 129, 130] or essential oil component cytotoxicity [131] and for the detection of cell proliferation in the presence of plant tannin extracts [132]. The impact of infections by enteric pathogens, diet-induced cellular responses and the regulation of inflammatory parameters have been determined as well using IPEC-J2 cell line. The latter comprises the expression of inflammatory key genes like proinflammatory IL-6, IL-8 or TNF-α in the presence of natural compounds such as apigenin by means of LPS-challenged IPEC-J2 cells [133-137]. IPEC-J2 cell line was also used for the determination of intracellular oxidative stress in the absence or presence of e.g. antioxidants like ascorbic acid [138-141]. Furthermore Kolodziejczak et al. performed experiments with different cell lines including IPEC-J2 for the investigation of prion protein uptake to enterocytes by means of 67kDa laminin receptor (67LR), which is believed to take part in their internalization and thus in the development of neurodegenerative disorders like bovine spongiform encephalopathy (BSE) [142].

Although some differences between *in vitro* cell culture and *in vivo* experiments have been observed using IPEC-J2 cells in comparison to native epithelium [143, 144], they possess an overall similar morphology and functionality to *in vivo* intestinal epithelial cells, including their ability to form microvilli as well as tight junctions [133], which makes them an appropriate tool to address various physiological questions. The knowledge acquired by means of employing porcine gastrointestinal epithelial cells may also be considered transferable on the human gastrointestinal tract, due to a highly similar physiology and anatomy [145-147].

1.3.   Perilla frutescens

Perilla frutescens (PF) is an annual herbaceous plant belonging to the family of Lamiaceae, which has been used in traditional Asian medicine for millennia. Whereas its leaves are a popular garnish, food coloring and seasoning, its seeds are commonly used for the production of oil rich in α-linolenic acid [148]. In traditional Chinese medicine PF is often applied in the form of mixtures containing different herbs for the treatment of mental disorders such as depression and depression-associated diseases [149-151]. Various *in vitro* and animal studies indicate a variety of promising effects of PF, which range beyond the alleviation of mental disorders to the treatment of stomach and bowel discomfort, to the amelioration of cold and flu-like symptoms, to beneficial effects in terms of food or fish allergy or poisoning as well as to the administration as sedative [112, 152-156]. Although *in vitro* experimental results might not unconditionally be transferable to the impact of PF on human health *in vivo*, there are indications for diverse wholesome properties of PF and its constituents, which are ascribed to its antioxidant, anti-allergic, antiviral and anti-inflammatory effects. PF exerts is antioxidant activity either by direct scavenging of ROS or via metal-chelating activity [112]. Moreover the expression of antioxidant enzymes was found to increase in macrophages [157], whereas ROS generation was decreased in stimulated human neutrophils after the application of PF extract [158, 159]. PF is also able to downregulate a variety of inflammatory markers, including the expression of proinflammatory TNF-α, IL-17A and IL-6 *in vitro* and *in vivo* [160-163] as well as the neutrophil-recruiting chemokine IL-8 and cyclooxygenase-2 [157, 162]. Amongst others the suppression of inflammatory processes has been observed by researchers with regard to airway and colon inflammation in mice [164-166]. Furthermore distinct anti-allergic properties of PF could be demonstrated in several *in vivo* rat or mice model studies, respectively [167-170]. Its application was found to cause the suppression of the Th2 immune response towards an allergen. Moreover the downregulation of allergy-associated cytokines and chemokines and the reduction of eosinophils and histamine release was reported after the administration of PF or the major PF compound rosmarinic acid (RA) in a murine model of allergic asthma [165, 168]. Consequently some studies attribute the anti-allergic activity of PF to high quantities of RA [167, 168]. However Asada et al. also suggested an isolated PF glycoprotein as active macromolecular compound against allergy-related

processes [171]. Besides PF anti-inflammatory and anti-allergic effects, suppression of human lung and colon cancer cell line [111, 112] as well as a human hepatoma cell line proliferation [110] and apoptosis-inducing genes was observed [110]. In rat or mice model studies as well as in *in vitro* cell culture experiments PF has furthermore been observed to possess beneficial effects on disorders affecting the kidneys [172-174] and on obesity and hyperlipidemia, thus potentially protecting against arteriosclerosis [175]. A high-fat diet animal model in combination with PF extract application caused less weight gain as well as lower triglyceride and less total cholesterol and LDL levels in the plasma. This finding was accompanied with the downregulation of related adipogenic genes [175, 176]. Kishi et al. reported a lowered glucose level and a decelerated development of diabetes *in vivo* after the application of PF tea in rats [177]. Moreover PF compounds luteolin and RA have been demonstrated to be effective inhibitors of α-glucosidase and aldose reductase *in vitro*, both of which potential targets for the treatment of diabetes [178, 179]. Apart from the administration of total PF extracts, a plethora of studies focus on RA as the major active component in PF due to its potent antioxidant activity [180, 181], its anti-carcinogenic, anti-allergic and anti-inflammatory effects. RA was observed to suppress the release of histamine from mast cells, neutrophilic infiltration in inflammation and the tumorgenesis of murine skin carcinogenesis [182-186]. Moreover suppression of mesangial cell proliferation *in vitro* was partly due to the presence of RA, which also caused the downregulation of cytokines and further genes involved in the development of various renal diseases [187]. Beyond that, RA was found to protect against liver injury, due to its antioxidant activity [188] and its ability to suppress proliferation genes in cells activated during liver injury [189]. However hepatic protection was found to be more pronounced by simultaneous administration of caffeic acid (CA), which resulted in the upregulation of de novo GSH synthesis and antioxidant enzymes [190]. CA was furthermore reported to enhance the activity of ɣ-glutamylcysteine synthetase [191], thus contributing to cellular protection mechanisms against ROS as well as to the detoxification of xenobiotics and adverse ROS reaction products. Protection against oxidative stress and inflammation in ethanol induced liver injury was also reported for perillyl alcohol, which downregulated proinflammatory cytokine TNF-α as well as restored alcohol related suppression of antioxidant enzyme and non-enzyme cellular defense systems [192]. Luteolin, a further PF compound, has been demonstrated to

possess anti-inflammatory, anti-allergic and antioxidant effects [193, 194] and was found to alleviate carcinogenesis of induced skin tumor in mice [118]. It also inhibited several proinflammatory cytokines including TNF-α and IL-6 [166] as well as allergic edema *in vivo* [193]. In addition PF compound apigenin exerted its effect on inflammation via the upregulation of anti-inflammatory cytokine IL-10 [166]. Since effects of PF have been observed *in vitro* and *in vivo*, it became a popular functional food within recent years. However, further *in vivo* studies will be necessary to include intestinal absorption and metabolism and thus the generation of metabolic products into the equation.

2. Aim of the study

The study is divided into four main chapters, which include several (bio-)analytical as well as biomolecular experiments to elucidate natural compounds effects on the activity of three enzymes with distinct functions in health and disease, on cell proliferation as well as on gene expression of a panel of cell cycle and cancer-related genes (Figure 1). The study of promising natural sources like plants and their extracts is of particular interest to researches and pharmaceutical companies to exploit their potentially beneficial effects on human health. In this regard, aim of this study was to establish methods and suitable control experiments, which eventually allow the disclosure of health-promoting properties of PF extracts.

In order to diversify PF extract compositions and encompass a wide range of compounds, extracts were prepared with different solvents, which ranged from polar to non-polar, thus resulting in different extraction yields, molecular compositions and reducing potentials. Experiments performed by means of a HILIC-RPLC coupling with MS detection moreover facilitate the comparative molecular characterization of PF extracts. The employed chromatographic separation provides insight into the composition of extracts by means of the detection of highly accurate molecular weights as well as retention times. Both of which may be used to correlate different PF extract polarity fractions with the observed outcome of enzymatic assays, cell proliferation or gene expression experiments.

To be able to identify enzyme-regulatory compounds assays of intestinal alkaline phosphatase, xanthine oxidase and glutathione-s-transferase ought to be adapted from photometric to MS detection to benefit from advantages provided by MS, which include the possibility to capture all assay components simultaneously and continuously. Later on the necessity of combining biochemical assay detection with chromatographic separation of PF extracts consequently results in the establishment of an online coupled continuous flow mixing system method. Requirements for the successful implementation of this setup include the assessment of organic solvent tolerance of employed enzymes as well as the optimization of a chromatographic separation.

Besides the detection of enzymatic activity, this study targets the investigation of PF extracts impact on cell proliferation and gene expression of a porcine jejunal epithelial cell line. Due

to artificial effects, which may arise in *in vitro* experiments, a comprehensive verification in the form of various control experiments ought to be implemented and discussed in this part of the study. This includes the generation of H_2O_2 and the stability of natural compounds in cell culture medium.
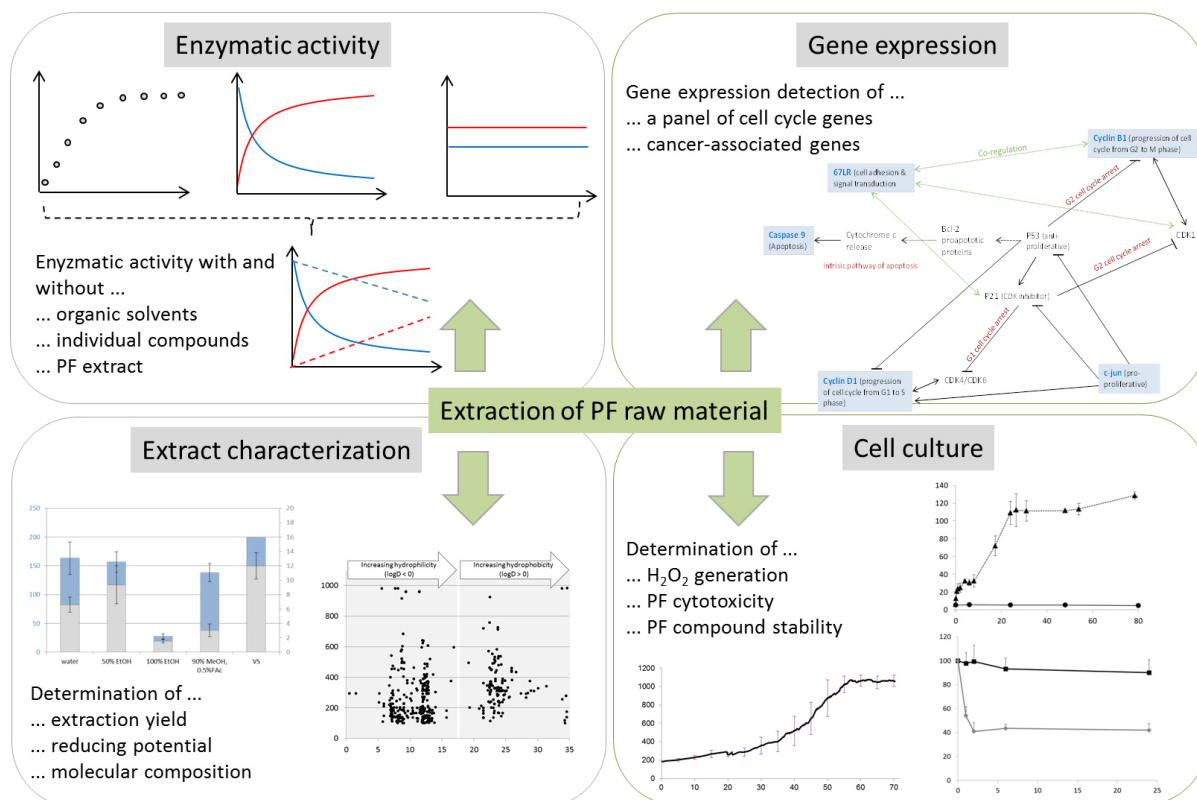
Figure 1 Overview of the four parts of the study, which includes the assessment of enzymatic activity using photometric and MS detection, the characterization of PF extracts and the determination of gene expression and cell proliferation in the presence of PF extracts.

3. Materials & Methods

3.1. Perilla frutenscens extract

PF water extract, which was provided as evaporated powder ("VS PF water extract") as well as PF var. crispa freeze-dried and milled leaves were supplied by Vital Solutions GmbH (Langenfeld, Germany) and Amino Up Chemicals Co., Ltd (Sapporo, Japan). VS PF water extract was specified with a given extraction yield of 1:5 (extraction residue after evaporation : freeze-dried and milled PF leaves). Further extracts from freeze-dried PF leaves were prepared with water, 50% ethanol (EtOH), 100% EtOH or 90% Methanol (MeOH) with 0.5% FAc. The procedures are depicted in Table 1. Further details on chemicals and instrumentation can be found in Appendix IV and V.

Table 1 Methods used for the extraction of freeze-dried and milled PF leaves

	Method 1		Method 2	
Freeze-dried & milled leaves	20 mg		500 mg	
	Extraction solvent	**Redissolution solvent**	**Extraction solvent**	**Redissolution solvent**
Extraction solvents & redissolution solvents	Water	80% MeOH	Water	Water
	90% EtOH	80% MeOH	50% EtOH	50% EtOH
	90% MeOH, 0.5% FAc	80% MeOH	100% EtOH	100% EtOH
			90% MeOH, 0.5% FAc	100% EtOH
Extraction solvent volume	0.75 mL		1 mL	
Extraction procedure	3 times: ice-cooled ultrasonic bath (10 min), centrifugation (3 000 rpm, 10 min), withdrawal and pooling of supernatants in another tube, evaporation		3 times: ice-cooled ultrasonic bath (10 min), centrifugation (1 500 rpm, 20 min), withdrawal and pooling of supernatants in another tube, evaporation	
Storage temperature	-20°C		-20°C	

The majority of experiments were performed using extracts prepared with method 2 (unless stated otherwise). Here, evaporated extracts were redissolved in the solvent used for extraction, except for 90% MeOH, 0.5% FAc extract, which was redissolved in 100% EtOH to maintain physiological relevance and avoid cytotoxic effects of MeOH in biomolecular experiments.

3.1.1. Extraction yield and total reducing potential

For extracts prepared by means of method 2, extraction yields as well as total reducing potentials were determined. Details on the experimental procedure can be found in Materials & Methods chapter of Appendix V.

3.2. Chromatographic analysis of Perilla frutescens extracts

PF extracts, which were prepared with different organic solvents, were analyzed in terms of differences in their molecular composition. For this purpose a chromatographic setup comprised of the serial coupling of a RPLC- and a HILIC column was used. The experimental setup was also employed for the investigation of PF stability in cell culture medium. Further details on the system can be found in the publication of Greco et al. [195] and in the following chapter.

3.2.1. General methodology

Two columns, i.e. Poroshell 120 EC-C18 (50.0 × 3.0 mm, 2.7 µm) (Agilent Technologies, Waldbronn, Germany) and ZIC® - HILIC column (150 × 2.1 mm, 5 µm, 200 Å) (Merck SeQuant, Umeå, Sweden) were coupled for the investigation of polar and non-polar compounds contained in PF extracts in one single run. In order to obtain highly accurate masses, chromatographically separated compounds were detected by means of a Time-of-flight (Tof) mass spectrometer series 6230 equipped with a Jet stream electrospray-ionization (ESI) source (Agilent Technologies). Mobile phases for RPLC separation were a mixture of solvent A, which was 10 mM NH_4Ac:ACN (90:10, v/v) and solvent B composed of 10 mM NH_4Ac aqueous solution:ACN (10:90, v/v). Mobile phases employed for HILIC separation were ACN and water, i.e. solvent C and D, respectively. Sample injection volume was 10 µL. Details on HPLC gradients and flows can be found in Table 2.

Table 2 Conditions applied for the chromatographic separation of PF extracts

Reversed-phase separation			HILIC separation		
Time [min]	B %	Flow [mL/min]	Time [min]	D %	Flow [mL/min]
0	0	0.05	0	0	0.4
7	0	0.05	6	0	0.4
12	50	0.05	13	40	0.4
13	50	0.10	32	40	0.4
22	100	0.10			
32	100	0.10			

Samples were detected in positive and negative ionization mode, respectively, with the following ToF-MS parameters: Gas temperature 325 °C, drying gas flow 10 L/min, nebulizer gas pressure 45 psi, sheath gas temperature 325 °C, sheath gas flow 7.5 L/min, capillary voltage 3000 V, fragmentor 100 V and m/z range 60-1700. MS calibration was performed beforehand and a calibration mixture (G1969–85001, Agilent Technologies) was delivered continuously throughout the entire run by means of an additional pump, thus enabling mass correction and accuracy of less than 20 ppm.

Data evaluation

Data were processed using MassHunter Qualitative Analysis Version B.02.00 (Agilent Technologies) as well as Agilent ProFinder Version B.06.00 (Agilent Technologies), the latter utilized for the automatic extraction of PF compounds. Further data evaluation was conducted with Windows Excel 2007 (Microsoft Inc). More details can be found in Appendix IV and V.

3.2.2. Molecular characterization of Perilla frutescens extracts

Extracts prepared from 500 mg freeze-dried and milled PF leaves were redissolved in 1 mL of the respective redissolution solvent (≙ "500 mg"/mL) listed in Table 1. They were then diluted in order to obtain a final sample concentration of "16.5 mg"/mL of which 10 µL were injected to be chromatographically separated by means of the method depicted in Table 2.

3.2.3. Stability of Perilla frutescens extract in cell culture medium

The stability of VS PF water extract in cell culture medium was investigated compared to extract solved in water. For this purpose VS PF water extract was mixed with either cell culture medium or water and incubated at 37°C. At time points 0, 1, 2, 6 and 24 h the mixtures were purified of proteins and high salt concentrations by means of solid-phase extraction (SPE) to be chromatographically separated afterwards by means of the method described in Table 2. Prior to SPE and LC-MS analysis samples were spiked with four different natural compounds in order to correct the experimental data for loss during SPE or for MS signal inconstancies, respectively. Consequently evaluated peak areas of PF extract compounds were corrected by means of the added spike compounds. Sample preparation procedures, details about data correction as well as cell culture medium composition and further chemicals utilized can be found in Appendix V.

3.3. Photometric determination of enzymatic activity

Enzymatic assays of intestinal alkaline phosphatase (iAP), xanthine oxidase (XOD) and glutathione-S-transferase (GST) were analyzed by means of photometric methods.

3.3.1. General methodology

Enzymatic activities were determined using a SLT Spectra plate reader (SLT Instruments, Crailsheim, Germany). Assay concentrations and additives, i.e. inhibitors, PF extracts or organic solvents can be found in Table 3. In all cases, assay components except for the enzyme were pipetted into a reaction tube or directly into a 96-well plate. Reaction was then started by addition of the respective enzyme. Unless stated otherwise all assays were conducted in 10 mM NH_4Ac pH 7.4. Suitable control measurements were performed in order to verify the absorption signal changes are due to enzymatic activity. These included the detection of all assay component combinations without the presence of the respective enzyme as well as the determination of assay formulation background absorption.

Table 3 Overview of photometric determination of iAP, XOD and GST assays (ACN = acetonitrile, IPA = isopropyl alcohol, ACE = acetone).

	Formulation of stock solutions		Assay concentrations		Additives
	Enzyme	Substrate(s)	Enzyme	Substrate(s)	Inhibitor / Extract / Solvent
iAP assay, discontinuous detection at 620 nm	10 mM NH_4Ac pH 6.0, 7.4 or 9.0	ATP, ADP or AMP in 10 mM NH_4Ac pH 6.0, 7.4 or 9.0	0.2 U/mL	40 µM ATP, ADP or AMP	-
XOD assay, discontinuous detection at 492 nm	10 mM NH_4Ac pH 7.4 or 200 mM phosphate buffer pH 7.4	Xanthine in 0.1 M $NH_3{:}H_2O$ (30:70 v/v), NH_2OH in 10 mM NH_4Ac pH 7.4	0.0125 or 0.04 U/mL	0.5 mM xanthine, 1 mM NH_2OH	-
GST assay, continuous detection at 340 nm	10 mM NH_4Ac pH 7.4	CDNB in 100% EtOH, GSH in 10 mM NH_4Ac pH 7.4	0.1 U/mL	0.2 mM GSH & 0.1/0.2/0.3/0.5/ 1.0 mM CDNB or 1 mM CDNB & 0.02/0.05/0.07/0.1/ 0.2/0.5 mM GSH	10, 20 or 30% MeOH/ACN/IPA/ ACE/EtOH or 0.2/0.5/0.8/1.0% (v/v) PF water, 90% MeOH, 0.5% FAc or 100% EtOH extract (prepared according to Method 1, Table 1)

Data evaluation

Data were analyzed using Microsoft Office Excel 2007 (Microsoft Inc). Data interpretation was conducted by comparing the slopes of trend lines, which were applied within the linear range of either substrate degradation or product generation curve at the onset of the enzymatic assay detection. Possible enzymatic activity changes in the presence of e.g. organic solvents or PF extracts were assessed by comparing assays containing those additives with the respective control assays without additives. Average values of control

assays were set as 100%. Further details can be found in the Materials & Methods chapter of Appendix I.

3.3.2. Intestinal alkaline phosphatase

Activity of iAP was determined with its physiological nucleotide substrates ATP, ADP and AMP in 10 mM NH_4Ac pH 6.0, 7.4 or 9.0. The enzymatically released inorganic phosphate (Pi) was detected by means of a color reaction at seven time points within 90 min. Detailed information about chemicals, assay procedure, instrumentation, data evaluation and statistics can be found in Appendix I.

3.3.3. Xanthine oxidase

Xanthine oxidase activity was determined either in 200 mM phosphate buffer pH 7.4 or 10 mM NH_4Ac pH 7.4 using photometric detection. In order to estimate the amount of nitrite generated by the reaction of NH_2OH and the secondary enzymatic product superoxide a calibration curve was prepared beforehand.

Calibration

Calibration was performed by preparing $NaNO_2$ stock solutions (Sigma-Aldrich) in 10mM NH_4Ac pH 7.4 or 200 mM phosphate buffer pH 7.4 (n≥3 each) (Table 4). 80 µL of the respective $NaNO_2$ concentration was added to 80 µL 0.02% sulfanilamide (Merck Chemicals, Darmstadt, Germany) solution followed by the addition of 80 µL 1% NED solution (Merck Chemicals) to a 96-well plate. After thorough mixing, the plate was incubated in the dark for 15 minutes at room temperature. The absorption was determined at 492 nm.

Table 4 Overview of chemicals and concentrations utilized for calibration measurements

Chemicals	Solved in	Final concentrations
$NaNO_2$	10 mM NH_4Ac pH 7.4 or 200 mM phosphate buffer pH 7.4	100, 50, 25, 12.5, 6.25, 3.13 1.56, 0 µM
Sulfanilamide 0.2 mg/mL (0.02%)	8% HCl	0.067 mg/mL
N-(1-naphthyl)ethylendiamine (NED) 10 mg/mL (1%)	H_2O (bidest.)	3.33 mg/mL

<u>Assay detection</u>

XOD activity was determined in aqueous solution 10 mM NH$_4$Ac pH 7.4 or 200 mM phosphate pH 7.4, respectively, by detecting enzymatically generated nitrite after 30 minutes with a XOD concentration of 0.0125 U/mL and 0.04 U/mL XOD (solely in 10 mM NH$_4$Ac pH 7.4) (n≥3). Generated nitrite quantity was calculated by means of the respective calibration curves either prepared in 200 mM phosphate buffer pH 7.4 or 10 mM NH$_4$Ac pH 7.4.

Progress of xanthine degradation was furthermore assessed by means of capturing the generation of nitrite in 10 mM NH$_4$Ac pH 7.4 at time points 0, 20, 40 and 60 minutes. After starting the enzymatic reaction, the assays were incubated at 37°C. 80 μL of the respective assay corresponding to the time point of interest were withdrawn from the tube and added to 80 μL 0.02% sulfanilamide to stop the reaction. The addition of 80 μL 1% NED solution then started the color reaction. The plate was incubated in the dark at room temperature for 15 minutes and the absorption was measured at 492 nm. Controls containing xanthine substrate and/or NH$_2$OH but not the enzyme and vice versa were performed to control the results.

3.3.4. Glutathione S-Transferase

GST activity was investigated using CDNB and GSH as substrates. The impact of different organic solvents and solvent concentrations as well as increasing concentrations of PF extracts on the generation of the enzymatically generated GSH-CDNB conjugate was tested. Due to its hydrophobicity CDNB stock was solved in 100% EtOH. Consequently all GST assays contain a small proportion of 2.5% EtOH, which was kept constant in all experiments.

<u>Determination of enzyme kinetics</u>

GST kinetics was determined by measuring various concentrations of CDNB with a constant concentration of GSH and vice versa (Table 3). Data were plotted as Lineweaver-Burk diagram with 1/v corresponding to the slopes of linear trend lines applied within the initial linear range of substrate generation.

<u>GST assay in the presence of organic solvents</u>

10, 20 and 30% of either MeOH, acetonitrile (ACN), isopropyl alcohol (IPA), acetone (ACE) or EtOH were added to the assay and the activity was determined in comparison to standard assays in 10 mM NH_4Ac pH 7.4.

<u>GST assay in the presence of PF extracts</u>

PF extracts used were prepared by means of extraction method 1 (Table 1). For the conduction of GST assays two extracts per treatment (water, 90% EtOH or 90% MeOH, 0.5% FAc) were redissolved in 200 µL 80% MeOH each and pooled. Thus extract of 40 mg freeze dried and milled PF leaves was redissolved in 400 µL 80% MeOH ($\triangleq$ "40 mg"/400 µL). Since the final GST assay volume was 250 µL, the addition of 0.2, 0.5, 0.8 or 1.0 % (v/v) redissolved PF extract "40 mg"/400 µL corresponded to extract prepared from 0.05 mg, 0.1025 mg, 0.2 mg or 0.25 mg freeze-dried & milled leaves respectively. Control experiments included the assessment of GST activity in the presence of the respective proportions of 80% MeOH as well as the progress of absorption of GSH and CDNB individually and combined in the absence of the enzyme.

3.4.   Mass spectrometric assays of enzymatic activity

Enzymatic assays were established to be measured with a real-time online continuous flow system and an online coupled continuous flow mixing system with MS detection. Measurements were either conducted with an MSQ Plus single quadrupole MS (Wissenschaftliche Gerätebau Dr. Ing. Herbert Knauer, Berlin, Germany) or with an ESI−Time-of-Flight (ToF) MS series 6230 (Agilent Technologies). MS parameters along with flow rates applied in both assays can be found in Table 5 and Table 6. Experimental setups are displayed and explained in Appendix I, III and IV.

Table 5 Single quadrupole parameters and flow rates applied for the detection of enzymatic assays using a real-time online continuous flow setup of an online coupled continuous flow mixing setup.

Single quadrupole MS	Real-time online continuous flow setup	Online coupled continuous flow mixing setup
m/z range	100-1000	
ESI mode	positive	
Needle V	3.5 kV	3.5 kV
Cone V	75 V	75 V
Temperature	225 °C	300 °C
Flow [μL/min]	10 (GST, iAP) or 20 (XOD)	Enzyme: 25 Substrate: 50 Inhibitor carrier flow / chromatography: 25

Table 6 ToF-MS parameters and flow rates applied for the detection of enzymatic assays using an online coupled continuous flow mixing setup.

Time-of-Flight MS	Online coupled continuous flow mixing setup
m/z range	100-1700
ESI mode	positive
Gas temperature	300°C
Drying gas flow	7 L/min
Sheath gas temperature	250°C
Sheath gas flow	5.5 L/min
Nebulizer operating pressure	45 psig
Capillary voltage	2000 V
Nozzle voltage	2000 V
Skimmer voltage	65 V
Fragmentor voltage	175 V
Flow [μL/min]	Enzyme: 25 Substrate: 50 Inhibitor carrier flow / chromatography: 25

3.4.1. Real-time online continuous flow setup

iAP, XOD and GST activity was investigated with a real-time online continuous flow setup in the presence of either individual compounds or PF extracts in order to characterize enzymatic regulation.

3.4.1.1. General methodology

Enzymatic activity was investigated with a single quadrupole MS. The enzymatic assay was continuously delivered by a syringe pump, which was connected to the ESI source through a PEEK Tubing (Figure 4). MS detection was started simultaneously with the addition of the enzyme to a reaction tube containing all further assay components. MS parameters are listed in Table 5, enzyme and substrate concentrations, assay formulations as well as additives like regulatory compounds or PF extracts are listed in Table 7. Further information about the experimental setup can be found in Appendix I.

Table 7 Overview of enzymatic assays measured with the real-time continuous flow setup

	Stock solution formulations		Assay concentrations		Additives
	Enzyme	Substrate(s)	Enzyme	Substrate(s)	Inhibitor / Extract / Solvents
iAP, continuous detection	iAP in 10 mM NH$_4$Ac pH 6.0, 7.4 or 9.0	ATP, ADP or AMP in 10 mM NH$_4$Ac pH 6.0, 7.4 or 9.0	0.2 U/mL	40 μM ATP, ADP or AMP	50, 100, 250, 400, 500, 750 μM GSH
XOD, Continuous detection	XOD in 10 mM NH$_4$Ac pH 7.4	Xanthine in 0.1 M NH$_3$:H$_2$O 30:70 (v/v)	0.02 or 0.04 U/mL	25 μM xanthine	1.25, 2.5, 6.25, 12.5, 25.0, 50.0 μg VS PF water extract in 500 μL assay volume
GST, continuous detection	GST in 10 mM NH$_4$Ac pH 7.4	CDNB in 100% EtOH, GSH in 10 mM NH$_4$Ac pH 7.4	0.3 U/mL	25 μM GSH & 25 μM CDNB	-

<u>Data evaluation</u>

Data were processed using Xcalibur software 2.1.0.1139 (Thermo Fisher Scientific Inc, Waltham, MA, USA) for assays captured with the MSQ Plus single quadrupole mass spectrometer (Wissenschaftliche Gerätebau Dr. Ing. Herbert Knauer) and Microsoft Office

Excel 2007 (Microsoft Inc). All detectable and identified EICs of individual assay components (substrate(s), intermediate(s) and product) were taken into account for data evaluation (Table 8). Abundances of evaluated m/z of each individual assay component were summed. Due to the assay procedure, which causes a time delay between start of MS recording and assay detection, the first 2 to 3 minutes of the assay detection were excluded from data evaluation. Further details on this can be found in Appendix I.

Data normalization was conducted by setting the highest value of each individual assay to 100%. For graphical depiction the average of each scan of substrate, intermediate or product traces of measured replicates was then calculated along with the respective standard deviations. Unless stated otherwise data evaluation procedure involved the application of an exponential trend line to the substrate degradation curve, thus allowing the numerical comparison of enzymatic activity, e.g. in the presence and absence of regulatory compounds. Detailed description hereto can be found in the Materials & Methods chapter of Appendix I.

Table 8 Overview of evaluated m/z detected with the MSQ Plus single quadrupole MS.

Enzyme	Substrate, intermediate(s) & product	Monoisotopic mass [g/mol]	m/z				
			$[M+H]^+$	$[M+Na]^+$	$[M+K]^+$	$[M-H+2Na]^+$	$[M-H+Na+K]^+$
iAP	Adenosine	267.1	268.1	290.1			
	AMP	347.1	348.1	370.1	386.0	392.0	408.0
	ADP	427.0	428.0	450.0	466.0	472.0	488.0
	ATP	507.0	508.0	530.0	546.0	552.0	568.0
XOD	Xanthine	152.0	153.0				
	Uric acid	168.0	169.0				
GST	GSH	307.1	308.1	330.1			
	CDNB	202.0	Not detectable				
	GSH-CDNB conjugate	473.1	474.1	496.1	512.1		

3.4.1.2.   Intestinal alkaline phosphatase

Activity of iAP was determined by means of utilizing its physiological nucleotide substrates ATP, ADP and AMP in 10 mM NH$_4$Ac pH 6.0, 7.4 or 9.0 as well as in the presence of increasing concentrations of GSH (Table 7). Further details on iAP assay formulations, sample preparation and data evaluation can be found in Appendix I.

3.4.1.3.   Xanthine oxidase

Xanthine oxidase activity was investigated without extract as well as in the presence of increasing quantities of VS PF water extract (Table 7).

Data evaluation

Contrary to data evaluation using an exponential trend line, numerical values to compare XOD regulation were obtained by applying a linear trend line applied to the linear range of substrate and product traces between minute 3 and 15 of the measurement. Slopes of trend lines were utilized as numerical values, which allowed the comparison of XOD activity in the presence and absence of additives.

3.4.1.4.   Glutathione S-transferase

Enzymatic assay of GST was adapted to be measured with a real-time online continuous flow setup. Mass spectrometric setting and assay concentrations can be found in Table 5 or Table 7, respectively.

3.4.2. Online coupled continuous flow mixing system

By means of the online coupled continuous flow mixing system biochemical assays were coupled to either the injection of individual compounds to be investigated on their regulatory activity or to a chromatographic separation of PF extracts in order to detect enzyme regulators.

3.4.2.1.   General methodology

The setup is described in detail in Appendix II, III and IV. The majority of measurements were conducted with an MSQ Plus single quadrupole MS (Wissenschaftliche Gerätebau Dr. Ing. Herbert Knauer) with crucial measurements being repeated with an ESI–ToF-MS (Agilent

Technologies) in order to obtain accurate molecular weights of unknown PF extract compounds. MS parameters and setup flow rates are listed in Table 5 and Table 6.

In order to verify the stability of the measurements, e.g. with regard to the occurrence of mass spectrometric signal suppression after the injection of compounds to the enzymatic assay, histidine was added as internal standard. 80 µM histidine were continuously delivered along with the enzyme by means of a syringe pump throughout the entire experimental run. It was priorly tested negative for regulatory activities towards the enzymes employed.

Table 9 Overview of enzymatic assays measured with the online coupled continuous flow mixing system

	Stock solution formulations		Assay concentrations		Additives
	Enzyme	Substrate(s)	Enzyme [U/mL]	Substrate(s)	Inhibitor / Extract / Solvents / Alternative substrate
iAP, continuous detection	iAP in 10 mM NH$_4$Ac pH 7.4	ATP, ADP or AMP in 10 mM NH$_4$Ac pH 7.4	2.4 U/mL	40 µM ATP, ADP or AMP	1, 2, 3, 4 mM GSH, PF extracts, 160 µM, 320 µM, 1 mM and 2 mM of alternative nucleotide substrates ATP, ADP or AMP
XOD, Continuous detection	XOD in 10 mM NH$_4$Ac pH 7.4	Xanthine in 0.1 M NH$_3$:H$_2$O (30:70 v/v)	0.032 U/mL	50 µM xanthine	50, 100, 200 µM allopurinol or PF extracts

Chromatographic separation

The injection volume was 2 µL and the chromatographic separation was conducted with a Luna PFP(2) column (100 Å, 2 mm IDx100 mm length, Phenomenex, Aschaffenburg, Germany). To improve the applied isocratic elution, different organic solvents and solvent proportions were added to the mobile phase and a moderate temperature gradient up to 70°C was applied to the column (Table 10). Detailed description on the method can be found in Appendix IV.

Table 10 Temperature gradient applied to the chromatographic column

Temperature	30 °C		50 °C		60 °C		70 °C
Temperature increase [°C/min]		1		0.5		0.5	
Duration [min]	1	20	1	20	1	20	40
Overall duration [min]	103						

Data evaluation

EICs of all adducts of substrate, possible intermediates and products were evaluated and summed (Table 8). Data were then normalized to the highest intensity value, which was set 100%. In case of the emergence of an enzymatic regulation after injection of PF extract, data were manually scanned for m/z eluting during the respective time range of regulation. Peaks of the respective PF molecules were displayed along with assay EICs. Their peak widths and shapes were manually compared with the peak shape of enzymatic regulation in order to conclude on the regulatory compound. If necessary, peak areas were evaluated using Achroma software tool [196]. The procedure of peak evaluation by means of Achroma is described in detail in Appendix II.

In case of data evaluation for experiments with the online coupled continuous flow mixing system coupled to the ESI-ToF-MS, procedure of automatic extraction of eluting m/z using Agilent ProFinder Version B.06.00 (Agilent Technologies) can be found in Appendix IV along with applied parameters. The calculation of logD values and the drawing of chemical formulas were realized with MarvinSketch 14.8.25.0 (http://www.chemaxon.com ChemAxonLtD, Budapest, Hungary).

3.4.2.2. *Intestinal alkaline phosphatase*

The activity of iAP was investigated by means of the online coupled continuous flow mixing system in the presence of GSH and after the injection of alternative nucleotide substrates. Furthermore PF extracts were injected to the system, followed by their chromatographic separation and introduction to the enzyme.

Injection of alternative substrates

iAP activity was observed after the injection of alternative nucleotide substrates, e.g. when AMP was used as substrate, ADP and ATP were injected to the system and so on. The experimental approach was conducted in order to investigate potential substrate preference of iAP as well as the system´s response to compounds interfering with the enzymatic reaction. In order to obtain numerical values, peak areas were evaluated with Achroma software tool. Detailed description of the experimental setup, assay concentrations, data evaluation and interpretation can be found in Appendix II.

Injection of iAP inhibitor GSH

iAP activity was investigated in the presence of increasing concentrations of GSH injected to the system, i.e. 1, 2, 3 and 4 mM with n≥3 each. Due to MS signal suppression effects, control experiments were established to correct the data.

For the purpose of data correction, ionization factors (IF) of enzymatic assay components were determined. Mixtures of defined substrate, intermediates and product concentrations were prepared (Table 11), filled into the superloop (compare Appendix IV, Figure 1) and introduced to the online coupled continuous flow mixing system. Furthermore heat-inactivated iAP was pumped to the system by means of a syringe pump. All further experimental conditions were comparable to the detection of iAP enzymatic assays (Table 5 and 7).

Table 11 Composition of mixtures for the determination of ionization factors prepared in 10 mM NH$_4$Ac pH 7.4.

MIX	ATP [µM]	ADP [µM]	AMP [µM]	Ado [µM]
1.0	10	10	10	10
1.1	20	20	20	20
1.2	40	40	40	40
2.0		10	10	10
2.1		20	20	20
2.2		40	40	40
3.0			10	10
3.1			20	20
3.2			40	40

The average mass spectrometric intensity was calculated for each individual nucleotide of each mixture. Intensity ratios of all assay components per mixture were then calculated by normalization of the average values with AMP = 1. The ratio values were then used to calculate the average of nucleotide IFs over all mixtures along with the standard deviations. Intensities of nucleotide substrate, intermediate and product contained within an iAP assay could then be corrected by means of the calculated IFs, which ultimately allowed the calculation of their approximate concentrations. Based on this calculation, a nucleotide mixture was prepared, which was filled into the superloop and pumped into the online coupled continuous flow mixing system along with heat-inactivated iAP to mimic the assay concentrations in the absence of enzymatic activity. This approach allowed the observation of nucleotide EIC responses to the injection of increasing GSH concentrations to the control assay.

Peak areas obtained by measuring the assay as well as the control in the presence of injected GSH were evaluated using Achroma software tool (Appendix II). Peak areas of controls were then subtracted from assay areas. Average values and standard deviations were calculated out of n=3 GSH injections per concentration.

Injection of PF extracts

VS PF water, water, 50% EtOH, 100% EtOH and 90% MeOH, 0.5% FAc extracts were redissolved so as to obtain a concentration of 0.5 g extracted freeze-dried and milled leaves solved in 1 mL redissolution solvent (Table 1, Method 2), i.e. "0.5 g"/mL. The injection volume was 2 µL, i.e. an equivalent of extract prepared from 1 mg freeze-dried and milled leaves was introduced into the system per run to be chromatographically separated with a 5% MeOH:95% NH$_4$Ac pH 7.4 (v/v) mobile phase and a temperature gradient applied to the column (Table 10). Comparable to the injection of iAP inhibitor GSH described above, control measurement using the calculated IF of nucleotides were included here as well.

3.4.2.3. Xanthine oxidase

XOD activity was investigated in the presence of increasing concentrations of allopurinol as well as after the injection of PF extracts. For the latter purpose a chromatographic separation was established using different organic solvents and solvent contents. Controls included the injection of 90% MeOH, 0.5% FAc PF extract redissolution solvent 100% EtOH

(Table 1) to the enzymatic assay as well as the chromatographic separation of 90% MeOH, 0.5% FAc extract in the presence of xanthine substrate but without XOD. Further details about the applied method and conditions as well as data evaluation and interpretation can be found in Appendix IV.

3.5. Determination of cell proliferation

The porcine jejunal epithelial cell line IPEC-J2, which originates from neonatal piglets, was employed for the study of cell proliferation and gene expression changes in the presence of PF extracts in comparison to control extracts containing no PF matter. Cells were kindly provided by Dr. Karsten Tedin (FU Berlin). The quantity of PF extracts administered to the cells was chosen as to mimic physiological conditions with the volume of cell culture medium (= 400 µL) atop of the adherent cells representing the jejunal lumen containing PF extract (Figure 2).

The general maintenance of cells is described in Appendix V along with growing conditions, cell culture medium composition and materials and chemicals utilized.
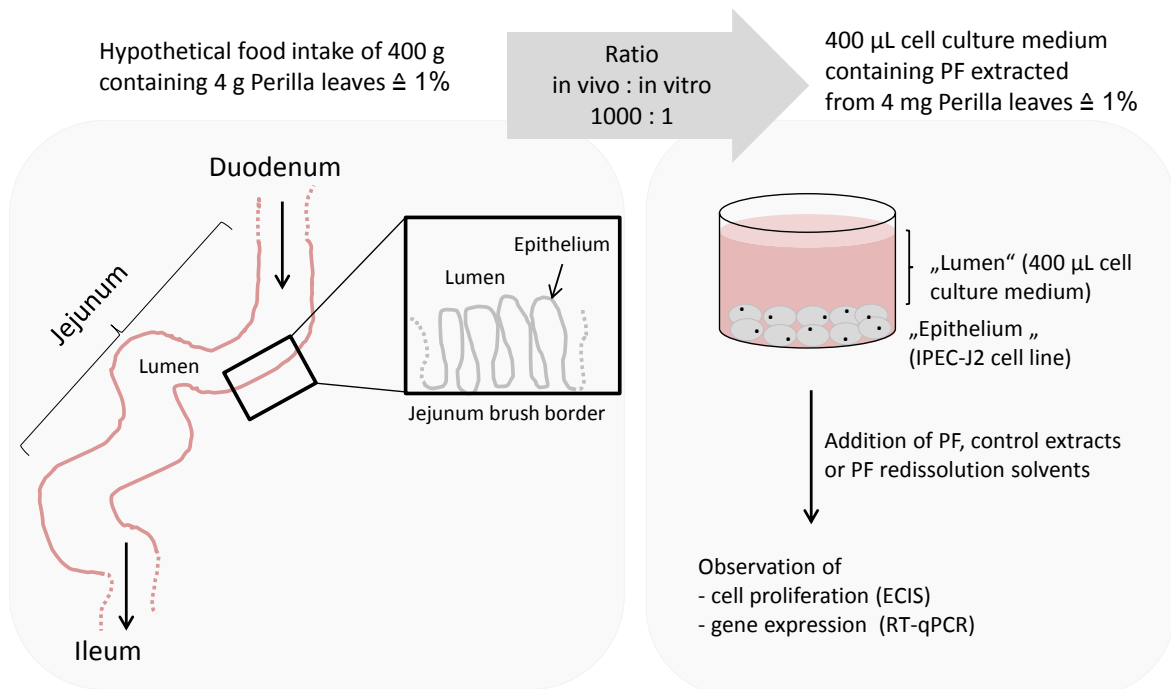
Figure 2 Transfer of *in vivo* to *in vitro* conditions in order to investigate the effect of PF extracts on cell physiology

3.5.1. Cell treatment with Perilla frutescens extracts

Cell proliferation was investigated by means of electric cell–substrate impedance sensing (ECIS) in order to assess the effects of PF extracts. ECIS allows the monitoring of impedance change, which is due to adherent cells overgrowing electrodes at the bottom of a well. Hence by means of seeding a low number of cells, their proliferation over time up to a confluent layer can be detected. For the assessment of cell proliferation the quantity of organic solvents, which is used to redissolve PF extracts (Table 1) was minimized to 1% of the total assay volume. Furthermore the effect of 1% of utilized redissolution solvents was tested beforehand in order to assess potential effects on the cells. Cells were then treated with increasing quantities of VS PF water extract, which corresponded to extract obtained from 4.0, 2.0, 1.6, 1.0 and 0.4 mg freeze-dried and milled PF leaves with n≥4 technical replicates each (hereafter referred to as "4.0 mg" , "2.0 mg", etc.). Further extracts, i.e. water, 50% EtOH, 100% EtOH and 90% MeOH, 0.5% FAc were applied in a quantity of "4 mg" and "0.4 mg" to the cells with n=9 technical replicates. PF quantities were calculated assuming the intake of a 400 g meal containing a specific amount of 10 or 1% PF, respectively. Figure 3 depicts the corresponding derivation of cell treatment using "0.4 mg" PF extracts, i.e. intake of a 400 g meal containing 1% PF.
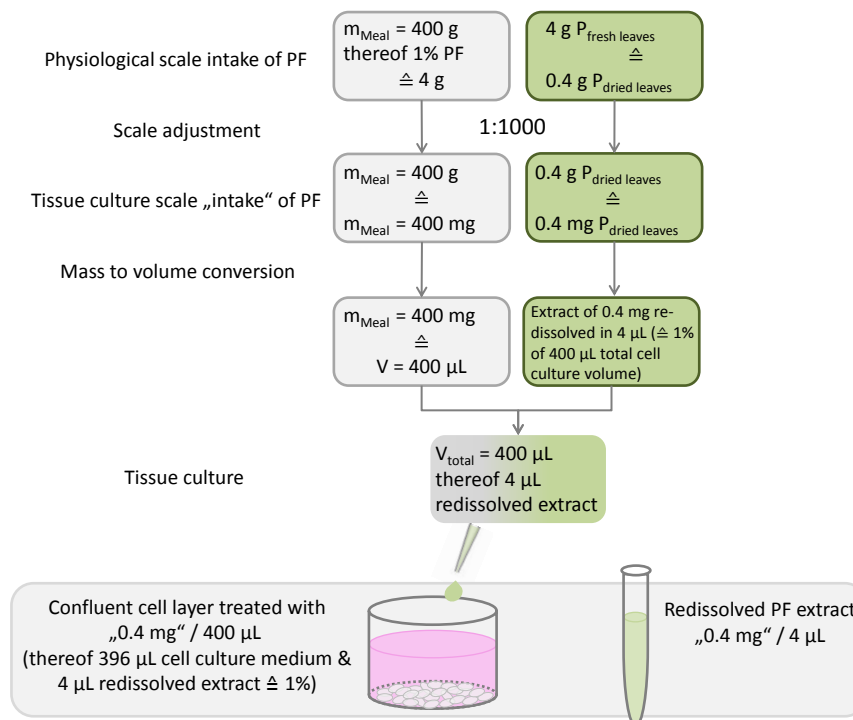
Figure 3 Application of PF extracts on IPEC-J2 cells exemplarily calculated for "0.4 mg" PF extract treatment.

3.5.2. Generation of H_2O_2 in cell culture medium

Possible generation of H_2O_2 in cell culture medium in the presence of PF extracts was detected in the absence of cells with "2.0 mg" VS PF water extract and "0.4 mg" VS PF water, water, 50% EtOH, 100% EtOH and 90% MeOH, 0.5% FAc extracts. For this purpose the respective PF extract quantity was solved in cell culture medium and H_2O_2 generation was measured photometrically at several time points within 80 hours along with negative controls containing no PF extract. Details about chemicals and experimental procedure can be found the Material & Methods chapter of Appendix V.

3.5.3. Cytotoxicity of Perilla frutescens extracts

Cytolysis of IPEC-J2 cells in the presence of PF extracts was determined by measuring the activity of released lactate dehydrogenase (LDH) with Cytotoxicity Detection Kit[PLUS] (Roche, Mannheim, Germany). For this purpose FBS content of cell culture medium had to be reduced to 1%. Preliminary experiments were therefore conducted to comparatively investigate cell proliferation with 5 % or 1 % FBS. 10,000 cells/well were seeded to 48-well plates with 400 µL cell culture medium containing either 5 % or 1 % FBS. Cell proliferation was investigated at several time points within 72 h using a Neubauer chamber.

For the assessment of cell toxicity in the presence of extracts, a confluent epithelial cell layer was mimicked by seeding 40,000 cells in 400 µL cell culture medium per well to 48-well plates. Cell treatment was conducted after cell adherence as described in Appendix V with "0.4 mg" "VS water extract", water, 50 % EtOH, 100 % EtOH and 90 % MeOH, 0.5 % FAc extracts in comparison to an untreated control at time points 0 h, 2 h, 6 h and 20 h. Cell toxicity assay was performed according to the manufacturers guidelines. Absorption was measured at 490 nm and 620 nm as reference wavelength.

3.6. Determination of gene expression

The effect of PF extracts on the expression of a panel of genes involved in cell cycle and cancer was investigated (Table 12). For this purpose cells were seeded at a concentration so as to obtain a confluent cell layer after adherence. Treatment was conducted as described in the Materials & Methods chapter of Appendix V using "0.4 mg" PF extracts (Figure 3). Controls included pure cell culture medium or 1% extract redissolution solvent (Table 1), respectively. At time point 0, 6 and 24 h after treatment cells were transferred to reaction

tubes, whereupon mRNA was extracted. In order to assess gene expression changes of reference and target genes a reverse transcription of extracted mRNA was conducted prior to RT-qPCR experiments. Further information about detailed experimental procedures, chemicals, data evaluation and calculation of significance can be found in Appendix V.

Table 12: Forward (fwd) and reverse (rev) primers of reference genes and target genes along with respective fragment length.

	Gene	Primer	Fragment length
Reference genes	Ubiquitin	fwd AGATCCAGGATAAGGAAGGCA rev GCTCCACCTCCAGGGTGAT	198
	GAPDH	fwd AGCAATGCCTCCTGTACCAC rev AAGCAGGGATGATGTTCTGG	187
	Actin beta	fwd AACTCCATCATGAAGTGTGAC rev GATCCACATCTGCRGGAAGG	234
	Histon H3	fwd ACTGGCTACAAAAGCCGCTC rev ACTTGCCTCCTGCAAAGCAC	232
Target genes	Caspase 9	fwd CTGACTGCCAAGCAAATGG rev GCCTGACAGCCGTGAGAG	104
	Cyclin B1	fwd GGATCACCAGGAACACGAAA rev GCTTCCTTTTTCAGAGGCAGT	187
	Cyclin D1	fwd GACGAGCTGCTGCAAATG rev GAAATGAACTTCACGTCTGTGG	188
	c-Jun	fwd ATGACTGCAAAGATGGAAACG rev TCACGTTCTTGGGGCACA	310
	67 kDa laminin receptor (67LR)	fwd AGCGAGCTGTGCTGAAGTTT rev GTGAGCTCCCTTGTTGTTGC	257

Data evaluation and statistical analysis was performed using Windows Excel 2010 (Microsoft Inc). To determine the relative mRNA gene expression changes, the previously described ΔΔCq method was applied (Livak and Schmittgen, 2001). For the presentation of data the gene expression is shown as log2 scale to depict the regulative impact of various PE extracts in comparison to the respective control experiments. Further information about detailed experimental procedures, chemicals, data evaluation and calculation of significance can be found in Appendix V.

4. Results & Discussion

A multitude of wholesome effects of PF are already established and are being discussed in a variety of scientific publications. Putting together further puzzle pieces may provide an increasingly complete picture to eventually gain full understanding of PF *in vitro* and *in vivo* modes of action. The effectiveness of PF extracts on three health and disease related enzymes – intestinal alkaline phosphatase, xanthine oxidase and glutathione S-transferase- was directly assessed using photometric as well as MS detection. In doing so, advantages and disadvantages as well as the distinctness of the employed methods could be examined in detail. The diversity of selected enzymes in terms of their physiological functionality and thus assay composition imposed specific requirements for successful assay adaptions. The applied experimental methods were consequently assessed with regard to their suitability for the detection of enzymatic activities. The comprehensive monitoring of substrate degradation as well as intermediate and product generation could be accomplished by means of real-time online measurements coupled to MS detection (Appendix I). Furthermore the assay transfer to an online coupled continuous flow mixing system enabled the investigation of individual PF compounds effects on enzymatic activity by means of combining biochemical assay detection with chromatographic separation (Appendix III). Necessary optimization steps include the establishment of a chromatographic separation and the finding of enzyme-compatible organic solvents (Appendix IV). Particular attention was given to assay validation, which was achieved by developing suitable control measurements and by employing a special software tool for the evaluation of atypical data (Appendix II). The here applied bioanalytical methods eventually enabled the investigation of enzymatic activity. Although being crucial biological catalyst, enzymes are merely a small part of a bigger picture, which is a cell, a tissue, an organ or an entire organism. For these reasons further experiments were performed to investigate the impact of PF on the proliferation of a porcine jejunal epithelial cell line and on the expression of a panel of genes involved in cell cycle and – if malfunctioning – in cell cycle dysregulation and cancer development. This chapter also approached drawbacks arising with *in vitro* tissue culture experiments like stability of extract compounds and hydrogen peroxide generation in cell culture medium. Bringing together both experimental moieties thus allows a circumspect

assessment of PF extract effects on cell physiology.

4.1. Enzymatic assay development – Adjustment of method parameters

Photometric detection of enzymatic activity is often employed for routine high-throughput screenings (HTS). Those standardized methods can be utilized for the discovery of new inhibitory molecules, which regulate enzymes e.g. involved in pathological conditions. The possibility to conduct enzymatic assays in physiological buffers, e.g. phosphate buffer, is one of the major arguments in favor of photometric detection. However, natural enzymatic substrates and their respective degradation products may not always be photometrically detectable. Although the utilization of chromogenic or fluorogenic and therewith artificial substrates is a possibility to overcome this issue, those have been shown to affect enzymatic specificity [197, 198]. A technique, which allows the use of most physiological substrates and simultaneously provides comprehensive knowledge of enzymatic action, is MS. By means of this detection method following the course of an enzymatic assay may not just include monitoring the physiological substrate degradation as well as the product generation, but also the increase and decrease of possible enzymatic intermediates [4] (Appendix I). To successfully adapt photometrical assays to MS detection several imperative optimization steps have to be executed (Figure 4). This includes the decrease of substrate and enzyme concentrations, the selection of a volatile buffer, the determination of a suitable pH value, the reduction of ion strength as well as the investigation of kinetic parameters [6, 14]. In the following those steps are exemplarily described by means of enzymatic assays of XOD, GST and iAP.
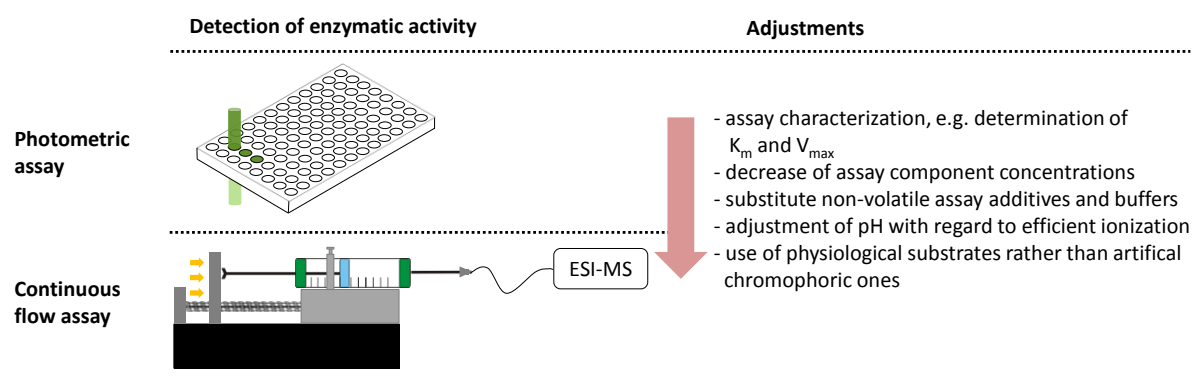
Figure 4 Enzymatic assay adaptation from photometric to MS detection (i.e. continuous flow assay)

4.1.1. Determination of buffer and pH impact

The selection of a suitable buffer or salt system is not only important with regard to its compatibility with the respective enzyme of interest, but must also meet the requirements and restrictions related to the analytical technique employed.

MS is a reliable and powerful method for the comprehensive analysis of enzymatic assays. However, the application of non-volatile buffers and high concentrations of salts have to be avoided in order to prevent contamination, impaired ionization and signal suppression effects [14, 199]. Nevertheless buffer-related difficulties can also emerge in photometric enzymatic assays. Side-reactions between assay components and buffer may falsify assay result using photometric detection. For instance the use of phosphate buffer is unsuitable for the determination of phosphatase assays like e.g. iAP, which assess enzymatic activity via phosphate release. Moreover additives like TRIS or ethanolamine have been shown to act as good phosphate acceptors for transphosphorylation reactions catalyzed by phosphatases [200, 201]. Although the presence of latter chemicals has been reported to also be able to enhance enzyme activity [202, 203], they nevertheless interfere with photometric phosphate detection and result in a lower quantity of detectable phosphate.

In general, alterations of the buffer system have been observed to affect enzymatic activity insofar as they can cause enzymatic inhibition, enzyme conformational changes or shifts of the enzymes pH optima [200, 202-208]. Thus, a successful assay adaption to MS detection requires the assessment of potential adverse effects of the MS-compatible buffer of choice on the enzyme. In this context, a reduction of enzymatic activity in MS-compatible volatile buffers compared to phosphate buffer has already been reported by de Jong et al. with acetylcholine esterase [34].

XOD activity has been widely investigated with photometric methods using phosphate buffer at pH 7.5 [209]. Therefore the activity of XOD was comparatively investigated using photometric detection in either well-established physiological phosphate buffer or volatile NH_4Ac buffer, which is suitable for MS detection (Figure 5).
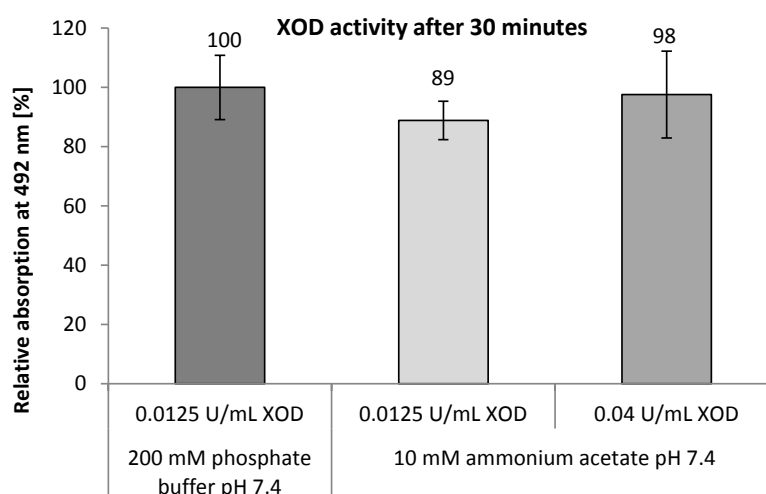
Figure 5 Photometrically detected XOD assay with 0.5 mM xanthine and 1 mM NH$_2$OH conducted either in 200 mM phosphate buffer pH 7.4 (A, dark grey colum) with 0.0125 U/mL XOD or in 10 mM NH$_4$Ac pH 7.4 with 0.0125 U/ml or 0.04 U/mL (A, light and mid-grey column). Columns represent relative generation of nitrite at time point 30 min with n≥3.

The activity of XOD was therefore comparatively assessed by means of measuring the absorption at time point 30 min (Figure 5). XOD activity can be observed by means of the superoxide released during xanthine substrate degradation to uric acid. Superoxide then oxidizes hydroxylamine to nitrite, which is followed by the formation of a colored complex after the addition of sulfanilamide and the azo dye NED [210, 211] (Figure 10). Nitrite formation was found to be slightly reduced in NH$_4$Ac solution compared to phosphate buffer (Figure 5, light and dark grey column respectively). Upon raising the enzyme concentration, the activity increased to a level comparable to assays conducted in phosphate buffer (Figure 5, mid-grey column). Furthermore XOD activity towards its substrate could be captured at several time points within 60 min in 10 mM NH$_4$Ac solution pH 7.4, which is reflected by an increase of absorption over time (Figure 6). However the amount of enzymatically generated nitrite in comparison to the quantity of xanthine available to the enzyme was found to be only minor throughout the whole experimental time (data not shown). Since the pH value of the buffer solution was 7.4, this finding may be attributed to minor superoxide stability, whose half-life highly depends on the pH value of the solution. It undergoes fast dismutation to H$_2$O$_2$ at physiological pH [212], which makes it a crucial factor for the here employed photometric XOD assay detection.

XOD assay in 10 mM NH₄Ac pH 7.4
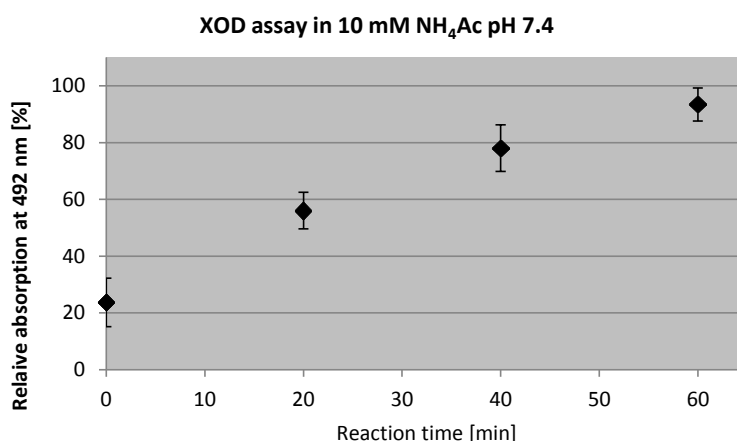
Figure 6 Relative nitrite generation within 60 minutes reaction time with 0.04 U/mL, 0.5 mM xanthine and 1 mM NH$_2$OH in 10 mM NH$_4$Ac pH 7.4.

Although various publications are available, which utilize radiolabeled substrates [213], employ fluorimetric quantification [214, 215] or follow XOD activity by means of UV detection [215, 216], the here employed assay might be considered particularly useful in terms of finding not only XOD inhibitors but also compounds able to scavenge the released superoxide [211]. Both would be reflected by the decrease of the absorption in comparison to XOD assay without the addition of an individual compound of interest or a complex mixture like e.g. a plant extract. Based on the pH-dependent superoxide dismutation reaction, the employed assay may not result in quantitative assessments of XOD activity, but would still allow qualitative assertion of the extent of an enzymatic regulation. Consequently, in the context of the described photometric XOD assay, the selection of a suitable pH value was found to be crucial in order to ensure adequate detection of enzymatic activity. Apart from considerations regarding effects of pH on the overall assay detection, enzymatic activity can also be affected directly by pH changes. Assay adaption may therefore be a compromise between maintaining sufficient enzymatic activity as well as assay detectability (Appendix I) [6, 14, 217] (Figure 7). Beyond that, the selection of a suitable pH value is an important factor in the context of MS measurements, since it distinctly affects ionization efficiency and thus the overall detection of assay components [14]. In this regard the activity of the highly pH dependent enzyme iAP, which shows its fastest substrate degradation at alkaline pH [41, 218, 219], was comparatively assessed by

means of a photometric as well as a MS approach. Using its physiological nucleotide substrates ATP, ADP or AMP [37, 220] the progress of catalysis was observed at alkaline pH 9.0, neutral/physiological pH 7.4 and acidic pH 6.0 by means of capturing inorganic phosphate released through enzymatic stepwise dephosphorylation reaction [42] (Figure 7 & Appendix I).
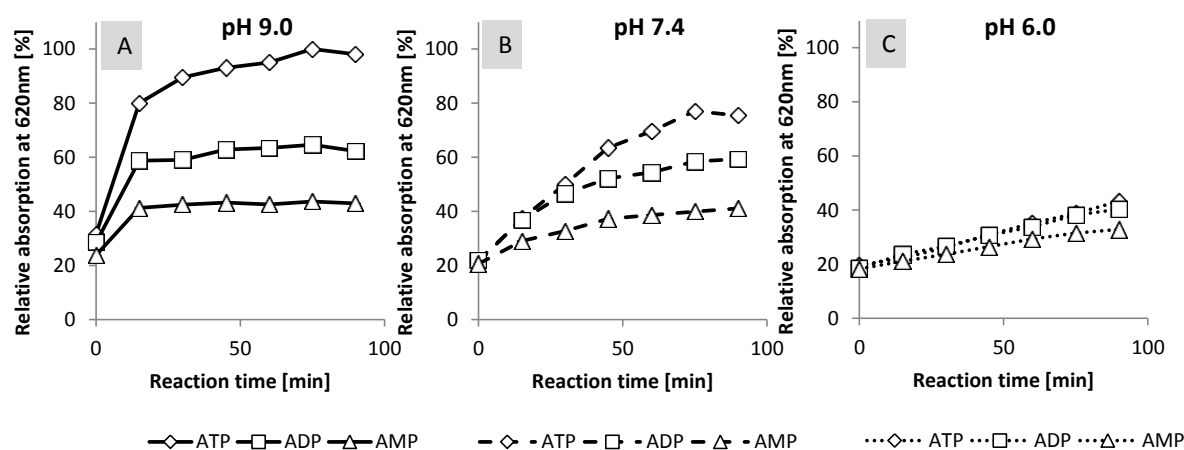
Figure 7 Enzymatic phosphate release from nucleotide substrates ATP ($\Diamond$), ADP ($\square$) or AMP ($\triangle$) at pH 9.0 (A), 7.4 (B) or 6.0 (C) with 0.2 U/mL iAP and 40μM of ATP, ADP or AMP. Enzyme assay with ATP substrate in pH 9.0 was set to 100% with the phosphate release of the other assays calculated accordingly. Standard deviations of all time points, all employed substrates and pH values are 9.3% ± 4.7. Final concentrations of enzymatically released phosphate at time point 90 min: **pH 9.0 (A)**: 120 μM ± 4.6 with ATP substrate, 67.9 ± 6.9 with ADP and 39.7 μM ± 1.8 with AMP; **pH 7.4 (B)**: 76.8 μM ± 5.5, 54.9 μM ± 8.8 and 30.1 μM ± 1.1; **pH 6.0 (C)**: 2.7 μM ± 0.4, 2.5 μM ± 0.2 and 2.0 μM ± 0.3.

At pH 9.0 the enzyme was observed to catalyze a fast and total dephosphorylation of its substrates, which is reflected by the initial steep increase of detectable phosphate followed by a nearly constant absorption. iAP is still active in pH 7.4 (B), whereas dephosphorylation is distinctly decreased in pH 6.0 (C). The release of phosphate was however not completed within the observed experimental time neither at neutral nor at acidic pH for all substrates (B, C). The reduced activity was discussed in previous publications, in which it is attributed to an inhibition of iAP by Pi and PPi at low pH values [221]. The photometrically observed pH dependency of enzymatic activity was also confirmed by iAP assays transferred and adapted to MS detection (Table 13 & Appendix I). However MS also allowed the observation of a stepwise enzymatic dephosphorylation with details about the progress of enzymatically

degraded substrate, generated intermediates as well as the final product adenosine (Figure 10, C(2) & Appendix I, Figure 4). Data evaluation of both, photometric as well as MS measurements, furthermore suggested a substrate preference of iAP towards ATP and ADP compared to AMP (Table 13 & Appendix I).

Table 13 iAP activity towards ATP, ADP or AMP substrates at pH 6.0, 7.4 or 9.0 detected photometrically or mass spectrometrically. Data is presented as substrate degradation rates [relative substrate degradation/min] for mass spectrometric assays or as slopes of trend lines [Δabsorption/Δtime] for photometric assays.

	Photometric assay Average value of n≥6: Δabsorption/Δtime ± standard deviation (SD)					
	pH 6.0	**SD**	**pH 7.4**	**SD**	**pH 9.0**	**SD**
ATP	1.350×10^{-3}	0.164×10^{-3}	5.856×10^{-3}	0.949×10^{-3}	19.73×10^{-3}	2.976×10^{-3}
ADP	1.650×10^{-3}	0.197×10^{-3}	5.033×10^{-3}	1.476×10^{-3}	12.27×10^{-3}	1.133×10^{-3}
AMP	1.083×10^{-3}	0.075×10^{-3}	2.467×10^{-3}	0.711×10^{-3}	7.133×10^{-3}	0.561×10^{-3}
	Mass spectrometric assay Average value of n≥5: relative substrate degradation/min ± standard deviation (SD)					
	pH 6.0	**SD**	**pH 7.4**	**SD**	**pH 9.0**	**SD**
ATP	10.17	0.734	38.1	13.63	575.6	58.12
ADP	8.43	4.379	27.42	15.47	751.7	128
AMP	7.001	1.175	11.48	5.379	121.9	32.33

4.1.2. Determination of a suitable substrate concentration

The understanding of enzymatic activity requires the consideration of certain kinetic parameters like Michaelis-Menten constant (K_M) or the maximum reaction rate (V_{max}). The determination of those is exemplarily presented for a photometrically detected GST assay. GSTs are part of the biotransformation phase II metabolism, which involves the detoxification of electrophilic xenobiotics by their conjugation with GSH to increase the water-solubility and thus facilitate excretion of harmful substances [222]. Consequently the assay contains two substrates, with CDNB mimicking the xenobiotic compound, which is "detoxified" by the enzymatic conjugation to the second substrate, reduced GSH [223-225]. Kinetic parameters were determined either with constant GSH and increasing CDNB concentrations or vice versa (Figure 8, A and B, respectively). Taking into account the calculated standard deviations, K_M values for both approaches were observed not to differ distinctly, which reflects a similar enzymatic substrate affinity towards GSH as well as CDNB. This is in accordance with previous findings of Enache et al. and Boušová et al., who detected

a similiar K_M for CDNB and GSH of ~0.100 mM or ~0.176 mM, respectively, for equine liver GST, albeit in phosphate buffer pH 6.5 [224, 225]. Although the here calculated V_{max} is not directly comparable due to its expression as $\triangle$abs/min (Figure 8) rather than µmol/min, the V_{max} values for varying GSH as well as varying CDNB concentrations were found also to lie in a similar range [224]. However the slight increase in V_{max} at a constant and high concentration of 1 mM CDNB (Figure 8, B) might be accounted to an enhanced accessibility of CDNB for the enzyme, since the availability of CDNB at low concentrations is presumably reduced based on the molecules hydrophobicity, which necessarily results in a poor solubility and a preferred aggregation of the compound in aqueous solution [226].
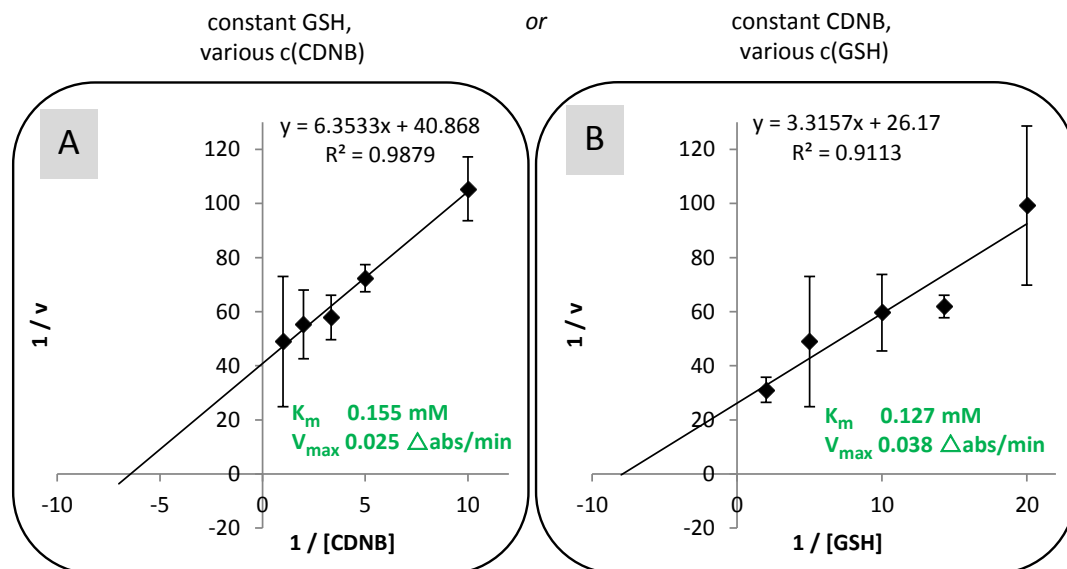
Figure 8 Lineweaver-Burk plots of GST assays with 0.1 U/mL GST in 10 mM NH$_4$Ac pH 7.4 with either constant 0.2 mM GSH and varying CDNB concentration (0.1, 0.2, 0.3, 0.5 and 1.0 mM) (A) or constant 1 mM CDNB and varying GSH concentration (0.02, 0.05, 0.07, 0.1, 0.2, 0.5 mM) (B).

Ge et al. performed kinetic analysis of GST using both a photometric and MS approach. Assays were conducted in 10 mM NH$_4$Ac pH 7.0 with 1 mM CDNB and increasing concentrations of GSH, making their study results comparable with the data presented in Figure 8 B [227]. They calculated a K_M value of 0.11 mM with photometric and 0.13 mM with MS detection, which for one is in high accordance to the results obtained here and for another shows the potential of MS and photometric detection to obtain highly comparable results for some enzymatic assays.

4.1.3. Determination of activity in the presence of organic solvents

To overcome the issues arising with hydrophobic enzymatic substrates like CDNB, the addition of low concentrations of organic solvent to an assay has already been proven to be a helpful means to enhance the solubility of non-polar assay components and simultaneously increase the substrate availability and thus the product formation [228-231]. The appropriate solvent, advantageous regarding CDNB solubility as well as maintenance of sufficient enzymatic activity, has to be evaluated by measuring the assay in the presence of different solvents and solvent concentrations (Figure 9). Besides being helpful in terms of enhancing the solubility of non-polar assay compounds, organic solvents are also a common requirement for chromatographic separations as they are for instance implemented into online coupled continuous flow mixing systems as discussed in chapter 4.4..
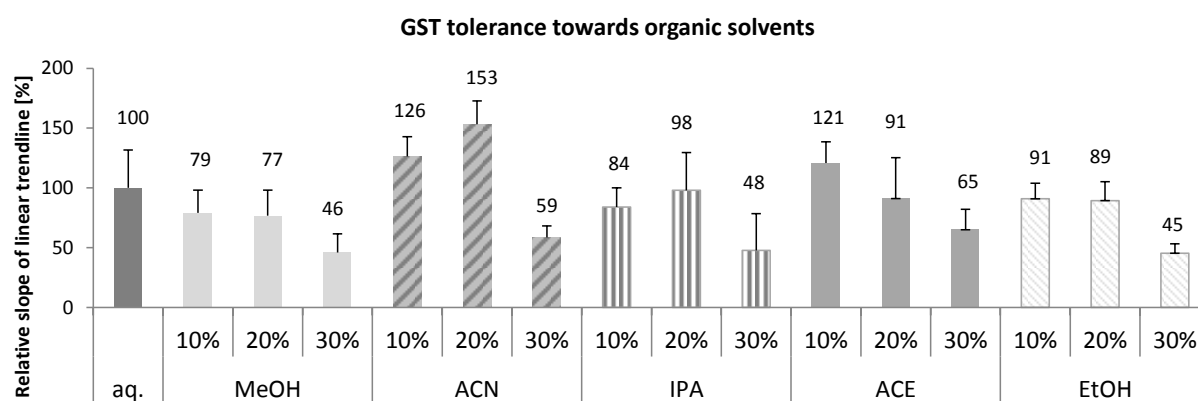
Figure 9 Photometric determination of GST tolerance to different organic solvents and solvent concentrations using 0.1 U/mL GST, 0.2 mM GSH, 1 mM CDNB in 10 mM NH_4Ac pH 7.4. Data is presented as relative slopes of linear trendlines of GST product formation with the average value of GST assays in purely aqueous solution (= aq.) set as 100%.

With most solvents and solvent concentrations, the activity of GST is decreased with up to merely 45% activity left with 30% EtOH compared to GST assays in purely aqueous solution (Figure 9, dark grey column). However a general tendency could be observed, whereupon the enzymatic product generation is increasing with decreasing solvent polarity [232]. This would confirm the assumption of a poor CDNB availability in entirely aqueous solution as discussed in chapter 4.1.2.. Nevertheless by improving the solubility of CDNB, organic

solvents also negatively affect the enzymatic activity, which leads to a reduction of product generation with the exception of 10% and 20% ACN and 10% ACE. Those solvents and concentrations can be assumed to enhance CDNB solubility and simultaneously maintain or even increase enzymatic activity. In contrast to the findings here, Scheerle et al. mostly observed distinctly lowered substrate degradation in the presence of organic solvents and no correlation between organic solvent polarity and enzymatic activity, however employing polar substrates [5]. In this case sufficient availability of the substrate is given in purely aqueous solution, wherefore the addition of organic solvents can be assumed to negatively affect the enzymatic activity without the advantage of improved substrate solubility. Nevertheless they also found an enhanced activity of glycoside hydrolases chitinase and lysozyme with assays containing EtOH or ACN and MeOH, respectively. The possibility for a preserved or even increased enzymatic activity in the presence of organic solvents has already been described and is amongst others ascribed to a stabilization of the enzymatic structure [228, 233-235].

4.2.   Photometrically vs. mass spectrometrically detected enzymatic assays

Photometric determination of enzymatic activity revealed distinct differences regarding the detectable assay components, whether it may be a direct detection of enzymatic substrate-formation with GST or the indirect determination of assay by-products like enzymatically released inorganic phosphate with iAP or superoxide with XOD (Figure 10, left column, grey shaded components). GST product generation was captured continuously via the direct detection of absorption changes caused by the formation of the GSH-CDNB conjugate (Figure 10, B(1)). In contrast, with iAP and XOD assays neither the decrease of substrate or the increase of the primary product is photometrically detectable. Both assays required the addition of mediator compounds, which eventually led to the formation of a colored complex via the reaction with secondary assay products P_i or superoxide, respectively (Figure 10, left column) [210, 211, 236-238]. Enzymatic activity was therefore investigated by means of quenching the enzymatic reaction at defined time points, which consequently resulted in a non-continuous assay detection (Figure 10, A(1) and C(1)).
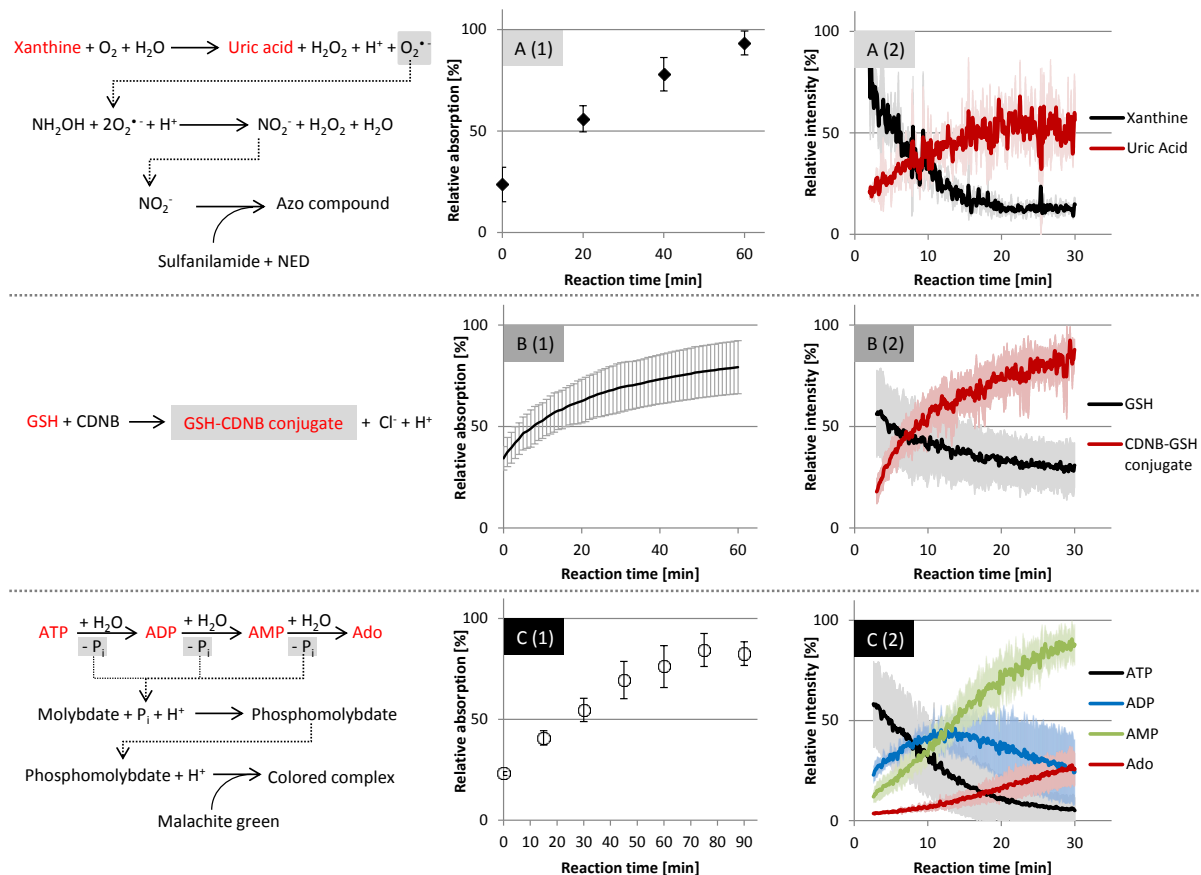
Figure 10 Comparison of XOD (A), GST (B) and iAP (C) photometric (1) and MS (2) assays. All assays were conducted in 10 mM NH_4Ac pH 7.4. MS-detectable assay components are marked red (left colum). Assay concentrations were as follows: A (1) with 0.5 mM xanthine, 1 mM NH_2OH, 0.04 U/mL XOD, A(2) with 25 µM xanthine, 0.02 U/mL XOD; B(1) with 0.2 mM GSH, 1 mM CDNB, 0.1 U/mL GST, B(2) with 25 µM GSH, 25 µM CDNB, 0.3 U/mL GST; C(1) 40 µM ATP, 0.2 U/mL iAP, C(2) 40 µM ATP, 0.2 U/mL iAP

In contrast the assay adaption to the real-time online MS setup allowed the continuous observation of enzymatic activity (Figure 10, A(2), B(2), C(2)). The utilization of MS detection furthermore enabled the reduction of most concentrations as well as a decrease of the overall experimental time. The necessary assay components could be limited to the respective enzyme and the corresponding substrate(s). Color-forming compounds like sulfanilamide and NED or malachite green molybdate, which were essential for the photometric detection, could be omitted entirely. Moreover, the reduction of concentrations to achieve MS compatible conditions enabled the measurement in purely aqueous solution, despite the presence of poorly water-soluble GST and XOD substrates, respectively (Figure 10, A(2), B(2)).

As already discussed in chapter 4.1.1. photometric assay of XOD might result in ambiguous findings with regard to the extent of enzymatic activity or inhibition, which can be ascribed firstly to the minor stability of the enzymatically released superoxide and secondly to the poor distinguishability between actual enzymatic inhibition and mere superoxide scavenging by compounds added to the assay. In contrast, by employing MS detection for the investigation of XOD activity both issues can be avoided. First results indicate that by adding the specific superoxide scavenger dihydroethidium (DHE) to the assay, a differentiation between enzymatic inhibition and released superoxide might be feasible in the presence of PF extract (data not shown). Furthermore by means of MS detection it became possible to directly capture substrate and product without the necessity of relying on superoxide stability. The benefits of being able to follow all assay components are also especially obvious for iAP assay. Besides the detection of the ATP substrate, the measurement revealed two intermediate products (ADP and AMP) and the generation of the final product Ado (Figure 10, C(2)) [42] (Appendix I), all of which non-detectable with the utilized photometric method (Figure 10, C(1)). Although Moss et al. already showed the formation of intermediates during ATP stepwise dephosphorylation, they had to perform a time-consuming multiple-step experimental procedure. Their method resulted in a non-continuous determination of iAP activity, which did not include the observation of adenosine product generation [42]. However, the determination of phosphate within iAP assay or superoxide within XOD assay, respectively, could not be realized with MS, but only via photometric detection. Hence it might be beneficial to conduct both methods to gain a comprehensive picture of enzymatic activity. In their studies Deng et al. and Ge et al. highlighted the competitiveness of MS detection with regard to the determination of enzymatic kinetics and inhibition analysis in comparison to classical spectroscopic approaches [227, 239]. Therefore photometric and MS measurements of enzyme kinetics can be considered to be complementary for certain assays.

4.3.   Enzymatic activity in the presence of regulatory compounds

The regulation of enzymes involved in the development and progress of diseases is a common therapeutical means for a successful alleviation, e.g the suppression of XOD activity with allopurinol for the treatment of gout [87]. Inhibition kinetics are usually investigated via

well-established and robust photometric approaches, which also offer the possibility for an automatized HTS. Those methods however lack important information in terms of observing all assay components. Therefore efforts have been made to use MS detection for the sensitive and quantitative HTS of enzymatic regulators [20, 21, 240, 241]. By utilizing MS detection a more comprehensive picture of enzymatic regulation can be obtained. This is of special interest with regard to multi-component assays, which include the generation of several intermediates (Figure 11).
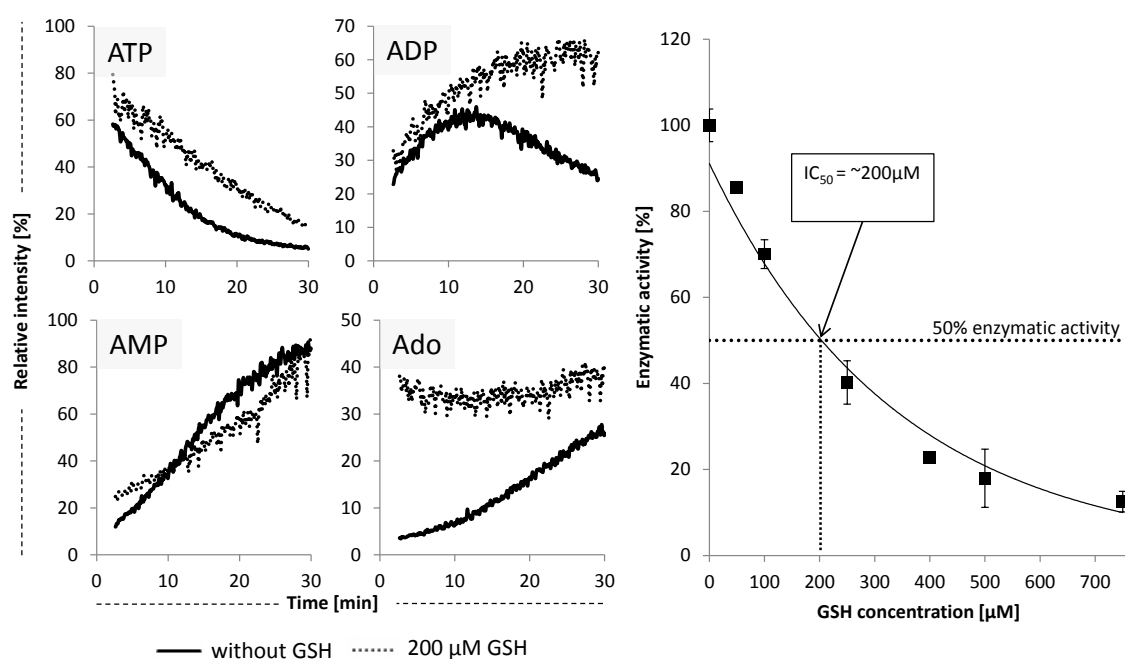
Figure 11 Direct comparison of individual iAP assay traces ATP, ADP, AMP and Ado in the presence (dotted traces) and in the absence (solid traces) of 200 µM GSH (left) as well as determination of IC_{50} value with increasing GSH concentrations (right). Assay composition was as follows: iAP assay with 0.2 U/mL iAP and 40 µM ATP in 10 mM NH_4Ac pH 7.4.

The stepwise ATP substrate dephosphorylation by iAP results in the generation of ADP and AMP intermediates as well as the final enzymatic product adenosine. Changes in the progress of individual nucleotide traces could be continuously followed, whereupon a distinctly decelerated degradation of ATP and ADP as well as generation of ADP, AMP and Ado was observed in the presence of the iAP inhibitor GSH (Figure 11, left, dotted traces) compared to assays without an inhibitor (solid traces). The addition of increasing GSH

concentrations to iAP assays revealed an IC_{50} of about 200 µM with the here applied conditions (Figure 11, right).

Besides the investigation of effects of single molecules on enzymatic activity, the addition of complex mixtures like e.g. plant extracts to enzymatic assays provides insight into possible regulatory effects. Although drawing conclusions about individual regulators is not possible in this case, the addition of a plant extract of interest to an enzymatic assay is an easy means to assess a mixtures regulatory potential. In this regard PF extracts, prepared with different organic solvents, were added to photometrically measured GST assays in 4 different concentrations (Figure 12, A). In contrast to EtOH extract, which lacked inhibitory effects, water and MeOH extracts were found to distinctly suppress GST activity. Due to the polarity of extraction solvents used, GST is inhibited rather by polar than moderately polar PF compounds as they would be present in the here applied non-inhibitory EtOH extract. Rohman et al. investigated the activity of different GSTs in the presence of onion bulb extracts and detected the most pronounced effects in the presence of a polar water extract compared to only minor inhibition caused by a non-polar hexane extract [242]. In contrast, no correlation between compound polarity and regulatory activity was found by Iio et al., who detected a distinct GST inhibition after addition of individual and mainly poorly water-soluble flavonols and flavones to the assay [243].

However, as fast and easy photometric determination of enzymatic activity may be, it can also lead to ambiguous results. The addition of complex mixtures or even individual compounds might be capable of interfering with photometric assay detection, either by overlaying absorption of mixture compounds at the wavelength of assay detection or by affecting the formation of a colored complex. Moreover, considering the photometric investigation of XOD assay, a distinction between an actual enzymatic inhibition and the scavenging of released superoxide by extract molecules is not feasible with the applied assay procedure. MS detection, which directly observes xanthine substrate and uric acid product may therefore help to elucidate enzymatic action without relying on the release of superoxide (Figure 10, A(2)). Xanthine oxidase assay was therefore measured in the presence of increasing concentrations of VS PF water extracts. Data evaluation revealed an extract concentration-dependent enzymatic inhibition (Figure 12, B), which is reflected by decreasing substrate degradation and product generation.
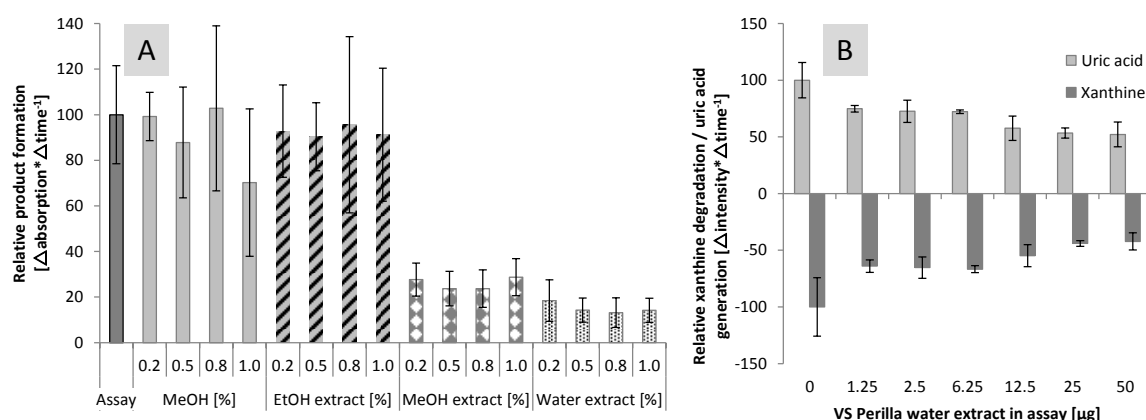
Figure 12 A: Photometrically determined GST activity with 0.1 U/mL GST, 0.2 mM GSH, 1 mM CDNB in 10 mM NH$_4$Ac pH 7.4 without extract (left dark grey colum) or 0.2, 0.5, 0.8 or 1.0% (v/v) of extract redissolution solvent 80% MeOH as controls (= "MeOH [%]") or 0.2, 0.5, 0.8 or 1.0% (v/v) water, 90% EtOH or 90% MeOH, 0.5% FAc PF extract (= "water extract [%]", "EtOH extract [%]" or "MeOH extract [%]"respectively). PF extracts were prepared using method 1 described in Table 1. **B**: Mass spectrometrically determined xanthine degradation and uric acid generation. Depicted columns represent the slopes of trend lines applied to the initial linear decrease (xanthine) and increase (uric acid). Assay composition were as follows, 0.004 U/mL XOD and 25 µM xanthine in 90% 10 mM NH$_4$Ac pH 7.4, 10% IPA (v/v) in the presence of increasing quantities of VS PF water extract redissolved in water in a total assay volume of 500 µL. PF extract quantities given here refer to the weight of the powder, which is obtained after extraction and extraction solvent evaporation.

Finding promising enzymatic regulation after applying a complex mixture consequently results in the isolation of single compounds, which are then further tested for their individual regulatory potential. The procedure mainly employed for this purpose is the so-called bioassay guided fractionation (Appendix III, Figure 5). This technique has been used e.g. by Huo et al. for the isolation of PF molecules, whereupon they were added to XOD assay to assess their impact on the enzymatic activity, which resulted in the finding of several inhibitory compounds including caffeic acid, rosmarinic acid and apigenin [244]. The employed procedure usually involves repeated fractionation, followed by the fractions exposure to the enzyme. Therewith the quantity of extracts compounds can be gradually narrowed down to eventually isolate enzyme-regulatory substances [191].

4.4.   Online coupled continuous flow mixing setup

A setup, which combines the chromatographic separation of a mixture with the direct MS detection of enzymatic activity, is the online-coupled continuous flow mixing setup (Figure 13, Bottom). The system has already been employed for a variety of different enzymes and applications, ranging from the screening of complex mixtures on enzyme regulatory molecules [27] to the determination of IC_{50} values of known enzymatic inhibitors [35, 245]. A comprehensive overview of publications regarding online coupled continuous flow mixing systems along with the investigated enzymes and the chromatographic methods used can be found in a recent publication (Appendix III, Table 2).

Again concentrations of enzyme and substrate have to be adapted from real-time continuous flow assays to the online coupled continuous flow mixing setup in order to detect the substrate as well as the generated product at sufficient MS intensity. The extent of substrate degradation is dependent on the reaction time provided by the length of reaction coil 2 (Appendix IV, Figure 1), which ensures the sufficient mixing of substrate and enzyme. Furthermore the interaction time between a regulatory compound injected to the system and the enzyme is dependent on the length of reaction coil 1, in which the flow containing the enzyme (Appendix IV, Figure 1, upper trace) is mixed with the chromatographically separated extract or with individual compounds injected to the system, respectively (Appendix IV, Figure 1, middle trace). Both reaction coils are knitted to improve the mixing of flows [246-248] and their length has to be adjusted in order to achieve the desired interaction time. However, opposed to the introduction of a single compound to the system, which is a straightforward means to investigate its regulatory potential on an enzyme of interest, the injection of a complex mixture requires the implementation of a chromatography. In this context several points have to be considered. Most importantly the addition of organic solvents, which are necessary for a chromatographic separation, has to be kept low and constant in order to maintain sufficient and consistent enzymatic activity (Figure 13). The separation was therefore established as isocratic elution, which however has the drawback of limiting the overall quantity of elutable compounds.
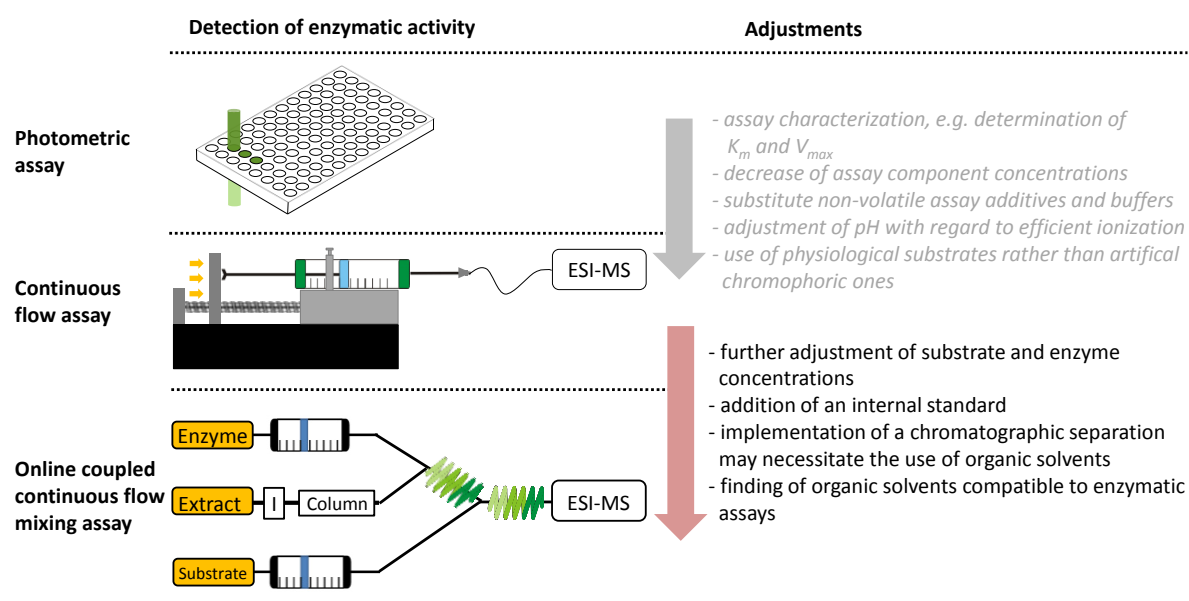
Figure 13 Enzymatic assay adaption from real-time continuous flow to the online coupled continuous flow mixing system

Method establishment is described in the following chapters, starting with the molecular characterization of PF extracts (chapter 4.4.1.) and proceeding with the enzymatic assay adaption (chapter 4.4.2.), which included comprehensive control experiments in order to validate the results after the injection of a known inhibitor (chapter 4.4.3.). The merging of established enzymatic assays and chromatographic separation of PF extracts is eventually discussed in chapter 4.4.4..

4.4.1. Molecular characterization of Perilla frutescens extracts & chromatographic method development

In order to estimate the quantity of elutable PF compounds within the online coupled continuous flow mixing system, molecular composition of extracts was characterized beforehand using a HILIC-RPLC coupling with UV and MS detection [195, 249]. By means of this method non-polar as well as polar compounds can be captured in a single run, which allows a comprehensive overview of the entirety of contained molecules. Knowledge about the polarity distribution of extract compounds is eminently important for the establishment of the chromatographic separation implemented into the online coupled continuous flow mixing system.
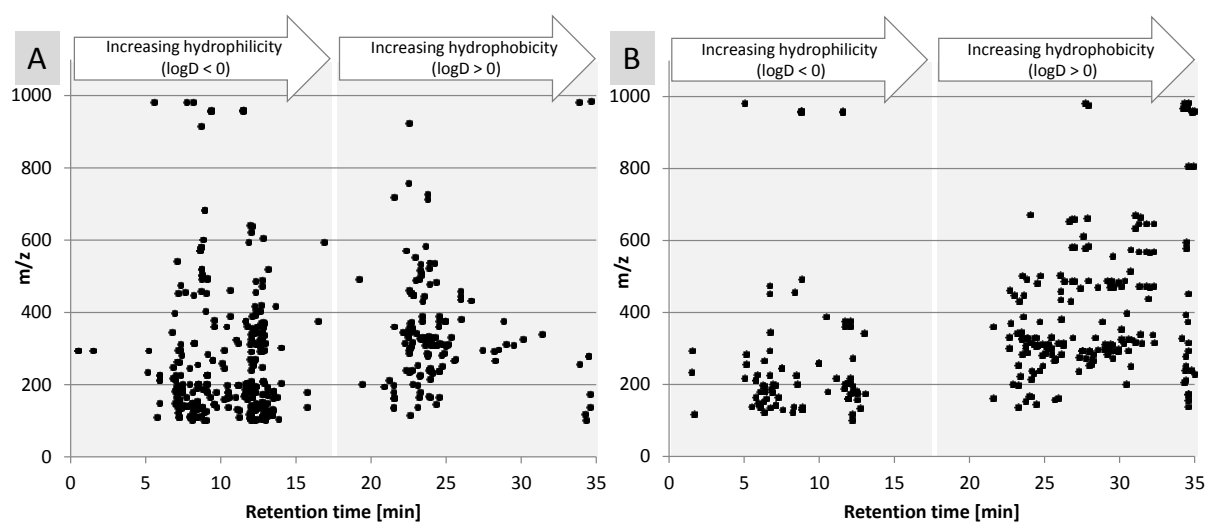
Figure 14 Exemplarily displayed chromatographic separation of PF water (A) and 100% EtOH extract (B) using the HILIC-RPLC coupling. Mass spectrometrically detected m/z of contained molecules are plotted against their RTs.

The molecular characterization of PF extracts revealed clear differences between the extracts, which can be ascribed to the use of different solvents for the extraction (Figure 14). The determination of the water extract composition showed distinctly more molecules to elute within the first 17 minutes of the chromatographic run, in which mainly compounds with logD values below 0, i.e. polar ones, can be found [195]. In contrast the separation of 100% EtOH extract was detected with an increase of eluting non-polar compounds after 25 minutes and a distinctly lower quantity within the "polar time range" up to minute 17, compared to PF water extract. Nevertheless both extracts contain polar compounds, which are potentially separable with the chromatographic method to be adapted for the utilization within the online coupled continuous flow mixing system. Due to the need of avoiding (high) organic solvent concentrations, which may negatively affect the enzyme, the chromatographic separation of PF extracts was first tested with an entirely aqueous isocratic elution. Chromatographic columns, which are stable to run with a 100% aqueous mobile phase, are available (Appendix IV, Supplementary material). However the quantity of eluting compounds as well as the MS intensities were found to be low (Figure 15, ✳). An efficient method to shorten the experimental time and to enhance the solubility and thus the elution of extract components is the application of a temperature gradient to the column [245]. The gradual heating of the mobile phase causes a decrease of its static permittivity, i.e. polarity,

59

which results in an increase of elution strength [250]. In accordance with the column specifications a moderate temperature gradient up to 70°C was applied (Figure 15 & Appendix IV, Figure 2). Due to the enhanced solution in the heated mobile phase an increasing quantity of eluting compounds (Figure 15, gray-shaded) and a distinct shift of retention times (Figure 15, arrows) was detected. Nevertheless also late-eluting compounds, like e.g. 623.1 or 639.1 (Figure 15), were still highly polar with logD values distinctly below 0 (Appendix IV, Table 3).

Figure 15 Chromatographic separation of PF water extract using a 100% aqueous mobile phase without (✳) and with (O) the application of a moderate temperature gradient (TG) up to 70°C. Shaded compounds only elute after the application of a TG. Arrows mark the shifts in RT of a selection of eluting compounds, which are due to the increasing temperature applied to the column.

Consequently a low amount of eluting compounds is expected after the injection of semi- to non-polar extracts with a 100% aqueous mobile phase. To extent the polarity spectrum and to further accelerate the separation low organic solvent proportions were added to the mobile phase and tested for their suitability within the online coupled continuous flow mixing system (Appendix IV, Figure 2). Besides being a necessary stability requirement with

most chromatographic columns, the use of organic solvents may also contribute to the improvement of MS intensities and signal stability (Appendix IV, Supplementary material, Figure S1) [14, 251]. Since organic solvents are likely to interfere with the enzyme´s catalytic activity (Appendix IV, Table 2, Figure 2 and Supplementary material) [5], their proportion has to be kept constant. This can either be achieved by performing an entirely isocratic separation (Appendix IV) or by the application of a counter gradient. By means of antagonizing the organic solvent proportion of the chromatographic gradient a constant solvent exposure to the enzyme can be preserved [26, 28, 29, 252, 253]. The additional flow will however cause the dilution of assay components and analytes, which potentially reduces the MS signal, wherefore a counter gradient was not applied here. Consequently a balance has to be found between the improvement of the separation by addition of an organic solvent and sufficient remaining enzymatic activity, wherefore the assessment of the enzymes compatibility with diverse organic solvents is a prerequisite for further measurements (Figure 9 & Appendix IV, Supplementary material). Moreover the injection of different PF extract polarities allows the comparison of chromatographic elution efficiency in terms of the contained polar, semi- and non-polar compounds (Appendix IV, Table). Due to the mostly polar properties of the employed mobile phases and the high content of polar compounds, most elutable features were found after the injection of PF water extract, followed by 50% EtOH extract and 90% MeOH, 0.5% FAc extract (Appendix IV). Injection of PF water extract revealed the best results with the applied most polar mobile phase containing 5% EtOH, whereas most elutable compounds of 50% EtOH and 90% MeOH, 0.5% FAc extract were observed with 5% IPA. Due to a higher static permittivity of the 10% EtOH and 5% IPA mobile phase [250], the finding of an improved elution efficiency for less polar extracts is reasonable. Consequently the lowest amount of compounds was found to elute with the non-polar 90% MeOH, 0.5% FAc PF extract and the most polar mobile phase of 5% EtOH (Appendix IV). Overall the applied chromatographic method was found to result in a good separation of PF extracts (Appendix IV, Figure 2). The plotting of known PF compound RTs vs their logDs revealed a logarithmic increase (Appendix IV, Figure 3). This correlation could then be utilized to tentatively assign unknown compounds e.g. like luteolin-6,8-di-C-glucoside (Appendix IV, Figure 3, B). Based on the observed logD values, the range of eluting molecule polarities can be determined. This is of special interest with regard to the detection

of enzymatic regulation by means of the online coupled continuous flow mixing system. The classification of inhibitors in terms of their chemical properties may be insightful for the finding and identification of further promising regulatory compounds.

4.4.2. Detection of an enzymatic assay

In terms of enzymatic assay detection various methods have been employed with the online coupled continuous flow mixing system, which range from UV [27, 248] to fluorescence [26, 28, 29, 252-255], MS detection [34, 35, 245] or a combination of UV or fluorescence with MS [27, 254] (Appendix III, Table 2). However UV and fluorescence detection methods require the use of artificial chromogenic or fluorogenic substrates, both of which can affect the enzymatic activity compared to the physiological substrate(s) [197, 256-258], which in most cases can be used with MS detection. Nevertheless a combination of UV or fluorescence with MS detection may facilitate a direct quantification of substrate degradation and product generation as well as the simultaneous determination of a regulatory compounds molecular weight. The elaborateness of those setups, which bring together multiple flows to be introduced, mixed and directed to the respective detection devices, requires equipment, which is not always available to the researcher. In this work a straightforward setup was therefore employed, which captured the assay traces as well as the injected compounds or the chromatographically separated mixtures by means of MS detection (Appendix II, III & IV). To be able to characterize unknown enzyme-regulatory compounds from complex mixtures, MS is a suitable method, since it provides the accurate molecular mass of a molecule of interest (Appendix IV, Table 3).

4.4.3. System characterization and control measurements

Prior to the merging of an enzymatic assay and a chromatographic separation using the online coupled continuous flow mixing system, the injection of known inhibitor(s) or an alternative enzymatic substrate served as control [27, 34, 35, 245, 254] to characterize the systems response to the presence of an enzyme-affecting molecule (Appendix IV, Supplementary material & Appendix II). Control measurements are presented by means of iAP assay. Its activity was determined in the presence of the inhibitor GSH as well as after the injection of alternative nucleotide substrates (Appendix II, Figure 4 and 5). The latter approach is exemplarily presented in Figure 16 using AMP as substrate. iAP degrades AMP to

adenosine, which results in a constant MS signal of the remaining AMP substrate and the adenosine product formed (Figure 16, Minute 5 to 10) [25, 35, 259].
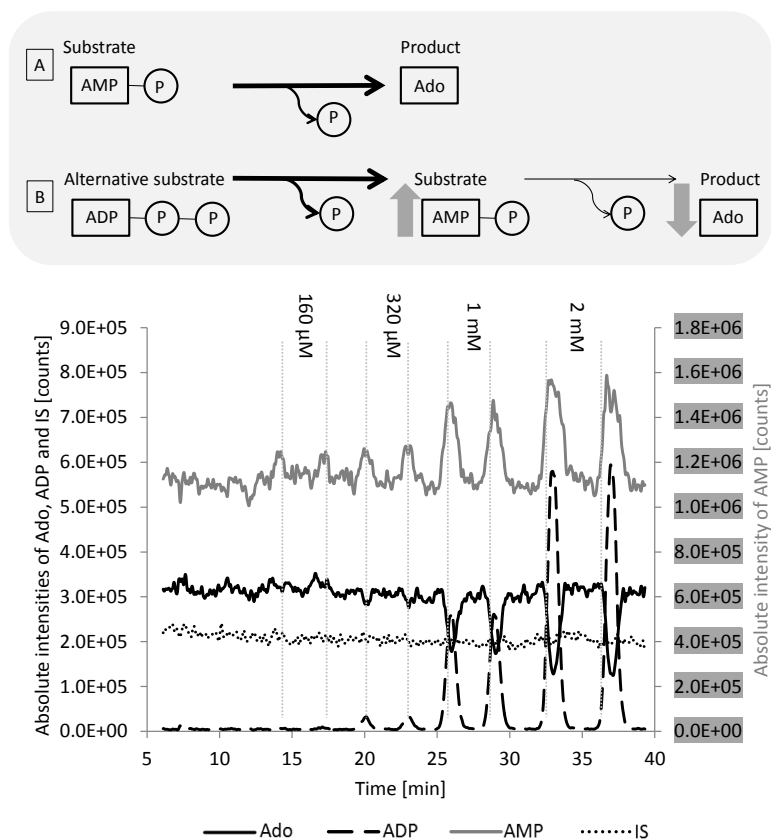
Figure 16 iAP assay detected with the online coupled continuous flow mixing system. Concentrations introduced to the system were 2.4 U/mL iAP, 80 µM AMP and 80 µM of the internal standard histidine (IS). Assay components formulation was 10 mM NH$_4$Ac pH 7.4, as were all used solvents. 160 µM, 320 µM, 1 mM and 2 mM ADP were successively injected to the system twice each (vertical lines). A: iAP assay, in which AMP substrate is dephosphorylated to adenosine. B: iAP assay with AMP substrate and injection of the alternative substrate ADP. ADP is primarily degraded to AMP by iAP, which results in an increase of AMP signal and a decrease in the final product adenosine (Ado).

Due to the enzyme´s preference towards ADP compared to AMP, the introduction of ADP to the system results in an increase of the AMP signal. Furthermore less AMP can be degraded to adenosine in the presence of high ADP concentrations, thus consequently causing a decrease of the Ado signal (Figure 16). Previous experiments, in which iAPs activity towards ATP and ADP was reported to be more pronounced compared to AMP (Appendix I) could thus be confirmed with the online coupled continuous flow mixing system (Appendix II).

Moreover, the application of this setup allowed a faster analysis of iAP activity towards nucleotide substrates due to the possibility of a consecutive injection of a multitude of samples in one experimental run.

Besides the investigation of alternative substrates, the iAP inhibitor GSH was injected to the system in increasing concentrations. As already observed by de Jong et al. [34] and de Boer et al. [35, 245] for acetylcholine esterase and cathepsin B, the presence of an inhibitory compound causes a temporary increase of substrate and simultaneous decrease of product signal. However injected concentrations of the GSH caused both, the ATP substrate as well as the dephosphorylation product traces of ADP and AMP to drop in intensity (Figure 17, A).
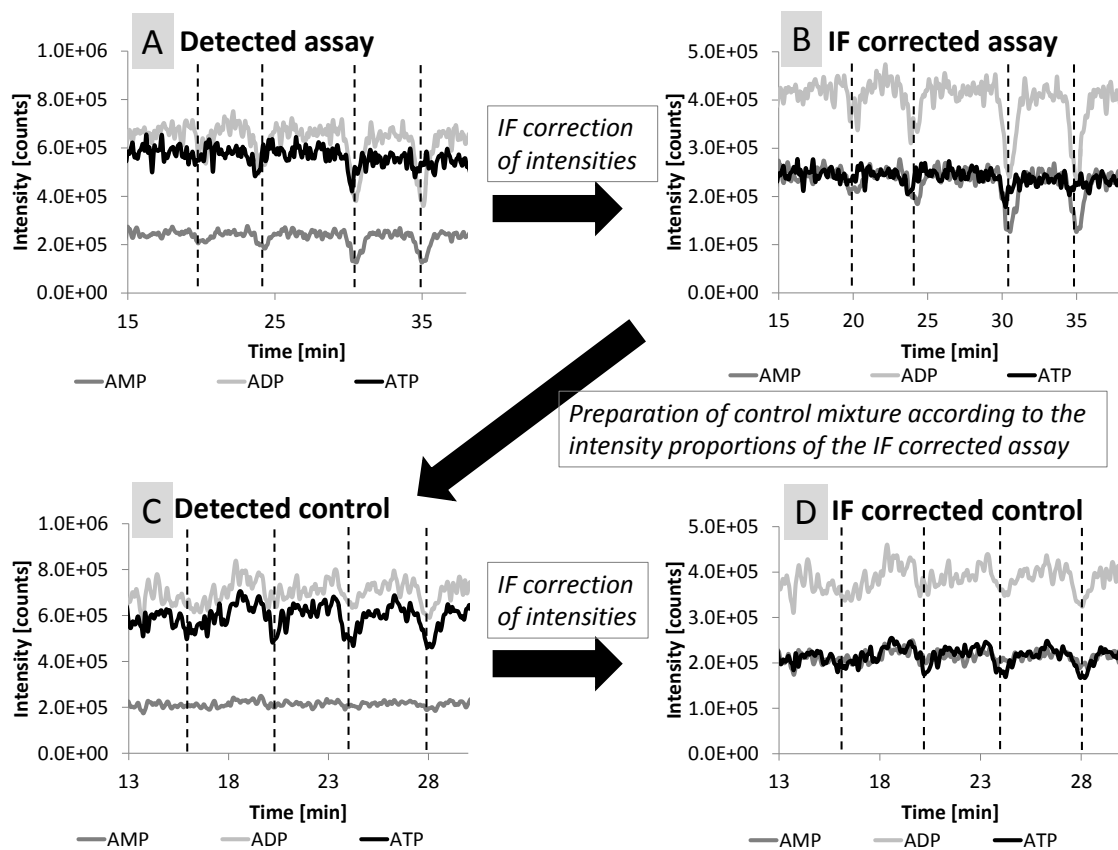
Figure 17 iAP assay (A) and control (C) in the presence of GSH injected (vertical dashed lines, GSH peaks are not shown for clarity reasons) to the online coupled continuous flow mixing system. Control and assay component intensities were corrected using ionization factors (B and D, respectively), which were determined priorly. Adenosine trace was omitted due to inferior intensity.

This has to be ascribed to MS signal suppression, since the inhibitory effect of GSH on iAP activity has already been determined in previous experiments by means of continuous flow assays (Figure 11). To be able to address the issue of MS signal suppression and to correct the assay data, control measurements were conducted. For this purpose the ionization efficiency of all assays components was determined by introducing mixtures containing known concentrations of the substrate ATP, the intermediates ADP and AMP as well as the product adenosine to the MS. Thusly determined ionization factors were used to correct assay intensities (Figure 17, B). Based on the resulting intensity proportions in B, concentrations of ATP, ADP, AMP and adenosine were calculated and used to prepare a "control mixture". To mimic the same conditions as present in the assay, iAP was heat-inactivated and introduced to the online coupled control system along with the nucleotide "control mixture" (Figure 17, C). Finally the correction of the control by means of the ionization factors resulted in highly similar intensities and intensity proportions of the control (D) and the assay (B) for all assay components. Using Achroma Software Tool (Appendix II, Figure 4) [196], correction of signal suppression in the presence of increasing GSH concentrations was conducted by calculating GSH-induced peak areas within the assay (Figure 17, B) and the control measurements (Figure 17, D). The subtraction of control peak areas from assay peak areas resulted in a GSH-concentration-dependent positive "peak signal" for ATP and negative "peak signals" for ADP and AMP, which reflects the inhibition of iAP by GSH (Figure 18).
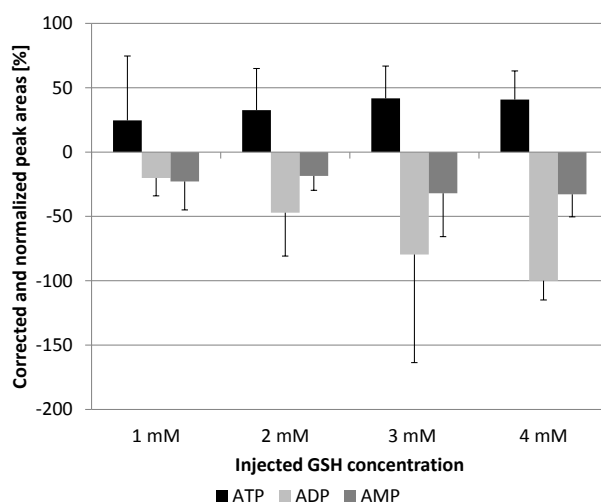
Figure 18 Normalized and corrected assay component peak areas after subtraction of control peak areas. Adenosine trace was omitted due to its inferior intensity.

The measurement of suitable controls is especially important in the presence of organic solvents, which are necessary for the implementation of a chromatographic separation into the online coupled continuous flow mixing system (compare chapter 4.4.1). They may alter enzymatic activity [5, 260], e.g. by causing denaturation of the enzyme [261, 262], enzymatic structure stabilization or alterations of substrate specificity [263]. In case of XOD assay to be adapted to the online continuous flow mixing system, several different organic solvents were tested for their suitability in terms of maintaining sufficient enzymatic activity (Appendix IV, Supplementary material). Furthermore prior to the introduction of PF extract to the system, XOD assay response towards the injection of the known XOD inhibitor allopurinol [87] was determined (Figure 19 & Appendix IV, Figure 4). The measurement was conducted in the presence of 10% IPA, which was found to distinctly affect XOD activity (Appendix IV, Supplementary material), in order to investigate its impact on the detection of XOD inhibition. The results clearly illustrate the capability of the system to capture an enzymatic regulation despite the presence of an organic solvent, which has been priorly shown to reduce XOD activity.
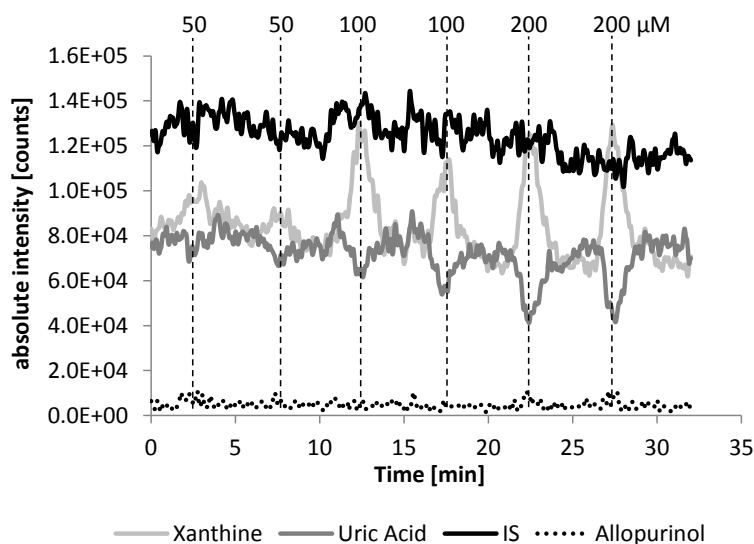
Figure 19 XOD xanthine substrate and uric acid product trace responses to the presence of the enzymatic inhibitor allopurinol. Assay concentrations as introduced to the system were as follows: 0.032 U/mL XOD, 50 µM xanthine and 80 µM histidine, which served as internal standard (IS). Allopurinol was injected in the following concentrations: 50 µM, 100 µM or 200 µM (dashed lines). All online coupled continuous flow mixing system flows contained 10% IPA.

4.4.4. Coupling of chromatography and enzymatic assay

Control measurements using IF data correction described in the previous chapter were also conducted for the detection of iAP activity after the injection of PF extract to the online coupled continuous flow mixing system. Using a mobile phase containing 5% MeOH for the chromatographic separation as well as a moderate temperature gradient up to 70°C, an enzymatic inhibition was captured approximately 45 minutes after injection of VS PF water extract to the system (Figure 20, A). The regulatory event was depicted by an increase of the ATP substrate trace and a decrease of dephosphorylation products ADP and AMP. Several compounds eluting within the time range of regulation could be found. Still none of them possessed the exact peak shape and retention time of the inhibition (Figure 20, A). Control experiments were therefore conducted to verify the presence of the captured inhibition (B).

A control mixture of iAP assay components was prepared and introduced to the system along with heat-inactivated iAP (compare chapter 4.4.3.). During the early stages of the experiment up to approximately 10 minutes, the ratio between ATP, ADP and AMP intensities is similar for the assay and the control mixture. The clear negative peak apparent for all traces at 13 to 15 minutes after injection of VS PF water extract can be found in both experiments (A & B) and is due to the elution of non- or barely retained polar extract compounds. In contrast to the control, injection of PF extract has a distinct effect on the subsequent course of iAP assay measurement, with the assay trace intensities of ADP and AMP remaining at a distinctly lower level (A) compared to the control (B). Compounds eluting during the time point of regulation are comparable within control and assay, with the control however not showing the observed inhibition. Hence the positive substrate and negative product peak captured during iAP assay detection are very likely not due to eluting compounds interfering with mass spectrometric intensity. Consequently, iAP can be assumed to be regulated by the presence of eluting VS PF water extract compound(s), although the inhibitor could not be identified, which might e.g. be due to the molecule not being ionizable.
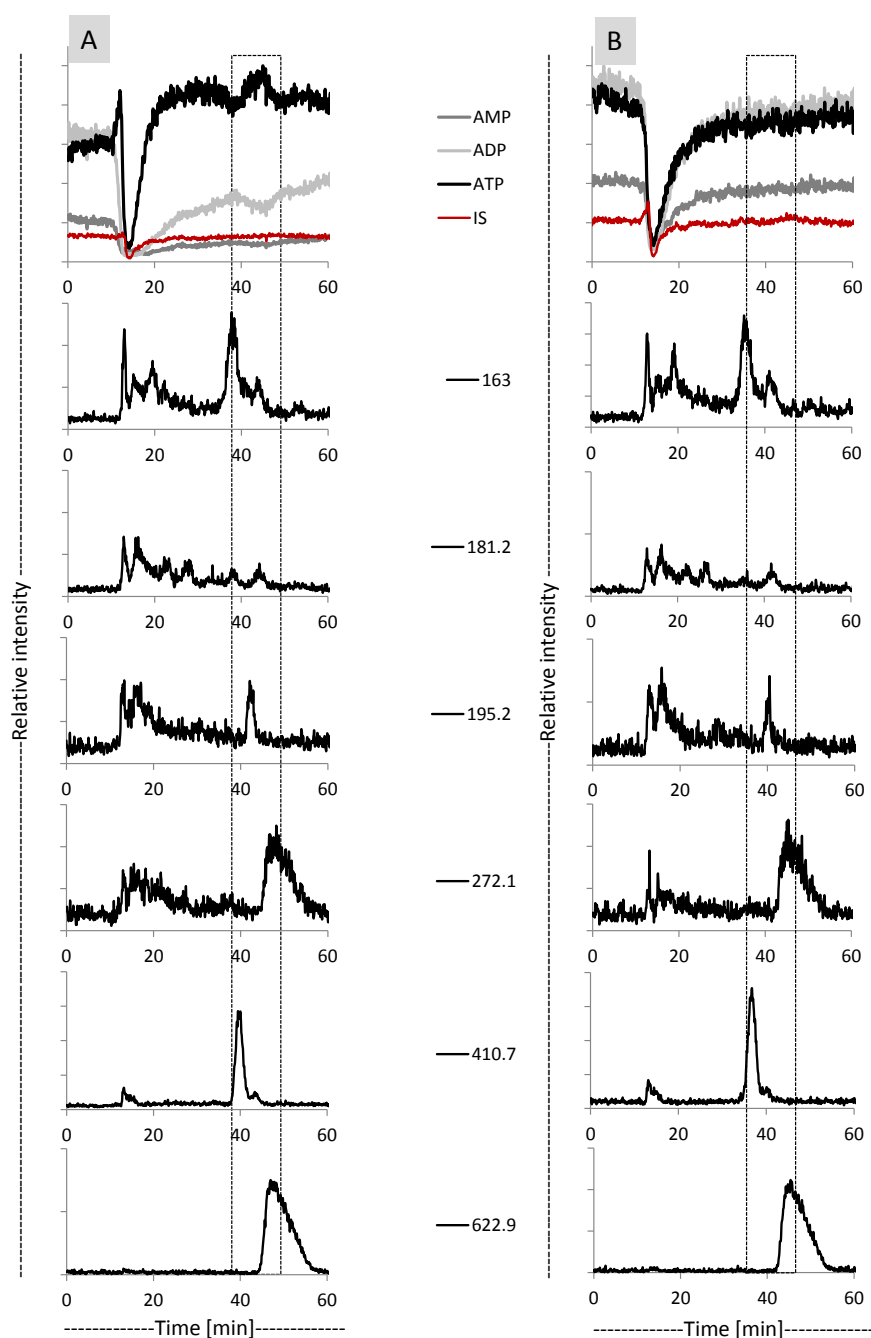
Figure 20 iAP assay (A) and control (B) measured with the online coupled continuous flow mixing system in the presence of VS PF water extract injected to the system. Assay concentrations introduced to the system were as follows 2.4 U/ml and 40 µM ATP substrate, whereas control measurements were performed using a mixture of iAP assay components (compare chapter 4.4.3.). PF extract is injected to both the assay and control measurement and is chromatographically separated using an isocratic elution with 5% MeOH and a temperature gradient up to 70°C. EICs of compounds eluting in the time range of regulation are displayed for iAP assay as well as control. Adenosine product trace was detected with minor intensity and is therefore not displayed.

Whereas iAP revealed a regulation after the injection of VS PF water extract, XOD assay was detected with an inhibition in the presence of chromatographically separated 90% MeOH, 0.5% FAc PF extract and a mobile phase organic solvent content of 5% IPA at approximately 18 minutes after extract injection (Figure 22, A & Appendix IV, Figure 5). The comparative assessment of PF extract chromatographic separation with 5% IPA revealed only a minor quantity of eluting compounds after the injection of water extract (Figure 21, A) or 50% EtOH extract (C) in comparison to 90% MeOH, 0.5% FAc extract (B) during the time range of XOD regulation.
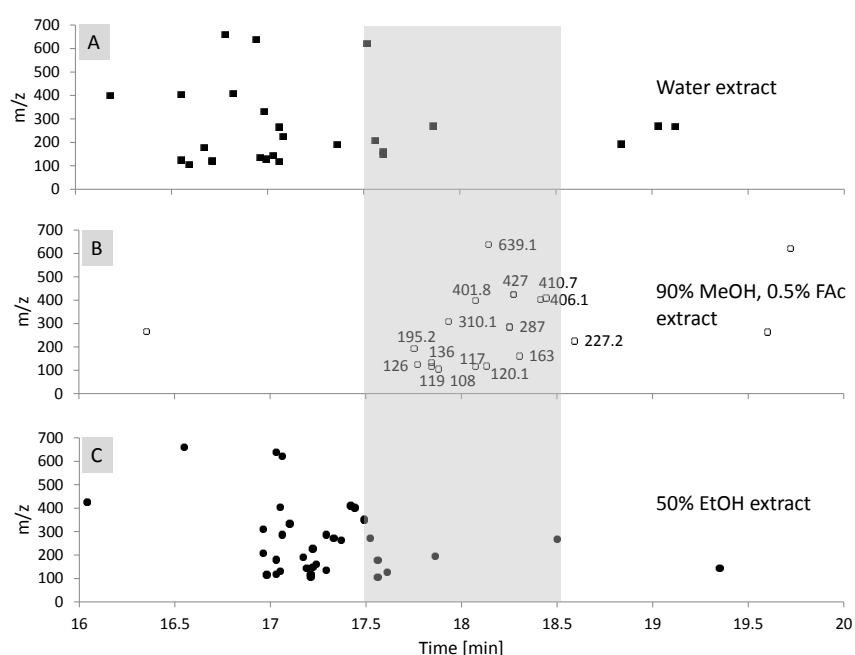
Figure 21 Elution of compounds in the time range of XOD inhibition between minute 17.5 and 18.5 (grey box) after injection of water (A), 90% MeOH, 0.5% FAc (B) or 50% EtOH extract (C) using a mobile phase containing 5% IPA and a temperature gradient up to 70°C.

Potential regulators could be limited to only a few, which possessed a retention time and peak shape similar to the observed inhibition (Appendix IV, Figure 6). An inhibitory activity of PF towards XOD has already been reported by Nakanishi et al. and Huo et al. [244, 264]. However, none of the therein mentioned compounds could be assigned to the here measured effect. This might be an indication for the finding of a new regulator with the applied setup. To verify the results, control measurements were conducted, which included a blank solvent injection (Figure 22, B). Neither the m/z´s eluting within the time range of

enzymatic regulation (Figure 21) nor an increase of substrate or a decrease of product signal were detected within the relevant time range. The control thus allowed ruling out the possibility of the observed regulation being due to the presence of the organic solvent or due to solvent impurities.
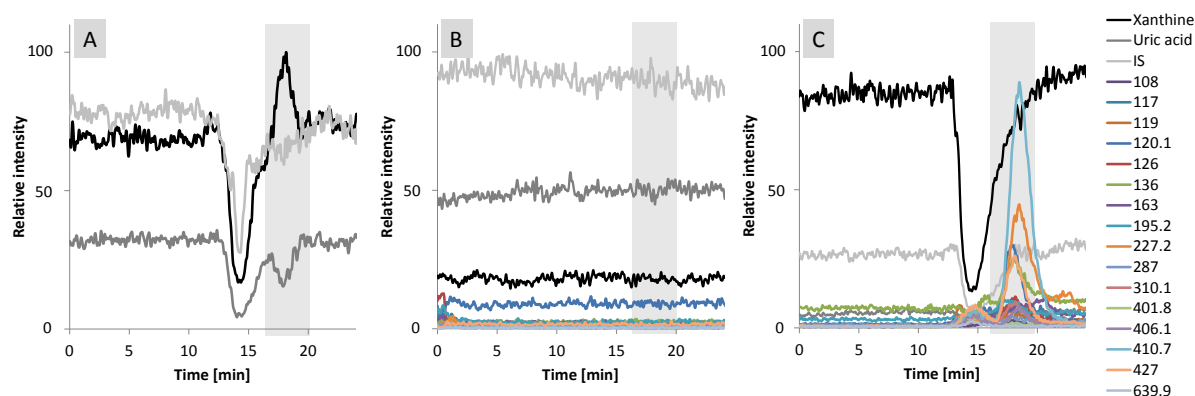
Figure 22 Online coupled continuous flow mixing system employed for the detection of XOD assay (A) and control measurements (B, C). Injection of 90% MeOH, 0.5% FAc PF extract to XOD assay. Chromatographic separation was conducted with a mobile phase of 5% IPA:95% 10 mM NH_4Ac pH 7.4 (v/v) and the application of a temperature gradient (A). Control measurement included the injection of 100% EtOH to XOD assay (B) or the introduction of 90% MeOH, 0.5% FAc PF extract to the system using solely xanthine substrate and no XOD (C).

An additional control was measured with solely xanthine substrate and chromatographically separated 90% MeOH, 0.5% FAc PF extract (Figure 22, C). By means of this measurement, the effect of eluting compounds on the substrate trace could be determined in order to exclude the possibility of an extract molecule with the same m/z as the substrate to be responsible for the observed positive peak signal. However both control measurements were found with no response to the presence of the extract, which confirms the finding of a XOD regulation.

4.5.   Conclusion - Enzymatic assays and Perilla frutescens extracts

The previous chapters comprehensively described the effect of PF extracts on the activity of the enzymes GST, iAP and XOD (Figure 12 A & B, Figure 20, Figure 22). In this regard the regulation of XOD can assumed to be of special interest, due to its involvement in several adverse health conditions. Excessive generation of its product uric acid causes hyperuricemia and gout. Moreover high levels of uric acid are extensively discussed as risk factors for hypertension and cardiovascular diseases amongst others [265, 266]. XOD was also

determined as source of oxidative stress due to the release of superoxide during (hypo-) xanthine degradation [267]. Due to its multiple roles in health and disease efforts have been made into the finding of natural substances able to suppress its activity [268, 269]. PF may therefore possess potential for the treatment of uric acid as well as superoxide associated diseases without the often adverse side effects of chemically synthesized medicinal drugs. Nevertheless severe pathological diseases like cancer unquestionably require the administration of drugs within the context of chemotherapeutical treatments. The utilization of those xenobiotic substances however triggers the action of enzymes involved in biotransformation processes including phase II GSTs. This family of enzymes is able to convert hydrophobic drugs to more hydrophilic derivates by conjugation to GSH, which results in the substances inactivation and facilitated elimination. This usually favored defense mechanism against potentially harmful chemicals may however lead to the premature clearance of administered drugs, which results in them being barely or non-effective towards the e.g. cancer afflicted target location [270]. Overexpression of GST in cancer cells is discussed to be related to decreased drug sensitivity due to an enhanced conversion and removal of the therapeutics [271, 272]. Besides targeting the regulation of GST on gene expression level, the finding of inhibitory substances might provide solutions for overcoming drug resistance [273].

A link between gene expression and cancer may also be existing for iAP. Some indications were found, which allow the conclusion of a tentative connection of its transcription to the tumorigenicity of HeLa x fibroblast cell hybrids [274]. A cancer-associated regulation has also been reported for further enzymes of the alkaline phosphatase type, including placenta AP and germ cell AP, which are closely related to iAP [275]. Besides its potential role in tumorigenesis, an enhanced presence of an intestinal AP variant has been found in patient with liver cirrhosis and diabetes mellitus [276]. However the significance of APs connection with pathological conditions and their contribution to the development and progression remains to be clarified.

iAPs multiple physiological functions have been unveiled during the last couple of decades. Its activity is linked to a variety of important regulatory processes, like the dephosphorylation and thus detoxification of bacterial LPS or the regulation of intestinal pH via the pH-dependent degradation of ATP [37, 39, 50, 277]. Its susceptibility to the inhibition

by natural substances like GSH [278] or L-phenylalanin [218, 279] may however imply a physiological relevance of iAP suppression, which has yet to be elucidated.

The inhibitory potential of PF extracts of the activity of XOD, GST and iAP could be investigated by means of the employed analytical methods. The detailed adaption and development of assays as well as the establishment of a chromatographic separation and the implementation of suitable controls were successfully conducted in order to comprehensively and critically investigate the activity of enzymatic assays with and without the addition of PF.

4.6.   Biomolecular assay development

In the following, the effect of PF extracts on the physiology of the porcine jejunal epithelial cell line IPEC-J2 was assessed. PF extracts were prepared with various organic solvents or solvent proportions, respectively, which results in distinct differences regarding their molecular composition, polarity of contained compounds (Figure 14) and total reducing potential (Appendix V, Figure 1). Thus their application in cell tissue experiments provides insight in terms of the most effective "polarity fraction". Experiments were conducted using electric cell-substrate impedance sensing (ECIS), which allows the observation of kinetics of adherent cells. By means of electrodes on the bottom of each well, AC impedance alterations, which result from the overgrowing of the electrodes by the cells, are captured (Figure 23). The cell proliferation can be measured continuously and in real-time in a non-invasive and label-free manner. The detection is reliable and the experimental preparation is easy and less time-consuming compared to manual counting or photometric determination of cell numbers.

Depending on the respective aspect to be investigated, cells are seeded either in a low or high density. By starting with a high cell number e.g. to obtain a confluent cell layer, the initial impedance signal is highest due to entirely covered electrodes. This approach is widely used for the assessment of cytotoxic effects of drugs or other substances, as it has been done by Pradhan et al. [280, 281] or Mueller at al. [131], who administered an anticancer drug on a breast cancer line or the compound 1,8-cineole, a common odorant, on the porcine jejunal epithelial cell line IPEC-J2, respectively. A low cell count may however be used in order to obtain a low impedance signal at the beginning of the measurement, which

allows to follow the slow overgrowing of the electrodes. In this regard, Masanetz et al. investigated the effect of different pine pollen extracts on the cell proliferation of a porcine ileal epithelial cell line (IPI-21) [105]. Hence, this approach is most suitable for the assessment of changes in cell proliferation after the application of a substance or a complex mixture [282-284].
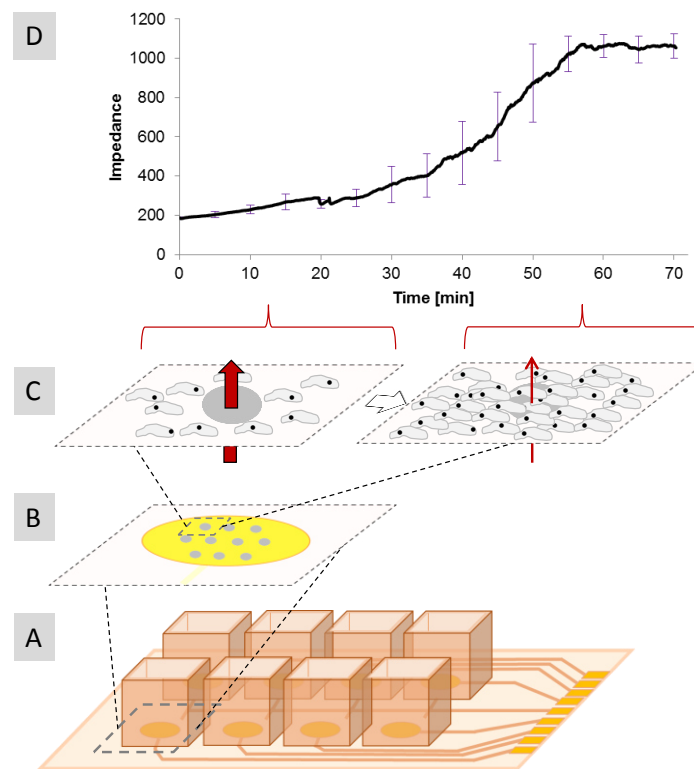
Figure 23 A: Scheme of ECIS slide with 8 wells. B: Electrodes on the bottom of each well, which C: detect the impedance alterations caused by cells gradually overgrowing the well bottom surface. D: The signal is displayed as continuous increase of impedance over time.

Apart from assessing the cell proliferation in the presence of PF extracts, a panel of genes involved in cell cycle progression and apoptosis and if misregulated in cancer development processes, was investigated to hint at prospective health-relevant areas of application for PF (Figure 24). Additionally cell toxicity of PF extracts was assessed by means of lactate-dehydrogenase (LDH) release. Comprehensive control experiments were established to address artificial effects arising with the conduction of *in vitro* cell culture experiments (Figure 24). Since various studies discuss not just the antioxidant, but also the *in vitro* and *in vivo* prooxidant activity of polyphenols, additional experiments were performed to capture a

potential generation of ROS and H_2O_2. In the presence of cell culture media constituents like transition metal ions, natural compounds are prone to degradation [285, 286]. The stability of PF extract under the applied experimental conditions was therefore investigated using a HILIC-RPLC coupling with MS detection [195, 249].
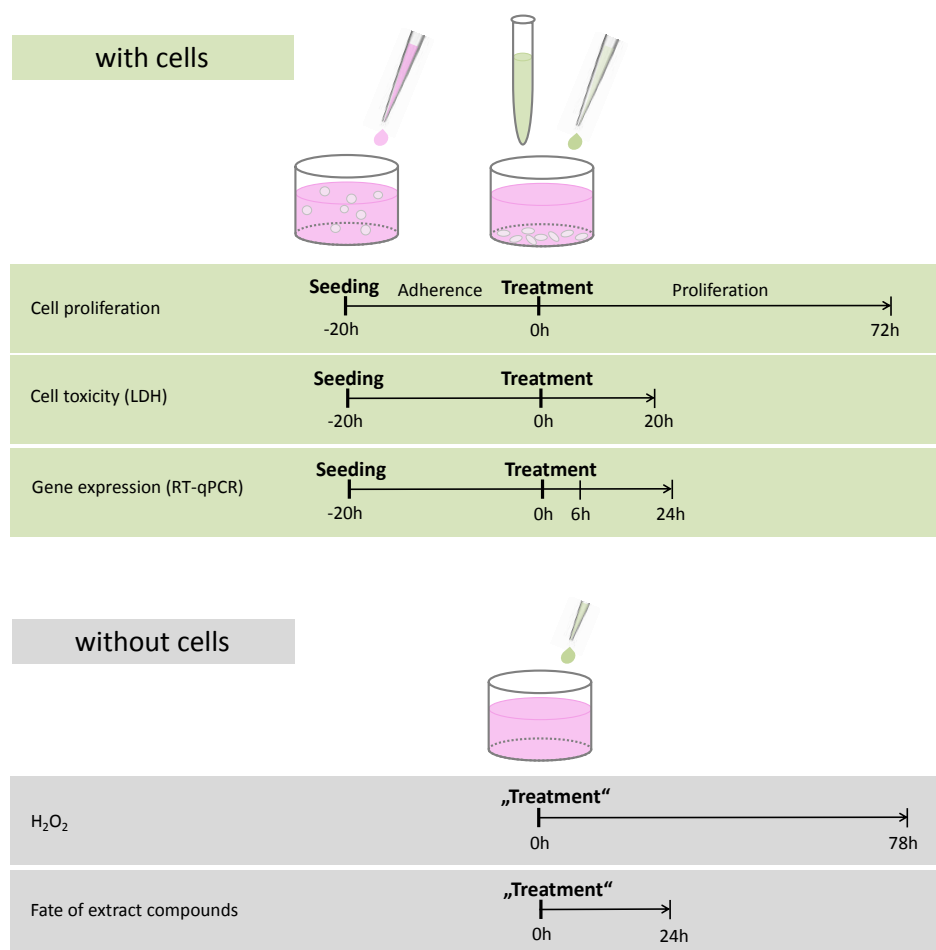
Figure 24 Assessment of cell proliferation in the presence of PF extracts and determination of cell toxicity (green) were performed with an initial cell concentration of 10 000 cells/well. Initial cell concentration for gene expression detection was 40 000 cells/well (green). Treatment with PF extracts was performed 20 h after seeding of cells for all experiments. Control measurements (grey) included the assessment of H_2O_2 generation in the presence of PF extract as well as the determination of PF compound stability in cell culture medium. Controls were conducted without cells.

4.6.1. Determination of cell proliferation

A suitable time point for the treatment of cells was determined by measuring the increase of impedance of untreated control cells (Figure 25, A, solid line) and simultaneously assessing the total cell number by manual counting using a Neubauer cell chamber (Figure 25, B). This

approach enabled the correlation of cell quantity with the impedance signal detected with ECIS. The initial slight increase of impedance (A) was found to be due to the adhesion of cells, which started proliferating only after approximately 25 hours (B). Comparable results were found by Mueller et al., who determined a cell settlement period of about 20 hours accompanied by an increase of impedance with the non-transformed porcine ileal epithelial cell line IPI-21 [287]. Hence cells were treated 20 hours after seeding to allow for a complete adherence and recovery.
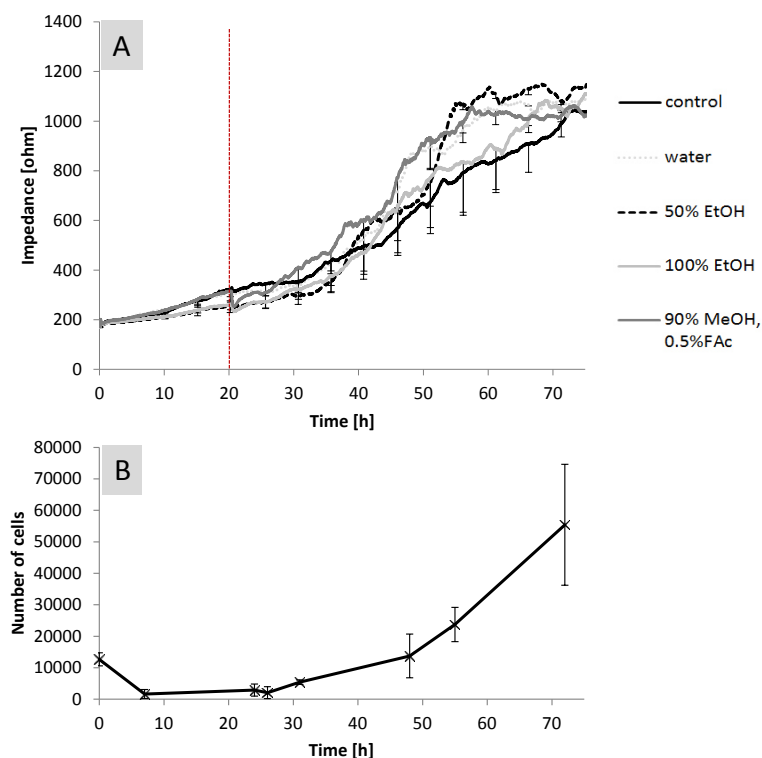
Figure 25 A: Cell proliferation in the presence of "control extracts" compared to an untreated control detected with ECIS. Time point of cell treatment is marked 20 h after seeding (red dashed line). For the treatment 1% of the total assay volume (= 400 µL) were replaced by "control extract" (= 4 µL), i.e. water, 50% EtOH, 100% EtOH or 90% MeOH, 0.5% FAc. In comparison a control was measured containing pure cell culture medium. B: Cell counting was done using a Neubauer cell chamber at defined time points. For this purpose cells were prepared in pure cell culture medium. In either case, standard deviation is calculated out of n=3.

Due to PF extracts being redissolved in water, 50% EtOH or 100% EtOH (Table 1, Method 2), respectively, a possible effect of the solvents on the cells was investigated by means of applying control extracts, which were prepared like PF extracts but without the addition of

PF matter (Appendix V). No significant effect of the solvents on the cell proliferation in comparison to cells in pure cell culture medium was detected (Figure 25, A).

In the following PF extract concentrations applied to the cells were chosen as to mimic physiological relevant quantities of 1 % to 10 % PF proportion of a whole meal (Figure 3). Decreasing concentrations of VS PF water extract, ranging from "4.0 mg" (≙ 10% of total food intake) to "0.4 mg" (≙ 1% of total food intake), were administered to the cells (Appendix V, Figure 2, A). The treatment revealed a pronounced effect at PF quantities above "1.0 mg", which was reflected by an immediate drop of the impedance signal after treatment (Appendix V, Figure 2, A). A low physiological quantity of "0.4 mg" was therefore used for all further measurements (Figure 26).
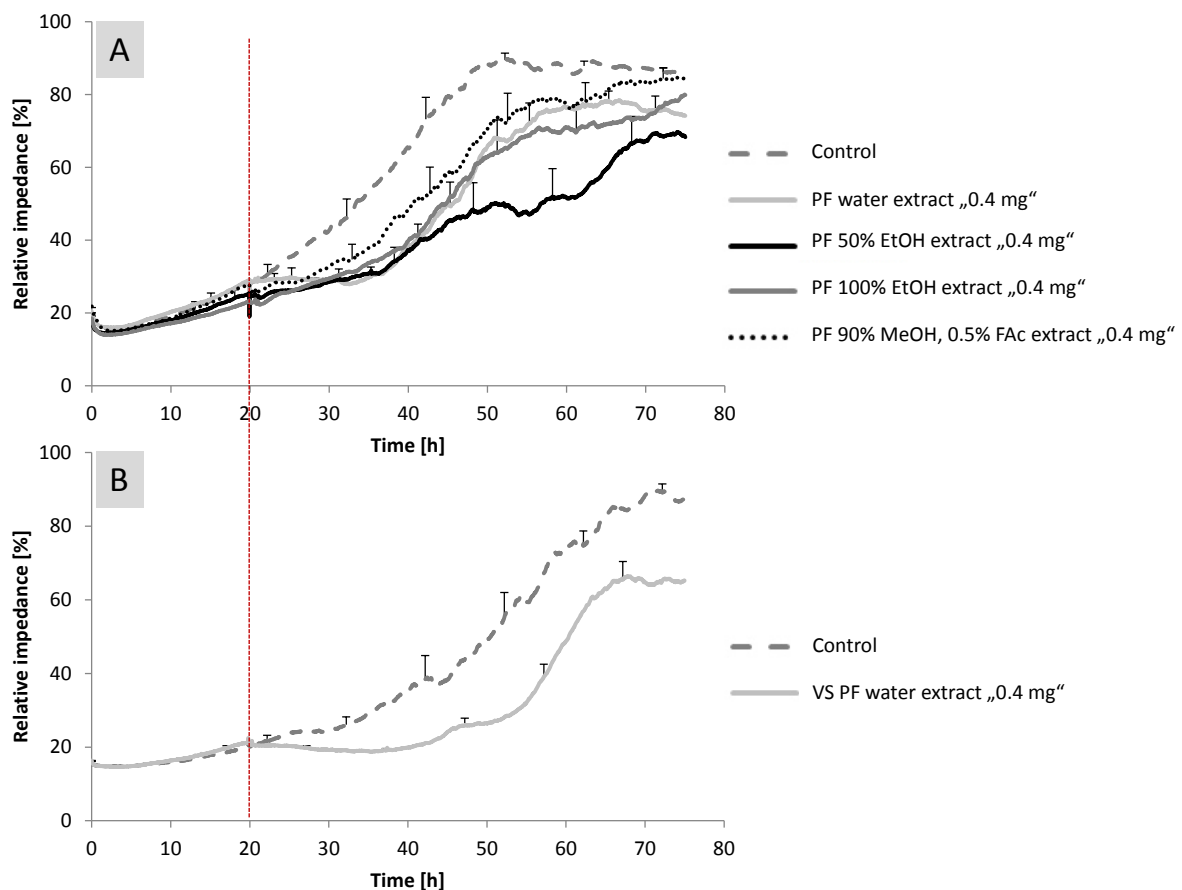
Figure 26 Assessment of cell proliferation after treatment with "0.4 mg" PF extracts. Time point of PF application at 20 h after seeding is marked (red dashed line). Positive SEM is displayed and was calculated out of n=9 for treatment and n=12 for untreated control measurements with pure cell culture medium (A) and n=8 for treatment with VS PF water extract and respective untreated controls in pure cell culture medium (B).

All PF extracts caused an inhibition of cell proliferation within few hours after treatment, which is reflected by the delayed increase of impedance signal (Figure 26) as well as by an immediate decrease of calculated p-values (Appendix V, Figure 3) compared to the control. VS PF water, self-made water and 50% EtOH extracts caused a long-term significant cell growth suppression, which correlates with the extent of their observed total reducing capacity (Appendix V, Figure 1). Nevertheless the results may be considered inconclusive, since the delayed increase of impedance can either be attributed to an actual suppression of cell proliferation or to apoptotic events occurring to a proportion of the cells. The latter event may reduce the number of cells to a point at which enough would still remain to slowly overgrow the electrodes, thus mimicking cell growth inhibition. Therefore potential cytotoxic effects of "0.4 mg" PF extracts were assessed by means of measuring the release of lactate dehydrogenase (LDH) from the cells after treatment with "0.4 mg" PF extracts, which would be associated with cells undergoing apoptosis (Figure 27).
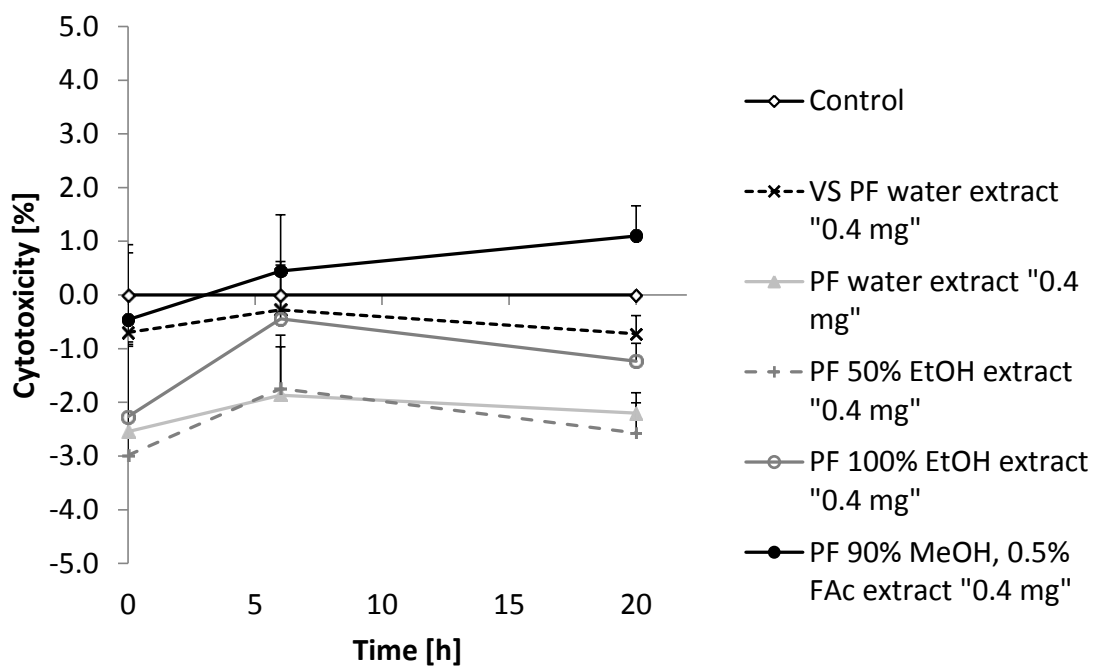
Figure 27 Determination of LDH release after treatment of cells with "0.4 mg" PF extracts 20 h after seeding (= 0 h). Time points of LDH detection were 0 h, 6 h and 20 h after PF application. Standard deviation is given and was calculated out of n=3. Percentage of cytotoxicity was calculated according to the manufacturer guidelines.

Compared to the untreated control no distinct release of LDH at time point 0 h, 6 h and 20 h after treatment could be detected. This finding supports the conclusion of an actual inhibitory effect of PF extracts on the cell proliferation (Figure 26) rather than apoptosis.

4.6.2. Determination of gene expression

The results obtained with the detection of cell proliferation were furthermore verified by measuring the expression of a panel of genes involved in cell cycle and apoptosis (Figure 28, blue boxes). They are part of a wide network with the tumor suppressor p53 as key regulator of cell cycle progression. p53 is able to induce cell growth arrest by means of cyclin B1 and D1 suppression as well as by controlling cyclin-dependent kinase (CDK) inhibitor p21 [288]. It furthermore regulates pro-apoptotic proteins of the Bcl-2 family, leading to cytochrome c release from mitochondria, which eventually induces caspase 9 and thus apoptosis [289]. The absence or impairment of p53 regulatory functions result in the development and progression of cancer [290].

In contrast, an important gene product required for cell cycle progression is c-jun, whose influence on cell proliferation includes the induction of cyclin D1 transcription as well as the suppression of anti-proliferative tumor suppressor p53 [291, 292]. Cyclin D1 in association with CDK4 and 6 promotes G1 phase progression as well as the transition to the S phase of the cell cycle. Cyclin B1, after forming a complex with CDK1, also plays a crucial role in the control of cell cycle progression and is predominantly expressed throughout G2 phase and mitosis [293].

Additionally the regulation of 67kDa laminin receptor (67LR) was determined. In normal cells this cell-surface receptor has crucial functions in cell adhesion and signal transduction, but has moreover been observed to be involved in pathological conditions like cancer or prion disease [294].
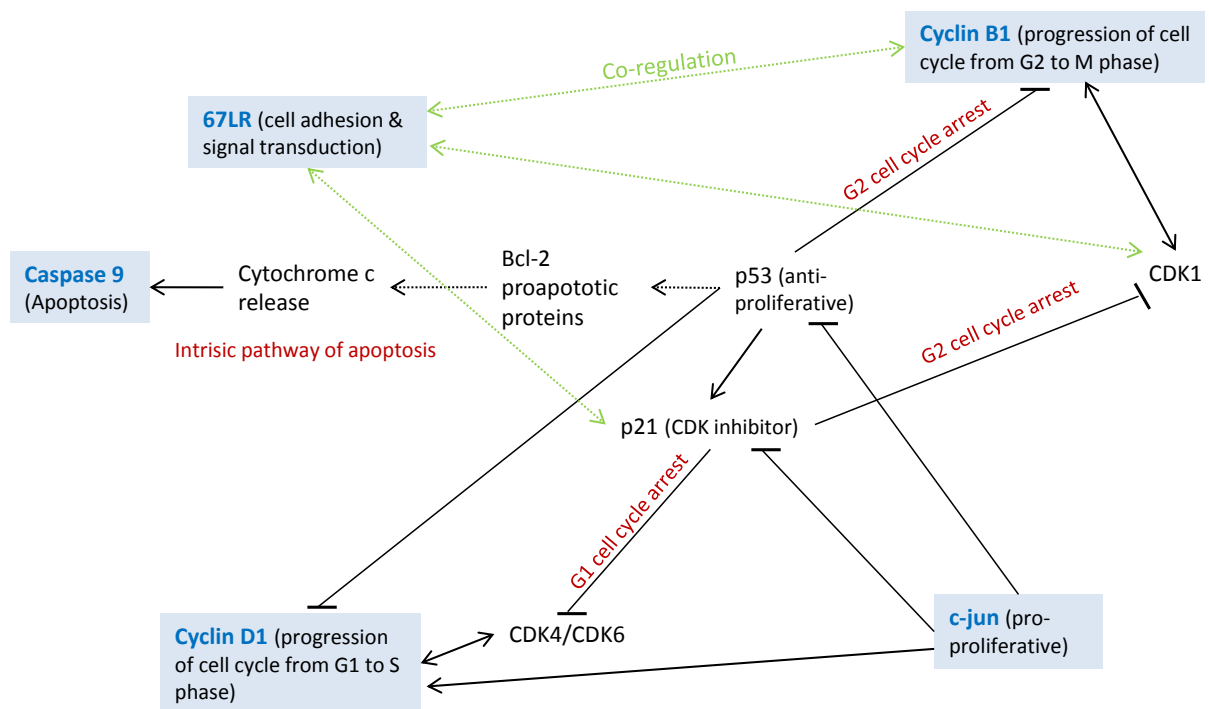
Figure 28 Panel of genes, whose expression was determined after the application of "0.4mg" PF extracts (blue boxes), embedded into a regulative network [288, 292, 295-304]

The expression of target genes was determined at 0, 6 at 24h after PF extract application to a confluent cell layer of IPEC-J2 cells. Caspase 9 was found to be non-regulated at all time points, which supports the findings obtained by LDH cytotoxicity assessment of PF being non-toxic to the cells (Figure 27). Cell cycle regulator genes cyclin D1, B1 and c-jun were detected to be downregulated (Appendix V, Figure 4) with cyclin D1 revealing an immediate response to the presence of PF extract at time point 0. In contrast downregulation of cyclin B1 became only apparent at time point 6h and 24h.

Several studies observed an inhibition of cancer cell proliferation in the presence of PF extract [110, 186, 305] or by PF compounds like RA [116], luteolin [118, 306], triterpene acids [307] and apigenin [308]. Since cyclin B1, D1 and c-jun expression has been reported to be increased in tumor cells [309-311], the capability of PF extract to downregulate those genes may be considered promising in the alleviation of cancerogenesis.

Furthermore, expression of 67LR was assessed. 67LR was detected to be downregulated by PF extracts at time point 0, 6 and 24 h, with PF 50% EtOH extract showing the most consistent effect (Appendix V, Figure 4). A connection between reduced 67LR expression and

cell cycle arrest has also been observed by Scheiman et al. [303]. The receptor gained particular interest due to its widely discussed association with cancer development and progression [312, 313], tumor-cell migration [314, 315] and angiogenesis [316]. Beyond that 67LR is involved in several pathological conditions by serving as cell-surface receptor for prions and various viruses [317, 318].

Although the observed suppression of genes was found to be not consistent with regard to the time points or the PF extract used (Appendix V, Figure 4), the results are in general agreement with the inhibition of IPEC-J2 cell proliferation after application of PF extracts (Figure 26).

4.6.3. Determination of H_2O_2 generation in cell culture medium

In vitro studies of cell lines in the presence of promising natural compounds and extracts is a common means to assess their effects on cells [102, 105]. However it has been found that significant quantities of H_2O_2 may be generated in cell culture [319], often due to high non-physiological partial oxygen pressure. The presence of moderate H_2O_2 concentrations has been found to result in cells undergoing apoptosis and to cause necrosis at more elevated levels [320]. However apart from being toxic, effects of H_2O_2 on cell physiology are wide ranging and often opposing. It may exert its effect on cells on many different levels, ranging from cytotoxicity [321-323] to the stimulation or inhibition of cell growth [324-327], to alterations of gene expression [328-330]. Studies applying H_2O_2 to cells to evaluate its effects however found distinctly different concentrations to result in the observed effects [324, 331, 332].

A major concern when dealing with H_2O_2 generation is its involvement in the formation of ROS. The oxidation of Fe(II) to Fe(III) via Fenton reaction is accompanied by the generation of highly reactive hydroxyl radicals formed from H_2O_2. Those are known to cause cell damage e.g. by means of lipid peroxidation [333]. Laughton et al. reported the generation of hydroxyl radicals from H_2O_2 [334]. They also found indications for superoxide released through oxidation of flavonoids, which can then contribute to the reduction of Fe(III) to Fe(II) via Haber-Weiss reaction [335], which again catalyzes the generation of hydroxyl radicals. Several publications are available, which discuss experimental findings in this context, often coming to the conclusion that the published effects in studies dealing with effects of natural

substances on cell physiology might not be due to the substance or extract applied, but rather due to H_2O_2 or ROS generation [336]. Halliwell et al. provide a comprehensive overview, which clearly summarizes the problematic nature of disregarding the matter of H_2O_2 generation by listing a distinct quantity of studies, which might have unknowingly encountered this issue [286, 337]. Promising *in vitro* results obtained in the presence of (natural) compounds like e.g. the widely investigated epigallocatechin gallate (EGCG) appear in a new light and are critically discussed accordingly [338]. Nakagawa et al. attribute the regulation of caspase-3 gene expression as well as the finding of apoptotic cell death in the presence of EGCG to H_2O_2 and ROS formation [339]. But also other compounds like catechin, quercetin, gallic acid and many more have been proven to form significant levels of H_2O_2 in cell culture [285, 319].

However, neither LDH release (Figure 27) nor regulation of caspase 9 gene expression were detected after treatment of IPEC-J2 cells with low physiological PF extract concentration of "0.4 mg", which is consistent with the here detected absence of distinct H_2O_2 generation (Appendix V, Figure 2 B). In contrast PF extract addition of "2.0 mg" resulted in a pronounced quantity of H_2O_2 up to ~130 µM with a steep initial increase during the first 24 hours of experiment. Cai et al. challenged the here employed cell line IPEC-J2 with increasing H_2O_2 concentrations and determined only low suppressive effects on cell viability of less than 10% below 500 µM H_2O_2 compared to up to 40% suppression beyond approximately 4 mM H_2O_2. However, in contrast to the experiments conducted here, they used a distinctly higher cell density, resulting in a confluent layer of cells, which for one thing might possess an improved resistance and for another thing results in an overall lower H_2O_2 exposure per cell [141]. In contrast other researchers observed apoptosis related DNA fragmentation after treatment of another cell line with merely 100 µM H_2O_2 [332]. Hence considering previous experimental findings regarding the effect of H_2O_2 on cells, the here detected concentration can be assumed to be at least partly responsible for the decreased cell proliferation detected with "2.0 mg" (Appendix V, Figure 2).

The application of higher VS PF water extract quantities (Appendix V, Figure 2A) is probably even more likely to cause H_2O_2 formation beyond the determined level. Consequently the determination of H_2O_2 formation is crucial for the validation of *in vitro* cell culture experiments. Its formation in cell culture is often related to oxidation and thus degradation

of extract compounds. However some compounds have been found to be unstable under *in vitro* conditions without generating significant H_2O_2 levels [285]. The absence of detectable H_2O_2 with "0.4 mg" PF extract is therefore not necessarily associated with the absence of natural compound degradation, wherefore PF extract stability was also examined using a HILIC-RPLC chromatographic separation (Appendix V, Table 2) [195, 249].

4.6.4. Determination of Perilla frutescens compound stability

The assessment of cell proliferation after treatment revealed an immediate effect on the cells for all PF extracts, which is reflected by the drop of p-values (Appendix V, Figure 3). The most pronounced and long-lasting significant effect was captured with "0.4 mg" VS PF water extract (Appendix V, Figure 3 A). The stability of PF in cell culture medium was therefore exemplarily assessed by the detection of the molecular composition of VS PF water extract at time points 0, 1, 2, 6 and 24h in comparison to control samples of extract prepared in water (Appendix V, Table 2). A variety of different molecules could be found in the employed extract based on previous findings of Buchwald-Werner et al., who analyzed the same PF material [163]. In addition to this, the development of a chromatographic separation discussed in a previous publication, allowed the tentative identification of further compounds based on their logD vs. retention time behavior (Appendix IV, Figure 3). In the following the stability of those known and tentatively identified PF compounds, i.e. RA or apigenin and luteolin as well as their O- or C- glucuronide or glucoside conjugates (Appendix V, Table 2 A-C & Figure 29), was investigated in order to draw conclusions on their potential to affect the physiology of IPEC-J2 cells. In comparison to PF extract controls prepared in water, which showed a stable abundance of all compounds within 24 h, in cell culture medium most of the compounds were found with decreasing abundance over time (Appendix V, Table 2 & Figure 29).
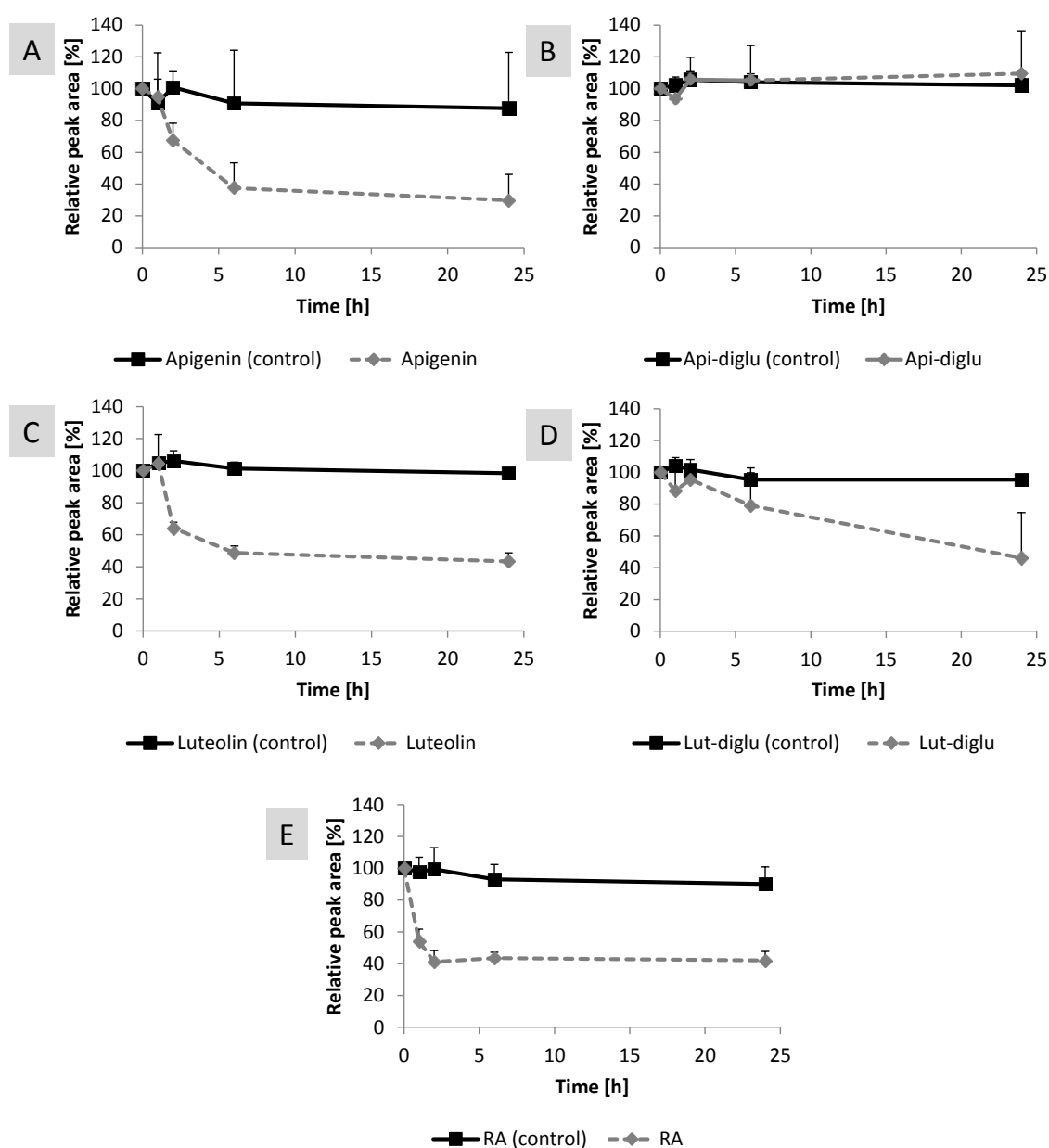
Figure 29 Stability of VS PF water extract compounds in the absence of cells either solved in cell culture medium (dashed grey) or water (bold black) as control at time points 0, 1, 2, 6 and 24 h. For clarity reasons, only positive standard deviations are given, which were calculated out of n=3. Diglu = diglucuronide moiety.

Apigenin has been demonstrated to be readily oxidized to form a reactive phenoxyl radical, but only in the presence of H_2O_2 or xanthine oxidase [340-342]. In contrast to the here captured distinct decrease of apigenin abundance (Appendix V, Table 2 A & Figure 29), Long et al. detected only a slight degradation in pure cell culture medium within the same time period [285]. However, they measured the stability of individual substances as opposed to

83

the mixture of a plethora of different compounds contained in PF extract. Those may chemically react with one another or with cell culture medium components, thus forming undesired decomposition products like e.g. H_2O_2 [336, 343-345]. This effect might furthermore be enhanced due to the here conducted experimental procedure, which included several purification and dilution steps prior to LC-MS analysis. The required quantity of VS PF water extract solved in cell culture medium was therefore increased compared to cell proliferation and gene expression experiments. Consequently, the generation of distinct quantities of H_2O_2 can be assumed. In the presence of transition metal ions H_2O_2 would be converted to hydroxyl radical, thus enhancing oxidation processes and therewith the degradation of PF extract compounds. Those aspects likely contribute to the degradation of apigenin with the here applied experimental conditions (Appendix V, Table 2). In contrast to apigenin and luteolin -the latter also revealing a fast degradation- their conjugates were detected with enhanced stability, which is especially apparent for apigenin 7-O-glycosides and 7-O-(di)glucuronides (Appendix V, Table 2 A & Figure 29 B). This would imply the involvement of the C7-OH group in the instability of non-conjugated apigenin and luteolin in cell culture medium. Musialik et al. determined the highest OH-acidity for C7-OH in polar organic solvents. This in turn may result in a deprotonation of the group and the formation of a phenolate anion, which was detected to readily react with radicals [346]. However C-conjugated apigenin, in which C7-OH is not blocked, was still detected to be stable during the experimental time range, which might be attributed to steric effects. In contrast the here observed O-conjugated luteolins were found to degrade over time. The presence of the B-ring catechol moiety might therefore contribute to their susceptibility to degradation compared to O-conjugated apigenin, which merely contains one OH-group in its B-ring (Appendix V, Table 2 A & B). In fact, O-substitution with glycosides or glucuronides was reported to stabilize flavonoids by Zenkevich et al. and Shirai et al., since it blocks OH-groups involved in antioxidant as well as pro-oxidant activities [347, 348]. Nevertheless, further mechanisms seem to be crucial for the stability of conjugated flavonoids.

Comparable to findings of Long et al., RA is rapidly degraded. Of all the compounds observed, it was found to be the most prone to decomposition in cell culture medium (Figure 29, E). Two catechol groups within its structure most likely result in the generation of two quinone moieties [349]. RA was furthermore reported to produce H_2O_2 and superoxide

[285, 350] and an iron catalyzed oxidation of RA was captured by Fujimoto et al., however in EtOH solution [349]. Some studies discuss the issue of a heightened oxygen partial pressure present in *in vitro* experiments as one of the main problems causing polyphenol oxidation and generation of H_2O_2 [351, 352]. However conducted control measurements, in which PF extract was solved in water, but otherwise treated like PF extract samples in cell culture medium, revealed no decrease of compounds within 24 h (Figure 29, A-D, bold black line). Although the presence of a non-physiological high oxygen concentration might contribute to the degradation of PF extract, it may only destabilize the compounds in combination with cell culture media. Components like metal catalyst are however more likely to impair PF extracts compound stability. In this regard, iron or copper ions, which are essential components of cell culture media, catalyze the generation of ROS via Haber-Weiss and Fenton reaction [334, 335, 353]. Jungbluth et al. proposed the degradation of flavonols in aqueous media in the context of a metal-catalyzed oxidation by Cu(II), Fe(II) or Fe(III) [354]. The possibility of flavonoid autooxidation was also described, whereupon phenoxyl radicals are generated [355, 356], which react with oxygen to form quinone products and superoxide in the presence of transition metals [334, 357]. In contrast flavonoids have also been observed to be able to chelate transition metals to form flavonoid-metal complexes at physiological pH, in this regard preventing metal catalyzed reactions [358-360]. The formation of those complexes is favored e.g. by a catechol moiety in the B-ring, as it is present in the structure of luteolin and rosmarinic acid [361, 362]. Metal-flavonoid complexes were even found to possess an enhanced superoxide scavenging activity compared to the parent flavonoid, in this manner e.g. exerting increased cytoprotective effects [363].

Beyond that, most wholesome properties ascribed to flavonoids are connected with their antioxidant activity. Their capability to capture ROS was found to be especially pronounced in the presence of some structural features, like a catechol moiety in the B-ring, a C3 and C5 hydroxyl substitution, a double bond between C2 and C3 and a C4 keto group [361, 364]. Luteolin and apigenin possess the latter three structural features, whereas only luteolin has a catechol moiety in the B-ring. However the processes causing a fast degradation of PF extract compounds in cell culture medium are apparently outbalancing their capability to scavenge ROS or chelate metal ions in the employed experimental setup. Consequently the

detected loss of flavonoid abundance would result in the generation of degradation products. In this regard Kern et al. detected the appearance of small phenolic acid degradation products like gallic acid after the rapid decrease of anthocyanidines in cell culture. Since gallic acid itself has been reported to inhibit cancer cell proliferation *in vitro* and *in vivo*, its generation will likely result in data misinterpretation [345, 365-367]. Oxidation mechanisms of flavonoids and the related generation of products were proposed by Zenkevich et al. and Jorgensen et al. by means of quercetin [348, 368]. Zhou et al. tentatively identified further oxidation products of quercetin, which included taxifolin, low molecular weight compounds and dimers. They moreover proposed the respective degradation pathways [369]. Dimerization, hydroxylation and the increase of decomposition products were also found by Sang et al. [343, 344], Zenkevich et al. [348] and Ramesova et al. [351] for EGCG, quercetin and luteolin. Furthermore adjacent hydroxyl-groups, as present in catechol type flavonoids like luteolin, facilitate a fast degradation via the formation of potentially harmful quinones and semiquinones [285, 368, 370-372]. With regard to the described literature, MS data was assessed for newly generated compounds (Appendix V, Table 2). Although some m/z were found to increase over time, they couldn´t be assigned to oxidation products discussed in the studies above. However, polar degradation products of PF extract compounds may not be present within the sample anymore due to the SPE purification procedure employed in this study. Increasing abundances of m/z were however not limited to low molecular weight products, which are likely to occur after chemical decomposition reactions. Compounds with high m/z were also found to increase, which might be due to chemical polymerization of the PF extract compounds in cell culture medium (Appendix V, Table 2, D).

4.7.   Conclusion - Effects of Perilla frutescens on cell proliferation and gene expression

The potential of PF extracts in terms of cell proliferation inhibition has been reported. Their effects were immediate and correlated with the observed reducing potential. The results were verified by the determination of PF cytotoxicity and by the measurement of a panel of cell cycle key-regulator genes. In this regard, the absence of LDH release and the non-regulated expression of caspase 9 confirmed the suppression of cell proliferation not to be due to cell toxicity or apoptosis-inducing effects of PF. This is furthermore supported by the

downregulation of cell cycle regulator genes c-jun, cyclin C1 and cyclin B1, the latter showing an immediate decrease at time point 0h. 67LR, which is mainly discussed for its connection to cancerogenesis, was also detected to be downregulated at time points 0, 6 and 24h. Moreover, control measurements were conducted, which included the detection of H_2O_2 generation, which was found to be absent at the applied low PF quantity of "0.4 mg". The assessment of PF extract stability in cell culture medium revealed PF compounds to be partly unstable in cell culture medium, which was reflected by a decrease of their abundance over time. However, effects of VS PF water, 50% EtOH and water extract on cell proliferation and the expression of cyclin D1 and 67LR were found to be immediate, i.e. at a time point at which non-degraded compounds would still be present in the medium. Furthermore PF concentration employed for the stability study was higher due to the implementation of several sample preparation procedures and thus dilution steps. For this reason a distinct generation of H_2O_2 as well as hydroxyl radicals, which would impair the compound stabilities, can be assumed. Although an effect of PF degradation products on the experimental outcome in the latter stages of experiments cannot be ruled out, the observed immediate impact of PF on cell proliferation and gene expression at time point 0 h is due to the presence of the extract rather than oxidation products.

5. Conclusion

This study is comprised of two main experimental parts, which consequently resulted in the establishment and employment of various methods in order to explore effects of PF extracts on enzymatic activity as well as on cell physiology. The impact of PF extract on the activity of three health-related enzymes was comparatively investigated by photometric as well as MS detection. Special emphasis was placed on the enzymatic assay adaption to MS detection as well as on the conduction of suitable control measurements to verify the results. In this regard MS revealed its great potential for the observation of multiple reaction intermediates as well as for enzymatic products non-detectable with classical photometric methods. For the finding of individual enzyme-regulatory compounds from complex mixtures an online coupled continuous flow mixing setup, which connects the advantages of MS detection, the implementation of a chromatographic separation and the ability to capture enzymatic activity in one single run, was employed. Eventually an inhibition of XOD and iAP was observed in the presence of chromatographically separated PF extracts. Results were verified by means of comprehensive control experiments, which included the injection of known inhibitors and alternative substrates.

Although the employed system required an extensive process of method establishment, online coupled continuous flow mixing system may prospectively obviate the need to conduct elaborate and time-consuming extract fractionation procedures, which are commonly performed in order to isolate and identify promising compounds from complex mixtures.

Apart from the observed regulation of enzymatic activity, further studies were conducted in order to identify the regulatory potential of PF extracts on the cell physiology of a porcine jejunal epithelial cell line. It was found that cell growth and gene expression of a panel of cell cycle and cancer related genes were downregulated by PF extracts, with a good correlation to the applied extracts respective reducing potentials. Based on the possible occurrence of a variety of artificial effects, which have often been neglected in past studies, comprehensive control experiments were conducted to verify the results. This included the determination of PF extract toxicity, which was measured by means of LDH release from the cells. Moreover H_2O_2 generation in cell culture medium and the stability of individual PF extract compounds

was assessed. In this regard H_2O_2 generation and PF toxicity could be excluded to be responsible for the detected inhibition of cell proliferation and regulation of gene expression. In contrast, PF compound stability was impaired in cell culture medium, which assumingly results in the generation of unknown degradation products. Nevertheless the detected immediate effect of PF extracts on cell physiology supports the assumption of regulatory potential of PF. Future investigations may however focus on the investigation of individual PF compounds and their effects on health and disease. Since most available studies investigate well-known PF components apigenin, luteolin or rosmarinic acid, whose beneficial effects are already established, the impact of e.g. glucuronidated and glucosylated flavonoids on physiological processes has yet to be determined. Moreover a comprehensive investigation of individual compounds promising with regard to enzyme-regulatory activity is required *in vitro* as well as *in vivo*. In order to assess the probability of them reaching their specific enzymatic target, their bioavailability *in vivo* has to be examined. This is of particular importance since a variety of flavonoids have been found to be metabolized and conjugated upon intestinal resorption.

Embedded in the context of detailed method establishment procedures, the here presented results thus reveal promising properties of PF. Various aspects of MS and photometric detection for the observation of enzymatic activities as well as PF effects on cell physiology have been discussed to outline advantages, but also various drawbacks of the employed methods.

6. References

1   Dennhart, N., Fukamizo, T., Brzezinski, R., Lacombe-Harvey, M. E. and Letzel, T. (2008) Oligosaccharide hydrolysis by chitosanase enzymes monitored by real-time electrospray ionization-mass spectrometry. J Biotechnol. **134**, 253-260

2   Stachowiak, K., Wilder, C., Vestal, M. L. and Dyckes, D. F. (1988) Rapid protein sequencing by the enzyme-thermospray liquid chromatographic/mass spectrometric method. J Am Chem Soc. **110**, 1758-1765

3   Kim, H. Y., Pilosof, D., Dyckes, D. F. and Vestal, M. L. (1984) On-line peptide sequencing by enzymic hydrolysis, high performance liquid chromatography, and thermospray mass spectrometry. J Am Chem Soc. **106**, 7304-7309

4   Yu, Z., Chen, L. C., Mandal, M. K., Nonami, H., Erra-Balsells, R. and Hiraoka, K. (2012) Online electrospray ionization mass spectrometric monitoring of protease-catalyzed reactions in real time. J Am Soc Mass Spectrom. **23**, 728-735

5   Scheerle, R. K., Grassmann, J. and Letzel, T. (2012) Real-time ESI-MS of Enzymatic Conversion: Impact of Organic Solvents and Multiplexing. Analytical Sciences. **28**, 607-612

6   Dennhart, N. and Letzel, T. (2006) Mass spectrometric real-time monitoring of enzymatic glycosidic hydrolysis, enzymatic inhibition and enzyme complexes. Anal Bioanal Chem. **386**, 689-698

7   Dennhart, N., Weigang, L. M. M., Fujiwara, M., Fukamizo, T., Skriver, K. and Letzel, T. (2009) 26 kDa endochitinase from barley seeds: Real-time monitoring of the enzymatic reaction and substrate binding experiments using electrospray ionization mass spectrometry. Journal of Biotechnology. **143**, 274-283

8   Pi, N., Hoang, M. B., Gao, H., Mougous, J. D., Bertozzi, C. R. and Leary, J. A. (2005) Kinetic measurements and mechanism determination of Stf0 sulfotransferase using mass spectrometry. Analytical Biochemistry. **341**, 94-104

9   Pi, N., Yu, Y., Mougous, J. D. and Leary, J. A. (2004) Observation of a hybrid random ping-pong mechanism of catalysis for NodST: A mass spectrometry approach. Protein Science. **13**, 903-912

10   Northrop, D. B. and Simpson, F. B. (1997) New concepts in bioorganic chemistry beyond enzyme kinetics: Direct determination of mechanisms by stopped-flow mass spectrometry. Bioorganic & medicinal chemistry. **5**, 641-644

11   Ganem, B., Li, Y. T. and Henion, J. D. (1991) Observation of Noncovalent Enzyme Substrate and Enzyme Product Complexes by Ion-Spray Mass-Spectrometry. J Am Chem Soc. **113**, 7818-7819

12   Lee, E. D., Mück, W., Henion, J. D. and Covey, T. R. (1989) Real-Time Reaction Monitoring by Continuous-Introduction Ion-Spray Tandem Mass Spectrometry J Am Chem Soc. **111**

13   Zea, C. J. and Pohl, N. L. (2004) Kinetic and substrate binding analysis of phosphorylase b via electrospray ionization mass spectrometry: a model for chemical proteomics of sugar phosphorylases. Analytical Biochemistry. **327**, 107-113

14   de Boer, A. R., Letzel, T., Lingeman, H. and Irth, H. (2005) Systematic development of an enzymatic phosphorylation assay compatible with mass spectrometric detection. Anal Bioanal Chem. **381**, 647-655

15   Hsieh, F. Y. L., Tong, X., Wachs, T., Ganem, B. and Henion, J. (1995) Kinetic Monitoring of Enzymatic Reactions in Real Time by Quantitative High-Performance Liquid Chromatography-Mass Spectrometry. Analytical Biochemistry. **229**, 20-25

16   Attwood, P. V. and Geeves, M. A. (2004) Kinetics of an enzyme-catalyzed reaction measured by electrospray ionization mass spectrometry using a simple rapid mixing attachment. Analytical Biochemistry. **334**, 382-389

17   Zechel, D. L., Konermann, L., Withers, S. G. and Douglas, D. J. (1998) Pre-Steady State Kinetic Analysis of an Enzymatic Reaction Monitored by Time-Resolved Electrospray Ionization Mass Spectrometry. Biochemistry. **37**, 7664-7669

18   Verdugo, D. E., Cancilla, M. T., Ge, X., Gray, N. S., Chang, Y.-T., Schultz, P. G., Negishi, M., Leary, J. A. and Bertozzi, C. R. (2001) Discovery of Estrogen Sulfotransferase Inhibitors from a Purine Library Screen. Journal of medicinal chemistry. **44**, 2683-2686

19   Gao, H. and Leary, J. A. (2003) Multiplex inhibitor screening and kinetic constant determinations for yeast hexokinase using mass spectrometry based assays. Journal of the American Society for Mass Spectrometry. **14**, 173-181

20   Cancilla, M. T., Leavell, M. D., Chow, J. and Leary, J. A. (2000) Mass spectrometry and immobilized enzymes for the screening of inhibitor libraries. Proceedings of the National Academy of Sciences. **97**, 12008-12013

21   Wu, J., Takayama, S., Wong, C. H. and Siuzdak, G. (1997) Quantitative electrospray mass spectrometry for the rapid assay of enzyme inhibitors. Chem Biol. **4**, 653-657

22   de Boer, A. R., Lingeman, H., Niessen, W. M. A. and Irth, H. (2007) Mass spectrometry-based biochemical assays for enzymeinhibitor screening. Trac-Trends Anal. Chem. **26**, 867-883

23   Newman, D. J. and Cragg, G. M. (2016) Natural Products as Sources of New Drugs from 1981 to 2014. Journal of natural products. **79**, 629-661

24   Baltz, R. H. (2006) Marcel Faber Roundtable: Is our antibiotic pipeline unproductive because of starvation, constipation or lack of inspiration? Journal of Industrial Microbiology and Biotechnology. **33**, 507-513

25   Kaufmann, C. M., Grassmann, J. and Letzel, T. (2016) HPLC method development for the online-coupling of chromatographic Perilla frutescens extract separation with xanthine oxidase enzymatic assay. Journal of Pharmaceutical and Biomedical Analysis. **124**, 347-357

26   Kool, J., Eggink, M., van Rossum, H., van Liempd, S. M., van Elswijk, D. A., Irth, H., Commandeur, J. N., Meerman, J. H. and Vermeulen, N. P. (2007) Online biochemical detection of glutathione-S-transferase P1-specific inhibitors in complex mixtures. J Biomol Screen. **12**, 396-405

27   Ingkaninan, K., de Best, C. M., van der Heijden, R., Hofte, A. J. P., Karabatak, B., Irth, H., Tjaden, U. R., van der Greef, J. and Verpoorte, R. (2000) High-performance liquid chromatography with on-line coupled UV, mass spectrometric and biochemical detection for identification of acetylcholinesterase inhibitors from natural products. Journal of Chromatography A. **872**, 61-73

28   Schebb, N. H., Heus, F., Saenger, T., Karst, U., Irth, H. and Kool, J. (2008) Development of a Countergradient Parking System for Gradient Liquid Chromatography with Online Biochemical Detection of Serine Protease Inhibitors. Analytical Chemistry. **80**, 6764-6772

29   Kool, J., van Liempd, S. M., Ramautar, R., Schenk, T., Meerman, J. H., Irth, H., Commandeur, J. N. and Vermeulen, N. P. (2005) Development of a novel cytochrome p450

bioaffinity detection system coupled online to gradient reversed-phase high-performance liquid chromatography. J Biomol Screen. **10**, 427-436

30   Hirata, J., Chung, L. P., Ariese, F., Irth, H. and Gooijer, C. (2005) Coupling of size-exclusion chromatography to a continuous assay for Subtilisin using a fluorescence resonance energy transfer peptide substrate: Testing of two standard inhibitors. Journal of Chromatography A. **1081**, 140-144

31   Kool, J., Giera, M., Irth, H. and Niessen, W. M. A. (2011) Advances in mass spectrometry-based post-column bioaffinity profiling of mixtures. Anal Bioanal Chem. **399**, 2655-2668

32   Letzel, T. (2008) Real-time mass spectrometry in enzymology. Anal Bioanal Chem. **390**, 257-261

33   Grassmann, J., Scheerle, R. K. and Letzel, T. (2012) Functional proteomics: application of mass spectrometry to the study of enzymology in complex mixtures. Anal Bioanal Chem. **402**, 625-645

34   de Jong, C. F., Derks, R. J. E., Bruyneel, B., Niessen, W. and Irth, H. (2006) High-performance liquid chromatography-mass spectrometry-based acetylcholinesterase assay for the screening of inhibitors in natural extracts. Journal of Chromatography A. **1112**, 303-310

35   de Boer, A. R., Letzel, T., van Elswijk, D. A., Lingeman, H., Niessen, W. M. A. and Irth, H. (2004) On-line coupling of high-performance liquid chromatography to a continuous-flow enzyme assay based on electrospray ionization mass spectrometry. Analytical Chemistry. **76**, 3155-3161

36   Li, D. Q., Zhao, J., Xie, J. and Li, S. P. (2014) A novel sample preparation and on-line HPLC–DAD–MS/MS–BCD analysis for rapid screening and characterization of specific enzyme inhibitors in herbal extracts: Case study of α-glucosidase. Journal of Pharmaceutical and Biomedical Analysis. **88**, 130-135

37   Lalles, J. P. (2010) Intestinal alkaline phosphatase: multiple biological roles in maintenance of intestinal homeostasis and modulation by diet. Nutr Rev. **68**, 323-332

38   Geddes, K. and Philpott, D. J. (2008) A new role for intestinal alkaline phosphatase in gut barrier maintenance. Gastroenterology. **135**, 8-12

39   Akiba, Y., Mizumori, M., Guth, P. H., Engel, E. and Kaunitz, J. D. (2007) Duodenal brush border intestinal alkaline phosphatase activity affects bicarbonate secretion in rats. Am J Physiol Gastrointest Liver Physiol. **293**, G1223-1233

40   Mizumori, M., Ham, M., Guth, P. H., Engel, E., Kaunitz, J. D. and Akiba, Y. (2009) Intestinal alkaline phosphatase regulates protective surface microclimate pH in rat duodenum. J Physiol. **587**, 3651-3663

41   Chappelet-Tordo, D., Fosset, M., Iwatsubo, M., Gache, C. and Lazdunski, M. (1974) Intestinal alkaline phosphatase. Catalytic properties and half of the sites reactivity. Biochemistry. **13**, 1788-1795

42   Moss, D. W. and Walli, A. K. (1969) Intermediates in the hydrolysis of ATP by human alkaline phosphatase. Biochim Biophys Acta. **191**, 476-477

43   Malo, M. S., Alam, S. N., Mostafa, G., Zeller, S. J., Johnson, P. V., Mohammad, N., Chen, K. T., Moss, A. K., Ramasamy, S., Faruqui, A., Hodin, S., Malo, P. S., Ebrahimi, F., Biswas, B., Narisawa, S., Millan, J. L., Warren, H. S., Kaplan, J. B., Kitts, C. L., Hohmann, E. L. and Hodin, R. A. (2010) Intestinal alkaline phosphatase preserves the normal homeostasis of gut microbiota. Gut. **59**, 1476-1484

44   la Sala, A., Ferrari, D., Di Virgilio, F., Idzko, M., Norgauer, J. and Girolomoni, G. (2003) Alerting and tuning the immune response by extracellular nucleotides. J Leukocyte Biol. **73**, 339-343

45   Ye, J. H. and Rajendran, V. M. (2009) Adenosine: an immune modulator of inflammatory bowel diseases. World J Gastroenterol. **15**, 4491-4498

46   Moss, A. K., Hamarneh, S. R., Mohamed, M. M. R., Ramasamy, S., Yammine, H., Patel, P., Kaliannan, K., Alam, S. N., Muhammad, N., Moaven, O., Teshager, A., Malo, N. S., Narisawa, S., Millán, J. L., Warren, H. S., Hohmann, E., Malo, M. S. and Hodin, R. A. (2013) Intestinal alkaline phosphatase inhibits the proinflammatory nucleotide uridine diphosphate. American Journal of Physiology - Gastrointestinal and Liver Physiology. **304**, G597-G604

47   Malo, M. S., Moaven, O., Muhammad, N., Biswas, B., Alam, S. N., Economopoulos, K. P., Gul, S. S., Hamarneh, S. R., Malo, N. S., Teshager, A., Mohamed, M. M. R., Tao, Q., Narisawa, S., Millán, J. L., Hohmann, E. L., Warren, H. S., Robson, S. C. and Hodin, R. A. (2014) Intestinal alkaline phosphatase promotes gut bacterial growth by reducing the concentration

of luminal nucleotide triphosphates. American Journal of Physiology - Gastrointestinal and Liver Physiology. **306**, G826-G838

48   Goldberg, R. F., Austen, W. G., Zhang, X. B., Munene, G., Mostafa, G., Biswas, S., McCormack, M., Eberlin, K. R., Nguyen, J. T., Tatlidede, H. S., Warren, H. S., Narisawa, S., Millan, J. L. and Hodin, R. A. (2008) Intestinal alkaline phosphatase is a gut mucosal defense factor maintained by enteral nutrition. P Natl Acad Sci USA. **105**, 3551-3556

49   Poelstra, K., Bakker, W. W., Klok, P. A., Kamps, J. A., Hardonk, M. J. and Meijer, D. K. (1997) Dephosphorylation of endotoxin by alkaline phosphatase in vivo. Am J Pathol. **151**, 1163-1169

50   Beumer, C., Wulferink, M., Raaben, W., Fiechter, D., Brands, R. and Seinen, W. (2003) Calf intestinal alkaline phosphatase, a novel therapeutic drug for lipopolysaccharide (LPS)-mediated diseases, attenuates LPS toxicity in mice and piglets. J Pharmacol Exp Ther. **307**, 737-744

51   Tuin, A., Poelstra, K., de Jager-Krikken, A., Bok, L., Raaben, W., Velders, M. P. and Dijkstra, G. (2009) Role of alkaline phosphatase in colitis in man and rats. Gut. **58**, 379-387

52   Bates, J. M., Akerlund, J., Mittge, E. and Guillemin, K. (2007) Intestinal Alkaline Phosphatase Detoxifies Lipopolysaccharide and Prevents Inflammation in Response to the Gut Microbiota. Cell host & microbe. **2**, 371-382

53   Bol-Schoenmakers, M., Fiechter, D., Raaben, W., Hassing, I., Bleumink, R., Kruijswijk, D., Maijoor, K., Tersteeg-Zijderveld, M., Brands, R. and Pieters, R. (2010) Intestinal alkaline phosphatase contributes to the reduction of severe intestinal epithelial damage. Eur J Pharmacol. **633**, 71-77

54   Riggle, K. M., Rentea, R. M., Welak, S. R., Pritchard, K. A., Jr., Oldham, K. T. and Gourlay, D. M. (2013) Intestinal alkaline phosphatase prevents the systemic inflammatory response associated with necrotizing enterocolitis. J Surg Res. **180**, 21-26

55   Chen, K. T., Malo, M. S., Moss, A. K., Zeller, S., Johnson, P., Ebrahimi, F., Mostafa, G., Alam, S. N., Ramasamy, S., Warren, H. S., Hohmann, E. L. and Hodin, R. A. (2010) Identification of specific targets for the gut mucosal defense factor intestinal alkaline phosphatase. American Journal of Physiology-Gastrointestinal and Liver Physiology. **299**, G467-G475

56   Montoya, C. A., Leterme, P. and Lalles, J.-P. (2006) A protein-free diet alters small intestinal architecture and digestive enzyme activities in rats. Reprod. Nutr. Dev. **46**, 49-56

57   Boudry, G., Lallès, J. P., Malbert, C. H., Bobillier, E. and Sève, B. (2002) Diet-Related Adaptation of the Small Intestine at Weaning in Pigs Is Functional Rather Than Structural. Journal of Pediatric Gastroenterology and Nutrition. **34**, 180-187

58   Sogabe, N., Mizoi, L., Asahi, K., Ezawa, I. and Goseki-Sone, M. Enhancement by lactose of intestinal alkaline phosphatase expression in rats. Bone. **35**, 249-255

59   Sogabe, N., Maruyama, R., Hosoi, T. and Goseki-Sone, M. (2007) Enhancement Effects of Vitamin K (Phylloquinone) or Vitamin K2 (Menaquinone-4) on Intestinal Alkaline Phosphatase Activity in Rats. Journal of Nutritional Science and Vitaminology. **53**, 219-224

60   Bamba, T., Vaja, S., Murphy, G. M. and Dowling, R. H. (1990) Effect of Fasting and Feeding on Polyamines and Related Enzymes along the Villus:Crypt Axis. Digestion. **46(suppl 2)**, 424-429

61   Stenson, W. F., Seetharam, B., Talkad, V., Pickett, W., Dudeja, P. and Brasitus, T. A. (1989) Effects of dietary fish oil supplementation on membrane fluidity and enzyme activity in rat small intestine. Biochemical Journal. **263**, 41-45

62   Narisawa, S., Huang, L., Iwasaki, A., Hasegawa, H., Alpers, D. H. and Millan, J. L. (2003) Accelerated fat absorption in intestinal alkaline phosphatase knockout mice. Mol Cell Biol. **23**, 7525-7530

63   Narisawa, S., Hoylaerts, M. F., Doctor, K. S., Fukuda, M. N., Alpers, D. H. and Millán, J. L. (2007) A novel phosphatase upregulated in Akp3 knockout mice. American Journal of Physiology - Gastrointestinal and Liver Physiology. **293**, G1068-G1077

64   Poss, W. B., Huecksteadt, T. P., Panus, P. C., Freeman, B. A. and Hoidal, J. R. (1996) Regulation of xanthine dehydrogenase and xanthine oxidase activity by hypoxia. American Journal of Physiology - Lung Cellular and Molecular Physiology. **270**, L941-L946

65   Cote, C. G., Yu, F. S., Zulueta, J. J., Vosatka, R. J. and Hassoun, P. M. (1996) Regulation of intracellular xanthine oxidase by endothelial-derived nitric oxide. Am J Physiol. **271**, L869-874

66   Parks, D. A., Bulkley, G. B. and Granger, D. N. (1983) Role of oxygen-derived free radicals in digestive tract diseases. Surgery. **94**, 415-422

67   Kuppusamy, P. and Zweier, J. L. (1989) Characterization of free radical generation by xanthine oxidase. Evidence for hydroxyl radical generation. Journal of Biological Chemistry. **264**, 9880-9884

68   Sorensen, L. B. (1965) Role of the intestinal tract in the elimination of uric acid. Arthritis & Rheumatism. **8**, 694-706

69   Faller , J. and Fox , I. H. (1982) Ethanol-Induced Hyperuricemia. New England Journal of Medicine. **307**, 1598-1602

70   Nakagawa, T., Hu, H., Zharikov, S., Tuttle, K. R., Short, R. A., Glushakova, O., Ouyang, X., Feig, D. I., Block, E. R., Herrera-Acosta, J., Patel, J. M. and Johnson, R. J. (2006) A causal role for uric acid in fructose-induced metabolic syndrome. American Journal of Physiology - Renal Physiology. **290**, F625-F631

71   Johnson, R. J., Segal, M. S., Sautin, Y., Nakagawa, T., Feig, D. I., Kang, D.-H., Gersch, M. S., Benner, S. and Sánchez-Lozada, L. G. (2007) Potential role of sugar (fructose) in the epidemic of hypertension, obesity and the metabolic syndrome, diabetes, kidney disease, and cardiovascular disease. The American Journal of Clinical Nutrition. **86**, 899-906

72   Feig, D. I., Kang, D.-H. and Johnson, R. J. (2008) Uric Acid and Cardiovascular Risk. The New England journal of medicine. **359**, 1811-1821

73   Grayson, P. C., Kim, S. Y., LaValley, M. and Choi, H. K. (2011) Hyperuricemia and incident hypertension: A systematic review and meta-analysis. Arthritis Care & Research. **63**, 102-110

74   Kang, D.-H. and Ha, S.-K. (2014) Uric Acid Puzzle: Dual Role as Anti-oxidantand Pro-oxidant. Electrolytes & Blood Pressure : E & BP. **12**, 1-6

75   Cronstein, B. N. and Terkeltaub, R. (2006) The inflammatory process of gout and its treatment. Arthritis Research & Therapy. **8**, 1-7

76   Cutler, R. G., Camandola, S., Malott, K. F., Edelhauser, M. A. and Mattson, M. P. (2015) The Role of Uric Acid and Methyl Derivatives in the Prevention of Age-Related Neurodegenerative Disorders. Curr Top Med Chem. **15**, 2233-2238

77   Davies, K. J., Sevanian, A., Muakkassah-Kelly, S. F. and Hochstein, P. (1986) Uric acid-iron ion complexes. A new aspect of the antioxidant functions of uric acid. Biochemical Journal. **235**, 747-754

78   Glantzounis, G. K., Tsimoyiannis, E. C., Kappas, A. M. and Galaris, D. A. (2005) Uric Acid and Oxidative Stress. Current Pharmaceutical Design. **11**, 4145-4151

79   Sautin, Y. Y., Nakagawa, T., Zharikov, S. and Johnson, R. J. (2007) Adverse effects of the classic antioxidant uric acid in adipocytes: NADPH oxidase-mediated oxidative/nitrosative stress. American Journal of Physiology - Cell Physiology. **293**, C584-C596

80   Maples, K. R. and Mason, R. P. (1988) Free radical metabolite of uric acid. Journal of Biological Chemistry. **263**, 1709-1712

81   Mittal, M., Siddiqui, M. R., Tran, K., Reddy, S. P. and Malik, A. B. (2013) Reactive Oxygen Species in Inflammation and Tissue Injury. Antioxidants & Redox Signaling. **20**, 1126-1167

82   Zhu, H. and Li, Y. R. (2012) Oxidative stress and redox signaling mechanisms of inflammatory bowel disease: updated experimental and clinical evidence. Experimental Biology and Medicine. **237**, 474-480

83   Liu, J., Wang, C., Liu, F., Lu, Y. and Cheng, J. (2015) Metabonomics revealed xanthine oxidase-induced oxidative stress and inflammation in the pathogenesis of diabetic nephropathy. Anal Bioanal Chem. **407**, 2569-2579

84   Grisham, M. B., Hernandez, L. A. and Granger, D. N. (1986) Xanthine oxidase and neutrophil infiltration in intestinal ischemia. Am J Physiol. **251**, G567-574

85   Phillis, J. W., Sen, S. and Cao, X. (1994) Amflutizole, a xanthine oxidase inhibitor, inhibits free radical generation in the ischemic/reperfused rat cerebral cortex. Neurosci Lett. **169**, 188-190

86   Higgins, P., Dawson, J., Lees, K. R., McArthur, K., Quinn, T. J. and Walters, M. R. (2012) Xanthine oxidase inhibition for the treatment of cardiovascular disease: a systematic review and meta-analysis. Cardiovasc Ther. **30**, 217-226

87   Pacher, P., Nivorozhkin, A. and Szabo, C. (2006) Therapeutic effects of xanthine oxidase inhibitors: renaissance half a century after the discovery of allopurinol. Pharmacol Rev. **58**, 87-114

88   Hayes, J. D. and Strange, R. C. (2000) Glutathione S-transferase polymorphisms and their biological consequences. Pharmacology. **61**, 154-166

89   Hayes, J. D. and Pulford, D. J. (1995) The glutathione S-transferase supergene family: regulation of GST and the contribution of the isoenzymes to cancer chemoprotection and drug resistance. Crit Rev Biochem Mol Biol. **30**, 445-600

90   Mannervik, B. and Danielson, U. H. (1988) Glutathione transferases--structure and catalytic activity. CRC Crit Rev Biochem. **23**, 283-337

91   Keen, J. H. and Jakoby, W. B. (1978) Glutathione transferases. Catalysis of nucleophilic reactions of glutathione. Journal of Biological Chemistry. **253**, 5654-5657

92   Pickett, C. B. and Lu, A. Y. (1989) Glutathione S-transferases: gene structure, regulation, and biological function. Annu Rev Biochem. **58**, 743-764

93   Hayes, J. D. and McLellan, L. I. (1999) Glutathione and glutathione-dependent enzymes represent a co-ordinately regulated defence against oxidative stress. Free Radical Res. **31**, 273-300

94   Mosialou, E., Ekström, G., Adang, A. E. P. and Morgenstern, R. (1993) Evidence that rat liver microsomal glutathione transferase is responsible for glutathione-dependent protection against lipid peroxidation. Biochemical Pharmacology. **45**, 1645-1651

95   Singhal, S. S., Saxena, M., Ahmad, H., Awasthi, S., Haque, A. K. and Awasthi, Y. C. (1992) Glutathione S-transferases of human lung: characterization and evaluation of the protective role of the alpha-class isozymes against lipid peroxidation. Arch Biochem Biophys. **299**, 232-241

96   Pickett, C. B., Telakowski-Hopkins, C. A., Argenbright, L. and Lu, A. Y. (1984) Regulation of glutathione S-transferase mRNAs by phenobarbital and 3-methylcholanthrene: analysis using cDNA probes. Biochem Soc Trans. **12**, 71-74

97   Hayes, J. D., Flanagan, J. U. and Jowsey, I. R. (2005) Glutathione transferases. Annu Rev Pharmacol Toxicol. **45**, 51-88

98   Listowsky, I., Abramovitz, M., Homma, H. and Niitsu, Y. (1988) Intracellular Binding and Transport of Hormones and Xenobiotics by Glutathiones-Transferases. Drug Metabolism Reviews. **19**, 305-318

99   Nicholson, D. W., Ali, A., Vaillancourt, J. P., Calaycay, J. R., Mumford, R. A., Zamboni, R. J. and Ford-Hutchinson, A. W. (1993) Purification to homogeneity and the N-terminal sequence of human leukotriene C4 synthase: a homodimeric glutathione S-transferase composed of 18-kDa subunits. P Natl Acad Sci USA. **90**, 2015-2019

100   Chang, M., Hong, Y., Burgess, J. R., Tu, C. P. and Reddy, C. C. (1987) Isozyme specificity of rat liver glutathione S-transferases in the formation of PGF2 alpha and PGE2 from PGH2. Arch Biochem Biophys. **259**, 548-557

101   Zandonai, R. H., Coelho, F., Ferreira, J., Mendes, A. K. B., Biavatti, M. W., Niero, R., Cechinel Filho, V. and Bueno, E. C. (2010) Evaluation of the proliferative activity of methanol extracts from six medicinal plants in murine spleen cells. Brazilian Journal of Pharmaceutical Sciences. **46**, 323-333

102   Gul, M. Z., Ahmad, F., Kondapi, A. K., Qureshi, I. A. and Ghazi, I. A. (2013) Antioxidant and antiproliferative activities of Abrus precatorius leaf extracts--an in vitro study. BMC Complement Altern Med. **13**, 53

103   Carraz, M., Lavergne, C., Jullian, V., Wright, M., Gairin, J. E., Gonzales de la Cruz, M. and Bourdy, G. (2015) Antiproliferative activity and phenotypic modification induced by selected Peruvian medicinal plants on human hepatocellular carcinoma Hep3B cells. Journal of Ethnopharmacology. **166**, 185-199

104   Siriwatanametanon, N., Fiebich, B. L., Efferth, T., Prieto, J. M. and Heinrich, M. (2010) Traditionally used Thai medicinal plants: In vitro anti-inflammatory, anticancer and antioxidant activities. Journal of Ethnopharmacology. **130**, 196-207

105   Masanetz, S., Kaufmann, C., Letzel, T. and Pfaffl, M. W. (2009) Effects of pine pollen extracts on the proliferation and mRNA expression of porcine ileal cell cultures. J Appl Bot Food Qual. **83**, 14-18

106   DeFeudis, F. V., Papadopoulos, V. and Drieu, K. (2003) Ginkgo biloba extracts and cancer: a research area in its infancy. Fundamental & Clinical Pharmacology. **17**, 405-417

107   Papadopoulos, V., Kapsis, A., Li, H., Amri, H., Hardwick, M., Culty, M., Kasprzyk, P. G., Carlson, M., Moreau, J. P. and Drieu, K. (2000) Drug-induced inhibition of the peripheral-type benzodiazepine receptor expression and cell proliferation in human breast cancer cells. Anticancer Res. **20**, 2835-2847

108   Brown, A. C., Shah, C., Liu, J., Pham, J. T. H., Zhang, J. G. and Jadus, M. R. (2009) Ginger's (Zingiber officinale Roscoe) inhibition of rat colonic adenocarcinoma cells proliferation and angiogenesis in vitro. Phytother Res. **23**, 640-645

109   Rhode, J., Fogoros, S., Zick, S., Wahl, H., Griffith, K. A., Huang, J. and Liu, J. R. (2007) Ginger inhibits cell growth and modulates angiogenic factors in ovarian cancer cells. BMC Complementary and Alternative Medicine. **7**, 1-9

110   Lin, C.-S., Kuo, C.-L., Wang, J.-P., Cheng, J.-S., Huang, Z.-W. and Chen, C.-F. (2007) Growth inhibitory and apoptosis inducing effect of Perilla frutescens extract on human hepatoma HepG2 cells. Journal of Ethnopharmacology. **112**, 557-567

111   Kwak, Y. and Ju, J. (2015) Inhibitory activities of Perilla frutescens britton leaf extract against the growth, migration, and adhesion of human cancer cells. Nutr Res Pract. **9**, 11-16

112   Lin, E. S., Chou, H. J., Kuo, P. L. and Huang, Y. C. (2010) Antioxidant and antiproliferative activities of methanolic extracts of Perilla frutescens. J Med Plants Res. **4**, 477-483

113   Xiaoguang, C., Hongyan, L., Xiaohong, L., Zhaodi, F., Yan, L., Lihua, T. and Rui, H. (1998) Cancer chemopreventive and therapeutic activities of red ginseng. Journal of Ethnopharmacology. **60**, 71-78

114   Kim, S.-J. and Kim, A. K. (2015) Anti-breast cancer activity of Fine Black ginseng (Panax ginseng Meyer) and ginsenoside Rg5. Journal of Ginseng Research. **39**, 125-134

115   Wong, V. K. W., Cheung, S. S. F., Li, T., Jiang, Z.-H., Wang, J.-R., Dong, H., Yi, X. Q., Zhou, H. and Liu, L. (2010) Asian ginseng extract inhibits in vitro and in vivo growth of mouse lewis lung carcinoma via modulation of ERK-p53 and NF-κB signaling. Journal of Cellular Biochemistry. **111**, 899-910

116   Xavier, C. P. R., Lima, C. F., Fernandes-Ferreira, M. and Pereira-Wilson, C. (2009) Salvia Fruticosa, Salvia Officinalis, and Rosmarinic Acid Induce Apoptosis and Inhibit Proliferation of Human Colorectal Cell Lines: The Role in MAPK/ERK Pathway. Nutrition and Cancer. **61**, 564-571

117   Olsson, M. E., Gustavsson, K.-E., Andersson, S., Nilsson, Å. and Duan, R.-D. (2004) Inhibition of Cancer Cell Proliferation in Vitro by Fruit and Berry Extracts and Correlations with Antioxidant Levels. J Agr Food Chem. **52**, 7264-7271

118   Ueda, H., Yamazaki, C. and Yamazaki, M. (2003) Inhibitory effect of Perilla leaf extract and luteolin on mouse skin tumor promotion. Biol Pharm Bull. **26**, 560-563

119   Yin, X., Zhou, J., Jie, C., Xing, D. and Zhang, Y. (2004) Anticancer activity and mechanism of Scutellaria barbata extract on human lung cancer cell line A549. Life Sciences. **75**, 2233-2244

120   Awad, W. A., Aschenbach, J. R. and Zentek, J. (2012) Cytotoxicity and metabolic stress induced by deoxynivalenol in the porcine intestinal IPEC-J2 cell line. J Anim Physiol an N. **96**, 709-716

121   Walle, T. (2004) Absorption and metabolism of flavonoids. Free Radical Biology and Medicine. **36**, 829-837

122   Spencer, J. P. E. (2003) Metabolism of Tea Flavonoids in the Gastrointestinal Tract. The Journal of Nutrition. **133**, 3255S-3261S

123   Scalbert, A. and Williamson, G. (2000) Dietary intake and bioavailability of polyphenols. Journal of Nutrition. **130**, 2073s-2085s

124   Miyake, Y., Shimoi, K., Kumazawa, S., Yamamoto, K., Kinae, N. and Osawa, T. (2000) Identification and Antioxidant Activity of Flavonoid Metabolites in Plasma and Urine of Eriocitrin-Treated Rats. J Agr Food Chem. **48**, 3217-3224

125   Yamamoto, N., Moon, J.-H., Tsushida, T., Nagao, A. and Terao, J. (1999) Inhibitory Effect of Quercetin Metabolites and Their Related Derivatives on Copper Ion-Induced Lipid Peroxidation in Human Low-Density Lipoprotein. Arch Biochem Biophys. **372**, 347-354

126   Brosnahan, A. J. and Brown, D. R. (2012) Porcine IPEC-J2 intestinal epithelial cells in microbiological investigations. Veterinary Microbiology. **156**, 229-237

127   Brown, D. R. and Price, L. D. (2007) Characterization of Salmonella enterica serovar Typhimurium DT104 invasion in an epithelial cell line (IPEC J2) from porcine small intestine. Veterinary Microbiology. **120**, 328-333

128   Liu, F., Li, G., Wen, K., Bui, T., Cao, D., Zhang, Y. and Yuan, L. (2010) Porcine Small Intestinal Epithelial Cell Line (IPEC-J2) of Rotavirus Infection As a New Model for the Study of Innate Immune Responses to Rotaviruses and Probiotics. Viral Immunology. **23**, 135-149

129   Diesing, A.-K., Nossol, C., Panther, P., Walk, N., Post, A., Kluess, J., Kreutzmann, P., Dänicke, S., Rothkötter, H.-J. and Kahlert, S. (2011) Mycotoxin deoxynivalenol (DON) mediates biphasic cellular response in intestinal porcine epithelial cell lines IPEC-1 and IPEC-J2. Toxicol Lett. **200**, 8-18

130   Diesing, A.-K., Nossol, C., Ponsuksili, S., Wimmers, K., Kluess, J., Walk, N., Post, A., Rothkötter, H.-J. and Kahlert, S. (2012) Gene Regulation of Intestinal Porcine Epithelial Cells IPEC-J2 Is Dependent on the Site of Deoxynivalenol Toxicological Action. PLoS ONE. **7**, e34136

131   Müller, J., Gruner, N., Almstätter, I., Kirsch, F., Buettner, A. and Pfaffl, M. W. (2012) Investigation into the metabolism of 1,8-cineole in an intestinal cell culture model and acquisition of its immune-modulatory effect via gene expression analysis. Flavour and Fragrance Journal. **27**, 405-413

132   Brus, M., Langerholc, T. and Škorjanc, D. (2013) Effect of hydrolysable tannins on proliferation of small intestinal porcine and human enterocytes. Acta argiculturae Slovenica. **Supplement 4**, 131–134

133   Schierack, P., Nordhoff, M., Pollmann, M., Weyrauch, K. D., Amasheh, S., Lodemann, U., Jores, J., Tachu, B., Kleta, S., Blikslager, A., Tedin, K. and Wieler, L. H. (2006) Characterization of a porcine intestinal epithelial cell line for in vitro studies of microbial pathogenesis in swine. Histochemistry and Cell Biology. **125**, 293-305

134   Stoy, A. C. F., Heegaard, P. M. H., Sangild, P. T., Ostergaard, M. V. and Skovgaard, K. (2013) Gene Expression Analysis of the IPEC-J2 Cell Line: A Simple Model for the Inflammation-Sensitive Preterm Intestine. ISRN Genomics. **2013**, 7

135   Mariani, V., Palermo, S., Fiorentini, S., Lanubile, A. and Giuffra, E. (2009) Gene expression study of two widely used pig intestinal epithelial cell lines: IPEC-J2 and IPI-2I. Vet Immunol Immunop. **131**, 278-284

136   Sargeant, H. R., Miller, H. M. and Shaw, M.-A. (2011) Inflammatory response of porcine epithelial IPEC J2 cells to enterotoxigenic E. coli infection is modulated by zinc supplementation. Molecular Immunology. **48**, 2113-2121

137   Farkas, O., Palócz, O., Pászti-Gere, E., Gálfi, P. (2015) Polymethoxyflavone Apigenin-Trimethylether Suppresses LPS-Induced Inflammatory Response in Nontransformed Porcine Intestinal Cell Line IPEC-J2. Oxidative Medicine and Cellular Longevity. **2015**, 10

138   Vergauwen, H., Tambuyzer, B., Jennes, K., Degroote, J., Wang, W., De Smet, S., Michiels, J. and Van Ginneken, C. (2015) Trolox and Ascorbic Acid Reduce Direct and Indirect Oxidative Stress in the IPEC-J2 Cells, an In Vitro Model for the Porcine Gastrointestinal Tract. PLoS ONE. **10**, e0120485

139   Paszti-Gere, E., Csibrik-Nemeth, E., Szeker, K., Csizinszky, R., Jakab, C. and Galfi, P. (2012) Acute Oxidative Stress Affects IL-8 and TNF-α Expression in IPEC-J2 Porcine Epithelial Cells. Inflammation. **35**, 994-1004

140   Kahlert, S., Junnikkala, S., Renner, L., Hynönen, U., Hartig, R., Nossol, C., Barta-Böszörményi, A., Dänicke, S., Souffrant, W.-B., Palva, A., Rothkötter, H.-J. and Kluess, J. (2016) Physiological Concentration of Exogenous Lactate Reduces Antimycin A Triggered Oxidative Stress in Intestinal Epithelial Cell Line IPEC-1 and IPEC-J2 In Vitro. PLoS ONE. **11**, e0153135

141   Cai, X., Chen, X., Wang, X., Xu, C., Guo, Q., Zhu, L., Zhu, S. and Xu, J. (2013) Pre-protective effect of lipoic acid on injury induced by H2O2 in IPEC-J2 cells. Molecular and Cellular Biochemistry. **378**, 73-81

142   Kolodziejczak, D., Da Costa Dias, B., Zuber, C., Jovanovic, K., Omar, A., Beck, J., Vana, K., Mbazima, V., Richt, J., Brenig, B. and Weiss, S. F. T. (2010) Prion Interaction with the 37-kDa/67-kDa Laminin Receptor on Enterocytes as a Cellular Model for Intestinal Uptake of Prions. Journal of Molecular Biology. **402**, 293-300

143   Bruch, M. and Mohr, E. (2015) Development of in vitro screening system for food habit related risk analysis. Journal of Experimental Biology and Agricultural Sciences. **3**, 384-393

144   Schmidt, L. D., Kohrt, L. J. and Brown, D. R. (2008) Comparison of growth phase on Salmonella enterica serovar Typhimurium invasion in an epithelial cell line (IPEC J2) and mucosal explants from porcine small intestine. Comparative Immunology, Microbiology and Infectious Diseases. **31**, 63-69

145   Guilloteau, P., Zabielski, R., Hammon, H. M. and Metges, C. C. (2010) Nutritional programming of gastrointestinal tract development. Is the pig a good model for man? Nutr Res Rev. **23**, 4-22

146   Deglaire, A. and Moughan, P. J. (2012) Animal models for determining amino acid digestibility in humans – a review. British Journal of Nutrition. **108**, S273-S281

147   Geens, M. M. and Niewold, T. A. (2011) Optimizing culture conditions of a porcine epithelial cell line IPEC-J2 through a histological and physiological characterization. Cytotechnology. **63**, 415-423

148   Asif, M. (2011) Health effects of omega-3,6,9 fatty acids: Perilla frutescens is a good example of plant oils. Oriental Pharmacy and Experimental Medicine. **11**, 51-59

149   Igarashi, M. and Miyazaki, Y. (2013) A Review on Bioactivities of Perilla: Progress in Research on the Functions of Perilla as Medicine and Food. Evid Based Complement Alternat Med. **2013**, 925342

150   Mao, Q.-Q., Huang, Z., Zhong, X.-M., Feng, C.-R., Pan, A.-J., Li, Z.-Y., Ip, S.-P. and Che, C.-T. (2010) Effects of SYJN, a Chinese herbal formula, on chronic unpredictable stress-induced changes in behavior and brain BDNF in rats. Journal of Ethnopharmacology. **128**, 336-341

151   Mao, Q.-Q., Zhong, X.-M., Li, Z.-Y., Feng, C.-R., Pan, A.-J. and Huang, Z. (2010) Herbal formula SYJN increases neurotrophin-3 and nerve growth factor expression in brain regions of rats exposed to chronic unpredictable stress. Journal of Ethnopharmacology. **131**, 182-186

152   Honda, G., Koezuka, Y., Kamisako, W. and Tabata, M. (1986) Isolation of Sedative Principles from Perilla frutescens. CHEMICAL & PHARMACEUTICAL BULLETIN. **34**, 1672-1677

153   Kang, R., Helms, R., Stout, M. J., Jaber, H., Chen, Z. and Nakatsu, T. (1992) Antimicrobial activity of the volatile constituents of Perilla frutescens and its synergistic effects with polygodial. J Agr Food Chem. **40**, 2328-2330

154   Kurita, N. and Koike, S. (1982) Synergistic Antimicrobial Effect of Acetic Acid, Sodium Chloride and Essential Oil Components. Agricultural and Biological Chemistry. **46**, 1655-1660

155   Buchwald-Werner, S., Fujii, H., Reule, C. and Schoen, C. (2014) Perilla Extract improves gastrointestinal discomfort in a randomized placebo controlled double blind human pilot study. BMC Complementary and Alternative Medicine. **14**, 1-10

156   Ito, N., Yabe, T., Gamo, Y., Nagai, T., Oikawa, T., Yamada, H. and Hanawa, T. (2008) Rosmarinic acid from Perillae Herba produces an antidepressant-like effect in mice through cell proliferation in the hippocampus. Biol Pharm Bull. **31**, 1376-1380

157   Lee, H. A. and Han, J. S. (2012) Anti-inflammatory Effect of Perilla frutescens (L.) Britton var. frutescens Extract in LPS-stimulated RAW 264.7 Macrophages. Prev Nutr Food Sci. **17**, 109-115

158   Chen, C.-Y., Leu, Y.-L., Fang, Y., Lin, C.-F., Kuo, L.-M., Sung, W.-C., Tsai, Y.-F., Chung, P.-J., Lee, M.-C., Kuo, Y.-T., Yang, H.-W. and Hwang, T.-L. (2015) Anti-inflammatory effects of

Perilla frutescens in activated human neutrophils through two independent pathways: Src family kinases and Calcium. Scientific Reports. **5**, 18204

159   Zekonis, G., Zekonis, J., Sadzeviciene, R., Simoniene, G. and Kevelaitis, E. (2008) Effect of Perilla frutescens aqueous extract on free radical production by human neutrophil leukocytes. Medicina (Kaunas). **44**, 699-705

160   Ueda, H. and Yamazaki, M. (1997) Inhibition of Tumor Necrosis Factor-α Production by Orally Administering a Perilla Leaf Extract. Bioscience, Biotechnology, and Biochemistry. **61**, 1292-1295

161   Yamazaki, M., Ueda, H. and Du, D. (1992) Inhibition by Perilla Juice of Tumor Necrosis Factor Production. Bioscience, Biotechnology, and Biochemistry. **56**, 152-152

162   Huang, B. P., Lin, C. H., Chen, Y. C. and Kao, S. H. (2014) Anti-inflammatory effects of Perilla frutescens leaf extract on lipopolysaccharide-stimulated RAW264.7 cells. Mol Med Rep. **10**, 1077-1083

163   Buchwald-Werner, S. (2012) Investigation of a Perilla frutescens special extract - Anti-inflammatory and immune-modulatory properties. Agro FOOD Industry Hi Tech. **23**, 38-41

164   Lim, H. J., Woo, K. W., Lee, K. R., Lee, S. K. and Kim, H. P. (2014) Inhibition of Proinflammatory Cytokine Generation in Lung Inflammation by the Leaves of Perilla frutescens and Its Constituents. Biomol Ther (Seoul). **22**, 62-67

165   Chen, M. L., Wu, C. H., Hung, L. S. and Lin, B. F. (2015) Ethanol Extract of Perilla frutescens Suppresses Allergen-Specific Th2 Responses and Alleviates Airway Inflammation and Hyperreactivity in Ovalbumin-Sensitized Murine Model of Asthma. Evid Based Complement Alternat Med. **2015**, 324265

166   Urushima, H., Nishimura, J., Mizushima, T., Hayashi, N., Maeda, K. and Ito, T. (2015) Perilla frutescens extract ameliorates DSS-induced colitis by suppressing proinflammatory cytokines and inducing anti-inflammatory cytokines. American Journal of Physiology - Gastrointestinal and Liver Physiology. **308**, G32-G41

167   Makino, T., Furuta, Y., Wakushima, H., Fujii, H., Saito, K. and Kano, Y. (2003) Anti-allergic effect of Perilla frutescens and its active constituents. Phytother Res. **17**, 240-243

168   Sanbongi, C., Takano, H., Osakabe, N., Sasa, N., Natsume, M., Yanagisawa, R., Inoue, K., Sadakane, K., Ichinose, T. and Yoshikawa, T. (2004) Rosmarinic acid in perilla extract

inhibits allergic inflammation induced by mite allergen, in a mouse model. Clin Exp Allergy. **34**, 971-977

169   Ueda, H. and Yamazaki, M. (2001) Anti-inflammatory and Anti-allergic Actions by Oral Administration of a Perilla Leaf Extract in Mice. Bioscience, Biotechnology, and Biochemistry. **65**, 1673-1675

170   Shin, T.-Y., Kim, S.-H., Kim, S.-H., Kim, Y.-K., Park, H.-J., Chae, B.-S., Jung, H.-J. and Kim, H.-M. (2000) Inhibitory Effect of Mast Cell-Mediated Immediate-Type Allergic Reactions in Rats by Perilla Frutescens. Immunopharmacology and Immunotoxicology. **22**, 489-500

171   Asada, M., Fukumori, Y., Inoue, M., Nakagomi, K., Sugie, M., Fujita, Y., Tomizuka, N., Yamazaki, Y. and Oka, S. (1999) Glycoprotein Derived from the Hot Water Extract of Mint Plant, Perilla frutescens Britton. J Agr Food Chem. **47**, 468-472

172   Makino, T., Ono, T., Matsuyama, K., Nogaki, F., Miyawaki, S., Honda, G. and Muso, E. (2003) Suppressive effects of Perilla frutescens on IgA nephropathy in HIGA mice. Nephrology Dialysis Transplantation. **18**, 484-490

173   Makino, T., Ito, M., Kiuchiu, F., Ono, T., Muso, E. and Honda, G. (2001) Inhibitory effect of decoction of Perilla frutescens on cultured murine mesangial cell proliferation and quantitative analysis of its active constituents. Planta medica. **67**, 24-28

174   Makino, T., Ono, T., Muso, E., Honda, G. and Sasayama, S. (1999) Suppressive effects of Perilla frutescens on spontaneous IgA nephropathy in ddY mice. Nephron. **83**, 40-46

175   Feng, L.-J., Yu, C.-H., Ying, K.-J., Hua, J. and Dai, X.-Y. (2011) Hypolipidemic and antioxidant effects of total flavonoids of Perilla Frutescens leaves in hyperlipidemia rats induced by high-fat diet. Food Research International. **44**, 404-409

176   Kim, M.-J. and Kim, H. K. (2009) Perilla leaf extract ameliorates obesity and dyslipidemia induced by high-fat diet. Phytother Res. **23**, 1685-1690

177   Kishi, H., Komatsu, W., Miura, Y., Kawanobe, T., Nonaka, T. and Ohhira, S. (2010) Effects of Habitual Perilla (Shiso) Tea Drinking on the Incidence of Diabetes Mellitus in Spontaneously Diabetic Trii (SDT)Rats. Biosci Biotech Bioch. **74**, 2490-2493

178   Ha, T. J., Lee, J. H., Lee, M.-H., Lee, B. W., Kwon, H. S., Park, C.-H., Shim, K.-B., Kim, H.-T., Baek, I.-Y. and Jang, D. S. (2012) Isolation and identification of phenolic compounds from the seeds of Perilla frutescens (L.) and their inhibitory activities against α-glucosidase and aldose reductase. Food Chem. **135**, 1397-1403

179   Paek, J. H., Shin, K. H., Kang, Y.-H., Lee, J.-Y. and Lim, S. S. (2013) Rapid Identification of Aldose Reductase Inhibitory Compounds from Perilla frutescens. BioMed Research International. **2013**, 8

180   Fadel, O., El Kirat, K. and Morandat, S. (2011) The natural antioxidant rosmarinic acid spontaneously penetrates membranes to inhibit lipid peroxidation in situ. Biochimica et Biophysica Acta (BBA) - Biomembranes. **1808**, 2973-2980

181   Petersen, M. and Simmonds, M. S. (2003) Rosmarinic acid. Phytochemistry. **62**, 121-125

182   Peake, P. W., Pussell, B. A., Martyn, P., Timmermans, V. and Charlesworth, J. A. (1991) The inhibitory effect of rosmarinic acid on complement involves the C5 convertase. International Journal of Immunopharmacology. **13**, 853-857

183   Englberger, W., Hadding, U., Etschenberg, E., Graf, E., Leyck, S., Winkelmann, J. and Parnham, M. J. (1988) Rosmarinic acid: a new inhibitor of complement C3-convertase with anti-inflammatory activity. Int J Immunopharmacol. **10**, 729-737

184   Osakabe, N., Takano, H., Sanbongi, C., Yasuda, A., Yanagisawa, R., Inoue, K.-I. and Yoshikawa, T. (2004) Anti-inflammatory and anti-allergic effect of rosmarinic acid (RA); inhibition of seasonal allergic rhinoconjunctivitis (SAR) and its mechanism. BioFactors. **21**, 127-131

185   Simpol, L. R., Otsuka, H., Ohtani, K., Kasai, R. and Yamasaki, K. (1994) Nitrile glucosides and rosmarinic acid, the histamine inhibitor from Ehretia philippinensis. Phytochemistry. **36**, 91-95

186   Osakabe, N., Yasuda, A., Natsume, M. and Yoshikawa, T. (2004) Rosmarinic acid inhibits epidermal inflammatory responses: anticarcinogenic effect of Perilla frutescens extract in the murine two-stage skin model. Carcinogenesis. **25**, 549-557

187   Makino, T., Ono, T., Muso, E., Yoshida, H., Honda, G. and Sasayama, S. (2000) Inhibitory effects of rosmarinic acid on the proliferation of cultured murine mesangial cells. Nephrology Dialysis Transplantation. **15**, 1140-1145

188   Osakabe, N., Yasuda, A., Natsume, M., Sanbongi, C., Kato, Y., Osawa, T. and Yoshikawa, T. (2002) Rosmarinic acid, a major polyphenolic component of Perilla frutescens, reduces lipopolysaccharide (LPS)-induced liver injury in D-galactosamine (D-GalN)-sensitized mice. Free Radic Biol Med. **33**, 798-806

189   Zhang, J. J., Wang, Y. L., Feng, X. B., Song, X. D. and Liu, W. B. (2011) Rosmarinic acid inhibits proliferation and induces apoptosis of hepatic stellate cells. Biol Pharm Bull. **34**, 343-348

190   Yang, S.-Y., Hong, C.-O., Lee, G. P., Kim, C.-T. and Lee, K.-W. (2013) The hepatoprotection of caffeic acid and rosmarinic acid, major compounds of Perilla frutescens, against t-BHP-induced oxidative liver damage. Food Chem Toxicol. **55**, 92-99

191   Park, H. Y., Nam, M. H., Lee, H. S., Jun, W., Hendrich, S. and Lee, K. W. (2010) Isolation of caffeic acid from Perilla frutescens and its role in enhancing gamma-glutamylcysteine synthetase activity and glutathione level. Food Chem. **119**, 724-730

192   Khan, A. Q., Nafees, S. and Sultana, S. (2011) Perillyl alcohol protects against ethanol induced acute liver injury in Wistar rats by inhibiting oxidative stress, NFκ-B activation and proinflammatory cytokine production. Toxicology. **279**, 108-114

193   Ueda, H., Yamazaki, C. and Yamazaki, M. (2002) Luteolin as an Anti-inflammatory and Anti-allergic Constituent of Perilla frutescens. Biological and Pharmaceutical Bulletin. **25**, 1197-1202

194   Jeon, I. H., Kim, H. S., Kang, H. J., Lee, H. S., Jeong, S. I., Kim, S. J. and Jang, S. I. (2014) Anti-inflammatory and antipruritic effects of luteolin from Perilla (P. frutescens L.) leaves. Molecules. **19**, 6941-6951

195   Greco, G., Grosse, S. and Letzel, T. (2013) Serial coupling of reversed-phase and zwitterionic hydrophilic interaction LC/MS for the analysis of polar and nonpolar phenols in wine. J Sep Sci. **36**, 1379-1388

196   Krappmann, M. and Letzel, T. (2012) Achroma: a software strategy for analysing (a-)typical mass-spectrometric data. Anal Methods-Uk. **4**, 1060-1071

197   Letzel, T., Sahmel-Schneider, E., Skriver, K., Ohnuma, T. and Fukamizo, T. (2011) Chitinase-catalyzed hydrolysis of 4-nitrophenyl penta-N-acetyl-beta-chitopentaoside as determined by real-time ESIMS: The 4-nitrophenyl moiety of the substrate interacts with the enzyme binding site. Carbohyd Res. **346**, 863-866

198   Bothner, B., Chavez, R., Wei, J., Strupp, C., Phung, Q., Schneemann, A. and Siuzdak, G. (2000) Monitoring Enzyme Catalysis with Mass Spectrometry. Journal of Biological Chemistry. **275**, 13455-13459

199   Sterling, H. J., Batchelor, J. D., Wemmer, D. E. and Williams, E. R. (2011) Effects of buffer loading for electrospray ionization mass spectrometry of a noncovalent protein complex that requires high concentrations of essential salts. Journal of the American Society for Mass Spectrometry. **21**, 1045-1049

200   Dayan, J. and Wilson, I. B. (1964) The Phosphorylation of Tris by Alkaline Phosphatase. Biochim Biophys Acta. **81**, 620-623

201   Wilson, I. B., Dayan, J. and Cyr, K. (1964) Some Properties of Alkaline Phosphatase from Escherichia coli : TRANSPHOSPHORYLATION. Journal of Biological Chemistry. **239**, 4182-4185

202   McComb, R. B. and Bowers, G. N., Jr. (1972) Study of optimum buffer conditions for measuring alkaline phosphatase activity in human serum. Clin Chem. **18**, 97-104

203   HETHEY, J., LAI, J., LOUTET, S., MARTIN, M. and TANG, V. (2002) Effects of Tricine, Glycine and Tris Buffers on Alkaline Phosphatase Activity. Journal of Experimental Microbiology and Immunology. **2**, 33-38

204   Ugwu, S. O. and Apte, S. P. (2004) The Effect of Buffers on Protein Conformational Stability. Pharmaceutical Technology. **28**

205   Krajewska, B. and Zaborska, W. (1999) The effect of phosphate buffer in the range of pH 5.80–8.07 on jack bean urease activity. Journal of Molecular Catalysis B: Enzymatic. **6**, 75-81

206   Atyaksheva, L. F., Chukhrai, E. S. and Poltorak, O. M. (2008) The catalytic properties of alkaline phosphatases under various conditions. Russ. J. Phys. Chem. **82**, 1947-1951

207   Bannister, A. and Foster, R. L. (1980) Buffer-induced activation of calf intestinal alkaline phosphatase. Eur J Biochem. **113**, 199-203

208   Ballou, G. A. and Luck, J. M. (1941) THE EFFECTS OF DIFFERENT BUFFERS ON THE ACTIVITY OF β-AMYLASE. Journal of Biological Chemistry. **139**, 233-240

209   Kostic, D. A., Dimitrijevic, D. S., Stojanovic, G. S., Palic, I. R., Dordevic, A. S. and Ickovski, J. D. (2015) Xanthine Oxidase: Isolation, Assays of Activity, and Inhibition. Journal of Chemistry. **2015**, 8

210   Elstner, E. F. and Heupel, A. (1976) Inhibition of nitrite formation from hydroxylammoniumchloride: a simple assay for superoxide dismutase. Anal Biochem. **70**, 616-620

211   Hippeli, S., Janisch, K., Kern, S., Ölschläger, C., Treutter, D., May, C. and Elstner, E. F. (2007) Antioxidant and immune modulatory activities of fruit and vegetable extracts after "cascade fermentation". Current Topics in Biochemical Research. **9**, 83-97

212   Elstner, E. F. (1990) Der Sauerstoff: Biochemie, Biologie, Medizin. BI-Wiss.-Verlag

213   Dougherty, T. M. (1976) A sensitive assay for xanthine oxidase using commercially available [14C]xanthine. Analytical Biochemistry. **74**, 604-608

214   Akaike, T., Ando, M., Oda, T., Doi, T., Ijiri, S., Araki, S. and Maeda, H. (1990) Dependence on O2- generation by xanthine oxidase of pathogenesis of influenza virus infection in mice. Journal of Clinical Investigation. **85**, 739-745

215   Beckman, J. S., Parks, D. A., Pearson, J. D., Marshall, P. A. and Freeman, B. A. (1989) A sensitive fluorometric assay for measuring xanthine dehydrogenase and oxidase in tissues. Free Radical Biology and Medicine. **6**, 607-615

216   Trujillo, M., Alvarez, M. a. N., Peluffo, G., Freeman, B. A. and Radi, R. (1998) Xanthine Oxidase-mediated Decomposition ofS-Nitrosothiols. Journal of Biological Chemistry. **273**, 7828-7834

217   Bisswanger, H. (2014) Enzyme assays. Perspectives in Science. **1**, 41-55

218   Ghosh, N. K. and Fishman, W. H. (1966) On the mechanism of inhibition of intestinal alkaline phosphatase by L-phenylalanine. I. Kinetic studies. J Biol Chem. **241**, 2516-2522

219   Morton, R. K. (1957) The kinetics of hydrolysis of phenyl phosphate by alkaline phosphatases. Biochem J. **65**, 674-682

220   Bours, M. J., Swennen, E. L., Di Virgilio, F., Cronstein, B. N. and Dagnelie, P. C. (2006) Adenosine 5'-triphosphate and adenosine as endogenous signaling molecules in immunity and inflammation. Pharmacol Ther. **112**, 358-404

221   Fernley, H. N. and Walker, P. G. (1967) Studies on alkaline phosphatase. Inhibition by phosphate derivatives and the substrate specificity. Biochem J. **104**, 1011-1018

222   Strange, R. C., Spiteri, M. A., Ramachandran, S. and Fryer, A. A. (2001) Glutathione-S-transferase family of enzymes. Mutat Res-Fund Mol M. **482**, 21-26

223   Dsilva, C. (1990) Inhibition and Recognition Studies on the Glutathione-Binding Site of Equine Liver Glutathione-S-Transferase. Biochemical Journal. **271**, 161-165

224   Enache, T. A. and Oliveira-Brett, A. M. (2015) Electrochemical evaluation of glutathione S-transferase kinetic parameters. Bioelectrochemistry. **101**, 46-51

225   Bousova, I., Hajek, J., Drsata, J. and Skalova, L. (2012) Naturally occurring flavonoids as inhibitors of purified cytosolic glutathione S-transferase. Xenobiotica. **42**, 872-879

226   Blokzijl, W. and Engberts, J. B. F. N. (1993) Hydrophobic Effects - Opinions and Facts. Angew Chem Int Edit. **32**, 1545-1579

227   Ge, X., Sirich, T. L., Beyer, M. K., Desaire, H. and Leary, J. A. (2001) A strategy for the determination of enzyme kinetics using electrospray ionization with an ion trap mass spectrometer. Anal Chem. **73**, 5078-5082

228   Simon, L. M., Laszlo, K., Vertesi, A., Bagi, K. and Szajani, B. (1998) Stability of hydrolytic enzymes in water-organic solvent systems. J Mol Catal B-Enzym. **4**, 41-45

229   Batra, R. and Gupta, M. N. (1994) Enhancement of Enzyme-Activity in Aqueous-Organic Solvent Mixtures. Biotechnol Lett. **16**, 1059-1064

230   Carrea, G. (1984) Biocatalysis in Water-Organic Solvent 2-Phase Systems. Trends Biotechnol. **2**, 102-106

231   Antonini, E., Carrea, G. and Cremonesi, P. (1981) Enzyme catalysed reactions in water - Organic solvent two-phase systems. Enzyme Microb Tech. **3**, 291-296

232   Griffiths, T. R. and Pugh, D. C. (1979) Correlations among solvent polarity scales, dielectric constant and dipole moment, and a means to reliable predictions of polarity scale values from cu. Coordination Chemistry Reviews. **29**, 129-211

233   Asakura, T., Adachi, K. and Schwartz, E. (1978) Stabilizing Effect of Various Organic-Solvents on Protein. Journal of Biological Chemistry. **253**, 6423-6425

234   Butler, L. G. (1979) Enzymes in Non-Aqueous Solvents. Enzyme Microb Tech. **1**, 253-259

235   Szabó, A., Kotormán, M., Laczkó, I. and Simon, L. M. (2006) Spectroscopic studies of stability of papain in aqueous organic solvents. Journal of Molecular Catalysis B: Enzymatic. **41**, 43-48

236   Grassmann, J., Hippeli, S., Vollmann, R. and Elstner, E. F. (2003) Antioxidative properties of the essential oil from Pinus mugo. J Agric Food Chem. **51**, 7576-7582

237   Baykov, A. A., Evtushenko, O. A. and Avaeva, S. M. (1988) A malachite green procedure for orthophosphate determination and its use in alkaline phosphatase-based enzyme immunoassay. Anal Biochem. **171**, 266-270

238   Henkel, R. D., VandeBerg, J. L. and Walsh, R. A. (1988) A microassay for ATPase. Anal Biochem. **169**, 312-318

239   Deng, G., Gu, R.-F., Marmor, S., Fisher, S. L., Jahic, H. and Sanyal, G. (2004) Development of an LC–MS based enzyme activity assay for MurC: application to evaluation of inhibitors and kinetic analysis. Journal of Pharmaceutical and Biomedical Analysis. **35**, 817-828

240   Liesener, A. and Karst, U. (2005) Monitoring enzymatic conversions by mass spectrometry: a critical review. Anal Bioanal Chem. **382**, 1451-1464

241   Cheng, X., Chen, R., Bruce, J. E., Schwartz, B. L., Anderson, G. A., Hofstadler, S. A., Gale, D. C., Smith, R. D., Gao, J., Sigal, G. B., Mammen, M. and Whitesides, G. M. (1995) Using Electrospray Ionization FTICR Mass Spectrometry To Study Competitive Binding of Inhibitors to Carbonic Anhydrase. J Am Chem Soc. **117**, 8859-8860

242   Rohman, M. M., Suzuki, T. and Fujita, M. (2009) Identification of a glutathione S-transferase inhibitor in onion bulb (Allium cepa L.) Australian Journal of Crop Science. **3**, 28-36

243   Iio, M., Kawaguchi, H., Sakota, Y., Otonari, J. and Nitahara, H. (1993) Effects of Polyphenols, Including Flavonoids, on Glutathione S-Transferase and Glutathione Reductase. Bioscience, Biotechnology, and Biochemistry. **57**, 1678-1680

244   Huo, L. N., Wang, W., Zhang, C. Y., Shi, H. B., Liu, Y., Liu, X. H., Guo, B. H., Zhao, D. M. and Gao, H. (2015) Bioassay-Guided Isolation and Identification of Xanthine Oxidase Inhibitory Constituents from the Leaves of Perilla frutescens. Molecules. **20**, 17848-17859

245   de Boer, A. R., Alcaide-Hidalgo, J. M., Krabbe, J. G., Kolkman, J., Boas, C. N. V., Niessen, W. M. A., Lingeman, H. and Irth, H. (2005) High-temperature liquid chromatography coupled on-line to a continuous-flow biochemical screening assay with electrospray ionization mass spectrometric detection. Analytical Chemistry. **77**, 7894-7900

246   Kaufman, A. D. and Kissinger, P. T. (1998) Extra-Column Band Spreading Concerns in Post-Column Photolysis Reactors for Microbore Liquid Chromatography. Current Separations **17**, 9-16

247   Engelhardt, H. and Neue, U. D. (1982) Reaction Detector with Three Dimensional Coiled Open Tubes in HPLC Chromatographia. **15**, 403-408

248   Schebb, N. H., Vielhaber, T., Jousset, A. and Karst, U. (2009) Development of a liquid chromatography-based screening methodology for proteolytic enzyme activity. J Chromatogr A. **1216**, 4407-4415

249   Greco, G., Grosse, S. and Letzel, T. (2014) Robustness of a method based on the serial coupling of reversed-phase and zwitterionic hydrophilic interaction LC–MS for the analysis of phenols. Journal of Separation Science. **37**, 630-634

250   Teutenberg, T., Wiese, S., Wagner, P. and Gmehling, J. (2009) High-temperature liquid chromatography. Part III: Determination of the static permittivities of pure solvents and binary solvent mixtures--implications for liquid chromatographic separations. J Chromatogr A. **1216**, 8480-8487

251   Kebarle, P. and Verkerk, U. H. (2009) Electrospray: From ions in solution to ions in the gas phase, what we know now. Mass spectrometry reviews. **28**, 898-917

252   Kool, J., Ramautar, R., van Liempd, S. M., Beckman, J., de Kanter, F. J., Meerman, J. H., Schenk, T., Irth, H., Commandeur, J. N. and Vermeulen, N. P. (2006) Rapid on-line profiling of estrogen receptor binding metabolites of tamoxifen. Journal of medicinal chemistry. **49**, 3287-3292

253   van Elswijk, D. A., Diefenbach, O., van der Berg, S., Irth, H., Tjaden, U. R. and van der Greef, J. (2003) Rapid detection and identification of angiotensin-converting enzyme inhibitors by on-line liquid chromatography–biochemical detection, coupled to electrospray mass spectrometry. Journal of Chromatography A. **1020**, 45-58

254   Schenk, T., Breel, G. J., Koevoets, P., van den Berg, S., Hogenboom, A. C., Irth, H., Tjaden, U. R. and van der Greef, J. (2003) Screening of natural products extracts for the presence of phosphodiesterase inhibitors using liquid chromatography coupled online to parallel biochemical detection and chemical characterization. J Biomol Screen. **8**, 421-429

255   Haselberg, R., Hempen, C., van Leeuwen, S. M., Vogel, M. and Karst, U. (2006) Analysis of microperoxidases using liquid chromatography, post-column substrate conversion and fluorescence detection. Journal of Chromatography B. **830**, 47-53

256   Neumann, U., Kubota, H., Frei, K., Ganu, V. and Leppert, D. (2004) Characterization of Mca-Lys-Pro-Leu-Gly-Leu-Dpa-Ala-Arg-NH2, a fluorogenic substrate with increased specificity constants for collagenases and tumor necrosis factor converting enzyme. Analytical Biochemistry. **328**, 166-173

257   Wolfson, A. J., Shrimpton, C. N., Lew, R. A. and Smith, A. I. (1996) Differential Activation of Endopeptidase EC 3.4.24.15 toward Natural and Synthetic Substrates by Metal Ions. Biochem Bioph Res Co. **229**, 341-348

258   Park, J. and Kim, Y. (2013) An improved fluorogenic substrate for the detection of alkaline phosphatase activity. Bioorganic & medicinal chemistry letters. **23**, 2332-2335

259   Krappmann, M., Kaufmann, C. M., Scheerle, R. K., Grassmann, J. and Letzel, T. (2014) Achroma Software-High-Quality Policy in (a-)Typical Mass Spectrometric Data Handling and Applied Functional Proteomics. Proteomics & Bioinformatics. **7**, 264-271

260   Zaks, A. and Klibanov, A. M. (1988) The effect of water on enzyme action in organic media. Journal of Biological Chemistry. **263**, 8017-8021

261   Hari Krishna, S. (2002) Developments and trends in enzyme catalysis in nonconventional media. Biotechnology Advances. **20**, 239-267

262   Ogino, H. and Ishikawa, H. (2001) Enzymes which are stable in the presence of organic solvents. Journal of Bioscience and Bioengineering. **91**, 109-116

263   Klibanov, A. M. (2001) Improving enzymes by using them in organic solvents. Nature. **409**, 241-246

264   Nakanishi, T., Nishi, M., Inada, A., Obata, H., Tanabe, N., Abe, S. and Wakashiro, M. (1990) Two new potent inhibitors of xanthine oxidase from leaves of Perilla frutescens Britton var. acuta Kudo. Chem Pharm Bull (Tokyo). **38**, 1772-1774

265   Dawson, J. and Walters, M. (2006) Uric acid and xanthine oxidase: future therapeutic targets in the prevention of cardiovascular disease? Br J Clin Pharmacol. **62**, 633-644

266   Landmesser, U., Spiekermann, S., Dikalov, S., Tatge, H., Wilke, R., Kohler, C., Harrison, D. G., Hornig, B. and Drexler, H. (2002) Vascular oxidative stress and endothelial dysfunction in patients with chronic heart failure: role of xanthine-oxidase and extracellular superoxide dismutase. Circulation. **106**, 3073-3078

267   Kruidenier, L., Kuiper, I., Lamers, C. B. and Verspaget, H. W. (2003) Intestinal oxidative damage in inflammatory bowel disease: semi-quantification, localization, and association with mucosal antioxidants. J Pathol. **201**, 28-36

268   Cos, P., Ying, L., Calomme, M., Hu, J. P., Cimanga, K., Van Poel, B., Pieters, L., Vlietinck, A. J. and Vanden Berghe, D. (1998) Structure-activity relationship and classification of

flavonoids as inhibitors of xanthine oxidase and superoxide scavengers. Journal of natural products. **61**, 71-76

269   Masuda, T., Shingai, Y., Takahashi, C., Inai, M., Miura, Y., Honda, S. and Masuda, A. (2014) Identification of a potent xanthine oxidase inhibitor from oxidation of caffeic acid. Free Radical Biology and Medicine. **69**, 300-307

270   Waxman, D. J. (1990) Glutathione S-transferases: role in alkylating agent resistance and possible target for modulation chemotherapy--a review. Cancer Res. **50**, 6449-6454

271   Tsuboi, K., Bachovchin, D. A., Speers, A. E., Spicer, T. P., Fernandez-Vega, V., Hodder, P., Rosen, H. and Cravatt, B. F. (2011) Potent and Selective Inhibitors of Glutathione S-transferase Omega 1 that Impair Cancer Drug Resistance. J Am Chem Soc. **133**, 16605-16616

272   Schisselbauer, J. C., Silber, R., Papadopoulos, E., Abrams, K., LaCreta, F. P. and Tew, K. D. (1990) Characterization of glutathione S-transferase expression in lymphocytes from chronic lymphocytic leukemia patients. Cancer Res. **50**, 3562-3568

273   Tew, K. D., Bomber, A. M. and Hoffman, S. J. (1988) Ethacrynic Acid and Piriprost as Enhancers of Cytotoxicity in Drug Resistant and Sensitive Cell Lines. Cancer Res. **48**, 3622-3625

274   Latham, K. M. and Stanbridge, E. J. (1990) Identification of the HeLa tumor-associated antigen, p75/150, as intestinal alkaline phosphatase and evidence for its transcriptional regulation. Proc Natl Acad Sci U S A. **87**, 1263-1267

275   Nageshwari, B. and Ramchander, M. (2013) Human alkaline phosphatases in health and disease: A mini review. International Journal of Research in Pharmaceutical Sciences. **4**, 371-379

276   Wolf, P. L. (1994) Clinical significance of serum high-molecular-mass alkaline phosphatase, alkaline phosphatase-lipoprotein-X complex, and intestinal variant alkaline phosphatase. J Clin Lab Anal. **8**, 172-176

277   Chen, K. T., Malo, M. S., Beasley-Topliffe, L. K., Poelstra, K., Millan, J. L., Mostafa, G., Alam, S. N., Ramasamy, S., Warren, H. S., Hohmann, E. L. and Hodin, R. A. (2011) A role for intestinal alkaline phosphatase in the maintenance of local gut immunity. Dig Dis Sci. **56**, 1020-1027

278   Fishman, W. H., Green, S. and Inglis, N. I. (1962) Organ-specific behavior exhibited by rat intestine and liver alkaline phosphatase. Biochim Biophys Acta. **62**, 363-375

279   Fishman, W. H., Green, S. and Inglis, N. I. (1963) L-phenylalanine: an organ specific, stereospecific inhibitor of human intestinal alkaline phosphatase. Nature. **198**, 685-686

280   Pradhan, R., Rajput, S., Mandal, M., Mitra, A. and Das, S. (2014) Electric cell-substrate impedance sensing technique to monitor cellular behaviours of cancer cells. RSC Advances. **4**, 9432-9438

281   Pradhan, R., Mandal, M., Mitra, A. and Das, S. (2014) Monitoring cellular activities of cancer cells using impedance sensing devices. Sensors and Actuators B: Chemical. **193**, 478-483

282   Yang, L., Arias, L. R., Lane, T. S., Yancey, M. D. and Mamouni, J. (2011) Real-time electrical impedance-based measurement to distinguish oral cancer cells and non-cancer oral epithelial cells. Anal Bioanal Chem. **399**, 1823-1833

283   Xiao, C. and Luong, J. H. T. (2005) Assessment of cytotoxicity by emerging impedance spectroscopy. Toxicol. Appl. Pharmacol. **206**, 102-112

284   Park, H. E., Kim, D., Koh, H. S., Cho, S., Sung, J. S. and Kim, J. Y. (2011) Real-time monitoring of neural differentiation of human mesenchymal stem cells by electric cell-substrate impedance sensing. J Biomed Biotechnol. **2011**, 485173

285   Long, L. H., Hoi, A. and Halliwell, B. (2010) Instability of, and generation of hydrogen peroxide by, phenolic compounds in cell culture media. Arch Biochem Biophys. **501**, 162-169

286   Halliwell, B. (2008) Are polyphenols antioxidants or pro-oxidants? What do we learn from cell culture and in vivo studies? Arch Biochem Biophys. **476**, 107-112

287   Muller, J., Thirion, C. and Pfaffl, M. W. (2011) Electric cell-substrate impedance sensing (ECIS) based real-time measurement of titer dependent cytotoxicity induced by adenoviral vectors in an IPI-2I cell culture model. Biosensors & Bioelectronics. **26**, 2000-2005

288   Schreiber, M., Kolbus, A., Piu, F., Szabowski, A., Möhle-Steinlein, U., Tian, J., Karin, M., Angel, P. and Wagner, E. F. (1999) Control of cell cycle progression by c-Jun is p53 dependent. Genes Dev **13**, 607-619

289   Hakem, R., Hakem, A., Duncan, G. S., Henderson, J. T., Woo, M., Soengas, M. S., Elia, A., de la Pompa, J. L., Kagi, D., Khoo, W., Potter, J., Yoshida, R., Kaufman, S. A., Lowe, S. W., Penninger, J. M. and Mak, T. W. (1998) Differential Requirement for Caspase 9 in Apoptotic Pathways In Vivo. Cell. **94**, 339-352

290   Hollstein, M., Sidransky, D., Vogelstein, B. and Harris, C. (1991) p53 mutations in human cancers. Science. **253**, 49-53

291   Shaulian, E. and Karin, M. (2001) AP-1 in cell proliferation and survival. Oncogene. **20**, 2390-2400

292   Shaulian, E., Schreiber, M., Piu, F., Beeche, M., Wagner, E. F. and Karin, M. (2000) The Mammalian UV Response: c-Jun Induction Is Required for Exit from p53-Imposed Growth Arrest. Cell. **103**, 897-908

293   Lim, S. and Kaldis, P. (2013) Cdks, cyclins and CKIs: roles beyond cell cycle regulation. Development. **140**, 3079-3093

294   Nelson, J., McFerran, N. V., Pivato, G., Chambers, E., Doherty, C., Steele, D. and Timson, D. J. (2008) The 67 kDa laminin receptor: structure, function and role in disease. Biosci Rep. **28**, 33-48

295   Chowdhury, I., Tharakan, B. and Bhat, G. K. (2008) Caspases - an update. Comp Biochem Physiol B Biochem Mol Biol. **151**, 10-27

296   Haupt, S., Berger, M., Goldberg, Z. and Haupt, Y. (2003) Apoptosis - the p53 network. J Cell Sci. **116**, 4077-4085

297   Kimura, S. H. and Nojima, H. (2002) Cyclin G1 associates with MDM2 and regulates accumulation and degradation of p53 protein. Genes to Cells. **7**, 869-880

298   Zhao, L., Samuels, T., Winckler, S., Korgaonkar, C., Tompkins, V., Horne, M. C. and Quelle, D. E. (2003) Cyclin G1 Has Growth Inhibitory Activity Linked to the ARF-Mdm2-p53 and pRb Tumor Suppressor Pathways1 1 D.E.Q. from the American Cancer Society (RSG-98-254-04-MGO) and NIH (RO1 CA90367), and by a grant from the NIH to M.C.H. (RO1 GM56900). Molecular Cancer Research. **1**, 195-206

299   Innocente, S. A., Abrahamson, J. L. A., Cogswell, J. P. and Lee, J. M. (1999) p53 regulates a G(2) checkpoint through cyclin B1. P Natl Acad Sci USA. **96**, 2147-2152

300   Seo, H. R., Lee, D. H., Lee, H. J., Baek, M., Bae, S., Soh, J. W., Lee, S. J., Kim, J. and Lee, Y. S. (2005) Cyclin G1 overcomes radiation-induced G2 arrest and increases cell death through transcriptional activation of cyclin B1. Cell Death Differ. **13**, 1475-1484

301   Satyanarayana, A., Hilton, M. B. and Kaldis, P. (2008) p21 Inhibits Cdk1 in the Absence of Cdk2 to Maintain the G1/S Phase DNA Damage Checkpoint. Molecular Biology of the Cell. **19**, 65-77

302   Taylor, W. R. and Stark, G. R. (2001) Regulation of the G2/M transition by p53. Oncogene. **20**, 1803-1815

303   Scheiman, J., Tseng, J. C., Zheng, Y. and Meruelo, D. (2010) Multiple functions of the 37/67-kd laminin receptor make it a suitable target for novel cancer gene therapy. Mol Ther. **18**, 63-74

304   Peer Zada, A. A., Singh, S. M., Reddy, V. A., Elsasser, A., Meisel, A., Haferlach, T., Tenen, D. G., Hiddemann, W. and Behre, G. (2003) Downregulation of c-Jun expression and cell cycle regulatory molecules in acute myeloid leukemia cells upon CD44 ligation. Oncogene. **22**, 2296-2308

305   Wang, Y., Huang, X., Han, J., Zheng, W. and Ma, W. (2013) Extract of Perilla Frutescens Inhibits Tumor Proliferation of HCC via PI3K/AKT Signal Pathway. African Journal of Traditional, Complementary, and Alternative Medicines. **10**, 251-257

306   Xavier, C. P. R., Lima, C. F., Preto, A., Seruca, R., Fernandes-Ferreira, M. and Pereira-Wilson, C. (2009) Luteolin, quercetin and ursolic acid are potent inhibitors of proliferation and inducers of apoptosis in both KRAS and BRAF mutated human colorectal cancer cells. Cancer Letters. **281**, 162-170

307   Banno, N., Akihisa, T., Tokuda, H., Yasukawa, K., Higashihara, H., Ukiya, M., Watanabe, K., Kimura, Y., Hasegawa, J.-i. and Nishino, H. (2004) Triterpene Acids from the Leaves of Perilla frutescens and Their Anti-inflammatory and Antitumor-promoting Effects. Bioscience, Biotechnology, and Biochemistry. **68**, 85-90

308   Wang, W. Q., Heideman, L., Chung, C. S., Pelling, J. C., Koehler, K. J. and Birt, D. F. (2000) Cell-cycle arrest at G2/M and growth inhibition by apigenin in human colon carcinoma cell lines. Mol Carcinogen. **28**, 102-110

309   Yu, M., Zhan, Q. and Finn, O. J. (2002) Immune recognition of cyclin B1 as a tumor antigen is a result of its overexpression in human tumors that is caused by non-functional p53. Molecular Immunology. **38**, 981-987

310   Maeda, S. and Karin, M. (2003) Oncogene at last—c-Jun promotes liver cancer in mice. Cancer Cell. **3**, 102-104

311   Diehl, J. A. (2002) Cycling to cancer with cyclin D1. Cancer Biol Ther. **1**, 226-231

312   Sanjuan, X., Fernandez, P. L., Miquel, R., Munoz, J., Castronovo, V., Menard, S., Palacin, A., Cardesa, A. and Campo, E. (1996) Overexpression of the 67-kD laminin receptor correlates with tumour progression in human colorectal carcinoma. J Pathol. **179**, 376-380

313   Ozaki, I., Yamamoto, K., Mizuta, T., Kajihara, S., Fukushima, N., Setoguchi, Y., Morito, F. and Sakai, T. (1998) Differential expression of laminin receptors in human hepatocellular carcinoma. Gut. **43**, 837-842

314   Martignone, S., Ménard, S., Bufalino, R., Cascinelli, N., Pellegrini, R., Tagliabue, E., Andreola, S., Rilke, F. and Colnaghi, M. I. (1993) Prognostic Significance of the 67-Kilodalton Laminin Receptor Expression in Human Breast Carcinomas. Journal of the National Cancer Institute. **85**, 398-402

315   Wewer, U. M., Taraboletti, G., Sobel, M. E., Albrechtsen, R. and Liotta, L. A. (1987) Role of laminin receptor in tumor cell migration. Cancer Res. **47**, 5691-5698

316   Bernard, A., Gao-Li, J., Franco, C. A., Bouceba, T., Huet, A. and Li, Z. (2009) Laminin receptor involvement in the anti-angiogenic activity of pigment epithelium-derived factor. J Biol Chem. **284**, 10480-10490

317   Gauczynski, S., Peyrin, J. M., Haik, S., Leucht, C., Hundt, C., Rieger, R., Krasemann, S., Deslys, J. P., Dormont, D., Lasmezas, C. I. and Weiss, S. (2001) The 37-kDa/67-kDa laminin receptor acts as the cell-surface receptor for the cellular prion protein. Embo J. **20**, 5863-5875

318   Morel, E., Andrieu, T., Casagrande, F., Gauczynski, S., Weiss, S., Grassi, J., Rousset, M., Dormont, D. and Chambaz, J. (2005) Bovine Prion Is Endocytosed by Human Enterocytes via the 37 kDa/67 kDa Laminin Receptor. Am J Pathol **167**, 1033-1042

319   Long, L. H., Clement, M. V. and Halliwell, B. (2000) Artifacts in cell culture: rapid generation of hydrogen peroxide on addition of (-)-epigallocatechin, (-)-epigallocatechin gallate, (+)-catechin, and quercetin to commonly used cell culture media. Biochem Biophys Res Commun. **273**, 50-53

320   Hampton, M. B. and Orrenius, S. (1997) Dual regulation of caspase activity by hydrogen peroxide: implications for apoptosis. FEBS Lett. **414**, 552-556

321   Chai, P. C., Long, L. H. and Halliwell, B. (2003) Contribution of hydrogen peroxide to the cytotoxicity of green tea and red wines. Biochem Biophys Res Commun. **304**, 650-654

322   Gulden, M., Jess, A., Kammann, J., Maser, E. and Seibert, H. (2010) Cytotoxic potency of H2O2 in cell cultures: Impact of cell concentration and exposure time. Free Radical Biology and Medicine. **49**, 1298-1305

323   Mao, Y., Song, G., Cai, Q., Liu, M., Luo, H., Shi, M., Ouyang, G. and Bao, S. (2006) Hydrogen peroxide-induced apoptosis in human gastric carcinoma MGC803 cells. Cell Biology International. **30**, 332-337

324   Davies, K. J. A. (1999) The Broad Spectrum of Responses to Oxidants in Proliferating Cells: A New Paradigm for Oxidative Stress. IUBMB Life. **48**, 41-47

325   Polytarchou, C., Hatziapostolou, M. and Papadimitriou, E. (2005) Hydrogen Peroxide Stimulates Proliferation and Migration of Human Prostate Cancer Cells through Activation of Activator Protein-1 and Up-regulation of the Heparin Affin Regulatory Peptide Gene. Journal of Biological Chemistry. **280**, 40428-40435

326   Ohguro, N., Fukuda, M., Sasabe, T. and Tano, Y. (1999) Concentration dependent effects of hydrogen peroxide on lens epithelial cells. Br J Ophthalmol. **83**, 1064-1068

327   Burdon, R. H. (1995) Superoxide and hydrogen peroxide in relation to mammalian cell proliferation. Free Radical Biology and Medicine. **18**, 775-794

328   Junn, E., Lee, K. N., Ju, H. R., Han, S. H., Im, J. Y., Kang, H. S., Lee, T. H., Bae, Y. S., Ha, K. S., Lee, Z. W., Rhee, S. G. and Choi, I. (2000) Requirement of Hydrogen Peroxide Generation in TGF-β1 Signal Transduction in Human Lung Fibroblast Cells: Involvement of Hydrogen Peroxide and Ca2+ in TGF-β1-Induced IL-6 Expression. The Journal of Immunology. **165**, 2190-2197

329   Chuang, Y.-Y. E., Chen, Y., Gadisetti, Chandramouli, V. R., Cook, J. A., Coffin, D., Tsai, M.-H., DeGraff, W., Yan, H., Zhao, S., Russo, A., Liu, E. T. and Mitchell, J. B. (2002) Gene Expression after Treatment with Hydrogen Peroxide, Menadione, or t-Butyl Hydroperoxide in Breast Cancer Cells. Cancer Res. **62**, 6246-6254

330   Martin, G., Andriamanalijaona, R., Mathy-Hartert, M., Henrotin, Y. and Pujol, J. P. (2005) Comparative effects of IL-1β and hydrogen peroxide (H2O2) on catabolic and anabolic gene expression in juvenile bovine chondrocytes. Osteoarthritis and Cartilage. **13**, 915-924

331   Bladier, C., Wolvetang, E. J., Hutchinson, P., de Haan, J. B. and Kola, I. (1997) Response of a primary human fibroblast cell line to H2O2: senescence-like growth arrest or apoptosis? Cell Growth Differ. **8**, 589-598

332   Li, J., Huang, C. Y., Zheng, R. L., Cui, K. R. and Li, J. F. (2000) Hydrogen peroxide induces apoptosis in human hepatoma cells and alters cell redox status. Cell Biol Int. **24**, 9-23

333   Halliwell, B., Aeschbach, R., Löliger, J. and Aruoma, O. I. (1995) The characterization of antioxidants. Food Chem Toxicol. **33**, 601-617

334   Laughton, M. J., Halliwell, B., Evans, P. J., Robin, J. and Hoult, S. (1989) Antioxidant and pro-oxidant actions of the plant phenolics quercetin, gossypol and myricetin. Biochemical Pharmacology. **38**, 2859-2865

335   Halliwell, B. and Gutteridge, J. M. (1984) Oxygen toxicity, oxygen radicals, transition metals and disease. Biochemical Journal. **219**, 1-14

336   Lapidot, T., Walker, M. D. and Kanner, J. (2002) Can Apple Antioxidants Inhibit Tumor Cell Proliferation? Generation of H2O2 during Interaction of Phenolic Compounds with Cell Culture Media. J Agr Food Chem. **50**, 3156-3160

337   Halliwell, B. (2009) The wanderings of a free radical. Free Radic Biol Med. **46**, 531-542

338   Lambert, J. D., Sang, S. and Yang, C. S. (2007) Possible controversy over dietary polyphenols: benefits vs risks. Chem Res Toxicol. **20**, 583-585

339   Nakagawa, H., Hasumi, K., Woo, J. T., Nagai, K. and Wachi, M. (2004) Generation of hydrogen peroxide primarily contributes to the induction of Fe(II)-dependent apoptosis in Jurkat cells by (-)-epigallocatechin gallate. Carcinogenesis. **25**, 1567-1574

340   Galati, G., Moridani, M. Y., Chan, T. S. and O'Brien, P. J. (2001) Peroxidative metabolism of apigenin and naringenin versus luteolin and quercetin: glutathione oxidation and conjugation. Free Radical Biology and Medicine. **30**, 370-382

341   Miyoshi, N., Naniwa, K., Yamada, T., Osawa, T. and Nakamura, Y. (2007) Dietary flavonoid apigenin is a potential inducer of intracellular oxidative stress: The role in the interruptive apoptotic signal. Arch Biochem Biophys. **466**, 274-282

342   Andueza, A., García-Garzón, A., Ruiz de Galarreta, M., Ansorena, E., Iraburu, M. J., López-Zabalza, M. J. and Martínez-Irujo, J. J. (2015) Oxidation pathways underlying the pro-oxidant effects of apigenin. Free Radical Biology and Medicine. **87**, 169-180

343   Sang, S., Yang, I., Buckley, B., Ho, C. T. and Yang, C. S. (2007) Autoxidative quinone formation in vitro and metabolite formation in vivo from tea polyphenol (-)-epigallocatechin-3-gallate: studied by real-time mass spectrometry combined with tandem mass ion mapping. Free Radic Biol Med. **43**, 362-371

344   Sang, S., Lee, M. J., Hou, Z., Ho, C. T. and Yang, C. S. (2005) Stability of tea polyphenol (-)-epigallocatechin-3-gallate and formation of dimers and epimers under common experimental conditions. J Agric Food Chem. **53**, 9478-9484

345   Kern, M., Fridrich, D., Reichert, J., Skrbek, S., Nussher, A., Hofem, S., Vatter, S., Pahlke, G., Rufer, C. and Marko, D. (2007) Limited stability in cell culture medium and hydrogen peroxide formation affect the growth inhibitory properties of delphinidin and its degradation product gallic acid. Mol Nutr Food Res. **51**, 1163-1172

346   Musialik, M., Kuzmicz, R., Pawłowski, T. S. and Litwinienko, G. (2009) Acidity of Hydroxyl Groups: An Overlooked Influence on Antiradical Properties of Flavonoids. The Journal of Organic Chemistry. **74**, 2699-2709

347   Shirai, M., Kawai, Y., Yamanishi, R., Kinoshita, T., Chuman, H. and Terao, J. (2006) Effect of a conjugated quercetin metabolite, quercetin 3-glucuronide, on lipid hydroperoxide-dependent formation of reactive oxygen species in differentiated PC-12 cells. Free Radic Res. **40**, 1047-1053

348   Zenkevich, I., Eshchenko, A., Makarova, S., Vitenberg, A., Dobryakov, Y. and Utsal, V. (2007) Identification of the Products of Oxidation of Quercetin by Air Oxygenat Ambient Temperature. Molecules. **12**, 654

349   Fujimoto, A., Shingai, Y., Nakamura, M., Maekawa, T., Sone, Y. and Masuda, T. (2010) A novel ring-expanded product with enhanced tyrosinase inhibitory activity from classical Fe-catalyzed oxidation of rosmarinic acid, a potent antioxidative Lamiaceae polyphenol. Bioorganic & medicinal chemistry letters. **20**, 7393-7396

350   Muñoz-Muñoz, J. L., Garcia-Molina, F., Ros, E., Tudela, J., GarcíA-Canovas, F. and Rodriguez-Lopez, J. N. (2013) PROOXIDANT AND ANTIOXIDANT ACTIVITIES OF ROSMARINIC ACID. Journal of Food Biochemistry. **37**, 396-408

351   Ramešová, Š., Sokolová, R., Degano, I., Bulíčková, J., Žabka, J. and Gál, M. (2011) On the stability of the bioactive flavonoids quercetin and luteolin under oxygen-free conditions. Anal Bioanal Chem. **402**, 975-982

352   Halliwell, B. (2003) Oxidative stress in cell culture: an under-appreciated problem? FEBS Letters. **540**, 3-6

353   Miller, D. M., Buettner, G. R. and Aust, S. D. (1990) Transition metals as catalysts of "autoxidation" reactions. Free Radical Biology and Medicine. **8**, 95-108

354   Jungbluth, G., Ruhling, I. and Ternes, W. (2000) Oxidation of flavonols with Cu(II), Fe(II) and Fe(III) in aqueous media. Journal of the Chemical Society, Perkin Transactions 2, 1946-1952

355   Canada, A. T., Giannella, E., Nguyen, T. D. and Mason, R. P. (1990) The production of reactive oxygen species by dietary flavonols. Free Radical Biology and Medicine. **9**, 441-449

356   Hajji, H. E., Nkhili, E., Tomao, V. and Dangles, O. (2006) Interactions of quercetin with iron and copper ions: Complexation and autoxidation. Free Radical Res. **40**, 303-320

357   Pietta, P. G. (2000) Flavonoids as antioxidants. Journal of natural products. **63**, 1035-1042

358   Fernandez, M. T., Mira, M. L., Florêncio, M. H. and Jennings, K. R. (2002) Iron and copper chelation by flavonoids: an electrospray mass spectrometry study. Journal of Inorganic Biochemistry. **92**, 105-111

359   Riha, M., Karlickova, J., Filipsky, T., Macakova, K., Rocha, L., Bovicelli, P., Silvestri, I. P., Saso, L., Jahodar, L., Hrdina, R. and Mladenka, P. (2014) In vitro evaluation of copper-chelating properties of flavonoids. RSC Advances. **4**, 32628-32638

360   Liu, Y. and Guo, M. (2015) Studies on Transition Metal-Quercetin Complexes Using Electrospray Ionization Tandem Mass Spectrometry. Molecules. **20**, 8583

361   Procházková, D., Boušová, I. and Wilhelmová, N. (2011) Antioxidant and prooxidant properties of flavonoids. Fitoterapia. **82**, 513-523

362   Brown, J. E., Khodr, H., Hider, R. C. and Rice-Evans, C. A. (1998) Structural dependence of flavonoid interactions with Cu2+ ions: implications for their antioxidant properties. Biochemical Journal. **330**, 1173-1178

363   Kostyuk, V. A., Potapovich, A. I., Strigunova, E. N., Kostyuk, T. V. and Afanas'ev, I. B. (2004) Experimental evidence that flavonoid metal complexes may act as mimics of superoxide dismutase. Arch Biochem Biophys. **428**, 204-208

364   León-González, A. J., Auger, C. and Schini-Kerth, V. B. (2015) Pro-oxidant activity of polyphenols and its implication on cancer chemoprevention and chemotherapy. Biochemical Pharmacology. **98**, 371-380

365   Kaur, M., Velmurugan, B., Rajamanickam, S., Agarwal, R. and Agarwal, C. (2009) Gallic Acid, an Active Constituent of Grape Seed Extract, Exhibits Anti-proliferative, Pro-apoptotic

and Anti-tumorigenic Effects Against Prostate Carcinoma Xenograft Growth in Nude Mice. Pharm Res. **26**, 2133-2140

366   Faried, A., Kurnia, D., Faried, L. S., Usman, N., Miyazaki, T., Kato, H. and Kuwano, H. (2007) Anticancer effects of gallic acid isolated from Indonesian herbal medicine, Phaleria macrocarpa (Scheff.) Boerl, on human cancer cell lines. Int J Oncol. **30**, 605-613

367   Romero, I., Paez, A., Ferruelo, A., Lujan, M. and Berenguer, A. (2002) Polyphenols in red wine inhibit the proliferation and induce apoptosis of LNCaP cells. BJU Int. **89**, 950-954

368   Jorgensen, L. V., Cornett, C., Justesen, U., Skibsted, L. H. and Dragsted, L. O. (1998) Two-electron electrochemical oxidation of quercetin and kaempferol changes only the flavonoid C-ring. Free Radic Res. **29**, 339-350

369   Zhou, A., Kikandi, S. and Sadik, O. A. (2007) Electrochemical degradation of quercetin: Isolation and structural elucidation of the degradation products. Electrochemistry Communications. **9**, 2246-2255

370   Hendrickson, H. P., Kaufman, A. D. and Lunte, C. E. (1994) Electrochemistry of catechol-containing flavonoids. Journal of Pharmaceutical and Biomedical Analysis. **12**, 325-334

371   Ramešová, Š., Sokolová, R., Tarábek, J. and Degano, I. (2013) The oxidation of luteolin, the natural flavonoid dye. Electrochimica Acta. **110**, 646-654

372   Awad, H. M., Boersma, M. G., Boeren, S., van Bladeren, P. J., Vervoort, J. and Rietjens, I. M. (2001) Structure-activity study on the quinone/quinone methide chemistry of flavonoids. Chem Res Toxicol. **14**, 398-408

Acknowledgment

First and foremost I would like to thank PD Dr. Thomas Letzel for his support, guidance and advice throughout the years we´ve been working together. In 2006 during my studies of biology I was lucky enough to do an internship in his group, during which I was first introduced to mass spectrometry. Besides being enthusiastic and a keen advisor on all things analytical, he was always able to create a work environment, which was warm, friendly, trustful and supportive.

Furthermore my gratitude goes to Prof. Dr. Michael Pfaffl for providing a harbor for all research non-analytical. Due to being submerged in the world of analytics most of the time, his advice and the opportunity to discuss different scientific perspectives as well as the exchange with colleagues from the institute of animal physiology and immunology were much-valued.

I also want to thank Prof. Dr. Wilfried Schwab and Prof. Dr. Dieter Langosch for their participation as examiner and chairman, respectively, during the defense of my doctor's thesis.

I´m also very much obliged to PD Dr. Johanna Graßmann, who is an inexhaustible source of knowledge, reliability, readiness to help, patience and kindness. I couldn´t have wished for a better supervisor, advisor and mentor.

For financial support I thank PD Dr. Thomas Letzel, the Vereinigung zur Milchwissenschaftlichen Forschung an der Technischen Universität München e.V., Vital Solutions GmbH and Amino Up Chemicals Co. Ltd..

For the provision of IPEC-J2 cells I thank Dr. Karsten Tedin.

I thank Vital Solutions GmbH and Amino Up Chemicals Co. Ltd. for the provision of Perilla frutescens plant material and water extract.

I´m especially grateful for the positive and supportive work atmosphere created by my fellow colleagues Sylvia Grosse, Dr. Romy Scheerle, Dr. Alper Aydin, Dr. Giorgia Greco, Dr. Christoforos Christoforidis, Therese Burkhardt, Lara Stadlmair, Dr. Michael Krappmann, Dr.

Scientific communications

Original peer reviewed scientific publications

Kaufmann, C.M., Graßmann, J., Treutter, D., Letzel, T., 2014. Utilization of real-time electrospray ionization mass spectrometry to gain further insight into the course of nucleotide degradation by intestinal alkaline phosphatase. *Rapid communications in mass spectrometry*, 28, 869-878

Krappmann, M.*, **Kaufmann, C.M.***, Scheerle, R.K., Graßmann, J., Letzel, T., 2014. Achroma Software-High-Quality Policy in (a-)Typical Mass Spectrometric Data Handling and Applied Functional Proteomics. *Proteomics & Bioinformatics*, 7(9), 264-271.

Burkhardt, T.*, **Kaufmann, C.M.***, Letzel T., Graßmann, J., 2015. Enzymatic Assays Coupled with Mass Spectrometry with or without Embedded Liquid Chromatography. *ChemBioChem*, 16(14), 1985-1992.

Kaufmann, C.M., Graßmann, J., Letzel, T., 2016. HPLC method development for the online-coupling of chromatographic Perilla frutescens extract separation with xanthine oxidase enzymatic assay. *Journal of Pharmaceutical and Biomedical Analysis*, 124, 347-357.

Kaufmann, C.M., Letzel, T., Graßmann, J., Pfaffl, M.W., 2016. Effect of Perilla frutescens Extracts on Porcine Jejunal Epithelial Cells. *Phytotherapy Research 2017, 31(2), 303–311*

*Equal contribution

Oral scientific presentation

Kaufmann, C.M.: Online coupled continuous flow system: The investigation of enzymatic activity in the presence of a chromatographically separated complex mixture. Requirements and Limitations.

24. Doktorandenseminar des AK Separation Science, GDCh, 05. - 07.01.2014, Hohenroda, Germany

Kaufmann, C.M.: Die asiatische ‚Wunderpflanze' Perilla frutescens — Inhaltsstoffe und deren regulative Funktion.

Semiar *Lebensmittel im Fokus*: *Wissenschaftliche Lösungen in der Industrie und an Universitäten,* 19.11.2015, Freising, Germany

Abstracts and posters presented at scientific meetings

Kaufmann, C.M., Graßmann, J., Letzel, T.: Mass spectrometric analysis of Perilla frutescens extracts and enzymatic assays for development of an online coupled system. *Anakon*, 22. – 25.03.2011, Zurich, Switzerland

Kaufmann, C.M., Graßmann, J., Letzel, T.: Establishment of control measurements for a multi-component enzymatic assay investigated with an online coupled continuous flow system. *Anakon*, 04. – 07.03.2013, Essen, Germany

Kaufmann, C.M., Graßmann, J., Letzel, T.: Multi-component enzymatic assay investigated with an online coupled continuous flow system and mass spectrometry. *Proteomics Forum*, 17. – 21.03.2013, Berlin, Germany

Curriculum vitae

Name	Christine Martina Kaufmann
Date of birth	April, 14th 1984
Place of birth	Mühlhausen/Thüringen, Germany

09/2010 – 12/2016	Research assistant at the Institute of Animal Physiology and Immunology, Technical University of Munich, Prof. Dietmar Zehn (former Institute of Physiology, Prof. Heinrich H.D. Meyer) and at the Chair of Urban Water Systems Engineering (Analytical Research Group), Technical University of Munich, Prof. Jörg E. Drewes
01/2010 - 07/2010	Diploma thesis (Dipl.-Biol.) at the Chair of Chemical-Technical Analysis, Technical University of Munich, Prof. Harun Parlar
10/2004 - 09/2010	Studies in Biology at the Technical University of Munich, Major "Technical Biology", Minors "Human biology" and "Immunology"
08/1999 - 07/2003	Secondary school and Graduation at Hans-Leinberger Gymnasium Landshut
08/1994 – 08/1999	Secondary school, Anna-Essinger Gymnasium Ulm

Appendix

Appendix I

Utilization of real-time electrospray ionization mass spectrometry to gain further insight into the course of nucleotide degradation by intestinal alkaline phosphatase

Christine M. Kaufmann, Johanna Graßmann, Dieter Treutter and Thomas Letzel

The following work was conducted in order to study the activity of intestinal alkaline phosphatase towards its physiological nucleotide substrates using a continuous flow setup and mass spectrometric detection.

The enzymatic activity was investigated at three different pH values, namely pH 6.0, 7.4 and 9.0, to be able to comparatively assess the substrate degradation, intermediate generation/degradation and product generation in detail. The experimental planning, conduction, data evaluation, literature research and the writing was done by me.

Utilization of real-time electrospray ionization mass spectrometry to gain further insight into the course of nucleotide degradation by intestinal alkaline phosphatase

Christine M. Kaufmann[1], Johanna Graßmann[1], Dieter Treutter[2] and Thomas Letzel[1]*

[1]Chair of Urban Water Systems Engineering, Technische Universität München, Am Coulombwall 8, 85748 Garching, Germany
[2]Institute of Fruit Science, Technische Universität München, Dürnast 2, 85354 Freising, Germany

RATIONALE: Related with its ability to degrade nucleotides, intestinal alkaline phosphatase (iAP) is an important participant in intestinal pH regulation and inflammatory processes. However, its activity has been investigated mainly by using artificial non-nucleotide substrates to enable the utilization of conventional colorimetric methods. To capture the degradation of the physiological nucleotide substrate of the enzyme along with arising intermediates and the final product, the enzymatic assay was adapted to mass spectrometric detection. Therewith, the drawbacks associated with colorimetric methods could be overcome.

METHODS: Enzymatic activity was comparatively investigated with a conventional colorimetric malachite green method and a single quadrupole mass spectrometer with an electrospray ionization source using the physiological nucleotide substrates ATP, ADP or AMP and three different pH-values in either methodological approach. By this means the enzymatic activity was assessed on the one hand by detecting the phosphate release spectrometrically at defined time points of enzymatic reaction or on the other by continuous monitoring with mass spectrometric detection.

RESULTS: Adaption of the enzymatic assay to mass spectrometric detection disclosed the entire course of all reaction components – substrate, intermediates and product – resulting from the degradation of substrate, thereby pointing out a stepwise removal of phosphate groups. By calculating enzymatic substrate conversion rates a distinctively slower degradation of AMP compared to ADP or ATP was revealed together with the finding of a substrate competition between ATP and ADP at alkaline pH.

CONCLUSIONS: The comparison of colorimetric and mass spectrometric methods to elucidate enzyme kinetics and specificity clearly underlines the advantages of mass spectrometric detection for the investigation of complex multi-component enzymatic assays. The entire course of enzymatic substrate degradation was revealed with different nucleotide substrates, thus allowing a specific monitoring of intestinal alkaline phosphatase activity. Copyright © 2014 John Wiley & Sons, Ltd.

The sphere of the enzymatic activity of intestinal alkaline phosphatase (iAP) is already known to be multifaceted, ranging from adjustment of intestinal pH-value to downregulation of lipid intestinal absorption[1] and to effects on immunity and inflammation.[2] The impact of iAP on immunity includes its capability to dephosphorylate lipopolysaccharide (LPS), the regulation of intestinal bacterial entry into the body and its involvement in the formation of adenosine by the breakdown of adenosine-5′-triphosphate (ATP), either possessing regulatory effects on inflammatory processes.[2–4]

Besides the modulatory function of iAP in inflammation, the enzyme takes part in intestinal pH regulation, whereby a drop in pH-value leads to a reduction in the activity of the enzyme and with that to an accumulation of ATP in the intestine, in this manner provoking bicarbonate secretion by

the stimulation of ATP receptors on enterocytes. The consequent rise in pH coincidently increases the activity of iAP, thus inducing an enhanced ATP breakdown followed by a reduced bicarbonate secretion.[1]

The investigation of enzymatic substrate degradation is usually conducted by means of applying colorimetric methods, which are often well established and therefore easy to handle. However, they predominantly provide information solely about either substrate degradation or product generation, resulting in a picture lacking important information or that is ambiguous.

In this regard, mass spectrometry (MS) has already proved its advantageous features, attested by the presence of a variety of studies investigating a considerable amount of different enzymes. Studies range from the determination of the kinetics of enzymes, including the assessment of inhibitor constants,[5–7] to the elucidation of noncovalent complexes[8,9] and conformational fluctuations associated with enzymatic catalysis.[10] Besides, elaborate setups like online coupled continuous flow approaches coupled with mass spectrometric detection have been applied for the finding of regulatory molecules in complex mixtures affecting enzymatic activity.[11,12]

* *Correspondence to:* T. Letzel, Chair of Urban Water Systems Engineering, Technische Universität München, Am Coulombwall 8, 85748 Garching, Germany.
  E-mail: t.letzel@tum.de

Concomitantly, MS detection provides the possibility to entirely capture the substrate and product trace continuously in real-time.[13] Moreover, detailed information about multiple reaction intermediates may be unveiled, which are usually not measureable with colorimetric methods.[14]

In fact the degradation of ATP by iAP has been shown to include the formation of intermediates, but in an elaborate and time-consuming procedure only monitoring single time points of enzymatic reaction and also disregarding the generation of adenosine.[15]

Because of its pH dependence, the activity of iAP has already been investigated in a wide range of pH-values using mainly the artificial substrate *p*-nitrophenyl phosphate.[16,17] However, it has been shown that the use of chromogenic substrates may significantly affect enzymatic specificity.[18] Due to the variety of important functions associated with the ability of iAP to degrade nucleotides and in view of the possibility provided by MS detection to employ a non-chromogenic substrate, enzymatic activity was tested with physiological substrates. An MS-compatible enzymatic assay was developed to enable the specific monitoring of all reaction intermediates present in the course of the reaction and to gain further insight into the enzymatic degradation of several substrates.

EXPERIMENTAL

Reagents and chemicals

Ammonium heptamolybdate (#RDHA31402) was purchased from Riedel de Häen (Seelze, Germany); malachite green oxalate (#3076) was purchased from VWR BDH prolabo (Darmstadt, Germany); poly(vinyl alcohol) (#363138), ammonium acetate (#A7330), ATP (#A2383), ADP (#A2754), AMP (#A1752), intestinal alkaline phosphatase from bovine intestinal mucosa (Enzyme Commission (EC) number 3.1.3.1., molecular weight (MW) ~160kDa) (#P7640), water LC-MS CHROMASOLV(R) (39253-1L-R) were purchased from Sigma-Aldrich (Steinheim, Germany).

Instrumentation

Photometric measurements were performed with a SLT Spectra plate reader (SLT Instruments, Crailsheim, Germany).

Mass spectrometric measurements were conducted with a MSQ Plus single quadrupole mass spectrometer (Wissenschaftliche Gerätebau Dr. Ing. Herbert Knauer, Berlin, Germany) equipped with an ESI source in the positive ionization mode. Mass spectrometric needle voltage was set at 3.5 kV, cone voltage at 75 V and temperature at 225°C. All samples were detected with a mass range of 100 to 1000 *m/z*.

Sample preparation for colorimetric determination of enzymatic activity

Reagents for malachite green assay, adapted from Henkel *et al.*[19] were always prepared freshly by thoroughly mixing a proportion of 16.7% of a 5.72% (w/v) ammonium heptamolybdate solution solved in 6 M HCl, 16.7% of a 2.32% (w/v) poly(vinyl alcohol) solution dissolved in

water (Milli-Q), 33.3% of a 0.081% (w/v) malachite green oxalate solution dissolved in water (Milli-Q) and 33.3% of water (Milli-Q).

Activity of iAP was investigated by means of colorimetric detection of inorganic (free) phosphate. Due to the reaction between malachite green molybdate and inorganic phosphate under acidic conditions a malachite green phosphomolybdate complex is formed that can be directly related to the phosphate released by the enzyme's activity.

The assay was conducted in 10 mM ammonium acetate solution (pH 6.0, 7.4 or 9.0) with either ATP, ADP or AMP employed as enzymatic substrates. Ammonium acetate was selected according to the work of Hogenboom *et al.*[20] and Dennhart and Letzel,[21] who have already been able to demonstrate its applicability for the investigation of enzymatic activity.

For each experiment phosphate release was determined at seven time points within 90 min. Therefore, seven individual enzymatic assays were prepared in 10 mM ammonium acetate solution with the respective pH-values with 0.2U/mL (≙ 44.64nM) iAP and 40 µM of the respective substrate (500 µL total volume). The reaction was started simultaneously by the addition of the enzyme to all assays.

In the case of time point 0, the enzyme was added to the assay, whereupon an aliquot was removed immediately and the enzymatic reaction was terminated by addition of malachite green reagent.

In case of time points 15, 30, 45, 60, 75 and 90 min an aliquot of one preliminarily prepared enzymatic assay was withdrawn and mixed with malachite green reagent to terminate the enzymatic reaction. The remaining assay was discarded. The aliquot/malachite green mixture was incubated for 20 min at room temperature and absorption was measured at 620 nm to detect the released phosphate. All experiments were performed six to nine times on two different days at room temperature.

Data evaluation in colorimetric experiments

Controls measured with the respective substrate in 10 mM ammonium acetate solution pH 6.0, 7.4 or 9.0 without enzyme revealed no increase in absorption. Therefore, an auto-dephosphorylation of the substrates could be excluded, whereupon a blank value correction was not implemented.

Data interpretation was conducted by comparing the slopes of trend lines within the initial linear range of phosphate release. The time interval for data evaluation was minutes 0 to 15 for enzymatic assays in pH 9.0, due to the faster reaction and minutes 0 to 30 for enzymatic assays in pH 6.0 or 7.4 (cf. Supplementary Table S1, Supporting Information).

Sample preparation for MS determination of enzymatic activity

Initially, different substrate and enzyme concentrations were tested with ATP substrate at pH 7.4. The most suitable combination was identified as that which resulted in a complete degradation of the substrate within 30 min and therewith in a considerable flattening of ATP substrate trace. iAP assays were performed in positive ionization mode, to maintain comparability to other enzymatic assays already established and in this context to prospectively conduct experiments with

multiplex enzymatic assays.[22] Even though higher intensities may be anticipated in negative mode, initial intensities of the nucleotides substrates between at least 150 000 counts for ATP substrate in pH 9.0 and up to 400 000 counts for AMP in pH 7.4 were obtained in positive mode.

Due to the pH-values applied and the disparity of available phosphate groups of the substrate, intermediates and of the product, different charge states of the assay components might be present. Therefore, the negatively charged groups might lead to a signal intensity underestimation of ATP and ADP towards AMP or adenosine. Nevertheless, the intensities of all assay components were exceedingly sufficient, thus enabling the assessment of the substrate degradation by means of an exponential trend line approach, also taking into account that quantification was not intended. The activity of iAPs was examined towards ATP, ADP or AMP in 10 mM ammonium acetate solution at pH 6.0, 7.4 or 9.0, respectively. The pH-value of the 10 mM ammonium acetate solution was checked daily and was readjusted to the respective value if necessary. All experiments were conducted 5 to 11 times on two different days at 21°C.

Initially, 40 μM of the respective substrate was mixed with 10 mM ammonium acetate solution pH 6.0, 7.4 or 9.0. The enzyme concentration of assays conducted at pH 6.0 or 7.4 was set to 0.2 U/mL (≙ 44.64 nM). Due to a distinct higher enzymatic activity at pH 9.0 (see Results, Figs. 4(a) and 4(b)), the concentration of enzyme was quartered to 0.05 U/mL (≙ 11.16 nM) to retain the viability of the data-evaluation procedure via the application of an exponential trend line. Controls were measured with all possible substrate-pH assay combinations but without enzyme to be able to exclude phosphate release related to mass spectrometric settings.

Reactions were always started together with mass spectrometric recording by pipetting the enzyme into the substrate/ammonium acetate solution, followed by a thorough and brief mixing. The assay was then drawn up into a 500 μL glass syringe (Hamilton-Bonaduz, Switzerland), clamped into a syringe pump (model 11 Plus, Harvard Apparatus, Hugo Sachs Elektronik, Hugstetten, Germany) and continuously pumped with 10 μL/min through a Peek tubing (1/16" × i.d. 0.13 mm, length 410 mm) into the source of the mass spectrometer. This procedure caused a time delay until the first signal could be detected and therefore the first 3 min of MS measurements were not considered for further data evaluation. Enzymatic reaction was recorded for 30 min.

Data evaluation in MS experiments

Data were processed using Xcalibur software 2.1.0.1139 (Thermo Fisher Scientific Inc., Waltham, MA, USA). The extracted ion chromatograms (EICs) of each assay component, obtained by using a m/z range of ±0.5 Da to the respective calculated m/z-value, were summed for the following compounds: Adenosine with m/z 268.1 and 290.1, i.e. [Adenosine+H]$^+$ and [Adenosine+Na]$^+$; AMP with m/z 348.1, 370.1, 386.0, 392.0 and 408.0; ADP with m/z 428.0, 450.0, 466.0, 472.0 and 488.0; ATP with 508.0, 530.0, 546.0, 552.0 and 568.0, i.e. [M+H]$^+$, [M+Na]$^+$, [M+K]$^+$, [M–H+2Na]$^+$ and [M–H+Na+K]$^+$. The EICs were smoothed with a Gaussian function using a 15-points function width. Further processing was conducted with Microsoft Office Excel 2007.

Table 1. Overview of iAP enzymatic activity towards ATP, ADP or AMP substrates at pH 6.0, 7.4 or 9.0 presented either as slopes of trend lines [Δabsorption/Δtime] for colorimetric experiments or substrate degradation rates [relative substrate degradation/min] for mass spectrometric assays along with the respective standard deviations (± value)

	Colorimetric assay			Mass spectrometric assay		
	Slope of linear trend line [Δabsorption/Δtime]			Degradation rate [relative substrate degradation/min]		
	pH 6.0	pH 7.4	pH 9.0	pH 6.0	pH 7.4	pH 9.0
ATP	$1.350 \times 10^{-3} \pm 0.164 \times 10^{-3}$	$5.856 \times 10^{-3} \pm 0.949 \times 10^{-3}$	$19.73 \times 10^{-3} \pm 2.976 \times 10^{-3}$	10.17 ± 0.734	38.10 ± 13.63	575.6 ± 58.12
ADP	$1.650 \times 10^{-3} \pm 0.197 \times 10^{-3}$	$5.033 \times 10^{-3} \pm 1.476 \times 10^{-3}$	$12.27 \times 10^{-3} \pm 1.133 \times 10^{-3}$	8.430 ± 4.379	27.42 ± 15.47	751.7 ± 128.0
AMP	$1.083 \times 10^{-3} \pm 0.075 \times 10^{-3}$	$2.467 \times 10^{-3} \pm 0.711 \times 10^{-3}$	$7.133 \times 10^{-3} \pm 0.561 \times 10^{-3}$	7.001 ± 1.175	11.48 ± 5.379	121.9 ± 32.33

At first each individual assay was normalized to 1 whereupon an exponential trend line was applied to the respective substrate trace from minute 3 to 30 for assays at pH 7.4 and 6.0 and minute 3 to 15 for assays at pH 9.0 (Table 1) resulting in Eqn. (1). The substrate degradation was observed until a plateau at a remaining intensity of 0.05 was reached, which reflected the termination of the reaction. y = 0.05 was therefore set as the end point of the reaction. By using Eqn. (1), the time (x) required for the enzyme to completely degrade the substrate (y = 0.05) was calculated, which was then inserted into Eqn. (2) to determine the enzymatic conversion rate.

$$y = a * \exp(bx) \tag{1}$$

$$\text{conversion rate} \left[\min^{-1}\right] = (c[\text{substrate}]/c[\text{enzyme}])/x \tag{2}$$

Statistics

Statistical analysis was performed in the same way for photometric and mass spectrometric data sets by applying Welch's t-test, which takes into account the extent of the respective standard deviations. Assays conducted with the same substrate at different pH or assays with ATP, ADP or AMP at the same pH-value were compared pairwise. Statistical significance was assumed for p-values of 0.05 to 0.01 (*), very significant for p-values of 0.01 to 0.001 (**) and extremely significant for p-values <0.001 (***).

RESULTS AND DISCUSSION

Intestinal pH regulatory mechanisms and the enzyme's contribution to inflammatory processes along with a variety of other functions are associated with the ability of iAP to dephosphorylate nucleotides.

Since ATP is naturally degraded to adenosine by the stepwise removal of its three phosphate groups,[15] possible intermediate products ADP and AMP were also used as substrates (Fig. 1).

Moreover, enzymatic activity was examined at three different pH-values (pH 6.0, 7.4 and 9.0). pH 9.0 was chosen, since the enzyme possesses its highest activity in alkaline medium.[17] Besides, the alkaline pH was selected to prospectively investigate regulatory compounds affecting enzymatic activity, which was similarly done previously by Vovk *et al.*, who studied inhibition of iAP at pH 9.0.[23] In

contrast, acidic pH 6.0 was selected due to pH-values present in the small intestine, that range from 5.5 to 7.5, and might even locally decrease further during intestinal inflammation.[24] In addition, pH 7.4 was chosen to represent the standard pH of physiological relevance.

Besides the employment of three different nucleotide substrates as well as three different pH-values, the activity of iAP was determined using on the one hand mass spectrometric detection and on the other a well-established photometric method. The absorption values obtained hereby are attributed to the overall release of phosphate. Besides its advantageous features like being well established and easy to handle, a main disadvantage of this procedure is the indistinguishability of the actual origin of released phosphate. A mass spectrometric assay was therefore established to comprehensively examine the course of the reaction, to obtain insight into the generation of all intermediates and to detect the final product adenosine. The gain in information provided by mass spectrometric measurements may thereby help to further elucidate pH-dependent substrate degradation and substrate preferences of iAP in a physiological context.

Colorimetric determination of iAP activity

The photometrical determination of enzymatic activity was conducted by observing the phosphate released from either ATP, ADP or AMP substrate at pH 6.0, 7.4 or 9.0.[25]

By comparing the initial increases of absorption of all assay compositions (data not shown) the most obvious differences in slopes between the substrates used were measured at pH 9.0, where the increase is highest for ATP, followed by ADP (62% compared to ATP) and lowest for AMP (36% compared to ATP) (Fig. 2). Due to the fact that nearly all phosphate is released during the first 15 min at pH 9.0, the differences in slopes may be explained by the availability of phosphate groups with either ATP or ADP or AMP substrate. This hypothesis was confirmed by finding the highest final amount of phosphate using ATP as substrate, followed by ADP and AMP at pH 9.0 (data not shown).

At pH 7.4 the increases in phosphate are considerably slower in case of all substrates compared to pH 9.0 (Fig. 2). However, just as at pH 9.0, most phosphate is released from ATP, followed by ADP and AMP. Although the difference in phosphate increase during the first 30 min is not significant between ATP and ADP substrate at pH 7.4, the mean value was detected to be slightly lower for ADP (86%) compared to ATP (100%), whereas it was
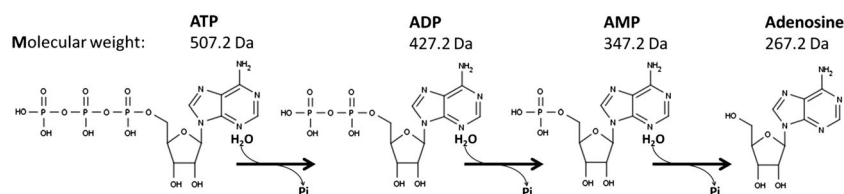
Figure 1. Enzymatic hydrolysis and stepwise removal of inorganic phosphate leads to the generation of the final iAP product adenosine. Nucleotide structures are given along with the average molecular weights of the respective neutral compounds.
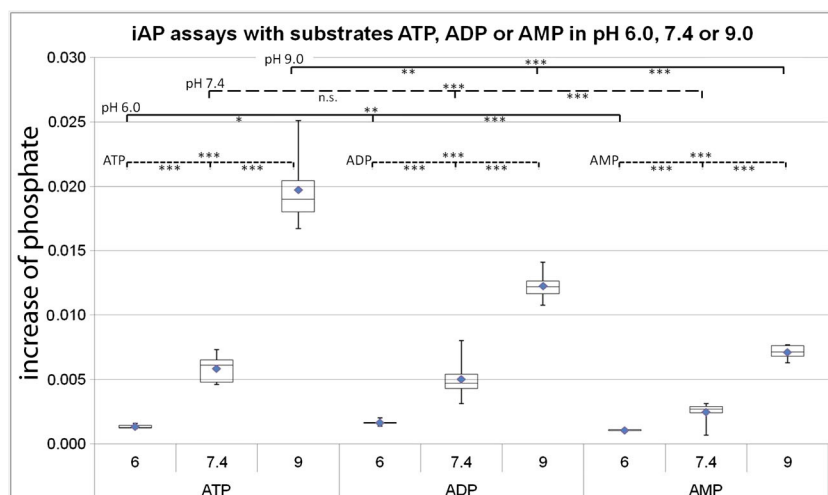
Figure 2. Box-and-whisker plot of numeric values of slopes of linear trend lines of initial phosphate increase photometrically detected; positive and negative whisker, first quartile, median and third quartile, mean value (♦), significant for p-values of 0.05 to 0.01 (*), very significant for p-values of 0.01 to 0.001 (**) and extremely significant for p-values <0.001 (***), not significant for values >0.05 (n.s.), n = 6–9.

significantly reduced with AMP substrate (42%) (Fig. 2). That is because the amount of available phosphate groups does not decrease markedly during the early stages of

reaction using ATP or ADP, since the breakdown of ATP or ADP substrate again results in the generation of ADP/AMP or AMP, respectively, which in turn serve as
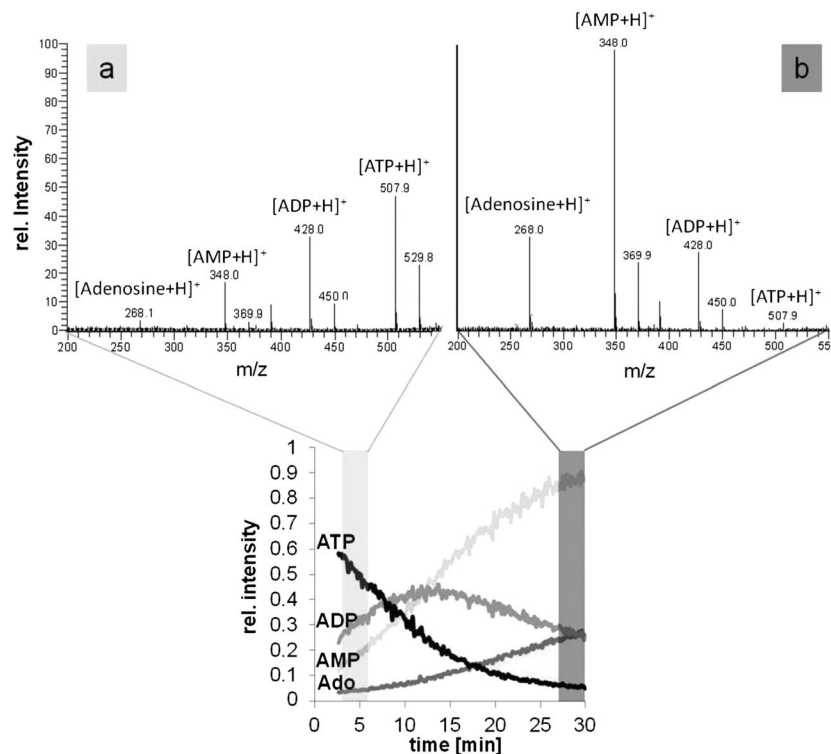
Figure 3. Assay component's signal changes within the m/z range 200 to 550 at pH 7.4 at the beginning of enzymatic conversion (a: average intensity of time range minute 3 to 6 corresponding to light grey area) and the end of the measurement (b: average intensity of time range minute 27 to 30 corresponding to dark grey area). Spectrum intensity maximum '100' corresponds to 2.63×10^5 counts. Prominent m/z within spectrum: [Ado+H]$^+$: 268.0; [AMP+H]$^+$: 348.0, [AMP+Na]$^+$: 369.9; [ADP+H]$^+$: 428.0, [ADP+Na]$^+$: 450.0; [ATP+H]$^+$: 507.9, [ATP+Na]$^+$: 529.8.

substrate. In contrast with AMP substrate merely the final product adenosine is generated. Therefore, with ATP or ADP compared to AMP substrate, it is more likely for the enzyme to encounter a substrate during the first stages of the reaction, indicating the availability of substrate as the rate-limiting step with AMP substrate at pH 7.4 and ATP, ADP and AMP substrate at pH 9.0.

At pH 6.0 enzymatic activity is distinctly reduced compared to alkaline or neutral pH, resulting in a considerably slower phosphate release from ATP (7% compared to pH 9.0), ADP (13% compared to pH 9.0) and AMP (15% compared to pH 9.0) (Table 1).

However, the differences in slopes (Fig. 2) between the three substrates are significant, with ADP leading to a faster increase in detectable phosphate (122%) than ATP (100%) and AMP (80% compared to ATP). At acidic pH the pyrophosphate synthesis by iAP is enhanced,[26,27] probably leading to an excess production of pyrophosphate with ATP compared to ADP substrate. Since the malachite

green assay does not respond to pyrophosphate,[28] its formation would lead to an underestimated phosphate release in the case of ATP substrate. In fact, mass spectrometric measurements (see below) revealed a tendency for faster degradation of ATP compared to that of ADP (83%) at pH 6.0.

Although the application of a colorimetric method to detect the enzymatic activity provides information about the effect of pH on the degradation of different nucleotide substrates, it also reveals several drawbacks. First of all a differentiation between the phosphate released from initial substrate or intermediate products is not achievable. Additionally, it cannot be clarified whether the phosphate groups are removed in a stepwise manner or if, for instance, pyrophosphate is released. This matter was first addressed by Moss *et al.*, who proved a stepwise removal from ATP resulting in ADP and AMP as intermediate products.[15] Nevertheless, this investigation was conducted at one pH-value, i.e. pH 9.5, and solely ATP was used as substrate. So to our best
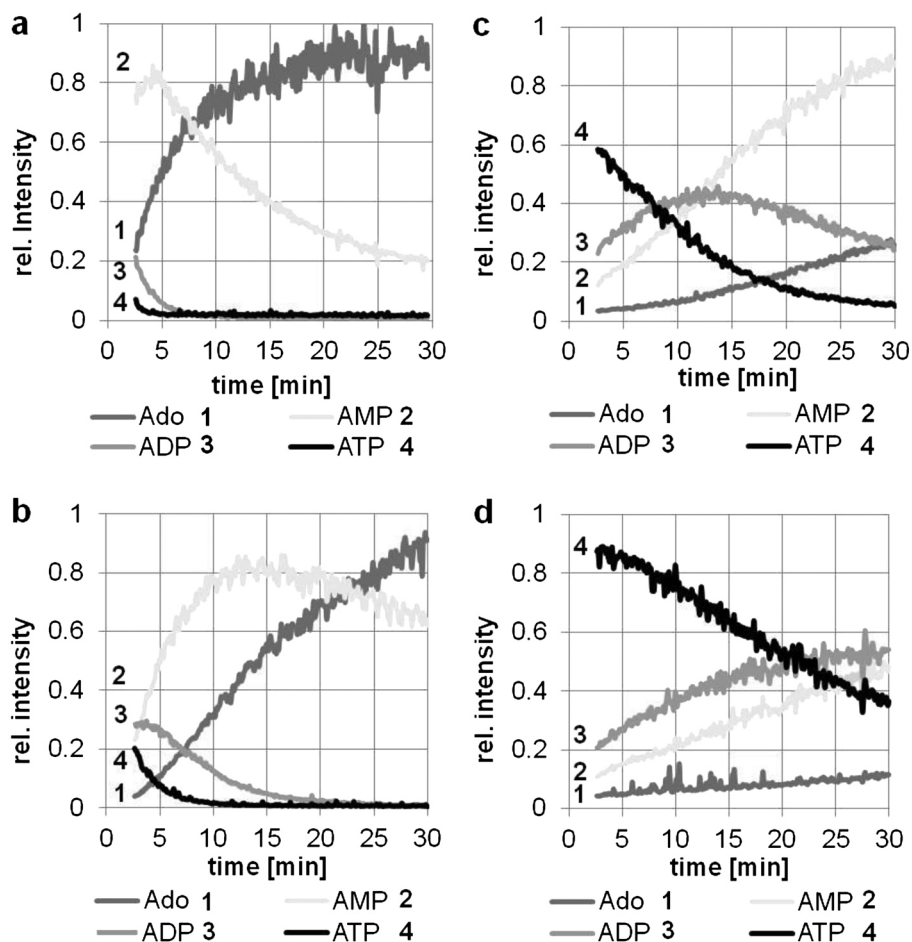
Figure 4. Mass spectrometric determination of enzymatic degradation of 40 μM ATP substrate: (a) iAP concentration 44.64 nM, pH 9.0; (b) iAP concentration 11.16 nM, pH 9.0; (c) iAP concentration 44.64 nM, pH 7.4; (d) iAP concentration 44.64 nM, pH 6.0; *m/z* evaluated, summarized and displayed here: Ado with *m/z* 268.1 and 290.1, i.e. [Ado+H]⁺ and [Ado+Na]⁺; AMP with *m/z* 348.1, 370.1, 386.0, 392.0 and 408.0; ADP with *m/z* 428.0, 450.0, 466.0, 472.0 and 488.0; ATP with 508.0, 530.0, 546.0, 552.0 and 568.0, i.e. [M+H]⁺, [M+Na]⁺, [M+K]⁺, [M–H+2Na]⁺ and [M–H+Na+K]⁺; n = 5–11.

knowledge, no information about detailed reaction kinetics, the degradation of ADP or AMP as substrates and also about the activity of iAP towards these three substrates at different pH-values is available. For these reasons, a mass spectrometric assay was established to obtain detailed data of the overall course of the reaction. In this regard Fig. 3 exemplarily shows the results of enzymatic ATP conversion at pH 7.4. Traces of ATP substrate, intermediates ADP and AMP and the final product adenosine are presented along with spectra revealing the shift of m/z signals associated with the degradation of ATP substrate (m/z 507.9, 529.8) and the generation of ADP (m/z 428.0, 450.0), AMP (m/z 348.0, 369.9) and adenosine (m/z 268.1).

MS determination of iAP activity

Applying the same concentrations as in the photometric assay, a nearly complete degradation of ATP within the first 5 min at pH 9.0 was revealed (Fig. 4(a)), that could not be assessed with photometric detection, due to merely detecting the overall phosphate release.

To enable the calculation of conversion rates by applying exponential trend lines to the substrate degradation trace, enzyme concentration at pH 9.0 was quartered to 11.16 nM, resulting in a quartering of enzymatic activity visible by the shift of AMP detection maximum from minute 4.18 with 44.64 nM (Fig. 4(a)) to minute 16.33 with 11.16 nM iAP (Fig. 4(b)). Figure 4 furthermore provides an overview of the ATP substrate degradation, the formation of ADP and AMP intermediates and the generation of the final product adenosine in 10 mM ammonium acetate solution at pH 9.0 (Figs. 4(a) and 4(b)), pH 7.4 (Fig. 4(c)) and pH 6.0 (Fig. 4(d)). In contrast to the photometric approach, for which the slopes of linear trend lines were used to obtain numeric values to enable the comparison of phosphate releases, in the case of MS-detected assays conversion rates were calculated and are presented in Fig. 5.

At pH 9.0 (Fig. 4(a), high enzyme concentration) the degradation of both ATP and ADP is completed within the first 7 to 8 min, whereas AMP slightly increases till minute 5 before also decreasing until minute 30. Furthermore, the AMP curve reveals a flattening, that is also reflected by the curve of the final product adenosine, both indicating a decelerated degradation of AMP at the end of the measurement.

By comparing the substrate degradation at pH 9.0 the conversion rate determined by mass spectrometry is highest for ADP (131%) and lowest for AMP (21% compared to ATP) (Fig. 5 and Table 1). The inferior conversion rate for ATP in comparison to ADP substrate might be associated with an initial substrate competition between ATP and the product ADP and AMP, eventually leading to a decreased degradation and therewith conversion rate of ATP.

Enzymatic assays with ADP substrate revealed a similar progress of fast enzymatic substrate degradation and related intermediate and product generation as those assays measured with ATP substrate (see Supplementary Figs. S2(a)–S2(c), Supporting Information). Like ATP substrate at pH 9.0, ADP substrate is completely degraded within approximately 10 min, revealing a comparable substrate preference for ATP and ADP. In contrast with AMP substrate at pH 9.0 a continuous decrease was observed over the whole measurement time, uncovering AMP as a comparatively poor substrate (21% compared to ATP, Supplementary Fig. S1(a), Supporting Information).

At pH 7.4 the degradation of ATP and simultaneously the generation of ADP are distinctively slower compared to assays conducted at pH 9.0 (Fig. 4(c)). After approximately 12 min a plateau is reached for ADP, i.e. formation from ATP and degradation to AMP is of similar velocity. Contrary to assays at pH 9.0 no decrease in AMP intensity was detected at neutral pH. However, generation of adenosine is apparent during the whole time of measurement, testifying to the degradation of AMP to adenosine, which in conclusion indicates a higher generation of AMP from ADP than degradation of AMP to adenosine.
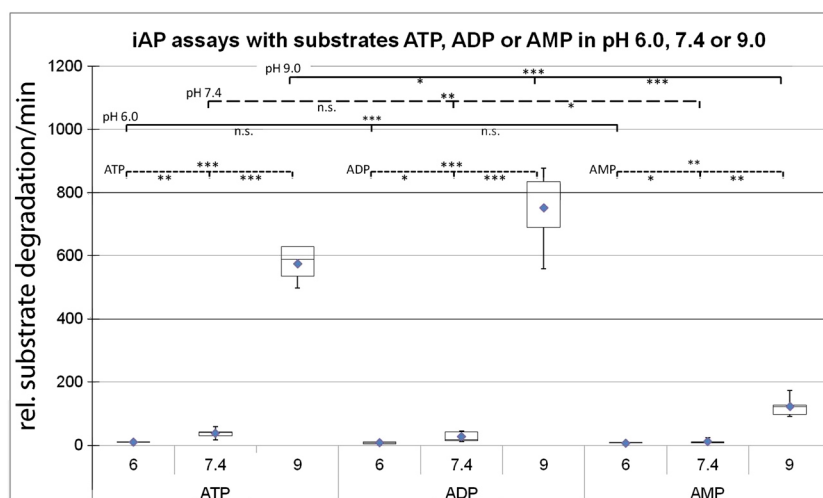
Figure 5. Box-and-whisker plot of substrate conversion rates calculated from exponential trend lines applied to the respective substrate traces mass spectrometrically detected; positive and negative whisker, first quartile, median and third quartile, mean value (◆), significant for p-values of 0.05 to 0.01 (*), very significant for p-values of 0.01 to 0.001 (**) and extremely significant for p-values <0.001 (***), not significant for values >0.05 (n.s.); n = 5–11.

Compared to ATP substrate the conversion rate with ADP substrate at pH 7.4 is decreased to 72% (Fig. 5), pointing out a less pronounced substrate competition at pH 7.4 in contrast to pH 9.0. This is attributed to a lower conversion rate of ATP at pH 7.4 (7%, Fig. 5) compared to the conversion rate of ATP at pH 9.0, resulting in a minor quantity of ADP generated at pH 7.4, which is insufficient to provoke substrate competition. Furthermore, a much more pronounced increase in AMP at pH 9.0 was detected from the beginning of the measurement compared to the increase in AMP at pH 7.4, which results in a higher amount of competitive substrate AMP at pH 9.0.

At pH 6.0 the average conversion rate with ATP substrate was calculated to be even slower (2%) than at pH 7.4 (7%) compared to pH 9.0 (Fig. 5). Nevertheless, an increase in products ADP, AMP and also a slight increase in adenosine was observed (Fig. 4(d)). Average conversion rate at pH 6.0 is highest for ATP, followed by ADP (83%, not significant) and AMP (69%), the latter significantly reduced compared to average ATP substrate conversion rate.

With ADP substrate, conversion rate at pH 6.0 was calculated to be only 1%, whereas at pH 7.4 it is 4% compared to the conversion rate of ADP at pH 9.0. Conversion rates with AMP substrate are 6% at pH 6.0 and 9% at pH 7.4 compared to conversion rate of AMP at pH 9.0. So the relationship between average values of conversion rates for assays at pH 6.0, 7.4 and 9.0 with ADP and AMP substrate is comparable to those obtained with ATP substrate (2% at pH 6.0, 7% at pH 7.4 compared to pH 9.0, Table 1), suggesting a similar response of the enzymatic activity to a decline in pH-value, which is independent of the nucleotide substrate used.

CONCLUSIONS

The mass spectrometric results revealed conversion rates that are considerably lower at pH 7.4 as well as pH 6.0 compared to pH 9.0, which is consistent with the data obtained photometrically (Table 1) and mostly also with data from the literature.[31,32] Furthermore, these findings are in accordance to results of Chappelet-Tordo *et al.* who observed a rise in enzymatic activity and a higher dissociation constant for the enzyme-inorganic phosphate complex with increasing pH-values.[17] Also Cocivera *et al.* demonstrated an increase in activity at alkaline pH and a considerably lower rate constant for the decomposition of the covalent enzyme-inorganic phosphate intermediate at acidic pH-values, thereby causing a lower availability of the enzyme's active site for further breakdown of substrate, indicating this step as rate-limiting.[29] Furthermore, Fernley and Walker demonstrated a decrease in Ki^a for Pi and PPi at less alkaline pH, suggesting a stronger inhibition of iAP by Pi and PPi at lower pH-values.[30]

However, in contrast to our results, Chappelet-Tordo *et al.*[17] found a considerably higher activity towards AMP substrate compared to ATP substrate at pH 10.0 and a comparable activity at pH 8.0. This indicates a preferred degradation of

AMP compared to ATP, although the substrate concentrations of AMP and ATP resulting in maximal velocity (Vm) of substrate conversion detected by Chappelet-Tordo *et al.* are comparable to those applied in this study.

It has been demonstrated in several investigations that diverse factors like type of buffer, ionic strength, metal ions, in particular Mg^{2+} and Zn^{2+}, may influence activity and specificity of iAP.[33,34] For instance, it has been shown that the order of degradation of ATP, ADP and AMP is reversed by addition of magnesium.[31] In this work no cations like Mg^{2+} or Zn^{2+} were added. However, it is unclear whether Chappelet-Tordo *et al.* used any additives, which in turn impedes a final conclusion regarding the disparity of experimental results. Anyhow, they applied buffers containing Tris in the case of pH 8 and ethanolamine at pH 10, both additives being good phosphate acceptors[35] which may result in a lower level of detectable phosphate with ATP.

Moreover, as mentioned before, the 'side reactions' of pyrophosphate formation may also mimic a lower phosphate release from ATP compared to AMP in the measurements of Chappelet-Tordo *et al.* More probably, however, is a difference in the enzyme used. In the study presented here iAP from bovine intestine was employed, whereas Chappelet-Tordo *et al.* used an enzyme originating from calf intestine. This enzyme however was proven in a later study to be heterogenic, i.e. to consist of different forms of the enzyme.[36] These, moreover, possess considerable different activities towards AMP.[37] So it may be assumed that, although a purification step was conducted, a heterogenic mixture of enzymes was used, probably showing markedly different substrate specificity.

In our opinion a lower degradation rate of AMP is more conceivable since the proximity of both the sugar residue and also the base of AMP may cause a steric hindrance or even the formation of interfering hydrogen bridge linkages between the nucleotide base and amino acids of the enzyme active site.

By further comparing the photometric and mass spectrometric measurements at pH 7.4 the results are similar, both revealing the highest enzymatic activity – reflected either by phosphate release or conversion rate – with ATP substrate, followed by ADP substrate (not significant) and AMP substrate (significant). AMP was again detected to be the poorest degradable substrate at pH 6.0, pointing out the clear substrate preference of iAP towards ATP and ADP. Nevertheless, substrate competition between ATP and ADP could be shown only by mass spectrometric detection, due to the ambiguous nature of colorimetric phosphate release detection. Mass spectrometric experiments clearly revealed a higher degradation rate for ADP compared to ATP at pH 9.0, but not at pH 7.4 or 6.0. Furthermore, mass spectrometric detection allowed a detailed investigation of the pH dependence of iAP by elucidating the degradation of substrate, intermediates and the generation of the final product. Increase or decrease of the catalytic activity of iAP due to pH-value shifts is of special interest since iAP takes part in intestinal pH regulation and is furthermore involved in inflammatory processes. In inflammation pH-values tend to become more acidic,[38] thus causing a lowered activity of iAP and therefore a tendency for higher ATP concentration, that would contribute to the progression of inflammatory processes.

---

[a]Ki = inhibition constant ($Ki = \frac{[E][I]}{[EI]}$) with [E] = concentration of the enzyme; [I] = concentration of the inhibitor and [EI] = concentration of the enzyme–inhibitor complex). Pi = inorganic phosphate and PPi = inorganic pyrophosphate.

Interestingly, the degradation of AMP to adenosine was demonstrated to be distinctively slower, but mainly in very alkaline medium. Nevertheless, a reduced degradation rate of AMP substrate compared to ATP or ADP degradation rates was also observed at physiological pH, although the difference was less pronounced. Physiological consequences in the context of this disparity that may be related to a more outstanding role for AMP in the context of inflammation or pH regulatory processes in the intestinal tract have to be enlightened in the future.

Acknowledgements

REFERENCES

[1] J. P. Lalles. Intestinal alkaline phosphatase: multiple biological roles in maintenance of intestinal homeostasis and modulation by diet. *Nutr. Rev.* **2010**, *68*, 323.

[2] M. J. Bours, E. L. Swennen, F. Di Virgilio, B. N. Cronstein, P. C. Dagnelie. Adenosine 5′-triphosphate and adenosine as endogenous signaling molecules in immunity and inflammation. *Pharmacol. Ther.* **2006**, *112*, 358.

[3] A. la Sala, D. Ferrari, F. Di Virgilio, M. Idzko, J. Norgauer, G. Girolomoni. Alerting and tuning the immune response by extracellular nucleotides. *J. Leukocyte Biol.* **2003**, *73*, 339.

[4] L. Antonioli, M. Fornai, R. Colucci, N. Ghisu, F. Da Settimo, G. Natale, O. Kastsiuchenka, E. Duranti, A. Virdis, C. Vassalle, et al. Inhibition of adenosine deaminase attenuates inflammation in experimental colitis. *J. Pharmacol. Exp. Ther.* **2007**, *322*, 435.

[5] X. Ge, T. L. Sirich, M. K. Beyer, H. Desaire, J. A. Leary. A strategy for the determination of enzyme kinetics using electrospray ionization with an ion trap mass spectrometer. *Anal. Chem.* **2001**, *73*, 5078.

[6] A. J. Norris, J. P. Whitelegge, K. F. Faull, T. Toyokuni. Analysis of enzyme kinetics using electrospray ionization mass spectrometry and multiple reaction monitoring: Fucosyltransferase V. *Biochemistry* **2001**, *40*, 3774.

[7] D. J. Wilson, L. Konermann. Mechanistic studies on enzymatic reactions by electrospray ionization MS using a capillary mixer with adjustable reaction chamber volume for time-resolved measurements. *Anal. Chem.* **2004**, *76*, 2537.

[8] B. Ganem, Y. T. Li, J. D. Henion. Observation of noncovalent enzyme substrate and enzyme product complexes by ion-spray mass-spectrometry. *J. Am. Chem. Soc.* **1991**, *113*, 7818.

[9] N. Dennhart, L. M. M. Weigang, M. Fujiwara, T. Fukamizo, K. Skriver, T. Letzel. 26 kDa endochitinase from barley seeds: Real-time monitoring of the enzymatic reaction and substrate binding experiments using electrospray ionization mass spectrometry. *J. Biotechnol.* **2009**, *143*, 274.

[10] P. Liuni, A. Jeganathan, D. J. Wilson. Conformer selection and intensified dynamics during catalytic turnover in chymotrypsin. *Angew. Chem. Int. Ed. Engl.* **2012**, *51*, 9666.

[11] A. R. de Boer, T. Letzel, D. A. van Elswijk, H. Lingeman, W. M. A. Niessen, H. Irth. On-line coupling of high-performance liquid chromatography to a continuous-flow enzyme assay based on electrospray ionization mass spectrometry. *Anal. Chem.* **2004**, *76*, 3155.

[12] C. F. de Jong, R. J. E. Derks, B. Bruyneel, W. Niessen, H. Irth. High-performance liquid chromatography-mass spectrometry-based acetylcholinesterase assay for the screening of inhibitors in natural extracts. *J. Chromatogr. A* **2006**, *1112*, 303.

[13] Z. Yu, L. C. Chen, M. K. Mandal, H. Nonami, R. Erra-Balsells, K. Hiraoka. Online electrospray ionization mass spectrometric monitoring of protease-catalyzed reactions in real time. *J. Am. Soc. Mass Spectrom.* **2012**, *23*, 728.

[14] N. Dennhart, T. Fukamizo, R. Brzezinski, M. E. Lacombe-Harvey, T. Letzel. Oligosaccharide hydrolysis by chitosanase enzymes monitored by real-time electrospray ionization-mass spectrometry. *J. Biotechnol.* **2008**, *134*, 253.

[15] D. W. Moss, A. K. Walli. Intermediates in the hydrolysis of ATP by human alkaline phosphatase. *Biochim. Biophys. Acta* **1969**, *191*, 476.

[16] R. K. Morton. The kinetics of hydrolysis of phenyl phosphate by alkaline phosphatases. *Biochem. J.* **1957**, *65*, 674.

[17] D. Chappelet-Tordo, M. Fosset, M. Iwatsubo, C. Gache, M. Lazdunski. Intestinal alkaline phosphatase. Catalytic properties and half of the sites reactivity. *Biochemistry* **1974**, *13*, 1788.

[18] T. Letzel, E. Sahmel-Schneider, K. Skriver, T. Ohnuma, T. Fukamizo. Chitinase-catalyzed hydrolysis of 4-nitrophenyl penta-N-acetyl-beta-chitopentaoside as determined by real-time ESIMS: The 4-nitrophenyl moiety of the substrate interacts with the enzyme binding site. *Carbohydr. Res.* **2011**, *346*, 863.

[19] R. D. Henkel, J. L. VandeBerg, R. A. Walsh. A microassay for ATPase. *Anal. Biochem.* **1988**, *169*, 312.

[20] A. C. Hogenboom, A. R. de Boer, R. J. Derks, H. Irth. Continuous-flow, on-line monitoring of biospecific interactions using electrospray mass spectrometry. *Anal. Chem.* **2001**, *73*, 3816.

[21] N. Dennhart, T. Letzel. Mass spectrometric real-time monitoring of enzymatic glycosidic hydrolysis, enzymatic inhibition and enzyme complexes. *Anal. Bioanal. Chem.* **2006**, *386*, 689.

[22] R. K. Scheerle, J. Grassmann, T. Letzel. Real-time ESI-MS of enzymatic conversion: Impact of organic solvents and multiplexing. *Anal. Sci.* **2012**, *28*, 607.

[23] A. I. Vovk, V. I. Kalchenko, S. A. Cherenok, V. P. Kukhar, O. V. Muzychka, M. O. Lozynsky. Calix 4 arene methylene-bisphosphonic acids as calf intestine alkaline phosphatase inhibitors. *Org. Biomol. Chem.* **2004**, *2*, 3162.

[24] S. G. Nugent, D. Kumar, D. S. Rampton, D. F. Evans. Intestinal luminal pH in inflammatory bowel disease: possible determinants and implications for therapy with aminosalicylates and other drugs. *Gut* **2001**, *48*, 571.

[25] C. H. Fiske. The colorimetric determination of phosphorus. *J. Biol. Chem.* **1925**, 66.

[26] N. Yoza, S. Onoue, Y. Kuwahara. Catalytic ability of alkaline phosphatase to promote P-O-P bond hydrolyses of inorganic diphosphate and triphosphate. *Chem. Lett.* **1997**, 491.

[27] R. V. Nayudu, L. Demeis. Energy transduction at the catalytic site of enzymes – Hydrolysis of phosphoester bonds and synthesis of pyrophosphate by alkaline-phosphatase. *FEBS Lett.* **1989**, *255*, 163.

[28] A. A. Baykov, O. A. Evtushenko, S. M. Avaeva. A malachite green procedure for ortho-phosphate determination and its use in alkaline phosphatase-based enzyme-immunoassay. *Anal. Biochem.* **1988**, *171*, 266.

[29] M. Cocivera, J. McManaman, I. B. Wilson. Phosphorylated intermediate of alkaline phosphatase. *Biochemistry* **1980**, *19*, 2901.

[30] H. N. Fernley, P. G. Walker. Studies on alkaline phosphatase. Inhibition by phosphate derivatives and the substrate specificity. *Biochem. J.* **1967**, *104*, 1011.

[31] R. H. Eaton, D. W. Moss. Inhibition of the orthophosphatase and pyrophosphatase activities of human alkaline-phosphatase preparations. *Biochem. J.* **1967**, *102*, 917.

[32] M. H. Jensen. Dephosphorylation of purine mononucleotides by alkaline phosphatases. Substrate specificity and inhibition patterns. *Biochim. Biophys. Acta* **1979**, *571*, 55.

[33] A. Bannister, R. L. Foster. Buffer-induced activation of calf intestinal alkaline phosphatase. *Eur. J. Biochem.* **1980**, *113*, 199.

[34] D. Hogarth, D. Jung, T. Murooka, S. Pun, M. Szeto. A decrease in the bovine intestinal mucosa alkaline phosphatase activity in the presence of inorganic phosphate. *J. Exp. Microbiol. Immunol.* **2002**, *2*, 6.

[35] J. Dayan, I. B. Wilson. The phosphorylation of Tris by alkaline phosphatase. *Biochim. Biophys. Acta* **1964**, *81*, 620.

[36] M. Besman, J. E. Coleman. Isozymes of bovine intestinal alkaline phosphatase. *J. Biol. Chem.* **1985**, *260*, 11190.

[37] F. J. Behal, M. Center. Heterogeneity of calf intestinal alkaline phosphatase. *Arch. Biochem. Biophys.* **1965**, *110*, 500.

[38] Z. Gerevich, Z. S. Zadori, L. Koles, L. Kopp, D. Milius, K. Wirkner, K. Gyires, P. Illes. Dual effect of acid pH on purinergic P2X(3) receptors depends on the histidine 206 residue. *J. Biol. Chem.* **2007**, *282*, 33949.

SUPPORTING INFORMATION

Additional supporting information may be found in the online version of this article at the publisher's website.

Utilization of real-time ESI-MS to gain further insight into the course of nucleotide degradation by intestinal alkaline phosphatase

Christine M. Kaufmann,[*] Johanna Graßmann,[*] Dieter Treutter, [‡] Thomas Letzel[*†]

[*] Chair of Urban Water Systems Engineering, Technische Universität München, Am Coulombwall 8, 85748 Garching, Germany
[‡] Institute of Fruit Science, Technische Universität München, Dürnast 2, 85354 Freising, Germany

[†] To whom correspondence should be addressed: Dr. Thomas Letzel,

Head of the Analytical Research Group, Phone: +49 (0)89 2891 3780, E-mail: t.letzel@wzw.tum.de,

Table S1

Overview of data evaluation procedures and enzyme concentration applied for colorimetric and mass spectrometric experiments.

Assay		Concentration of substrate/enzyme	Data evaluation
Colorimetric	pH 6.0	40µM/44.64nM	Linear trend line within minute 0 to 30
	pH 7.4		
	pH 9.0		Linear trend line within minute 0 to 15
Mass spectrometric	pH 6.0	40µM/44.64nM	Exponential trend line within minute 3.0 to 30
	pH 7.4		
	pH 9.0	40µM/11.16nM	Exponential trend line within minute 3.0 to 15
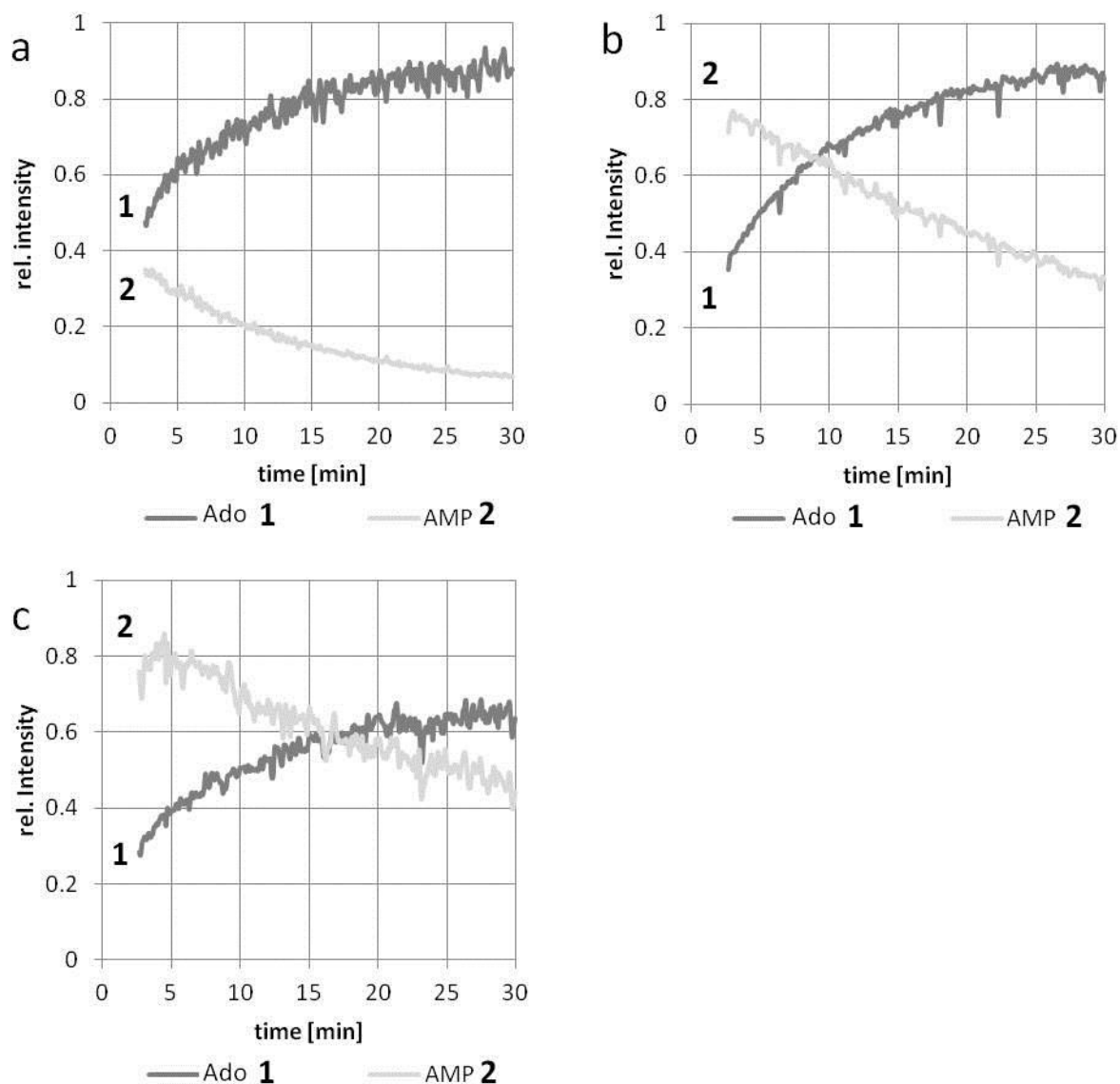
Figure S1

All assays were conducted in 10mM ammonium acetate buffer with 40µM AMP substrate; a: iAP concentration 11.16nM, pH 9.0; b: iAP concentration 44.64nM, pH 7.4; c: iAP concentration 44.64nM, pH 6.0; m/z evaluated, summarized and displayed here: Ado with m/z 268.1 and 290.1, i.e. $[Ado+H]^+$ and $[Ado+Na]^+$; AMP with m/z 348.1, 370.1, 386.0, 392.0 and 408.0, i.e. $[M+H]^+$, $[M+Na]^+$, $[M+K]^+$, $[M-H+2Na]^+$ and $[M-H+Na+K]^+$; n = 5 – 11.
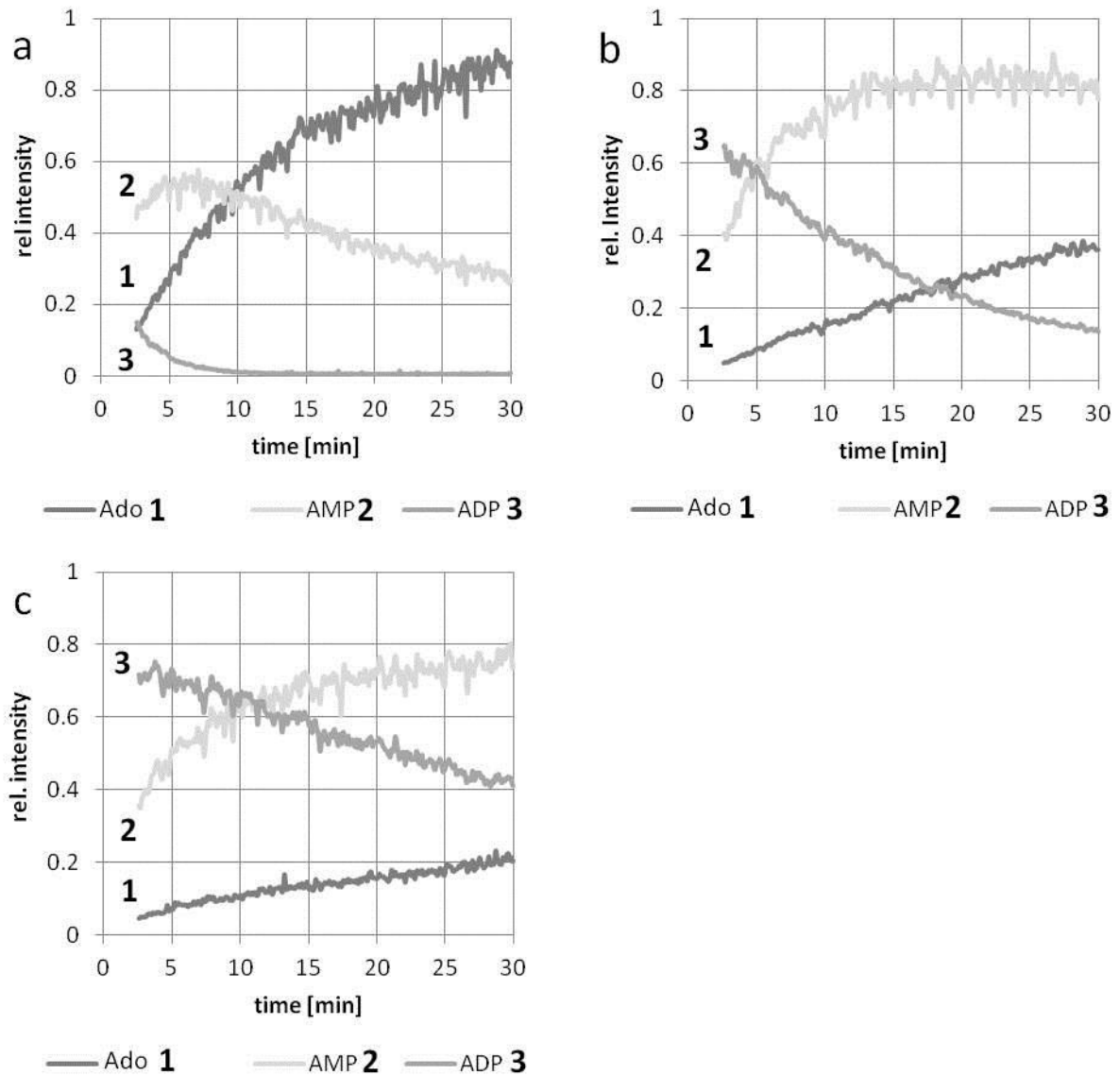
Figure S2

 All assays were conducted in 10mM ammonium acetate buffer with 40µM ADP substrate; a: iAP concentration 11.16nM, pH 9.0; b: iAP concentration 44.64nM, pH 7.4; c: iAP concentration 44.64nM, pH 6.0; m/z evaluated, summarized and displayed here: Ado with m/z 268.1 and 290.1, i.e. $[Ado+H]^+$ and $[Ado+Na]^+$; AMP with m/z 348.1, 370.1, 386.0, 392.0 and 408.0; ADP with m/z 428.0, 450.0, 466.0, 472.0 and 488.0, i.e. $[M+H]^+$, $[M+Na]^+$, $[M+K]^+$, $[M-H+2Na]^+$ and $[M-H+Na+K]^+$; n = 5 – 11.

Appendix II

Achroma Software-High-Quality Policy in (a-)Typical Mass Spectrometric Data Handling and Applied Functional Proteomics

Michael Krappmann*, Christine M. Kaufmann*, Romy K. Scheerle, Johanna Grassmann and Thomas Letzel

*equal contribution of the authors

The following publication shows the evaluation of atypical mass spectrometric data using Achroma software tool. The evaluation procedure is outlined by means of specific examples of enzymatic assays, which were conducted with an online coupled continuous flow mixing system. Data processing is described in detail, followed by the introduction of different features of Achroma.

Intestinal alkaline phosphatase assay data was conducted and evaluated by me. This also applies to the related text passages and graphics. General parts of the publication, i.e. introduction and conclusion were written by all parties involved.

Achroma Software-High-Quality Policy in (a-)Typical Mass Spectrometric Data Handling and Applied Functional Proteomics

Michael Krappmann[1#], Christine M Kaufmann[2#], Romy K Scheerle[2], Johanna Grassmann[2] and Thomas Letzel[2]*

[1]*University of Applied Sciences, Am Hofgarten 4, 85354 Freising, Weihenstephan, Germany*
[2]*Chair of Urban Water Systems Engineering, TU München, Am Coulombwall, 85748 Garching, Germany*
[#]*Equal contribution of the authors*

Abstract

Data evaluation of mass spectrometric raw data is an essential step to obtain high-quality results. In our days an exorbitant amount of raw data are produced in analytical (bio)chemistry due to the utilization of sophisticated experimental setups. The recently published free software Achroma has been developed to overcome increasing data processing challenges by providing the possibility of a comprehensive data analysis (http://openmasp.hswt. de/pages/project/achroma.php). To illustrate (a-)typical data evaluation, an online coupled continuous flow system hyphenated with mass spectrometric detection was applied to investigate enzymatic activity changes in the presence of regulatory molecules and alternative substrates. The extended software strategy, the processing as well as evaluation of data is presented in detail based on enzymatic assays of intestinal alkaline phosphatase (iAP) and acetylcholine esterase (AChE). Different Achroma data evaluation modules enabled a high quality analysis. This included the elucidation of enzymatic substrate preferences by means of the calculation of negative and positive peak areas as well as the identification of an inhibitory molecule by comparing different mass spectra with regard to their overall composition. The possibility of an automatically performed validity control to monitor the systems robustness furthermore emphasized the usefulness of Achroma software regarding its applicability in the area of 'functional proteomics' data handling.

Graphical Abstract
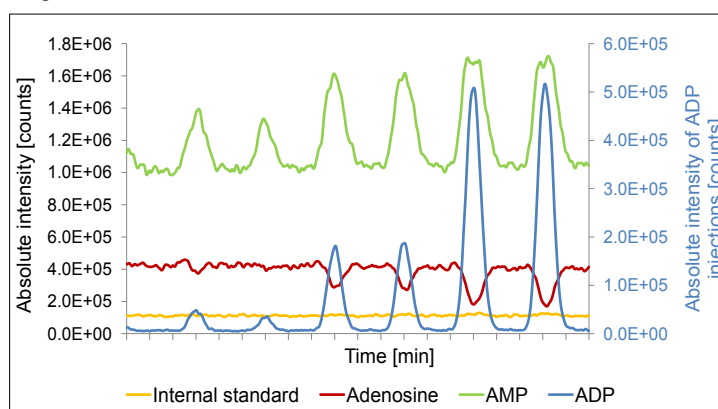
Challenges regarding (a-)typical data processing and their overcoming by applying Achroma Software are outlined.

Data evaluation includes e.g. the assessment of data quality and the calculation of peak area.

Keywords: Functional proteomics; Enzyme; Data evaluation software; Online-coupled continuous flow system; Chromatography; Mass spectrometry

Abbreviations: LC: Liquid Chromatography; MS: Mass Spectrometry; EIC: Extracted Ion Chromatograms; AChE: Acetylcholine Esterase; SRM/MRM: Selective or Multiple Reaction Monitoring; IS: Internal Standards; openMASP: Open Source Modular Analytical Software Platform

Introduction

Mass spectrometry (MS) combined with liquid chromatography (LC) is nowadays a key technology in the field of analytical chemistry. Research areas like 'small compound screening' in food and environmental chemistry and also the investigation of large molecules like proteins may lead to a plethora of data, which need to be processed, evaluated and interpreted. Beyond that, (LC-) MS is a key technology in

the field of 'functional proteomics', as part of experimental setups used to monitor enzymatic reactions in real-time or to study the formation of non-covalent complexes [1-6].

The rapid improvement of analytical instruments and thereby the emergence of new and complex experimental setups further contribute to an increasing amount of data and in this manner to data evaluation challenges. One single experiment may result in thousands of mass spectra and extracted ion chromatograms (EIC), depending on the complexness of the analyzed mixtures, the measurement time and the number of substrate and product traces, especially in multiplexing approaches.

In this regard, the application of an online coupled continuous flow system to detect changes in enzymatic activity in the presence of regulatory molecules may result in the emergence of complex data sets. This well-established technique has already been applied for the detection of interactions between proteins and compounds of interest [7], for the detailed investigation of enzyme inhibitors [8,9] or even on the screening of complex mixtures for unknown enzyme regulatory compounds [8-10]. The applicability of this systems has already been proven for the investigation of several enzymes, i.e. acetylcholine esterase (AChE) [9,8], phosphodiesterase [10], glutathione S-transferase [11] and cathepsin B [8]. In the presented work the setup was applied for the investigation of AChE and iAP enzymatic assays, either to find regulatory molecules from complex mixtures or to detect the enzymatic response to alternative substrates. Both applications were found to result in unusual data sets, which enclose the presence of positive and negative peaks within the assay EICs. The introduction of complex mixtures with unknown composition furthermore necessitated a fast and easy identification of potential enzyme regulatory compounds. Standard software provided by LC/MS hardware vendors is usually expensive and often does not comprise all functions required for entire data analysis. Researchers may have to conduct additional procedures like the export of data and further handling with common spread sheet software. This software type however in most cases lacks certain requirements for a detailed data evaluation. Thus, the development of new software allowing automated data handling and rapid as well as easy data interpretation and data evaluation is essential. Consequently, a special free software–Achroma–was developed and applied to clearly visualize, process and analyze a large amount of chromatographic and mass spectrometric data. So far, the Achroma software includes several independent data handling modules, like a) 'chromatogram comparison' for the calculation of a quotient of particular EICs to track signal inconstancies, b) 'signal recognition' of positive and negative peak signals (incl. signal area calculation) and c) 'signal comparison' tool. Latter enables the discovery of differences between two spectra at two different defined time points, e.g. comparing the EICs baseline range with a signal of enzymatic regulation. In contrast to common data evaluation software the possibility of a data quality examination was implemented into Achroma software to obtain helpful information about the robustness of the applied experimental setup. Automatically performed signal recognition and signal comparison furthermore provide a distinct reduction of elaborate manual data processing time.

In contrast to other available software tools for selective or multiple reaction monitoring (SRM/MRM) [12], e.g. like Skyline [13] or ATAQS [14], Achroma provides the calculation of negative peak areas, which may occur in continuous flow experiments of enzymatic activity determination in the presence of regulatory compounds. By adding the possibility of a difference spectrum calculation, Achroma software tool further stands out from classical SRM/MRM software regarding helpful features for functional proteomics data evaluation. Achroma software and its features were exemplarily employed on AChE and iAP enzymatic assays to evaluate data quality features and to illustrate application-oriented data evaluation. The enzymatic assay data were

processed with respect to a) performing data quality control and signal robustness assessment via EIC correlation of an internal standard (IS) and the EIC of an assay component, b) monitoring signal changes of iAP enzymatic assay induced by the injection of competitive substrates and c) screening of single compounds contained in complex mixtures on their regulatory effect on AChE, e.g. inhibitory effects.

Materials and Methods

Reagents and chemicals

All compounds for the enzymatic assays were purchased from Sigma-Aldrich (Steinheim, Germany): AChE from *Electrophorus electricus* type VI-S (AChE, Enzyme Commission (EC) number 3.1.1.7, M_w ~280 kDa), acetylcholine chloride (AChCl, M_w 181.7 Da), galanthamine hydrobromide from *Lycoris* sp. (M_w 368.3 Da), iAP from bovine intestinal mucosa (EC 3.1.3.1., M_w ~160 kDa), Adenosine 5′-triphosphate (ATP, M_w 507.2 Da), Adenosine 5'-diphosphate (ADP, M_w 427.2 Da), Adenosine 5'-monophosphate (AMP, M_w 347.2 Da), LC-MS grade reagent water, LC-MS grade methanol and ammonium acetate (M_w 77.1 Da, >98%). L-histidine (M_w 155.16 Da) served as internal standard and was obtained from Merck Chemicals (Darmstadt, Germany).

A house dust extract sample was used for screening experiments. The sample was taken from a household with visible mould infestation and was prepared as follows: 0.5 g house dust was sieved and the particle fraction ≤ 63 μm was extracted with 5 mL methanol/H_2O (84:15). 1 mL was evaporated to dryness, resolved in methanol/H_2O (20:80), filtered with a 45 μm RC-filter and used for application in enzymatic assays.

Instrumentation

Online coupled continuous flow system: The experiments were performed using an online coupled continuous flow system with sample introduction part (Injector, Rheodyne, California, sample loop volume: 2 μL) as presented in Figure 1.

In setup 1 (Figure 1, middle trace: light grey dashed line), the enzymatic activity of iAP was measured towards its nucleotide substrate AMP. Activity changes in AMP substrate degradation along with adenosine (Ado) product generation, caused by the introduction of additional AMP substrate as well as increasing concentrations of the competitive nucleotide substrates ADP and ATP [15], were investigated. Concentration of the enzyme and the AMP substrate introduced to the system were 2.4 U/mL and 80 μM, respectively. Both were solved in 10 mM ammonium acetate pH 7.4.

Setup 2 (Figure 1, middle trace: black solid line) was used for the determination of the AChE activity with regard to an enzymatic regulation potentially caused by a chromatographically separated house dust mixture of unknown molecules. Initial concentrations were set to 0.05 nM of AChE and 10 μM of acetylcholine, either solved in
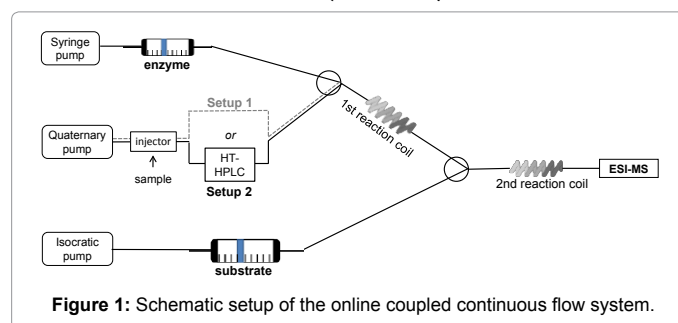
Figure 1: Schematic setup of the online coupled continuous flow system.

10 mM ammonium acetate pH 7.4. Internal standard L-histidine was introduced to the systems along with the enzyme solutions and was set to an initial concentration of 80 μM. In both setups the enzyme was provided in a syringe (2.5 mL, Hamilton-Bonaduz, Switzerland) located in a syringe pump with a flow rate set to 25 μL/min (Figure 1, upper trace) (Model 11 Plus, Harvard Apparatus, Hugo Sachs Elektronik, Hugstetten, Germany). Substrate solution was filled in a superloop (volume 10 mL, Amersham Biosciences, Uppsala, Sweden) and introduced to the system with a flow rate of 50 μL/min (Figure 1, bottom trace). Samples were injected into the continuous flow delivered by the quaternary pump via an injector (Rheodyne, California, sample loop volume: 2 μL). The quaternary pump flow rate (1100 series, Agilent Technologies, Waldbronn, Germany) was set to 25 μL/min, taking the sample either directly to the first reaction coil (setup 1) or along to the chromatographic column (setup 2). The isocratic pump (1260 series, Agilent Technologies, Waldbronn, Germany) was connected to the superloop for pumping the substrate solution to the system (Figure 1, bottom trace). Pumps were controlled by ChemStation software (version B.04.03, Agilent Technologies, Waldbronn, Germany). Reaction coils 1 and 2 (Teflon, 0.25 mm ID) were knitted as described in literature [16] to provide a sufficient mixing of enzyme and injected sample (reaction coil 1, flow-through time of ~1.3 min) and of the enzyme-sample mixture with the substrate (reaction coil 2, flow-through time of ~2.9 min), respectively. Apart from reaction coil 1 and 2 all further modules in both setups were connected with PEEK tubing. In setup 1, 10 mM ammonium acetate pH 7.4 was delivered continuously by the quaternary pump (Figure 1, middle trace). In setup 2 an isocratic eluent flow with 90% 10 mM ammonium acetate pH 7.4 with 10% methanol was used to separate the sample on a high temperature-compatible Zirchrom PBD column (100x1 mm, 3 μm) (ZirChrom Separations, Inc., Anoka, MN, USA), which was integrated into a column oven (HT HPLC 2000, Scientific Instruments Manufacturer GmbH, Oberhausen, Germany) (Figure 1, middle trace). The organic solvent concentration tolerable for AChE was preliminarily tested [17], whereupon 10% methanol was found to be suitable to maintain sufficient enzymatic activity. A temperature gradient was applied to improve the chromatographic separation. Initial temperature was set 30°C, followed by a linear temperature increase up to 120°C within a time range of 20 min, whereupon 120°C was held for 10 min. After completion of the gradient, the column was automatically reconditioned to the starting temperature of 30°C.

Mass spectrometric assay detection: Samples were analyzed using a single quadrupole mass spectrometer (MSQ Plus, Wissenschaftliche Gerätebau Dr. Ing. Herbert Knauer GmbH, Berlin, Germany) equipped with an electrospray ionization source in positive ionization mode. Mass spectrometric parameters were as follows: 300°C probe temperature, 3.5 kV needle voltage and 75 V cone voltage. In setup 1, the mass range for the iAP assay component detection was 100-1000 m/z, whereas in setup 2, the mass range for experiments performed with AChE was 100-800 m/z.

The following signals were analyzed in the AChE assay with the substrate acetylcholine: substrate signal m/z 146 (M)$^+$ and product signal m/z 104 (M–CH$_3$COOH)$^+$.

For data evaluation of iAP assays, related m/z signals were summarized, using m/z 268.1 and 290.1, i.e. (Ado+H)$^+$ and (Ado+Na)$^+$; m/z 348.1, 370.1, 386.0, 392.0 and 408.0, i.e. (AMP+H)$^+$, (AMP+Na)$^+$, (AMP+K)$^+$, (AMP-H+2Na)$^+$ and (AMP-H+Na+K)$^+$ and m/z 428.0, 450.0, 466.0, 472.0 and 488.0, i.e. (ADP+H)$^+$, (ADP+Na)$^+$, (ADP+K)$^+$, (ADP-H+2Na)$^+$ and (ADP-H+Na+K)$^+$.

Data evaluation

Mass spectrometric data was acquired using Xcalibur software 2.1.0.1139 (Thermo Fisher Scientific Inc., Waltham, MA, USA). For data evaluation with Achroma software either an entire Xcalibur data file was processed directly with an Xcalibur-implemented file converter tool, followed by a further conversion step with Achroma converter software or individual EICs of interest were transferred to Office Excel, whereupon further processing was again performed with Achroma converter (Figure 2).

The latter procedure leads to a minor amount of information, only containing data of particular EICs, which is sufficient in case of known m/z values of interest and advantageous regarding the reduction of the final data volume and file sizes. In contrast by converting the entire Xcalibur data file the mass spectrometric information recorded is entirely preserved. A more detailed explanation regarding the conversion of raw data is provided on the Achroma web page [18].

Data interpretation of enzymatic assays was accomplished by applying several Achroma modules after smoothing the data: 'Chromatogram comparison' tool allows the calculation of a quotient of two independent EICs, e.g. the traces of an internal standard and an assay component. Hence, the ratio obtained enables the correction of experimental data for intensity irregularities.

Moreover, enzymatic regulation manifested as negative or positive peaks present in the EIC traces was detected with 'signal recognition' module to assess peak areas, thereby obtaining numerical values that correspond to an alteration of enzymatic activity, whether it is inhibitory or activating. Further evaluation of data was carried out using 'spectra comparison'. By means of this module, regulatory molecules affecting enzymatic activity can be easily identified by comparing the mass spectrum of a time point of altered enzymatic activity with the mass spectrum of a non-regulated time range. In doing so, differences

Figure 2: Data evaluation steps from data acquisition to data processing with Achroma software.
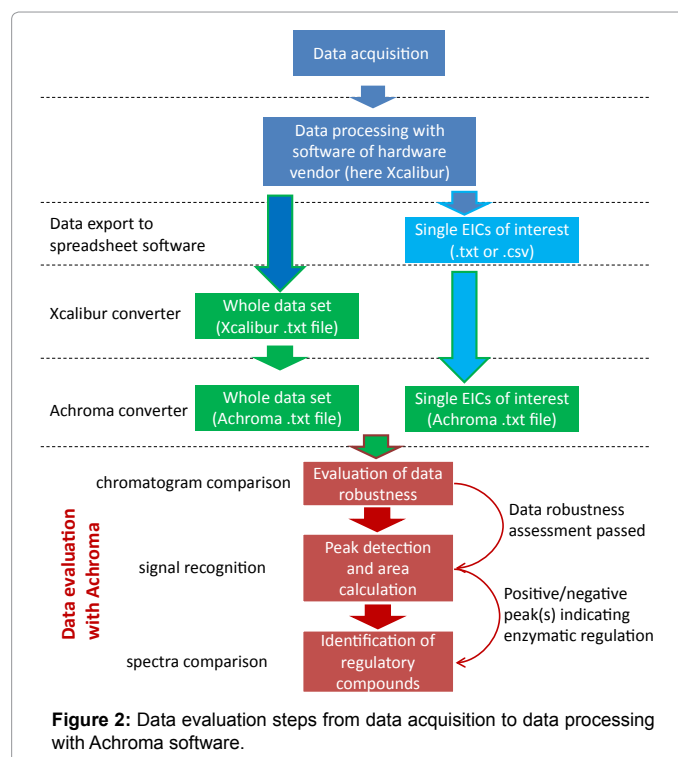
regarding the total composition of both spectra or merely the alteration of single m/z signal intensities respectively can be revealed. Temporarily emerging m/z values or m/z values with a distinct increase of intensity are presented as negative signals and vice versa.

Results and Discussion

A continuous flow system coupled with MS detection (Figure 1) was applied to study enzymatic activity of iAP and AChE, respectively. Temporary increases or decreases of mass spectrometric substrate or product traces in the presence of inhibiting or activating molecules can be used to identify regulatory molecules from complex mixtures. In the absence of regulatory molecules, a constant trace of substrate and product is continuously detected, which reflects an unchanged enzymatic activity.

The presence of *e.g.* an inhibiting molecule is reflected by a temporary increase of substrate intensity (positive peak) and a simultaneously occurring decrease of product intensity (negative peak). In this regard, the evaluation of positive as wells as negative peak signals to assess enzymatic activity changes is inevitable. To address this need a former Achroma software version was developed and recently published [19]. Data quality and also the overall data evaluation procedure was considered applying three modules of Achroma software-'signal recognition', 'spectra comparison' and 'chromatogram comparison'.

The handling and processing of raw data with a new Achroma version (incl. additional functionality like an extended file converter tool) is demonstrated by means of iAP enzymatic activity measured with the online coupled continuous flow system in section 3.1 (Figure 1 and Setup 1). A further verification of proper data analysis is shown by the evaluation of AChE enzymatic assay measured in the presence of a chromatographically separated complex real house dust extract, which was introduced to the system (Figure 1 and Setup 2).

Intestinal alkaline phosphatase assay data evaluation

iAP is able to dephosphorylate the nucleotide AMP, thereby generating the nucleoside product adenosine. iAP (Figure 1, upper trace) and AMP (Figure 1, bottom trace) were introduced to the online coupled continuous flow system, resulting in a constant AMP substrate trace and an enzymatically dephosphorylated Ado product trace. Enzyme and substrate concentrations were chosen to obtain an enzymatic substrate conversion rate that results in a sufficient mass spectrometric substrate as well as product trace intensity. The injection of different concentrations of substrate AMP or alternative substrates ADP or ATP led to the generation of intermediates and an altered Ado product generation, which is due to the enzyme´s ability to dephosphorylate its substrates in a stepwise manner [15].

As previously investigated, iAP activity measurements towards AMP compared to ADP and ATP revealed the enzyme´s preference to dephosphorylate the latter two with a rate about twice and thrice as high, respectively [15].

ADP and ATP injections (Figure 1, middle trace) consequently caused a reduced generation of the final product Ado, which is solely formed through AMP dephosphorylation. Additionally, injected ADP or ATP are largely degraded to AMP or AMP and ADP by the removal of one or two phosphate groups, respectively [20].

Assessment of signal stability and overall data quality: After successfully adapting iAP enzymatic assay to the online coupled continuous flow system, first experiments showed recurring drops within assay component traces. To investigate whether these inconstancies are due to mass spectrometric detection or related to changes of enzymatic activity, data was assessed with Achroma software module 'chromatogram comparison'. The extent of signal inconstancies within the course of internal standard and assay component traces (substrate, intermediates or product) can easily be displayed, compared and corrected (Figure 3). By doing so, actual enzymatic activity changes due to the presence of regulatory molecules and events of system-related intensity loss can be distinguished. This data correction step is therefore particularly important, since signal inconstancies might lead to a feigning of enzyme regulation. 'Chromatogram comparison' tool hence provides the possibility to monitor and correct assay EICs for signal detection irregularities and potentially assign them either to signal suppression effects due to injected molecules, pumping inconsistencies, system leakage or others.

Assay traces of the internal standard (IS) and the substrate AMP (Figure 3) are selected by entering the respective masses into the provided input field of Achroma software (Figure 3, solid black line, exemplary m/z range 155 to 156 and 347 to 348). By means of chromatogram comparison the data were edited by calculating the quotient of those molecule EICs, resulting in a constant and consistent ratio which is corrected for signal inconstancies (Figure 3C).

A tolerance interval can be additionally selected (Figure 3, dashed line box and Figure 3C) to control the resulting EIC after correction. The tolerance interval is shown as additional lines below and above the calculated quotient chromatogram (Figure 3C). The correction procedure applied to the data might therefore also reveal further inconstancies beyond the events of obvious signal losses, which would be clearly revealed as signals ranging out of the tolerance interval set. Those exceeding signals might therefore be accounted to enzymatic regulation events, which were previously concealed by the more dominant signal inconstancies. In case of the data set exemplarily used, no further irregularity is apparent, visible by the trace´s course lying within the tolerance limit of 10%.
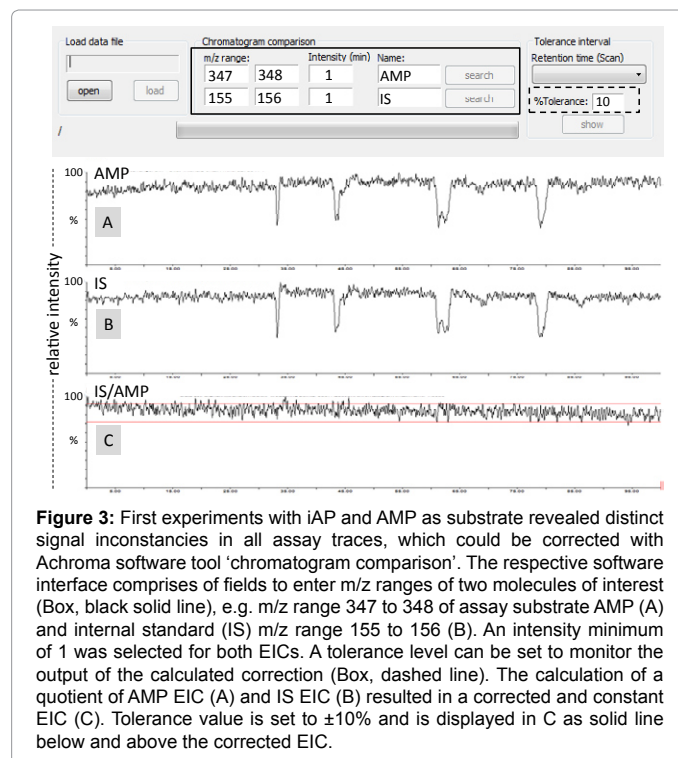
Figure 3: First experiments with iAP and AMP as substrate revealed distinct signal inconstancies in all assay traces, which could be corrected with Achroma software tool 'chromatogram comparison'. The respective software interface comprises of fields to enter m/z ranges of two molecules of interest (Box, black solid line), e.g. m/z range 347 to 348 of assay substrate AMP (A) and internal standard (IS) m/z range 155 to 156 (B). An intensity minimum of 1 was selected for both EICs. A tolerance level can be set to monitor the output of the calculated correction (Box, dashed line). The calculation of a quotient of AMP EIC (A) and IS EIC (B) resulted in a corrected and constant EIC (C). Tolerance value is set to ±10% and is displayed in C as solid line below and above the corrected EIC.

After successfully examining the quality of the data set, evaluation regarding the effects of an alternative substrate introduced to iAP assay as well as the finding of regulatory molecules were accomplished by applying additional Achroma software modules.

Enzymatic regulation in the presence of alternative substrates: The activity of iAP towards its substrate AMP was investigated in the presence of different concentrations of injected AMP and alternative substrates ADP and ATP. Changes in Ado product and intermediate generation as well as enzymatic preferences regarding nucleotide substrates ought to be detected and analyzed. Data processing is exemplarily described by means of iAP enzymatic assay with AMP substrate and ADP injections to the online coupled continuous flow system (Figure 4). Evaluation was performed by entering the *m/z* of an assay component of interest into the respective input field (Figure 4, I) to display the corresponding EIC traces of the product (Ado), the substrate (AMP) and the competitive substrate (ADP) (Figure 4A-C). EIC smoothing was conducted with a moving average algorithm, similar to the Savitzky-Golay algorithm (Figure 4, III) [18].

Subsequently, peak recognition was automatically performed with Achroma software by selecting the provided option "negative signals" (Figure 4, II) in case of data showing mainly negative peaks (Figure 4A) and vice versa (Figure 4B and C). If necessary, the software provides the possibility to manually adjust the starting and end point of individual peaks (Figure 4, IV). Alterations of trace intensities of product Ado (Figure 4A), substrate AMP (Figure 4B) and competing substrate ADP (Figure 4C) were further evaluated using the peak areas obtained from Achroma Software (Figure 4D). A peak area average value of four
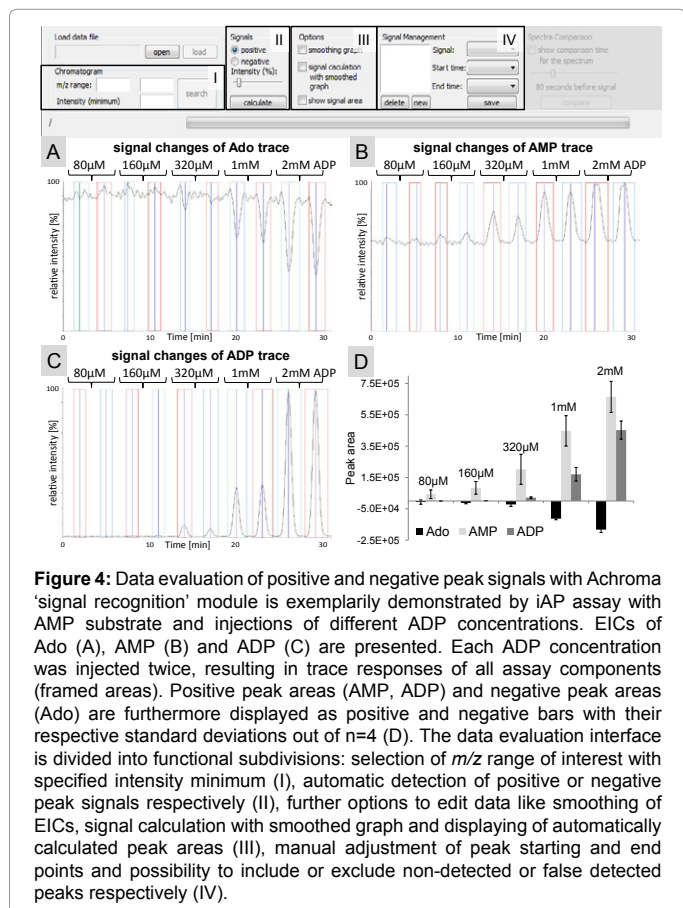
injections of ADP was calculated for Ado, AMP as well as ADP. The decrease of trace intensities is presented as negative bars, whereas the intensity increases are displayed as positive bars (Figure 4D).

Injection of 80 μM and 160 μM ADP solutions to the iAP assay with AMP substrate led to a preferred and complete degradation of ADP in reaction coil 1 (Figure 4C) and in this manner to an associated slight increase of AMP (Figure 4B) and of the final product Ado (Figure

Figure 4: Data evaluation of positive and negative peak signals with Achroma 'signal recognition' module is exemplarily demonstrated by iAP assay with AMP substrate and injections of different ADP concentrations. EICs of Ado (A), AMP (B) and ADP (C) are presented. Each ADP concentration was injected twice, resulting in trace responses of all assay components (framed areas). Positive peak areas (AMP, ADP) and negative peak areas (Ado) are furthermore displayed as positive and negative bars with their respective standard deviations out of n=4 (D). The data evaluation interface is divided into functional subdivisions: selection of *m/z* range of interest with specified intensity minimum (I), automatic detection of positive or negative peak signals respectively (II), further options to edit data like smoothing of EICs, signal calculation with smoothed graph and displaying of automatically calculated peak areas (III), manual adjustment of peak starting and end points and possibility to include or exclude non-detected or false detected peaks respectively (IV).

Figure 5: Dependency between calculated peak areas of Ado (■), AMP (✳), ADP (♦) and ATP (▲) and the injection of AMP, ADP or ATP in different concentrations (80 μM, 160 μM, 320 μm, 1 mM and 2 mM); internal standard (IS) peak areas are presented as well (O). Standard deviations shown are calculated out of n=4.

4A). ADP concentration above 160 µM caused a more pronounced and gradual increase of AMP intensities and a progressive decrease of the Ado level, which can be explained by the availability of non-degraded, enzymatically favored substrate ADP. High levels of competing ADP therefore resulted in the generation of mainly AMP and a further reduced Ado generation. Detailed data evaluation with AMP, ADP and ATP injections was performed in the same manner as described and is comparatively displayed in Figure 5.

The injection of additional AMP to the system led to a distinct increase of AMP peak areas, which is likely due to the inability of iAP to degrade the majority of AMP injected to the system. The rise of Ado product level was consequently found to be minor and only slightly increased for all AMP concentrations (Figure 5A).

In contrast, data examination with ADP injections revealed a more pronounced increase of AMP intermediate product peak areas (Figure 5B), which reflects the enzymatic substrate preference towards ADP compared to AMP. The simultaneous decrease of Ado furthermore indicates the preferred degradation of ADP to AMP rather than AMP to Ado (Figure 5B). The non-linearity of AMP peak areas with increasing ADP concentrations injected might be accounted to a substrate saturation occurring above a certain level of injected ADP (Figure 5B). This results in an increasing amount of non-degraded ADP and concurrently less generated AMP, due to the systems limited reaction time span (Figure 1, 2nd reaction coil). To verify the thesis of actual substrate saturation and to exclude the possibility of mass spectrometric signal suppression effects, controls containing no enzyme were measured in the online coupled continuous flow system. 80, 160, 320, 1000 and 2000 µM AMP was injected respectively, investigating the peak area progression with increasing concentrations. Data evaluation of AMP peak areas with Achroma showed a linear increase up to 2 mM of injected AMP (data not shown), which in turn supports the assumption of the non-linear AMP increase visible in Figure 5B to be due to substrate saturation.

The injection of ATP to the system furthermore reduces the generation of Ado, which is again due to the enzymes substrate preference towards ATP and ADP. Minor concentrations of injected ATP resulted in a distinct increase of AMP and only a slight rise of ADP levels, which is accounted to the enzyme´s ability to rapidly degrade ATP as well as a major proportion of the thereby generated ADP to AMP within the reaction time span provided (Figure 1, 2nd reaction coil) (Figure 5C). ATP injections of 1mM and beyond led to a flattening of AMP, ADP and Ado peak area progression, which is again attributed to substrate saturation.

Within the time ranges of assay component peak calculations, also the peak areas of the internal standard were assessed (Figure 5A-C). The absence of distinct intensity changes in the course of the internal standard EIC furthermore confirms the finding of negative peaks within the EIC of Ado to be an actual alteration in enzyme activity rather than mere signal suppression.

In this manner the signal recognition tool of Achroma software supports a more detailed data interpretation by providing the possibility to calculate positive and negative peak areas as well as regulation effects.

Identification of regulatory molecules and differences in spectra composition and intensities: Injection of alternative substrates to iAP enzymatic assay resulted in the emergence of negative and positive peaks within the assay component EICs. To be able to investigate the spectra composition, which corresponds to the time point of altered substrate degradation, 'spectra comparison' module was exemplarily
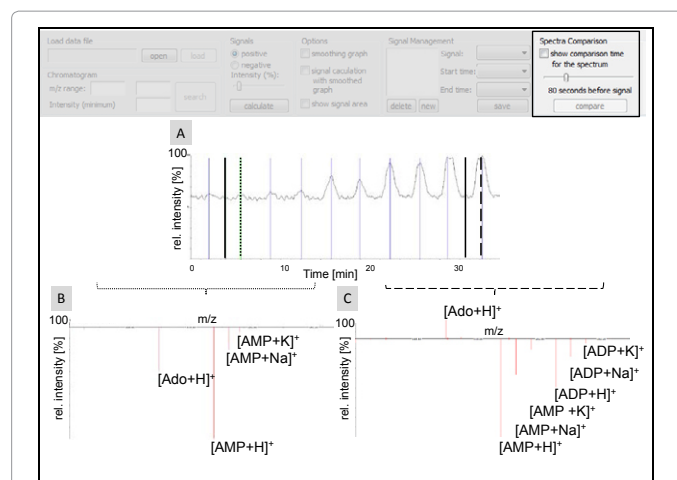
Figure 6: 'Spectra comparison' interface of the Achroma software and data evaluation of signal peaks: Injection of 80 µM (A, left dashed line) and 2 mM ADP (A, right dashed line) with no injection baseline time points (A, dark solid lines); difference spectrum of 80 µM ADP injection (B); difference spectrum of 2 mM ADP injection (C). AMP and ADP appeared as positively charged ions, either with proton, sodium or potassium. Ado was solely detected as protonated ion.

applied for the data evaluation of ADP injections (compare Figure 4 and 5B). The module is convenient in terms of investigating differences between two different spectra or even provides the possibility to identify signal intensity changes, *e.g.* caused by the injection of a competitive molecule like ADP. To illustrate the procedure of data evaluation with spectra comparison, two independent signals present in the AMP substrate trace were exemplarily selected (Figure 6A, dashed lines, corresponding to the injection of 80 µM ADP and 2 mM ADP). In both cases the time point of the respective assay baseline spectrum is marked as solid black line (manually set to 80 seconds prior to the respective peak maximum; see Figure 6, top right).

A spectra comparison was automatically performed by subtracting the spectrum corresponding to the selected peak maximum (Figure 6A, dashed lines) from the reference baseline spectrum corresponding to the selected minimum (Figure 6A, solid lines). Molecules possessing higher intensities within the selected peak spectrum compared to the reference peak spectrum are therefore displayed as negative signal and vice versa (Figure 6B and 6C) [19]. The injection of 80 µM ADP (Figure 6A, left dashed line) results in an increase of Ado and AMP signal and no detectable ADP signal (Figure 6B). As already discussed and displayed in Figure 4 at low ADP concentrations, the total amount of ADP can be enzymatically degraded to AMP and Ado, therefore causing negative signals for both molecules in the spectra comparison data evaluation.

Injection of 2 mM ADP (Figure 6A, right dashed line) however reveals a decrease of Ado and an increase of AMP as well as the emergence of ADP signals and co-occurring increases of ADP and AMP Na- and K adducts (Figure 6C).

With high ADP concentrations introduced to the system, ADP can be only partially degraded to AMP, resulting in a negative signal of remaining ADP and a distinctively higher negative signal for AMP. The positive Ado signal visible in the spectrum reflects the reduced amount of the final enzymatic product Ado, which is generated in lower quantity due to the presence of the favored ADP substrate.

Acetylcholine esterase assay data evaluation

The identification of regulatory substances from complex mixtures

is an emerging research area, which becomes more and more important within the scope of pharmaceutical, environmental or nutritional issues [1,8,21]. In a current project different house dust extracts were used for the screening of their regulatory influence on enzymatic systems. The investigation of the extract and especially their partially unknown molecular composition led to a large amount of data that had to be evaluated.

Enzymatic activity response and identification of regulatory molecules from complex mixtures: The identification of negative and/or positive EIC peak areas, indicating enzymatic regulation, and simultaneously the evaluation of the related mass spectra detected at time points of regulation, serve as a basis for the finding of enzyme regulatory compounds. In this regard, the effects of house dust extracts were investigated on their influence on AChE activity.

A positive control was included by spiking the house dust extract with the known AChE inhibitor galanthamine. The spiked extract sample was injected to the system and chromatographically separated by HT-HPLC (Figure 1, setup 2, middle trace) before it was introduced to the continuous flow containing AChE (Figure 1, upper trace). Data evaluation with the Achroma 'signal recognition' module revealed two negative peaks, which were automatically identified and tagged in the continuous trace of the assay product choline (Figure 7A, light and dark grey area). The negative peaks may therefore indicate the presence of an AChE regulatory compound contained in the house dust sample. The peak areas in the product trace can be easily calculated with Achroma and may also provide further information about the strength of an enzymatic regulation. After calculating and analyzing the recognized negative signal peaks, software module 'spectra comparison' was applied. By comparing the spectrum underlying a negative peak signal time range with a constant signal time range spectrum (baseline), information about differences between their compositions was obtained (Figure 7B and 7C). Subsequently regulatory extract compounds can be easily identified by means of their

m/z. The spectrum comparison of the negative signal 1 (Figure 7A, 7B and 7D, light grey area) with the constant non-regulated baseline spectrum (Figure 7A, dashed line) revealed no significant characteristic difference of m/z signals. In contrast, the comparison of the negative peak 2 spectrum (Figure 7A and 7C, dark grey area) with the baseline spectrum (Figure 7A, dashed line) showed a distinct difference, which is displayed as negative spectrum signal with a m/z of 288 (Figure 7C). The signal is only apparent in the spectrum of the negative peak 2 area and seems to affect the activity of AChE. To verify this finding, the EIC of m/z 288 was visualized (Figure 7E), hereby revealing a retention time, which is identical with the time point of the negative EIC peak signal within the (choline) product trace. Since the house dust extract was spiked with a known AChE inhibitor, m/z 288 could be assigned to galanthamine $(M+H)^+$, therewith clearly showing the applicability of the experimental setup as well as the benefits of Achroma software for a comprehensive data analysis.

Conclusion

Achroma software features were presented in detail, in this manner demonstrating the software to be a powerful and beneficial tool. It supports a fast and wide-ranging interpretation of (a-)typical mass spectrometrically detected enzymatic assay data, e.g. data which are obtained with an online coupled continuous flow system. The three modules 'signal recognition', 'signal comparison' and 'chromatogram comparison' discussed in this work provide several possibilities regarding data evaluation. Negative and positive signal peak areas within the trace of a substrate, intermediate and/or product EIC could be assessed for iAP enzymatic assay with 'signal recognition' module. Detailed examination of the recorded mass spectrometric data thus revealed the enzyme´s substrate preference towards ADP and ATP in comparison to AMP. Besides the injection of alternative substrates, negative and positive peaks are often related to events of enzymatic regulation, *e.g.* caused by an inhibitor. In this context AChE activity was investigated in the presence of chromatographically separated house dust extracts, spiked with a known AChE inhibitor as positive control. An enzymatic assay response related to the inhibitor added could be detected and evaluated with Achroma modules 'signal recognition' and 'spectra comparison'. The latter provided the comparative assessment of mass spectrometric spectra, detected at different time points to identify the compound responsible for AChE inhibition. Besides the finding of newly emerging molecule signals, e.g. like enzyme inhibiting or activating compounds from complex mixtures, also intensity changes could be easily identified.

The third module, 'chromatogram comparison', provides an easy means to control and correct mass spectrometric data for signal loss or signal inconstancies. It was therefore employed to assess signal inconstancies within iAP enzymatic assay traces in comparison to the course of an internal standard also taken along. The calculation of a quotient and in this manner the correction of assay EICs revealed the nature of signal loss events as related to mass spectrometric detection rather than enzymatic regulation.

Achroma software was shown to be efficient for the analysis of mass spectrometric data, whose evaluation has been too complex, time consuming or even impossible heretofore. However, further adaptions are necessary to fully exploit the improvement potential. For this purpose the functionality of Achroma software will be transferred into an open source modular analytical software platform (openMASP) to revise and expand the modules explained in this work. By switching to the open source platform the implemented code of Achroma will
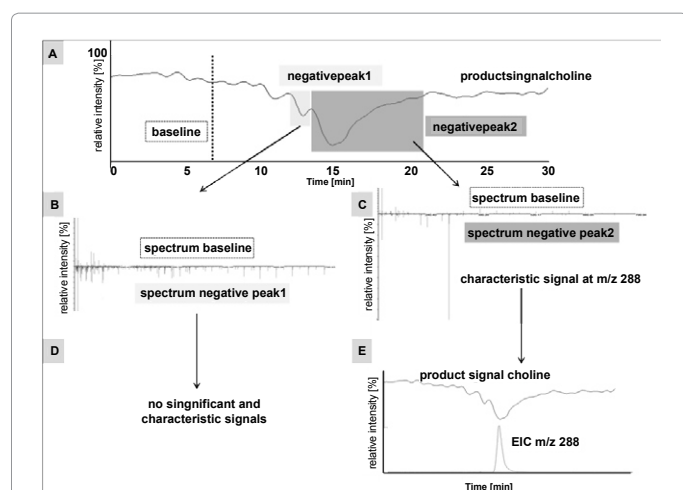
Figure 7: Screening of a house dust extract on its regulatory influence on AChE activity. Detection of negative signals and calculation of signal areas present in the course of the product trace was performed with the 'signal recognition' software tool (A). Comparison of the product EIC baseline spectrum with the spectra corresponding to the negative peak areas was done with 'spectra comparison' tool (B,C). No significant difference of baseline spectrum to negative peak 1 spectrum was detected (B,D). A potentially enzyme regulatory substance was identified, reflected by a characteristic difference between baseline spectrum and negative area spectrum (m/z 288, C). EIC of regulatory substance revealed the concurrence of the compound´s retention time and the time point of regulation (D).

be free, open and downloadable for users, in this manner enabling the participation of external software developers/analysts in improving and adjusting the software functions or even adding new modules to the analytical software platform. Until then every potential user can download the Achroma software for free and may use it as helpful as it is. Further information regarding software and hardware requirements can be found in a previous publication [19] or on the Achroma web page [18].

References

1. Grassmann J, Scheerle RK, Letzel T (2012) Functional proteomics: application of mass spectrometry to the study of enzymology in complex mixtures. Anal Bioanal Chem 402: 625-645.

2. Greis KD (2007) Mass spectrometry for enzyme assays and inhibitor screening: an emerging application in pharmaceutical research. Mass Spectrom Rev 26: 324-339.

3. Letzel T (2008) Real-time mass spectrometry in enzymology. Anal Bioanal Chem 390: 257-261.

4. Ruotolo BT, Verbeck GF, Thomson LM, Gillig KJ, Russell DH (2002) Observation of conserved solution-phase secondary structure in gas-phase tryptic peptides. J Am Chem Soc 124: 4214-4215.

5. Dennhart N, Letzel T (2006) Mass spectrometric real-time monitoring of enzymatic glycosidic hydrolysis, enzymatic inhibition and enzyme complexes. Anal Bioanal Chem 386: 689-698.

6. Kaltashov IA, Fenselau C (1997) Stability of secondary structural elements in a solvent-free environment: the alpha helix. Proteins 27: 165-170.

7. Hogenboom AC, de Boer AR, Derks RJ, Irth H (2001) Continuous-flow, on-line monitoring of biospecific interactions using electrospray mass spectrometry. Anal Chem 73: 3816-3823.

8. Kool J, Giera M, Irth H, Niessen WM (2011) Advances in mass spectrometry-based post-column bioaffinity profiling of mixtures. Anal Bioanal Chem 399: 2655-2668.

9. de Jong CF, Derks RJE, Bruyneel B, Niessen W, Irth H (2006) High-performance liquid chromatography-mass spectrometry-based acetylcholinesterase assay for the screening of inhibitors in natural extracts. J Chromatogr A 1112: 303-310.

10. Schenk T, Breel GJ, Koevoets P, van den Berg S, Hogenboom AC, et al. (2003) Screening of natural products extracts for the presence of phosphodiesterase inhibitors using liquid chromatography coupled online to parallel biochemical detection and chemical characterization. J Biomol Screen 8: 421-429.

11. Kool J, Eggink M, van Rossum H, van Liempd SM, van Elswijk DA, et al. (2007) Online biochemical detection of glutathione-S-transferase P1-specific inhibitors in complex mixtures. J Biomol Screen 12: 396-405.

12. Colangelo CM, Chung L, Bruce C, Cheung KH (2013) Review of software tools for design and analysis of large scale MRM proteomic datasets. Methods 61: 287-298.

13. MacLean B, Tomazela DM, Shulman N, Chambers M, Finney GL, et al. (2010) Skyline: an open source document editor for creating and analyzing targeted proteomics experiments. Bioinformatics 26: 966-968.

14. Brusniak MY, Kwok ST, Christiansen M, Campbell D, Reiter L, et al. (2011) ATAQS: A computational software tool for high throughput transition optimization and validation for selected reaction monitoring mass spectrometry. BMC bioinformatics 12: 78.

15. Kaufmann CM, Grassmann J, Treutter D, Letzel T (2014) Utilization of real-time electrospray ionization mass spectrometry to gain further insight into the course of nucleotide degradation by intestinal alkaline phosphatase. Rapid Commun Mass Spectrom 28: 869-878.

16. Schebb NH, Vielhaber T, Jousset A, Karst U (2009) Development of a liquid chromatography-based screening methodology for proteolytic enzyme activity. J Chromatogr A 1216: 4407-4415.

17. Scheerle RK, Grassmann J, Letzel T (2012) Real-time ESI-MS of enzymatic conversion: impact of organic solvents and multiplexing. Anal Sci 28: 607-612.

18. Krappmann (2012) open MASP.

19. Krappmann M, Letzel T (2012) Achroma: a software strategy for analysing (a-)typical mass-spectrometric data. Analytical Methods 4: 1060-1071.

20. Moss DW, Walli AK (1969) Intermediates in the hydrolysis of ATP by human alkaline phosphatase. Biochim Biophys Acta 191: 476-477.

21. Shi SY, Zhou HH, Zhang YP, Jiang XY, Chen XQ, et al. (2009) Coupling HPLC to on-line, post-column (bio)chemical assays for high-resolution screening of bioactive compounds from complex mixtures. TrAC-Trends Anal Chem 28: 865-877.

Appendix III

Enzymatic Assays Coupled with Mass Spectrometry with or without Embedded Liquid Chromatography

Therese Burkhardt*, Christine M. Kaufmann*, Thomas Letzel and Johanna Grassmann

*equal contribution of the authors

The following publication outlines several experimental approaches for the determination of enzymatic activity detected with mass spectrometry. The discussed setups are utilized for various applications in the context of enzymatic assays. This includes the detection of enzymatic activity with or without the addition of regulatory compounds or the measurement of multiplex assays amongst others.

Data and chapter outlining intestinal alkaline phosphatase enzymatic assay was conducted and evaluated on my part. Moreover the collection of literature data regarding the online coupled continuous flow mixing system with special emphasis to the injected compounds and the chromatographic method employed was done by me.

General parts of the publication, i.e. introduction and conclusion were written by all parties involved.

Enzymatic Assays Coupled with Mass Spectrometry with or without Embedded Liquid Chromatography

Therese Burkhardt, Christine M. Kaufmann, Thomas Letzel,* and Johanna Grassmann[a]

This article reviews monitoring strategies for enzymatic assays coupled with mass spectrometric detection. This coupling has already been shown to be helpful in providing versatile and detailed knowledge about enzyme kinetics. Various available publications address two general approaches. 1) The continuous-flow setup allows real-time determination of substrate degradation. Simultaneously, resulting product or potential intermediates can be detected. 2) The online coupled continuous-flow mixing assay allows the direct coupling of an enzymatic assay to chromatographic separation of complex mixtures. The latest efforts in improving the methodology have been made with regard to miniaturization. This is especially advantageous with regard to reducing costly consumption of chemicals. Finally, these developments are applicable for diverse bioanalytical purposes in the realms of pharmaceutical, biotechnological, food, and environmental research.

Introduction

Enzymatic reactions are of interest because their catalysis not only reflects biological function, but also enables the effective chemical production of various organic molecules (in so-called "white biotechnology"). As a result of their individual and unique properties in terms of specificity and catalytic efficiency, enzymes play essential roles in the fields of environmental and water research[1] and of food and nutrition,[2] as well as in the chemical,[3] pharmaceutical,[4] and biotechnological[4a, 5] industries.

Conventionally, enzymatic reactions are analyzed either continuously with spectroscopic techniques (e.g., photometry, fluorescence) or offline by LC-MS, GC-MS, or CE-MS techniques using the inactivated reaction solutions. Nowadays, the conditions for these enzymatic reactions can also be designed in a manner in which they are coupled directly and online to mass spectrometric detection.[6] The apparent advantage of MS detection is the opportunity to use physiological substrates. Artificial or labeled substrates, which are usually necessary in spectroscopic measurements, might alter the enzymatic activity.[7] In addition to this, MS detection allows for the utilization of low substrate and enzyme concentrations. Combined with low flow rates (nL min^{-1} up to 5 µL min^{-1}) a cost-effective measurement is enabled. This sensitive technique further offers the potential for simultaneous and online detection of all ionizable assay components: substrate, product(s), and potential intermediates.

With respect to MS requirements, volatile buffer systems are needed for direct coupling, resulting in partially non-physiolog-

ical conditions. However, despite this modification of the "conventional" assay conditions, enzymes still remain active, so that their reactions can be monitored. MS-compatible additives, often mandatory for enzymatic reactions, can be used as well, but in significantly lower concentrations. Addition of organic solvents, to prevent surface sticking of assay components and to lower surface tension (in the desolvation process of the MS ion source), might improve the experimental outcome.[8] However, limitations such as signal suppression or denaturation processes in the electrospray ion source should also be taken into account. Table 1 provides an overview of representative enzymatic assays established with mass spectrometric detection along with their potential areas of application. Further examples can be found in the literature.[6a–f]

Determination of Reaction Profiles and Cleavage Specificities by Using a Continuous-Flow Assay (without HPLC)

Single assays

A basic way to measure enzymatic reactions coupled to MS is direct injection by means of a (syringe) pump (Figure 1A, top). In this setup, buffer, substrate, enzyme (and additives) are mixed and filled into a syringe. Subsequently, the reaction mixture is directly introduced into the mass spectrometric source. Syringe-pump assays provide the opportunity to assess enzymatic kinetics as a result of the continuous nature of the measurement. The simultaneous measurement of substrate, product, and intermediates furthermore gives additional insight into the enzyme's mode of action.

A selection of studies is discussed in the forthcoming section and summarized in Table 1. This highlights the wide range of possibilities for studying the behavior of different enzymes with MS. In this regard, the investigation of different dephos-

[a] T. Burkhardt,+ C. M. Kaufmann,+ Prof. Dr. T. Letzel, Dr. J. Grassmann
Chair of Urban Water Systems Engineering, Technical University of Munich (TUM)
Am Coulombwall, 85748 Garching (Germany)
E-mail: t.letzel@tum.de
[+] These authors contributed equally to this work.

Table 1. Selection of enzymatic assays established with mass spectrometric detection and their application area.		
Enzyme	Possible application	Application area
acetylcholinesterase[11, 24]	screening for pesticides[25]	environmental analysis
	Alzheimer's disease therapy[26]	pharmaceutical industry
	chemical weapon screening[27]	defense and safety industry
chitinase and chitosanase[11]	design of new chemotherapeutics,[28] production of antimicrobial agents,[29]	pharmaceutical industry, food industry, agriculture
	production of agricultural control chemicals,[29–30]	
	preparation of D-glucosamine for osteoarthritis therapy[28b]	
chymotrypsin[11]	diagnostic test for pancreatic exocrine insufficiency[31]	medical research
cytochrome p450 (not published)	bioremediation of trace organic chemicals[32]	environmental applications
elastase[11]	skincare products and chronic obstructive pulmonary disease therapy	cosmetics industry, pharmaceutical industry
intestinal alkaline phosphatase[9]	anti-inflammatory regulation, maintenance of intestinal homeostasis[33]	pharmaceutical industry
laccase (not published)	bioremediation of trace organic chemicals[1a, 34]	environmental applications
myeloperoxidase (not published)	Parkinson's disease therapy[35]	pharmaceutical industry
	screening for antioxidants[36]	food chemistry and analytics, cosmetics industry
xanthine oxidase (not published)	gout therapy[37]	pharmaceutical industry
glutathione S-transferase (not published)	cancer treatment[38]	pharmaceutical industry
pepsin[39]	mucosal damage after gastric reflux[40]	pharmaceutical industry
trypsin[39]	involvement in pancreatitis[41]	pharmaceutical industry
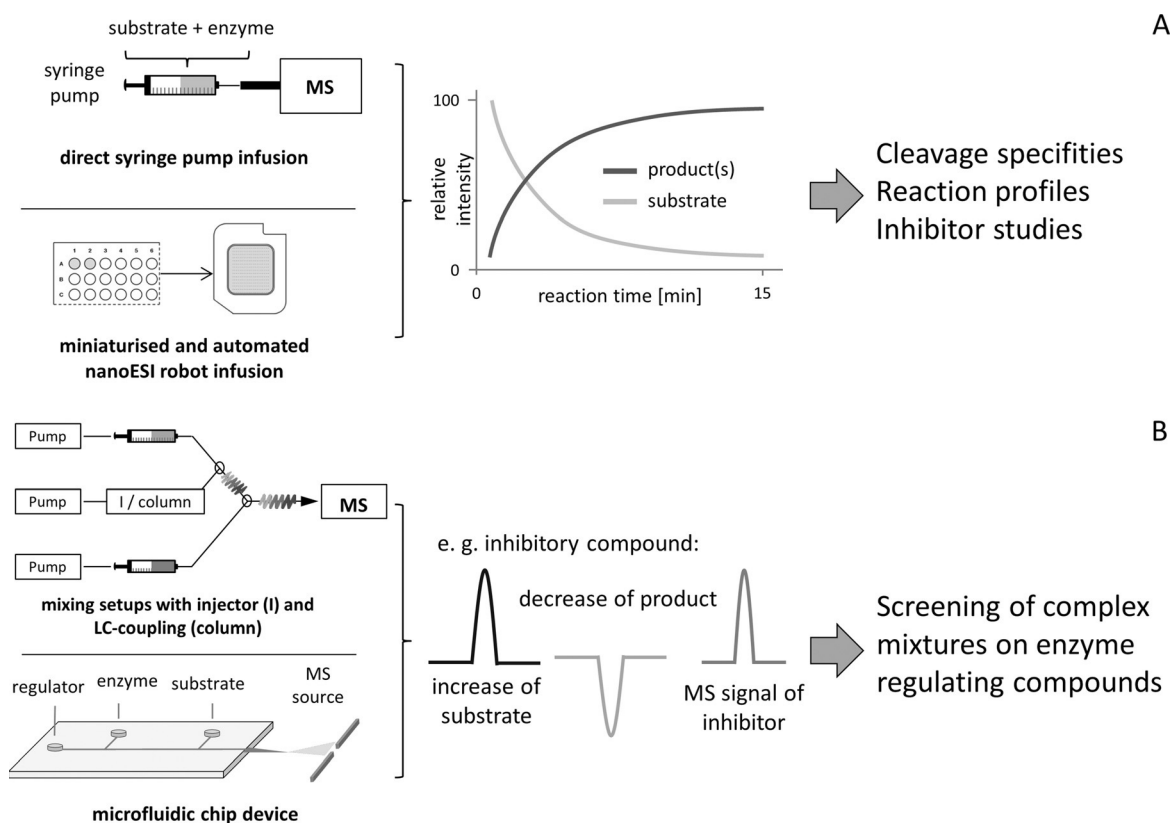
Figure 1. Overview of coupling techniques for studying enzymatic reactions by continuous-flow measurements. Basic approaches, miniaturization, and resulting data are shown schematically for A) a syringe pump assay, and B) the online coupled continuous-flow setup. Adapted from R. K. Scheerle, PhD thesis, TU München.

phorylation products of intestinal alkaline phosphatase is presented as an example. The degradation of the initial substrate, ATP, to the first product, ADP, can be observed. Subsequently, ADP is further degraded to AMP and finally to adenosine (Figure 2). Thus, mass spectrometric detection has the potential to identify enzymatically generated intermediates that would likely be disregarded with use of conventional spectroscopic methods.[9]
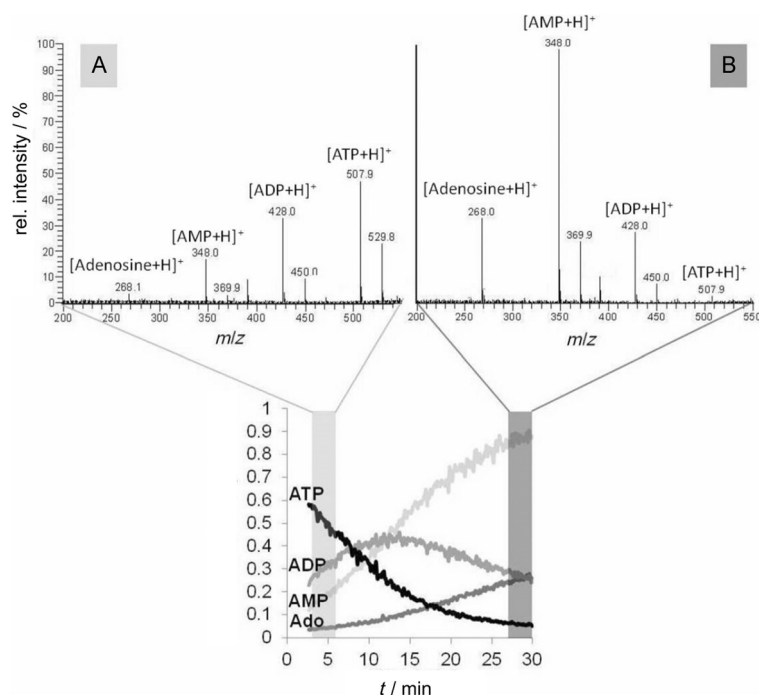
Figure 2. Direct syringe pump infusion assay with intestinal alkaline phosphatase and its substrate ATP. Mass spectra A) at the beginning, and B) at the end of measurement time. Time courses of substrate ATP and of intermediates ADP and AMP, as well as of the final product adenosine, are shown at the bottom.

Another study elucidated the hydrolysis profiles of chitosanases and chitinases. In the process, different cleavage patterns for these hydrolyzing enzymes could be evaluated with the aid of the continuous-flow technique.[10]

Multiplex assays

Mass spectrometric real-time online detection of enzymatic reactions can also be employed to assess enzymatic binding and catalytic preferences in the presence of multiple substrates. Vice versa, multiplex assays—that is, the simultaneous measurements of two or even more enzymes—can also be conducted in one single experiment. This approach is not only time- and cost-efficient but provides high information value with regard to kinetics and mutual enzymatic interactions. Figure 3 presents a multiplex experiment using chitinase and chymotrypsin in comparison with their single enzymatic assays. In this way, substrate degradation and product formation could be detected for both enzymes simultaneously. More-

over enzymatic activities were found to be almost as high in the multiplex approach as in the single assays (78% for chitinase and 94% for chymotrypsin). Further examples can be found in Scheerle et al.[11]
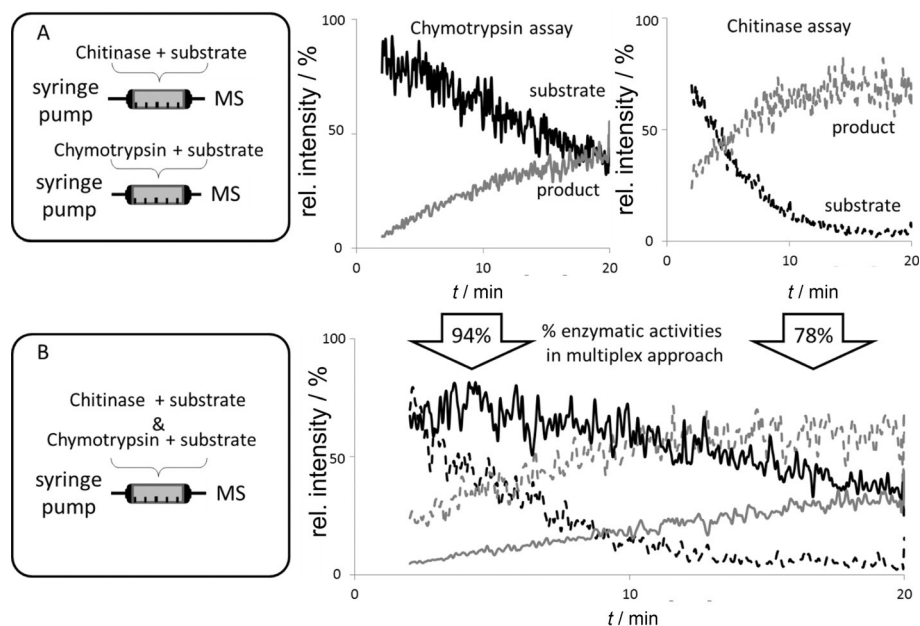
Investigation of Inhibitors by Using a Continuous-Flow Assay or the Online Coupled Continuous-Flow Mixing Assay

Determination of kinetic parameters

The described continuous-flow setup allows the addition of individual compounds to an assay for investigation of their capability in regulating an enzyme of interest. Those regulatory compounds can either inhibit or enhance the catalysis efficiencies of the enzymatic reactions. Figure 4 representatively illustrates the effect of the inhibitor (−)-epigallocatechin 3-gallate (EGCG) on the formation of nitrotyrosine by the enzyme myeloperoxidase and the remaining enzyme activity. The introduction of increasing concentrations of, for example, inhibitors provides an easy screening method for single compounds with respect to their regulatory potential and enables the determination of IC_{50} values. Regulator-associated changes in kinetic parameters such as K_m and v_{max} can furthermore elucidate the character of inhibition—whether it is competitive, noncompetitive, or uncompetitive. In recent years, interest has emerged in identifying enzymatic regulators from complex natural sources, such as plant extracts. For this purpose, an online coupled mixing assay can be applied, as demonstrated in the next section.

Figure 3. Direct syringe pump infusion assay with the enzymes chitinase and chymotrypsin. A) Individual enzymatic reactions of chitinase and chymotrypsin in the presence of their corresponding substrates, in comparison with B) the multiplex approach, in which both enzymes were measured simultaneously in one assay.
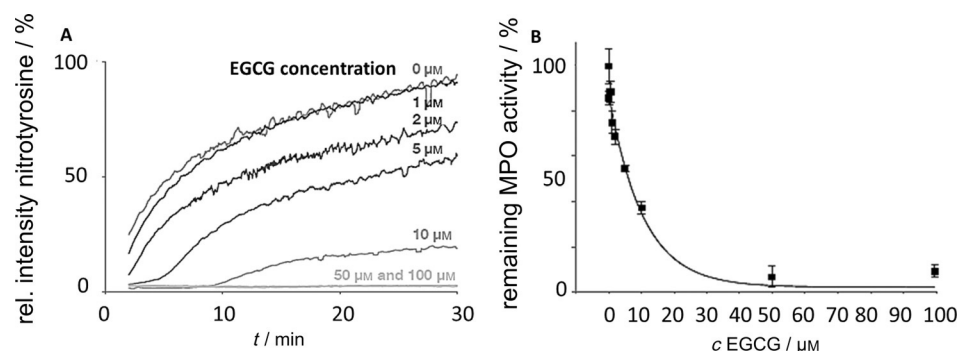
Figure 4. Inhibition studies with the enzyme myeloperoxidase (MPO), tyrosine as substrate, and EGCG as inhibitor. A) Product formation (nitrotyrosine, NitroTyr) in the presence of different inhibitor concentrations (0–100 μM EGCG). B) Relative myeloperoxidase activity plotted against the EGCG concentration for determination of the IC_{50} value.

Complex mixtures

Usually, complex mixtures are tested on contained enzyme regulators by high-throughput screening techniques, which involve time-consuming isolation and sample-processing procedures. This entails extract fractionation followed by the exposure of the enzymatic target to the collected fractions (Figure 5; "Conventional Screening").[12] In this manner the number of compounds is gradually narrowed down, thus providing the possibility to reveal a potential new drug. Other studies represent a combination of identification (by MS) and functionality (by spectroscopy)[13] (Figure 5; "Combined Bioassays"). However, the need for fast and integrated analytical methods led to the development of new screening ap-

proaches. These setups would ideally enable the identification of a regulator by its molecular weight (i.e., chemical information) and simultaneously allow the determination of its functionality, both detected by mass spectrometry (Figure 5; online coupled bioassay). This resulted in the development of a so-called "online coupled continuous-flow mixing assay" (Figure 1 B; top).[14]

The combination of chromatographic separation with a biochemical assay offers the possibility to screen for regulators in complex matrices (Table 2). To couple chromatography and bioassay, one has to face some challenges. Primarily, a chromatographic separation typically needs addition of an organic solvent to the mobile phase for effective elution of hydrophobic compounds from the reversed-phase chromatographic column. Beyond this, most chromatographic columns require the addition of at least small proportions of organic solvents to maintain stability. On the other hand, organic solvents affect enzymatic activity, through denaturation, interference with substrate binding, direct inhibition, and other negative effects.[11,14–15] For this reason various solvents have to be tested for their influence on the enzyme(s) of interest before application in the mixing assay.[11] In order to maintain constant or-
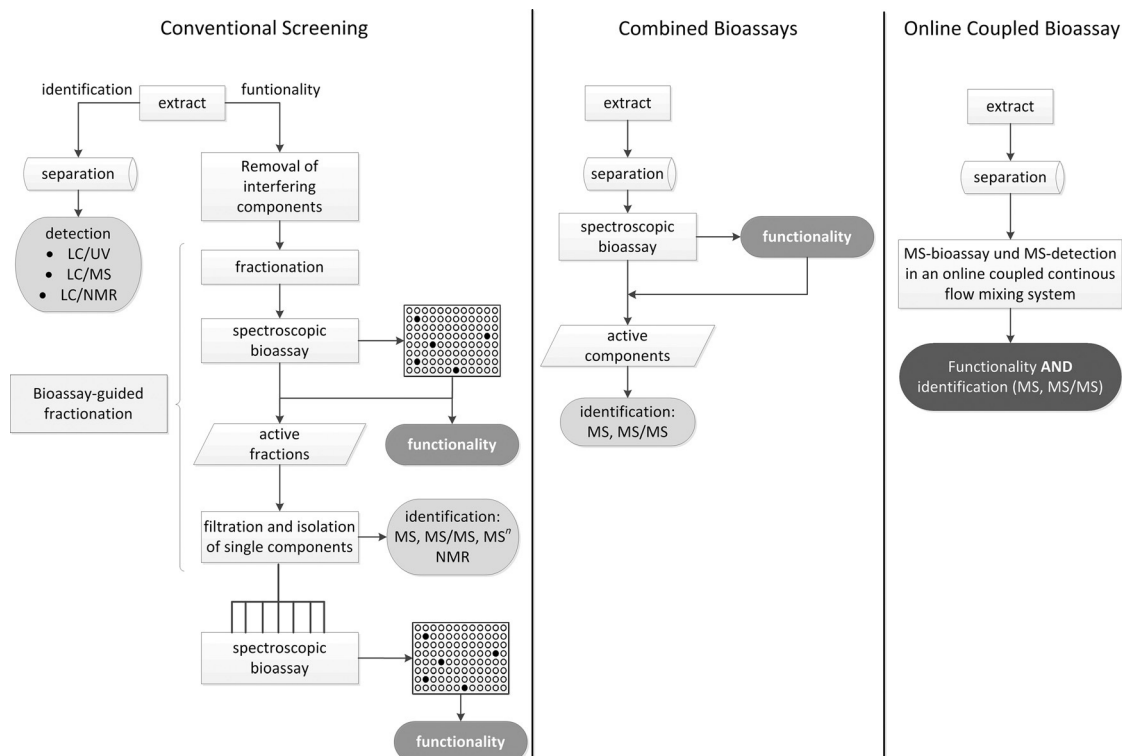
Figure 5. Workflow comparison for three different methodological approaches with regard to the assessment of functional bioassays.

Table 2. Publication overview of online coupled continuous-flow setups previously employed to investigate the activities of various enzymes in the presence of known inhibitors and/or complex mixtures. Chromatographic separation parameters and methods of assay detection are given.

Enzyme(s)	Injection of/separation of	Chromatographic column	Eluent	Enzymatic assay detection	T [°C]	Ref.
acetylcholine esterase	narcissus extract, known inhibitors physostigmine, galanthamine, and carbachol	LiChrospher RP SelectB (Merck)	40% MeOH or 30% MeOH (isocratic)	UV	n.s.	[15a]
phosphodi-esterase	natural products extracts, known inhibitors theophylline and papaverine	Luna C18 (Phenomenex)	5–95% MeOH (gradient)	fluorescence	n.s.	[13a]
acetylcholine esterase	narcissus extract, known inhibitor galanthamine	Luna C18 (Phenomenex)	21.5–78.5% MeOH (gradient)	MS	n.s.	[20]
cathepsin B	five flavonoids, known inhibitors E-64 and leupeptin	ODS Hypersil RP-C18 (Agilent Technologies)	45.5% MeOH (isocratic)	MS	25 (constant)	[14]
	red clover extract (*Trifolium pratense* L.), known inhibitors E-64 and leupeptin, fungi sample		9.5–90.5% MeOH (gradient)	MS	25 (constant)	[14]
xanthine oxidase	*Perilla frutescens* extract	Synergi Polar-RP (Phenomenex)	100% aqueous (isocratic)	MS	30–70 (gradient)	unpub. data
xanthine oxidase, intestinal alkaline phosphatase	*Perilla frutescens* extract	Luna PFP (Phenomenex)	5% isopropyl alcohol, 5% ethanol, 10% ethanol or 5% MeOH (isocratic)	MS	30–70 (gradient)	unpub. data
cathepsin B	tea extract, known inhibitors CA-074, E-64, leupeptin	DiamondBond C18 (ZirChrom)	10% MeOH (isocratic)	MS	90–208	[16]
trypsin, thrombin	inhibitors of the benzamidine type	Luna C18 (2) (Phenomenex)	5–95% MeOH (gradient and countergradient)	fluorescence	n.s.	[18a]
cytochrome P450	various inhibitors	Luna C18 (2) (Phenomenex)	5–95% MeCN (gradient and countergradient)	fluorescence	n.s.	[18d]
estrogen receptor α	bioaffinity profiling with 14 different metabolites	Prodigy C18 (Phenomenex)	5–95% MeOH (gradient and countergradient)	fluorescence	n.s.	[18c]
acetylcholine binding protein	bioaffinity profiling	Xterra C18 MS column (waters)	≈70% MeOH (isocratic) or ≈20% MeOH to ≈100% MeOH (gradient)	fluorescence	n.s.	[42]
glutathione S-transferase	eight ligands and synthesized GST inhibitors	Luna C18 (2) (Phenomenex)	5–95% MeOH (gradient and countergradient)	fluorescence	n.s.	[18b]
protease	two inhibitors	n.a.	n.a.	fluorescence (FRET)	n.s.	[43]
protease	two inhibitors	size-exclusion guard column Biosep S-2000 (Phenomenex)	100% aqueous	fluorescence (FRET)	n.s.	[19b]
microperoxidases	microperoxidases	Prontosil 120-5-phenyl column (Bischoff Chromatography)	10% MeCN to 30% MeCN (gradient)	fluorescence	n.s.	[44]
angiotensin-converting enzyme	inhibitors: for example, hydrolyzed whey proteins	Altech Ultima C18	2–95% MeOH (gradient and countergradient)	fluorescence	RT	[45]
proteases	proteases	ion-exchange (CM-825 cation-exchange column, Shodex) or size-exclusion chromatography (TSK-Gel G2000SWXL column, Tosoh)	100% aqueous	UV	n.s.	[19a]
glutathione S-transferase	mycotoxin patulin	Supelco Discovery RP18 column (Sigma–Aldrich)	50% MeOH (isocratic) or ≈5% MeOH to 85% MeOH	fluorescence	n.s.	[46]

n.a.: not available, n.s.: not specified.

ganic solvent exposure to the enzyme, isocratic separation over the entire measurement time is favored, to ensure a consistent substrate and product signal.[15] Isocratic elution, however, distinctly decreases the amount of compounds that can be eluted from the chromatographic column. A considerable improvement in chromatographic performance—even when an isocratic flow is applied—can be achieved by means of a temperature gradient.[16] With increasing temperature, the

static permittivity or dielectric constant, and hence the polarity, of the chromatographic eluent decreases.[17] This results in enhanced solubility of rather nonpolar compounds and thus in reduced retention times and finally in increasing numbers of eluting compounds. In assays with enzymatic reactions, the employment of a temperature gradient can therefore serve as an effective substitute for an organic solvent gradient. However, high-temperature liquid chromatography (HTLC) necessitates thermally stable column materials. Conventional silica columns are unsuitable for HTLC application due to their comparatively low temperature stability of up to 70–80 °C. Nevertheless, they do enable the use of moderate temperature gradients, which can also result in distinct reductions of retention times.

A different approach, which has already been employed in several studies, is the introduction of a so-called countergradient[18] (Table 2). By antagonizing a gradient with increasing organic solvent concentrations necessary for LC separation, a constant and low amount of solvent can be maintained to ensure stable enzymatic activity.

To avoid the use of organic solvents entirely, whilst nevertheless maintaining the capacity of the system for separation, ion-exchange or size-exclusion chromatography columns might represent the means of choice, although only a few studies are yet available[19] (Table 2). Subsequently to successful chromatography, the separated compounds are successively introduced into the flow containing the enzyme (Figure 1 B, top). The enzyme/compound mixture is then introduced into the substrate flow. A change in mass spectrometrically detected substrate degradation and product formation indicates a regulatory event (Figure 2 B). These alterations in enzymatic activity can be captured in various ways, by colorimetric,[15a] fluorimetric, or mass spectrometric recording (Table 2).[14,15b,16,20]

With use of colorimetric detection at a defined wavelength, information about either the substrate or the product might be lost. Additional assay components absorbing at the detection wavelength might furthermore lead to incorrect data interpretation. Fluorescence detection might be used for measurements focusing on known reaction products, for which it is a very sensitive and selective method. However, only mass spectrometric detection provides the possibility to detect all ionizable compounds simultaneously (Figure 6), including known and unknown enzymatic intermediates, as well as the corresponding enzymatic inhibitor or stimulator. The regulatory compound is captured as a mass spectrometric peak within the timespan of enzymatic regulation (Figure 6, black trace). In this regard, the elution of, for example, an inhibitor leads to an increase in the substrate trace (Figure 6, dark gray trace) and a decrease in product formation (Figure 6, light gray trace). With the aid of an internal standard (IS), the stability of the system can be assessed (Figure 6, black dotted trace), to allow distinction between actual regulation events and mass spectrometric signal suppression.
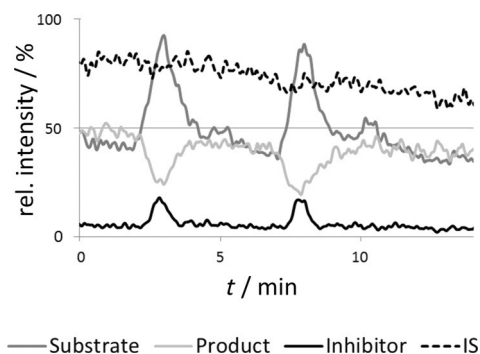
Figure 6. Online coupled xanthine oxidase bioassay after a double injection of the known inhibitor allopurinol. The uric acid product trace decreases and the xanthine substrate trace increases when allopurinol is present. IS is the internal standard.

Miniaturization: Directions for Future Research

The various advantages of the described coupling techniques can further be enhanced by miniaturization. The consumption of enzyme and substrate can be distinctly decreased. With regard to the components to be investigated, enzymatic assays can be conducted with use of lower quantities, in order to achieve environmentally or physiologically relevant concentrations.

For continuous-flow assays a nanoliter mixing/spraying device that combines a robot part with an ESI chip can be used (Figure 1 B, bottom). Previous investigations have already shown the great potential of robotic automation as a routine device for studying enzymatic reactions.[21]

Miniaturization of the online coupled continuous-flow setups can be achieved on a microfluidic chip device (Figure 1 B, bottom). The possibility of conducting enzymatic reactions on a chip in continuous-flow mode has also already been demonstrated.[15b,22] Current research focuses on the development of a microfluidic chip for the analytical, zero-death-volume investigation of enzymatic reactions. This reaction chip is designed in such a manner as to enable direct coupling to a mass spectrometer.[23]

Conclusion

The application of real-time online continuous-flow setups facilitates comprehensive analysis of enzymatic reactions and their regulation. The use of mass spectrometric detection usually allows easy and fast assessment of all ionizable assay components, including enzymatically formed intermediates. Experiments to investigate substrate cleavage specificities, substrate preference, multiplex approaches, or the determination of IC$_{50}$ values represent further promising areas of application. Beyond that, the continuous-flow coupling of a bioassay to a chromatographic separation enables the screening of complex mixtures for their potential to inhibit or stimulate enzymes of interest. Various adaptations, meeting different requirements in terms of separation and detection, might support the application of online coupled continuous-flow setups for a wide range of enzymatic assays, inhibitor screenings, and

investigation of complex (natural) mixtures in functional proteomics and metabolomics. Further development with regard to assay miniaturization should result in time- and cost-efficient methods to analyze and assess functional enzymatic reactions in nanoflow ranges.

Acknowledgement

Keywords: continuous-flow assays · enzymes · functional proteomics · mass spectrometry · metabolomics

[1] a) T. D. Sutherland, I. Horne, K. M. Weir, C. W. Coppin, M. R. Williams, M. Selleck, R. J. Russell, J. G. Oakeshott, *Clin. Exp. Pharmacol. Physiol.* **2004**, *31*, 817–821; b) M. A. Rao, R. Scelza, F. Acevedo, M. C. Diez, L. Gianfreda, *Chemosphere* **2014**, *107*, 145–162.

[2] a) D. Panyam, A. Kilara, *Trends Food Sci. Technol.* **1996**, *7*, 120–125; b) G. A. Tucker, L. Woods, *Enzymes in Food Processing*, Springer, New York, NY, **1995**.

[3] a) A. Schmid, F. Hollmann, J. B. Park, B. Bühler, *Curr. Opin. Biotechnol.* **2002**, *13*, 359–366; b) K. M. Koeller, C.-H. Wong, *Nature* **2001**, *409*, 232–240.

[4] a) T. Palmer, P. L. Bonner, *Enzymes: Biochemistry, Biotechnology, Clinical Chemistry*, Elsevier, Amsterdam, **2007**; b) J. P. Rasor, E. Voss, *Appl. Catal. A* **2001**, *221*, 145–158.

[5] a) V. B. Urlacher, S. Lutz-Wahl, R. D. Schmid, *Appl. Microbiol. Biotechnol.* **2004**, *64*, 317–325; b) M. K. Bhat, *Biotechnol. Adv.* **2000**, *18*, 355–383; c) K.-E. Jaeger, T. Eggert, *Curr. Opin. Biotechnol.* **2002**, *13*, 390–397.

[6] a) T. Letzel, *Anal. Bioanal. Chem.* **2008**, *390*, 257–261; b) K. D. Greis, *Mass Spectrom. Rev.* **2007**, *26*, 324–339; c) A. R. de Boer, H. Lingeman, W. M. A. Niessen, H. Irth, *Trac-Trends Anal. Chem.* **2007**, *26*, 867–883; d) K. F. Geoghegan, M. A. Kelly, *Mass Spectrom. Rev.* **2005**, *24*, 347–366; e) A. Liesener, U. Karst, *Anal. Bioanal. Chem.* **2005**, *382*, 1451–1464; f) J. Grassmann, R. K. Scheerle, T. Letzel, *Anal. Bioanal. Chem.* **2012**, *402*, 625–645; g) M. T. Reetz, M. H. Becker, H.-W. Klein, D. Stöckigt, *Angew. Chem. Int. Ed.* **1999**, *38*, 1758–1761; *Angew. Chem.* **1999**, *111*, 1872–1875.

[7] T. Letzel, E. Sahmel-Schneider, K. Skriver, T. Ohnuma, T. Fukamizo, *Carbohydr. Res.* **2011**, *346*, 863–866.

[8] A. R. de Boer, T. Letzel, H. Lingeman, H. Irth, *Anal. Bioanal. Chem.* **2005**, *381*, 647–655.

[9] C. M. Kaufmann, J. Grassmann, D. Treutter, T. Letzel, *Rapid Commun. Mass Spectrom.* **2014**, *28*, 869–878.

[10] a) N. Dennhart, L. M. M. Weigang, M. Fujiwara, T. Fukamizo, K. Skriver, T. Letzel, *J. Biotechnol.* **2009**, *143*, 274–283; b) M. Zitouni, M. Fortin, R. K. Scheerle, T. Letzel, D. Matteau, S. Rodrigue, R. Brzezinski, *Appl. Microbiol. Biotechnol.* **2013**, *97*, 5801–5813.

[11] R. K. Scheerle, J. Grassmann, T. Letzel, *Anal. Sci.* **2012**, *28*, 607–612.

[12] C. F. B. Holmes, *Toxicon* **1991**, *29*, 469–477.

[13] a) T. Schenk, G. J. Breel, P. Koevoets, S. van den Berg, A. C. Hogenboom, H. Irth, U. R. Tjaden, J. van der Greef, *J. Biomol. Screening* **2003**, *8*, 421–429; b) R. J. Derks, A. C. Hogenboom, G. van der Zwan, H. Irth, *Anal. Chem.* **2003**, *75*, 3376–3384.

[14] A. R. de Boer, T. Letzel, D. A. van Elswijk, H. Lingeman, W. M. A. Niessen, H. Irth, *Anal. Chem.* **2004**, *76*, 3155–3161.

[15] a) K. Ingkaninan, C. M. de Best, R. van der Heijden, A. J. P. Hofte, B. Karabatak, H. Irth, U. R. Tjaden, J. van der Greef, R. Verpoorte, *J. Chromatogr. A* **2000**, *872*, 61–73; b) A. R. de Boer, B. Bruyneel, J. G. Krabbe, H. Lingeman, W. M. Niessen, H. Irth, *Lab Chip* **2005**, *5*, 1286–1292.

[16] A. R. de Boer, J. M. Alcaide-Hidalgo, J. G. Krabbe, J. Kolkman, C. N. V. Boas, W. M. A. Niessen, H. Lingeman, H. Irth, *Anal. Chem.* **2005**, *77*, 7894–7900.

[17] T. Teutenberg, S. Wiese, P. Wagner, J. Gmehling, *J. Chromatogr. A* **2009**, *1216*, 8480–8487.

[18] a) N. H. Schebb, F. Heus, T. Saenger, U. Karst, H. Irth, J. Kool, *Anal. Chem.* **2008**, *80*, 6764–6772; b) J. Kool, M. Eggink, H. van Rossum, S. M. van Liempd, D. A. van Elswijk, H. Irth, J. N. Commandeur, J. H. Meerman, N. P. Vermeulen, *J. Biomol. Screening* **2007**, *12*, 396–405; c) J. Kool, R. Ramautar, S. M. van Liempd, J. Beckman, F. J. de Kanter, J. H. Meerman, T. Schenk, H. Irth, J. N. Commandeur, N. P. Vermeulen, *J. Med. Chem.* **2006**, *49*, 3287–3292; d) J. Kool, S. M. van Liempd, R. Ramautar, T. Schenk, J. H. Meerman, H. Irth, J. N. Commandeur, N. P. Vermeulen, *J. Biomol. Screening* **2005**, *10*, 427–436.

[19] a) N. H. Schebb, T. Vielhaber, A. Jousset, U. Karst, *J. Chromatogr. A* **2009**, *1216*, 4407–4415; b) J. Hirata, L. P. Chung, F. Ariese, H. Irth, C. Gooijer, *J. Chromatogr. A* **2005**, *1081*, 140–144.

[20] C. F. de Jong, R. J. E. Derks, B. Bruyneel, W. Niessen, H. Irth, *J. Chromatogr. A* **2006**, *1112*, 303–310.

[21] R. K. Scheerle, J. Grassmann, T. Letzel, *Anal. Methods* **2011**, *3*, 822–830.

[22] a) S. Benetton, J. Kameoka, A. Tan, T. Wachs, H. Craighead, J. D. Henion, *Anal. Chem.* **2003**, *75*, 6430–6436; b) K. Kanno, H. Maeda, S. Izumo, M. Ikuno, K. Takeshita, A. Tashiro, M. Fujii, *Lab Chip* **2002**, *2*, 15–18; c) J. Wang, *Electrophoresis* **2002**, *23*, 713–718; d) J. Svobodová, S. Mathur, A. Muck, T. Letzel, A. Svatos, *Electrophoresis* **2010**, *31*, 2680–2685.

[23] S. Ohla, D. Belder, *Curr. Opin. Chem. Biol.* **2012**, *16*, 453–459.

[24] M. Krappmann, C. M. Kaufmann, R. K. Scheerle, J. Grassmann, T. Letzel, *J. Proteomics Bioinform.* **2014**, *7*, 264–271.

[25] C. S. Pundir, N. Chauhan, *Anal. Biochem.* **2012**, *429*, 19–31.

[26] a) N. Tabet, *Age Ageing* **2006**, *35*, 336–338; b) V. N. Talesa, *Mech. Ageing Dev.* **2001**, *122*, 1961–1969.

[27] G. M. Murray in *Encyclopedia of Analytical Chemistry*, Wiley, Hoboken, **2006**.

[28] a) M. J. Dixon, O. A. Andersen, D. M. van Aalten, I. M. Eggleston, *Bioorg. Med. Chem. Lett.* **2005**, *15*, 4717–4721; b) N. Dahiya, R. Tewari, G. S. Hoondal, *Appl. Microbiol. Biotechnol.* **2006**, *71*, 773–782.

[29] S. B. Chavan, M. V. Deshpande, *Biotechnol. Prog.* **2013**, *29*, 833–846.

[30] a) D. Somashekar, R. Joseph, *Bioresour. Technol.* **1996**, *55*, 35–45; b) N. Thadathil, S. P. Velappan, *Food Chem.* **2014**, *150*, 392–399.

[31] R. W. Ammann, E. Tagwecher, H. Kashiwagi, H. Rosenmund, *Am. J. Dig. Dis.* **1968**, *13*, 123–146.

[32] a) D. G. Kellner, S. A. Maves, S. G. Sligar, *Curr. Opin. Biotechnol.* **1997**, *8*, 274–278; b) S. Kumar, *Expert Opin. Drug Metab. Toxicol.* **2010**, *6*, 115–131.

[33] a) K. T. Chen, M. S. Malo, L. K. Beasley-Topliffe, K. Poelstra, J. L. Millan, G. Mostafa, S. N. Alam, S. Ramasamy, H. S. Warren, E. L. Hohmann, R. A. Hodin, *Dig. Dis. Sci.* **2011**, *56*, 1020–1027; b) J. P. Lallès, *Nutr. Rev.* **2010**, *68*, 323–332; c) M. Mizumori, M. Ham, P. H. Guth, E. Engel, J. D. Kaunitz, Y. Akiba, *J. Physiol.* **2009**, *587*, 3651–3663; d) M. J. Bours, E. L. Swennen, F. Di Virgilio, B. N. Cronstein, P. C. Dagnelie, *Pharmacol. Ther.* **2006**, *112*, 358–404.

[34] a) C. S. Karigar, S. S. Rao, *Enzyme Res.* **2011**, 805187; b) U. Kües, *Curr. Opin. Biotechnol.* **2015**, *33*, 268–278; c) R. Chandra, P. Chowdhary, *Environ. Sci. Processes Impacts* **2015**, *17*, 326–342.

[35] a) D. K. Choi, S. Pennathur, C. Perier, K. Tieu, P. Teismann, D. C. Wu, V. Jackson-Lewis, M. Vila, J. P. Vonsattel, J. W. Heinecke, S. Przedborski, *J. Neurosci.* **2005**, *25*, 6594–6600; b) D. L. Lefkowitz, J. Mone, S. S. Lefkowitz, *Curr. Immunol. Rev.* **2010**, *6*, 123–129.

[36] J. Grassmann, S. Hippeli, R. Vollmann, E. F. Elstner, *J. Agric. Food Chem.* **2003**, *51*, 7576–7582.

[37] P. Pacher, A. Nivorozhkin, C. Szabo, *Pharmacol. Rev.* **2006**, *58*, 87–114.

[38] a) D. M. Townsend, K. D. Tew, *Oncogene* **2003**, *22*, 7369–7375; b) D. M. Townsend, V. L. Findlay, K. D. Tew in *Methods in Enzymology, Vol. 401: Glutathione Transferases and gamma-Glutamyl Transpeptidases* (Eds.: H. Sies, L. Packer), Academic Press, San Diego, **2005**, pp. 287–307.

[39] Z. Yu, L. C. Chen, M. K. Mandal, H. Nonami, R. Erra-Balsells, K. Hiraoka, *J. Am. Soc. Mass Spectrom.* **2012**, *23*, 728 – 735.

[40] N. Johnston, P. W. Dettmar, B. Bishwokarma, M. O. Lively, J. A. Koufman, *Laryngoscope* **2007**, *117*, 1036 – 1039.

[41] M. Hirota, M. Ohmuraya, H. Baba, *J. Gastroenterol.* **2006**, *41*, 832 – 836.

[42] J. Kool, G. E. de Kloe, B. Bruyneel, J. S. de Vlieger, K. Retra, M. Wijtmans, R. van Elk, A. B. Smit, R. Leurs, H. Lingeman, I. J. de Esch, H. Irth, *J. Med. Chem.* **2010**, *53*, 4720 – 4730.

[43] J. Hirata, F. Ariese, C. Gooijer, H. Irth, *Anal. Chim. Acta* **2003**, *478*, 1 – 10.

[44] R. Haselberg, C. Hempen, S. M. van Leeuwen, M. Vogel, U. Karst, *J. Chromatogr. B* **2006**, *830*, 47 – 53.

[45] D. A. van Elswijk, O. Diefenbach, S. van der Berg, H. Irth, U. R. Tjaden, J. van der Greef, *J. Chromatogr. A* **2003**, *1020*, 45 – 58.

[46] N. Schebb, H. Faber, R. Maul, F. Heus, J. Kool, H. Irth, U. Karst, *Anal. Bioanal. Chem.* **2009**, *394*, 1361 – 1373.

Appendix IV

HPLC method development for the online-coupling of chromatographic *Perilla frutescens* extract separation with xanthine oxidase enzymatic assay

Christine M. Kaufmann, Johanna Grassmann and Thomas Letzel

The publication comprehensively describes the development and special requirements of a chromatographic method, which is to be implemented into an online coupled continuous flow system. The separation of PF extracts was tested with two different columns, the application of a temperature gradient and different low organic solvent contents added to the mobile phase. PF extract were injected to the system in order to identify compounds able to regulate xanthine oxidase. Moreover the established method allowed the tentative identification of unknown m/z contained in PF. Conduction of data and evaluation and writing were done on my part.

HPLC method development for the online-coupling of chromatographic *Perilla frutescens* extract separation with xanthine oxidase enzymatic assay

Christine M. Kaufmann, Johanna Grassmann, Thomas Letzel *

Chair of Urban Water Systems Engineering, Technical University of Munich, Am Coulombwall, 85748 Garching, Germany

ABSTRACT

Enzyme-regulatory effects of compounds contained in complex mixtures can be unveiled by coupling a continuous-flow enzyme assay to a chromatographic separation. A temperature-elevated separation was developed and the performance was tested using *Perilla frutescens* plant extracts of various polarity (water, methanol, ethanol/water). Owning to the need of maintaining sufficient enzymatic activity, only low organic solvent concentrations can be added to the mobile phase. Hence, to broaden the spectrum of eluting compounds, two different organic solvents and various contents were tested. The chromatographic performance and elution was further improved by the application of a moderate temperature gradient to the column. By taking the effect of eluent composition as well as calculated logD values and molecular structure of known extract compounds into account, unknown features were tentatively assigned. The method used allowed the successful observation of an enzymatic inhibition caused by *P. frutescens* extract.

© 2016 Elsevier B.V. All rights reserved.

1. Introduction

The assessment of health-promoting properties of natural extracts with regard to their antioxidative and anti-inflammatory capacity or their capability to regulate the activity of health- or disease related enzymes is a developing field of research. Most studies either focus on the investigation of whole extracts or on single known compounds to assess their impact on physiological parameters [1,2]. Especially the extent of an immunological response or changes in cellular gene expression of health-related enzymes may indicate the benefits of extracts or single compounds. Nevertheless those alterations are not necessarily correlated to the abundance of the proteinaceous gene product or to the activity of the translated enzyme [3]. This realization consequently eventuated in a major interest in the direct assessment of enzyme-regulatory effects of an extract or single compound. The investigation of whole extracts however results in only incomplete information about actual molecules able to inhibit or activate enzymatic catalytic activity. Most researchers therefore initially focus on the study of

extract compositions by employing LC-UV or LC–MS techniques, followed by the isolation, purification and identification of single molecules [4]. Subsequently, these compounds can be investigated by introducing them successively to enzymatic assays to determine their regulatory potential.

By employing the so called online coupled continuous flow system, drug screening and determination of enzymatic activity can be combined [5,6]. Therewith the effects of chromatographically separated mixtures on enzymatic activity can directly be assessed. Alterations of substrate degradation and product generation, due to the presence of regulatory compounds, can be observed with mass spectrometric detection. This system has already been utilized in order to determine biochemical interactions [7] and assess IC_{50} values of single compounds [8–10]. In contrast to the injection of single molecules, the injection of mixtures necessarily resulted in the implementation of a chromatographic separation to the system [10]. This setup was thus applied to screen complex extracts for inhibitory molecules affecting the activity of enzymes like cathepsin B [10] or acetylcholine esterase [8,11].

On this basis, the effects of *Perilla frutescens* leave extracts towards xanthine oxidase (XOD) were investigated in the current study. In this regard a suitable HPLC method was developed to enable the direct coupling of extract separation and XOD enzymatic assay.

Abbreviations: XOD, xanthine oxidase; IS, internal standard; ROS, reactive oxygen species; RC, reaction coil.

* Corresponding author.
E-mail address: T.Letzel@tum.de (T. Letzel).

Perilla is frequently used as herbal medicine, herb or garnish in the Asian region and has been found to possess a variety of health-promoting effects [12], like working anti-allergic [13], antioxidative [14] and anti-inflammatory [15]. Perilla's advantageous features are related to a plethora of different phenolic compounds, whose individual impact on health has been extensively investigated as well [16,17]. Flavonoids like luteolin, apigenin as well as their glycosides and glucuronides or phenolic acids like caffeic acid and rosmarinic acid are known to possess health-promoting properties (e.g. alleviating the progress of inflammatory processes) [18]. Extract compounds may also be able to avert the exposure of harmful reactive oxygen (ROS) to cells by direct scavenging [19] or by inhibiting enzymes [20] involved in the generation of ROS, like e.g. XOD. Besides its participation in the release of superoxide during substrate degradation [21], XOD is part of the nucleotide metabolism and is also known to be involved in the development of hyperuricemia, in this manner also contributing to the pathogenesis of gout [21]. Molecules able to inhibit the activity of XOD would therefore not only reduce the accumulation of uric acid but also alleviate oxidative stress. Since several extracts as well as natural phenolic compounds have already been shown to regulate the enzyme [22,23], in this study Perilla extracts were screened in order to unveil molecules potentially affecting its activity.

2. Experimental

2.1. Reagent and chemicals

Xanthine oxidase from bovine milk, xanthine, allopurinol, rosmarinic acid, water LC–MS CHROMASOLV®, isopropyl alcohol (IPA) CHROMASOLV® for HPLC, formic acid and ammonium acetate were purchased from Sigma-Aldrich (Steinheim, Germany). Histidine was obtained from Merck (Darmstadt, Germany). Absolute ethanol, acetic acid (#A0820) and ammonia 32% were purchased from AppliChem (Darmstadt, Germany). Methanol HiPerSolv CHROMANORM® for LC–MS and acetonitrile were obtained from VWR (Darmstadt, Germany). *P. frutescens* water extract as well as *P. frutescens* (var. crispa) freeze-dried Perilla leaves were kindly provided by Vital Solutions GmbH and Vital Solutions GmbH (Langenfeld, Germany) and Amino Up Chemicals Co., Ltd (Sapporo, Japan).

2.2. Preparation of P. frutescens extracts

P. frutescens freeze-dried and milled leaves were extracted with ethanol (EtOH)-water (50:50, v/v) or methanol (MeOH)-water-formic acid (FAc) (90:9.5:0.5, v/v/v), respectively. For this purpose 500 mg freeze-dried and milled leaves were weighed, followed by the addition of 5 mL extraction solvent. After thorough mixing, the Perilla-solvent mixture was sonicated for 10 min at 4 °C and centrifuged afterwards for 20 min at 1500 rpm. The supernatant was transferred to another tube and the extraction procedure was repeated twice. The collected supernatant was evaporated to dryness (miVac Duo concentrator, GeneVac, Ipswich, England) and stored at −20 °C until use. Perilla water extract was provided in form of extracted and evaporated powder. Extracted Perilla was redissolved as required, whereby water extract was redissolved in water, 50% EtOH extract in EtOH-water (50:50, v/v) and 90% MeOH, 0.5% FAc extract in 100% EtOH.

2.3. Instrumentation and experimental setup

The online coupled continuous flow setup is comprised of three traces, each of which delivering either enzymatic assay components (Fig. 1, upper and bottom trace) or potentially regulatory compounds introduced to the system individually or as chromatographically separated mixture (Fig. 1, middle trace).

Enzyme solution was provided in a syringe (2.5 mL, Hamilton-Bonaduz, Switzerland) located in a syringe pump (Model 11 Plus, Harvard Apparatus, Hugo Sachs Elektronik, Hugstetten, Germany), which was set to a flow rate of 25 µL/min (Fig. 1, upper trace). Substrate solution was filled in a superloop (volume 10 mL, Amersham Biosciences, Uppsala, Sweden) and introduced to the system with a flow rate of 50 µL/min (Fig. 1, bottom trace). Samples were injected (Injector, Rheodyne, California, sample loop volume: 2 µL) into a continuous flow of 25 µL/min delivered by a quaternary HPLC pump (1100 series, Agilent Technologies, Waldbronn, Germany) and thus taken along (Fig. 1, middle trace).

Pumps were controlled by ChemStation software (version B.04.03, Agilent Technologies). Reaction coils (RC) 1 and 2 (Teflon, 0.25 mm ID) were knitted as described in literature [24] to provide a sufficient mixing of enzyme with the sample injected (RC 1, reaction time ~1.3 min) or of the enzyme-sample mixture with the substrate (RC 2, reaction time ~2.9 min), respectively. XOD and histidine stock solution were prepared in ammonium acetate (NH_4Ac) (pH 7.4, 10 mM), whereas xanthine stock was dissolved in water-NH_3 (0.1 M) (70:30, v/v), due to its low solubility in neutral aqueous solutions. Initial concentrations of the assay components were 0.032 U/mL for the enzyme XOD along with 80 µM histidine, latter serving as internal standard, (Syringe, Fig. 1, upper trace) and 50 µM xanthine (Superloop, Fig. 1, bottom trace). Due to the confluence of continuously delivered flows (Fig. 1, upper, middle and bottom trace), final concentrations of assay components in RC2 were 0.008 U/mL of XOD, 20 µM of histidine and 25 µM of xanthine, respectively.

2.3.1. Separation of P. frutescens extracts

Dried Perilla extracts were redissolved to a final concentration of 0.5 g extracted freeze-dried leaves/mL and introduced to the system equipped with chromatographic column (Fig. 1, middle trace, injection valve with 2 µL sample loop). The chromatographic performance of Luna PFP(2) column (100 Å, 2 mm IDx100 mm length, Phenomenex, Aschaffenburg, Germany) was tested with an isocratic elution using different low organic solvent concentrations and the application of a moderate temperature gradient up to 70 °C (Table 1), thus without conflict to the column specifications. The column was installed into a column oven (HT HPLC 2000, Scientific Instruments Manufacturer GmbH, Oberhausen, Germany) and equipped with a SecurityGuard Cartridge System (Phenomenex) with PFP(2) material precolumn (Phenomenex). It was flushed after each extract injection using a gradient up to Acetonitril (ACN):water (50:50, v/v), followed by the reconstitution to the respective eluent.

The temperature gradient was started simultaneously with the Perilla extract injection. The heated chromatographic eluent flow was cooled down to 30 °C before it was mixed with the flow containing the enzyme (Fig. 1, RC1). Chromatographic separation was performed using either EtOH−NH_4Ac (pH 7.4, 10 mM) (5:95, v/v), EtOH−NH_4Ac (pH 7.4, 10 mM) (10:90, v/v) or isopropyl alcohol (IPA)-NH_4Ac (pH 7.4, 10 mM) (5:95, v/v). In case of a chromatographic separation performed with 5% EtOH or 5% IPA, the enzyme was solved in NH_4Ac solution (pH 7.4, 10 mM)-the respective solvent (95:5, v/v). This led to an organic solvent concentration of 5% in RC1. The substrate was solved in NH_4Ac solution (pH 7.4, 10 mM)-respective solvent (85:15, v/v), resulting in a final organic solvent concentration of 10% in RC2 (Fig. 1). For a chromatographic separation using 10% EtOH, XOD as well as xanthine substrate were solved in NH_4Ac (pH 7.4, 10 mM)-EtOH (90:10, v/v), resulting in a solvent concentration of 10% in RC1 and RC2. Final organic solvent proportion of 10% in RC2 was chosen for all experiments to maintain a
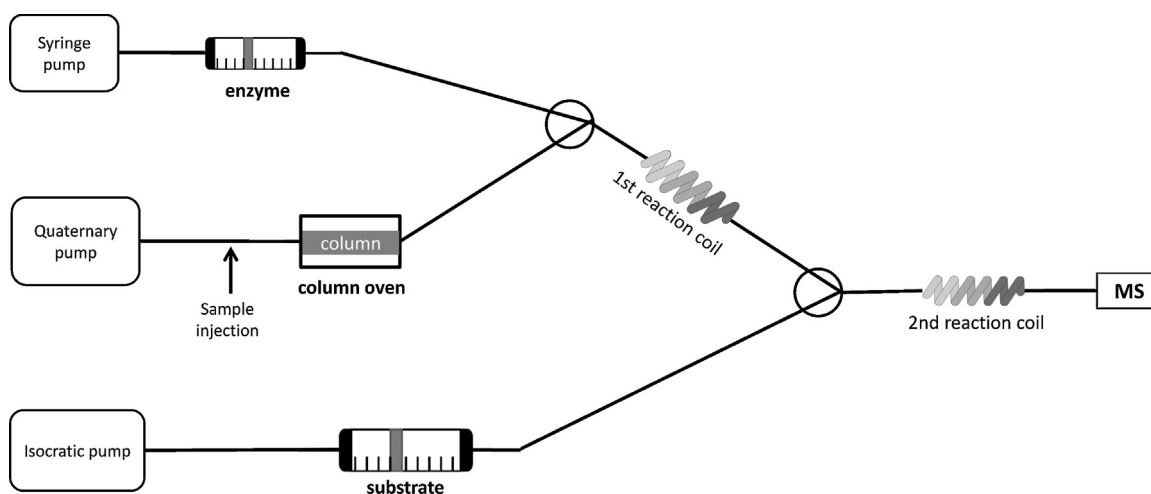
Fig. 1. Online coupled continuous flow system.

Table 1
Temperature gradient applied to the column.

Temperature	30 °C		50 °C		60 °C		70 °C
Temperature increase/min		1 °C/min		0.5 °C/min		0.5 °C/min	
Duration	1 min	20 min	1 min	20 min	1 min	20 min	40 min
Overall duration	103 min						

comparable efficiency of in-source solvent evaporation, compound detection and intensity in mass spectrometry.

2.3.2. Injection of xanthine oxidase inhibitor allopurinol

The enzymatic response to the presence of 50, 100 and 200 μM of the known XOD inhibitor allopurinol [21] was tested without the implementation of a chromatographic column.

Allopurinol was manually injected with a 100 μL syringe (Hamilton-Bonaduz) into the sample introduction part of the online coupled continuous flow system (Fig. 1, middle trace). The continuous flow (to take the inhibitor along) contained 10% IPA, as were the enzyme and substrate solution (Fig. 1, upper and bottom trace). This resulted in a final solvent proportion of 10% IPA in RC2.

2.3.3. Mass spectrometric detection

Development and establishment of the experimental setup and the majority of experiments were performed using a single quadrupole mass spectrometer (MSQ Plus, Wissenschaftliche Gerätebau Dr. Ing. Herbert Knauer GmbH, Berlin, Germany) equipped with an electrospray ionization (ESI) source in positive ionization mode. Mass spectrometric parameters were as follows: 300 °C probe temperature, 3.5 kV needle voltage and 75 V cone voltage and a mass range of 100–1000 m/z. Crucial measurements were repeated by hyphenating the online coupled continuous flow system to a ESI −Time-of-Flight (ToF) mass spectrometer (Agilent Technologies) as detector. Measurements were again detected in positive ionization mode with a mass range of 100–1300 m/z. Here, the parameters were as follows: 300 °C gas temperature, 7 L/min drying gas flow, 250 °C sheath gas temperature, 5.5 L/min sheath gas flow, 45 psig nebulizer operating pressure, 2000 V capillary voltage, 2000 V nozzle voltage, 65 V skimmer voltage and 175 V fragmentor voltage. Assessment of ToF-MS measurement accuracy was determined by calculating the molecular weight deviations from at least five of a total of eight known masses present in each measurement. This included assay components xanthine and uric acid, the internal standard histidine as well as several known and verified *P. frutescens* compounds.

2.3.4. Data evaluation

Data were processed using Xcalibur software 2.1.0.1139 (Thermo Fisher Scientific Inc., Waltham, MA, USA) in case of measurements detected with the single quadrupole MS. The extracted ion chromatograms (EIC) were obtained by using an m/z range of ± 0.5 Da to the respective calculated m/z value of substrate and product: xanthine with m/z 153, i.e. [M + H]⁺ and uric acid with m/z 169, i.e. [M + H]⁺ and internal standard histidine with m/z 156, i.e. [M + H]⁺. Compound peaks originating from the injection of *P. frutescens* extracts were evaluated manually with Xcalibur software. Assay as well as extract compound EICs were smoothed with a Gaussian function using a 15 points function width. Further processing was conducted with Microsoft Office Excel 2007. For comparative data evaluation, time point of plant extract injection was set as time point 0.

In case of allopurinol inhibitor injections, negative and positive peak areas within the product and substrate trace were calculated with Achroma software tool [25].

Data (for experiments conducted with ToF-MS) was processed using MassHunter Qualitative Analysis Version B.02.00 (Agilent Technologies) and Agilent ProFinder Version B.06.00 (Agilent Technologies). ProFinder parameters applied for the automatic extraction of Perilla extract compound retention times (RT) and molecular weights were set to a peak filter of 600 counts peak height, ion species to "positive ions" with H⁺, Na⁺ and K⁺, "charge state" to 1 and the "expected RT" to ±4.00 min. The extracted EICs were smoothed with a Gaussian function using 9 points function width and 5000 points Gaussian width and then exported to Windows Excel 2007 for further data evaluation. LogD of compounds at pH 7.4 was determined with MarvinSketch Calculator Plugin 14.8.25.0 (ChemAxonLtD, Budapest, Hungary).

3. Results and discussion

The direct and continuous-flow coupling of the chromatographic separation (Fig. 1) of a *P. frutescens* extract to an enzymatic assay required the consideration of various optimization steps.

They are described in the following to be able to unveil potential enzyme-regulatory compounds.

3.1. Selection of suitable organic modifiers

Organic solvent gradients, commonly applied for purposes of chromatographic separation, are of limited suitability for the applied experimental setup [10]. In order to maintain a constant and sufficient enzymatic activity the solvent content has to be kept constant and low. Preliminary tests with several organic solvents in different concentrations were conducted to identify the most suitable ones (compare Supplementary material) [26]. Using low concentrations of MeOH, ACN, EtOH and IPA, respectively, added to the assay, MeOH was found to be the most negatively affecting one. 10% EtOH and 10% IPA revealed a comparably medium suppression of XOD activity, with EtOH showing slightly less reduction of activity (Supplementary material). Following experiments were therefore conducted using low EtOH or IPA concentrations as organic modifier for the separation of Perilla extracts.

3.2. Implementation of a chromatographic separation

To encompass a wide range of different Perilla compounds and to comprehensively examine the chromatographic separation, a polar water extract, a semi-polar 50% EtOH extract and a non-polar 90% MeOH, 0.5%FAc Perilla extract were injected into the system. Experiments were conducted with a Quadrupole mass spectrometer or a Time-of-flight mass spectrometer (ToF-MS) for detection, respectively. The latter has to be used for compounds with similar molecular weight to distinguish them by their empirical formula.

To improve the chromatographic separation and simultaneously increase the amount of eluting compounds, a moderate temperature gradient up to 70 °C was applied. Initial experiments, with a column that allows a 100% aqueous mobile phase, enabled the utilization of temperature gradients in the absence of organic solvents [9]. Most compounds revealed distinctly earlier RTs (up to approximately forty minutes) compared to measurements without temperature gradient (Supplementary material, Table S1). This effect is reflecting the decreasing static permittivity and therewith an enhanced elution strength of the heated mobile phase [27].

Since the addition of low organic solvent concentrations may further augment the amount of compound elution, either 5% EtOH, 10% EtOH or 5% IPA, respectively, were added to the mobile phase. The associated increase of elution strength, the decrease of surface tension as well as the improvement of mass spectrometric signal were found to increase the quantity of detectable Perilla compounds compared to a purely aqueous mobile phase (Supplementary material, Fig. S1).

However, data analysis revealed the highest total amount of eluting compounds for water extract, followed by 50% EtOH extract and 90% MeOH extract, independent of the organic modifier applied (data not shown). The decreasing polarity of extracts, with water extract molecules being the most polar, followed by 50% EtOH and 90% MeOH extracts, necessarily results in an increased proportion of retained compounds on the unpolar column.

The evaluation of the retention time distribution however revealed a decreasing amount of total eluting features in the order 5% IPA > 10% EtOH > 5% EtOH for 50% EtOH and 90% MeOH extract (Table 2, "number of eluting compounds"). In contrast water extract was observed with a similar quantity for 5% IPA and 10% EtOH and a distinct increase with 5% EtOH content. These observations can be explained by the different polarities of the extracts in combination with the elution strength of the mobile phases employed. In this regard, the mainly non-polar properties of 90% MeOH extract resulted in the least effective elution using 5% EtOH mobile phase

content, which possesses the lowest elution strength (Table 2, "number of eluting compounds") [27].

Considering the systems flow-through time (Fig. 1, RC1 and RC2), compound elution in time range of minute 14–20 was defined to comprise of highly polar, non- or barely retained molecules (Table 2, "non-retained compounds"). Due to a higher proportion of polar compounds, most compounds were detected at that time range within the water extract, followed by 50% EtOH extract and 90% MeOH extract. This fact was true for all organic solvents and contents applied (data not shown).

In the following, the effect of the mobile phase was investigated in more detail by focusing on the behavior of individual known and unknown compounds contained in Perilla water extract (Fig. 2). This extract was selected due to the highest quantity of eluting features. The majority revealed a similar elution profile for mobile phase 10% EtOH and 5% IPA with only few exceptions (Fig. 2, e.g. Cp6), whereas RTs were distinctly higher with 5% EtOH (Fig. 2, e.g. Cp3, Cp7 and Cp8). Some compounds were also found to be absent with the more polar eluent, compared to 10% EtOH or 5% IPA (Fig. 2, e.g. *m/z* Cp1, Cp2 or Cp6). Beyond the examination of RT behavior, the observation of mass spectrometric in source fragmentation allowed the structural 'feature prediction' of several compounds [28]. Compounds Cp4 and Cp5 could be ascribed to be apigenin 7-O-diglucuronide (Cp4) and luteolin-diglucuronide or scutellarein-diglucuronide (Cp5), by means of their respective monoglucuronide and flavonoid-core fragments (Fig. 2, F1 and F2 and Table 3). Moreover, features Cp1 and Cp2 correspond to apigenin-glucuronide and luteolin- or scutellarein-glucuronide. The finding of monoglucuronides as well as diglucuronides was furthermore verified by a previous study, in which the same Perilla water extract had been used as here [29]. Due to their high similarity in terms of molecular weight, structure and logD, diglucuronide constitutional isomers (Table 3 and Fig. 2, Cp4 and Cp5) could only be sufficiently separated with 5% EtOH eluent. logD provides a good measure to predict the water solubility of a compound dependent on the pH of the solution. In this regard, the calculated low logD values for either diglucuronide are attributed to the occurrence of three negatively charged functional groups within the molecules at pH 7.4.

The employment of 10% EtOH or 5% IPA consequently led to a shift of RTs, which resulted in a nearly co-elution of those highly water-soluble compounds (Table 3, compare also *m/z* 611.1619). Hence, with the applied setup, an isomeric separation might only be realizable with the employment of 5% EtOH organic modifier.

Further compounds, which were already verified to be present within the injected Perilla water extract [29], are a C-glycosylated flavonoid (Fig. 2 and Table 3, Cp5) and the rosmarinic acid (Table 3). Both could be captured with 5% EtOH, 10% EtOH and 5% IPA eluent along with the respective fragment ions described in literature (Table 3). Apart from this, a detailed molecular characterization of unknown compounds was accomplished by an extensive literature research, which included mainly studies dealing with Perilla in particular or its plant family Lamiaceae or subfamily Nepetoideae (Table 3). Furthermore their accurate *m/z*, which was determined in this study using a ToF-MS, was employed for the calculation of chemical formulas. Based on the logD vs. RT behavior of known compounds (Table 3, No. 1–7 and 12 and Fig. 3A), unidentified features were then tentatively assigned (Fig. 3B) [30].

Since the logD values for most known (and detected) compounds increase with RT in a nearly logarithmic manner (exemplarily presented for 10% EtOH mobile phase, Fig. 3, A), unknown compounds were assumed in this study to fit into the observed trend. Therefore literature described compounds contained in Lamiaceae or Perilla, which are not possessing logD values fitting into the logarithmic trend (Table 3, e.g. No. 8, 9, 10 with logD values −2.02, −2.1, −2.48) were disregarded. In contrast, the

Table 2
Comparison of number of eluting extract compound in relation to extract and organic modifier; < or >: the amount of eluting compounds differs between 15 and 25 features, comparing the respective organic solvents, « or » for difference, that exceeds 25 features and ≤ or ≥ for differences between 5 to 15 features, =for differences lower than 5 features. * First compounds can be mass spectrometrically detected after approx. 14 min due to the systems volume and thus flow-through time.

Elution	Extract	Eluting compounds with organic modifier
Number of eluting compounds	Water extract	5% EtOH » 10% EtOH ≤ 5% IPA
	50% EtOH extract	5% EtOH < 10% EtOH « 5% IPA
	90% MeOH extract	5% EtOH < 10% EtOH « 5% IPA
Non retained compounds (initial time- minute 14*-20)	Water extract	5% EtOH < 10% EtOH = 5% IPA
	50% EtOH extract	5% EtOH = 10% EtOH ≤ 5% IPA
	90% MeOH extract	5% EtOH < 10% EtOH « 5% IPA

No.	[M+H]+
F1	(271.0607)
F2	(287.0551)
Cp1	(447.0927)
Cp2	(463.0874)
Cp3	(595.1658)
Cp4	(623.1254)
Cp5	(639.1203)
Cp6	(588.3019)
Cp7	(628.2970)
Cp8	(880.3254)
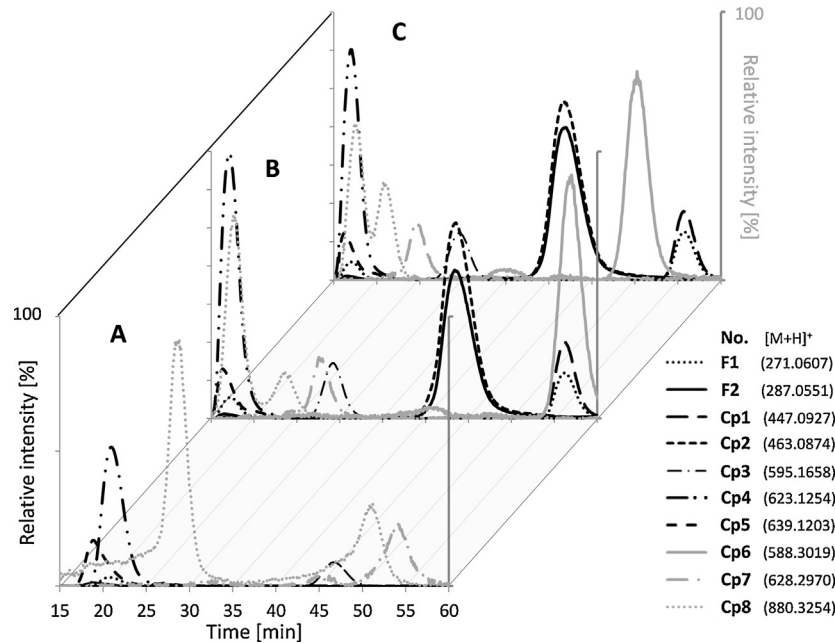
Fig. 2. Results of isocratic separation of Perilla water extract with 5% EtOH (A), 10% EtOH (B) and 5% IPA (C) displayed by means of exemplarily selected compounds (Cp) and their fragments (F) if available. *m/z*'s of light grey peaks Cp6-8 refer to the secondary y-axis, due to their inferior intensities. 100% relative intensity of primary y-axis corresponds to 1.2×10^6 (A), 7.0×10^5(B) and 7.0×10^5 (C); 100% relative intensity of secondary y-axis corresponds to 2.0×10^4 (A, B) and 1.8×10^4 (C).
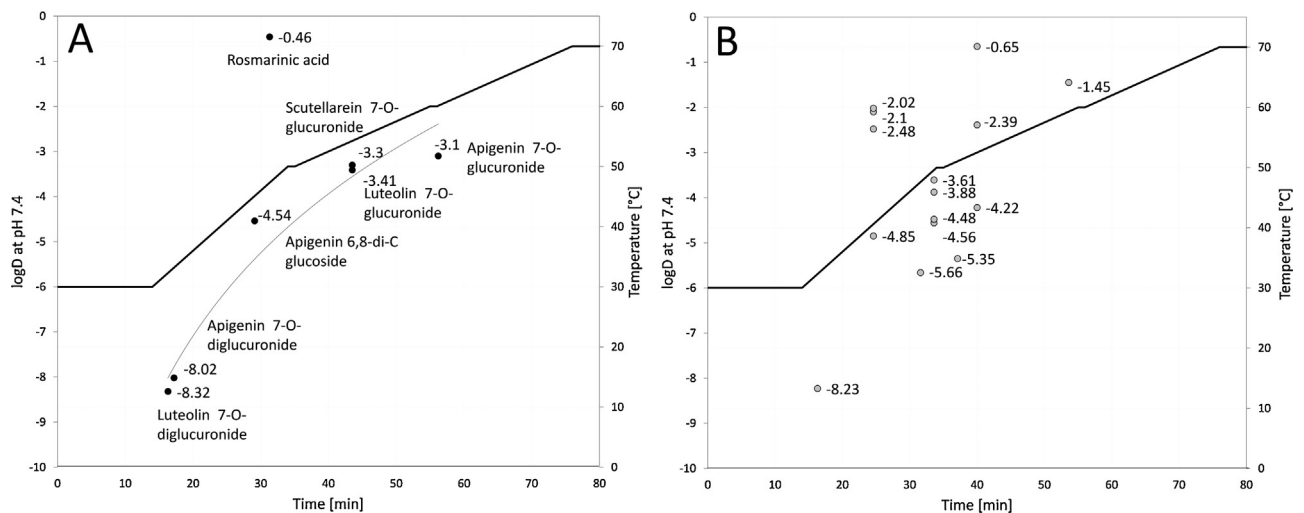
Fig. 3. Plot of logD values at pH 7.4 (primary y-axis) against RT (x-axis) of known Perilla compounds (A) and unassigned compounds found in Lamiaceae/Nepetoideae literature sources (B). Chromatographic separation was carried out isocratically with 10% EtOH. Progress of temperature gradient is presented as bold black line (secondary y-axis). Due to the time delay caused by the systems dead volume, first compounds are mass spectrometrically captured with a RT of approx. 13 min. Temperature gradient is therefore adjusted accordingly with a gradient starting point of minute 13.

presence of luteolin di-C-glucoside with *m/z* 611.1606 (Table 3, No. 11) can be reasonably assumed, considering its logD of −4.85 as well as its connaturality to the contained compound apigenin di-

C-glucoside (Table 3) [29]. The absence of related fragmentation products in this case might be due to the low abundance.

Table 3

List of observed *m/z* values detected in Perilla water extract with a ToF–MS along with the calculated accurate *m/z* values, calculated molecular formula and calculated in-source fragment *m/z* values along with respective deviations in ppm and logD values at pH 7.4. RTs of compounds are given for 5% EtOH, 10% EtOH and 5% IPA mobile phase. References are marked as (*) for literature dealing with Perilla, (+) for literature discussing compounds from Lamiaceae family and/or Nepetoideae subfamiliy and (×) for literature in which the core-flavonoid was found without glycosylation or glucuronisation.

No.	Observed m/z/calculated m/z (deviation [ppm])	Calculated molecular formula	RT with eluents			Observed fragment m/z / calculated m/z (deviation [ppm])	Fragment m/z from literature	Perilla/Lamiaceae compounds from literature	logD at pH 7.4
			5% E	10% E	5% I				
1	639.1203 / 639.1192 (-1.72)	$C_{27}H_{26}O_{18}$	18.8 27.1	16.3	16.2	287.0551 / 287.05500 (0.35)	287 [45]	Luteolin 7-O-diglucuronide [44, 45]*	-8.32
2	Cp5					F2		Scutellarein 7-O-diglucuronide [45]*	-8.23
3	623.1254 / 623.1243 (-1.77) Cp4	$C_{27}H_{26}O_{17}$	21.0	17.2	17.0	271.0607 / 271.06009 (-2.3) F1, 447.0927 / 447.09217 (-1.2)	271 [45]	Apigenin 7-O-diglucuronide [18, 44, 45]*	-8.02
4	447.0927 /447.0922 (-1.12) Cp1	$C_{21}H_{18}O_{11}$		56.2	55.7	271.0607 / 271.06009 (-2.3) F1		Apigenin 7-O-glucuronide [44, 46]+*	-3.1
5	463.0874 / 463.0871 (-0.65)	$C_{21}H_{18}O_{12}$		43.5	41.8	287.0555 / 287.05500 (-1.74)	287 [45]	Luteolin 7-O-glucuronide [18, 44, 45]*	-3.41
6	Cp2					F2		Scutellarein 7-O-glucuronide [18, 44, 45]*	-3.3
7	595.1658 / 595.1657 (-0.17) Cp3	$C_{27}H_{30}O_{15}$	46.6	29.1	29.7	577.1534 / 577.1553 (3.3), 475.1219 / 475.1236 (3.6)	577 [M-H2O]+, 475 [M-120]+ [47, 48]	Apigenin 6,8-di-C-glucoside (Vicenin 2) [44, 49]*	-4.54
8	611.1619 / 611.1606 (-2.13)	$C_{27}H_{30}O_{16}$	37.5 43.9	24.6	24.8			Quercetin-rhamno-glucoside (Rutin) [50]+	-2.02
9								Morin O-rutinoside[51]*×	-2.1
10								Luteolin-di-O-glucoside [52, 53]+	-2.48
11								Luteolin 6,8-di-C-glucoside (Lucenin-2) [54]+	-4.85
12	361.0931 / 361.0920 (-3.05)	$C_{18}H_{16}O_8$	46.5	31.3	30.5	163.0397 / 163.0390 (-4.3),	161 [M-H]-, 179 [M-	Rosmarinic acid [14, 18, 44]*	-0.46

Table 3 (*Continued*)

						181.0504 / 181.0495 (-5.0)	H]·[55]		
13	479.0812 / 479.0815 (0.63)	$C_{21}H_{18}O_{13}$	48.3 58.9	33.6	32.9	303.0498 / 303.0499 (0.33)		Morin 3-O-glucuronide/ [51][x]	-4.56
14								Morin 7-O-glucuronide [51]*[x]	-3.88
15								6-Hydroxyluteolin 7-O-glucuronide [53][+]	-3.61
16								Quercetin 3-glucuronide[56][+]	-4.48
17	579.1704 / 579.1708 (0.69)	$C_{27}H_{30}O_{14}$		40.0	39.4			Apigenin 7-O-rutinoside [50, 52, 53][+]	-0.65
18								Chrysin 6,8-di-C-glucoside [57][+]	-4.22
19								Chrysin-7-O-glucoside-8-C-glucoside [57][+]	-2.39
20	433.1132 / 433.1129 (-0.69)	$C_{21}H_{20}O_{10}$		53.6	55.0			Apigenin 7-O-glucoside [19, 20]*	0.08
21								Apigenin 8-C-glucoside (Vitexin) / Apigenin-6-C-glucoside (Isovitexin) [58][+]	-1.35 / -1.45
22	625.1389 / 625.1399 (1.6)	$C_{27}H_{28}O_{17}$	39.9 45.3	31.6	30.5			Luteolin 7-glucuronide 3'-glucoside[53, 59][+]	-5.66
23	609.1445 / 609.1450 (0.8)	$C_{27}H_{28}O_{16}$	56.5	37.1	36.5			Apigenin 7-glucuronide 4'-glucoside	-5.35
24	588.3019 / Unknown **Cp6**	unknown		57.0	50.3			unknown	-
25	628.2961 / Unknown **Cp7**	unknown	54.1	27.6	24.7			unknown	-
26	880.3254 / Unknown **Cp8**	$C_{31}H_{60}O_{28}$	28.6 51.2	17.6 23.6	17.4 20.8			unknown	-

For some *m/z* values observed in Perilla, various possibilities were found in literature, e.g. *m/z* 479.0815 with calculated logDs of −3.61, −3.88, −4.56 and −4.48 (Fig. 3B and Table 2, No. 13–16).

Since the flavonoid Morin has already been demonstrated to be contained in Perilla, two options were taken into consideration to tentatively assign the feature. Either one was calculated with
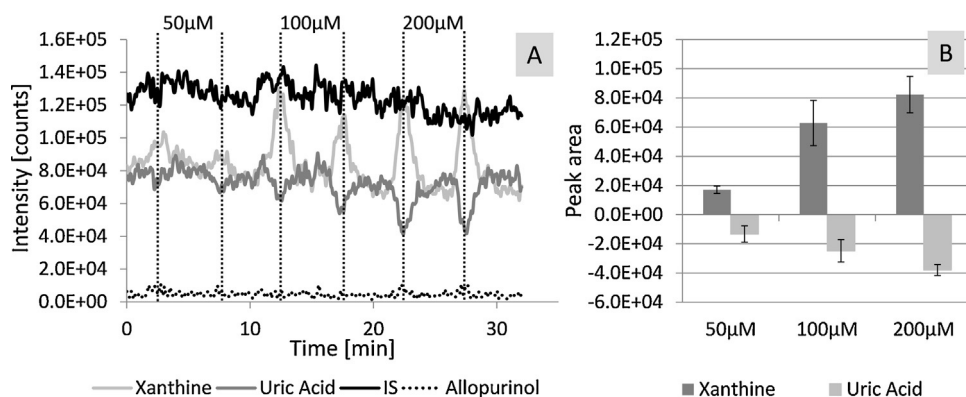
Fig. 4. Injection of either 50 μM, 100 μM or 200 μM allopurinol. EIC substrate and product trace responses to the presence of the inhibitor (A). Peak areas of substrate and product of n = 3 allopurinol injections per concentration were calculated with Achroma software [41] and displayed along with their respective standard deviations (B).

slightly different logD value depending on the site of glucuronidation (Table 3, −4.56 and −3.88, No. 13, 14).

In general, glycosylated and glucuronidated features were found to be the most prominent species of molecules to be eluted from the column (Fig. 3A). Their observed logD values range from −8.32 to −3.1 and is clearly indicating high water solubility. The divergence of rosmarinic acids logD vs. RT behavior (Fig. 3A, logD −0.46), might be explained by its different molecular structure and thus chemical properties. Its elution is assumed to be dependent on parameters like different charge state and quantity of potential hydrogen bond donors compared to glycosylated and glucuronidated flavonoids. The molecules discontinuous conjugated system in comparison to the continuous conjugated system of flavonoids luteolin, apigenin and scutellarein may furthermore explain the different elution behavior. The increase of potential hydrogen-bond-forming hydroxyl-groups with the addition of glucoside or glucuronide side chains can be assumed to result in an enhanced formation of hydrogen bonds, which would result into a stronger interaction of the compound with the stationary phase of the column in comparison to rosmarinic acid. As revealed by the elution of rosmarinic acid, also compounds with less water solubility could be captured with the setup applied. Hence, the employment of low organic solvent mobile phases was shown to be a good means to elute promising Perilla extract compounds for the further investigation of their effect on enzymatic activity.

3.3. Injection of a known xanthine oxidase inhibitor

Initially, the systems response to a regulatory molecule was evaluated by injecting three concentrations of the known XOD inhibitor allopurinol [21]. This validation was carried out under "worst case conditions"; i.e. tests were performed with a final concentration of 10% IPA in RC2 (Fig. 1), since it was found to significantly reduce XOD activity (Supplementary material). The system's consistency was furthermore controlled by the addition of an internal standard (Fig. 4A, IS).

The injection of all three allopurinol concentrations resulted in an enzymatic inhibition, which is reflected by an increase of mass spectrometric substrate intensity and a concurring decrease of the product signal (Fig. 4, A). The calculation of peak signal areas showed an inhibitor concentration dependent response with only minor peak areas after 50 μM allopurinol injection and a distinctly superior effect with 200 μM (Fig. 4, B). Internal standard EIC in turn was detected with negligible fluctuation, which can be considered without 'signal suppression' to the substrate and product trace response in the presence of the inhibitor. Allopurinol was only slightly detectable during the measurement (Fig. 4), which might either be due to its stable and complete binding to XOD and/or to
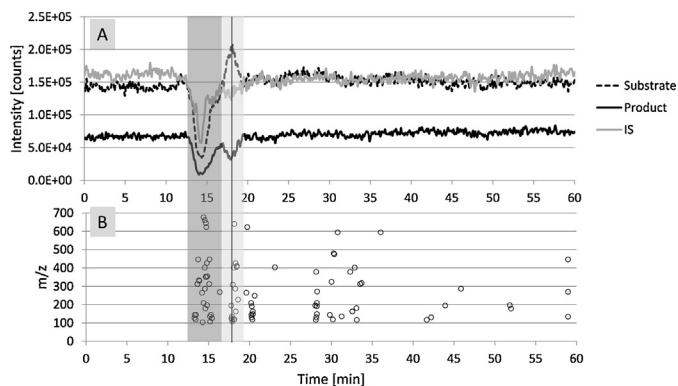
Fig. 5. Xanhine oxidase assay (A) in the presence of 90% MeOH, 0.5%FAc Perilla extract, chromatographically separated with 5% IPA eluent and the application of a temperature gradient (B). RTs of eluting extract compounds are presented in B (○). Dark grey area corresponds to an event of signal suppression, due to the elution of a considerate number of non-retained extract compounds. Light grey area highlights the time point of regulation (A) and the respective eluting extract compounds (B).

a minor protonation and therefore detection efficiency with the experimental conditions applied. Due to the finding of an assay response to the introduction of an inhibitory molecule, despite the presence of activity-affecting organic solvents, the applicability of the system for the detection of enzyme-regulatory molecules could be demonstrated. Hence, the optimized chromatographic separation was employed for the investigation of effects of *P. frutescens* extracts on the enzyme

3.4. Online coupled continuous flow system—enzymatic assay of xanthine oxidase

Enzymatic assay traces were examined with regard to a potentially regulation after injection and separation of *P. frutescens* extracts. A clear drop in intensity of all assay traces including the internal standard was observed due to a considerable amount of non-retained extract compounds, which elute approximately 13–15 min after injection to the system (Fig. 5,A and B, dark grey area).

In contrast, an increased substrate amount accompanied with a decline in product generation could be found between minute 17 and 20 with 90% MeOH, 0.5% FAcPerilla extract and 5% IPA eluent (Fig. 5A). No decline in signal intensity of the internal standard was observed within the respective time range of potential enzymatic regulation, which would furthermore confirm the presence of an inhibitor.

By plotting the *m/z* values of eluting extract compounds at that time range, the number of molecules potentially responsible for XOD inhibition could be limited (Fig. 5B, light grey area). Peak shape and peak width of possible regulatory molecule EICs were examined with regard to similarities to the peaks of enzymatic regulation (Fig. 6). Peaks of *m/z* 117, 120.1, 126, 136, 195.2 and 427 were found to possess the most fitting peak shape, whereas e.g. peaks of *m/z* 406.1, 410.7 and 227.2 revealed a different shape and RT as peaks within the substrate and product trace.

A majority of compounds, which eluted within the time range of inhibition could be subsequently assigned to accurate *m/z* by employing a ToF-MS (Table 4). After calculating possible molecular formulas, followed by literature and database research, various purine base derivatives similar to xanthine could be found (Table 4). The potential for those compounds to inhibit XOD has already been described by Hsieh et al., which includes the capability of adenine to act as inhibitor of XOD [31]. *m/z* value 136.0622, detected to elute within the relevant time range, was therefore considered to be the purine base adenine. Enzymatic activity towards adenine results in the generation of 2,8-dihydroxyadenine with an *m/z* of 168.05159, which ultimately prevents the enzyme from degrading further xanthine [31]. Despite indications of adenine to be present within the extract, no generation of *m/z* 168.05159 could be observed, which is either indicative of high enzyme-product-complex stability or of adenine not being responsible for the observed inhibition.

Nakanishi et al. and Huo et al. detected potent XOD inhibitors in *P. frutescens* extracts [32]. The reported *m/z* values were however not observed within the experimental polarity range after injection of Perilla extracts to the online coupled continuous flow system. Compounds discussed by Nakanishi et al. were probably not captured with the online-coupled continuous flow system due to the rather poor water solubility having a logD of 3.39. This also applies for flavonoids luteolin and apigenin, both are already known as potent XOD inhibitors [33,34]. Nevertheless their logD was calculated to be above 0, which may prevent both molecules, although present in Perilla water extract (data not shown), from eluting in the here applied setup. Huo et al. reported further compounds, e.g. caffeic acid, to possess inhibitory effects on XOD activity. Although being water soluble, they were not detected to elute, which might be due to a relatively low concentration and/or them being not ionized in the experimental setup applied here.

Due to detection of a variety of different possible structures and the quantity of co-eluting compounds within the range of inhibition, no final statement can be made about a single compound responsible for the inhibition. Moreover, a synergistic effect of different molecules might as well be the cause of the observed inhibition.

4. Conclusion

The applicability of an online coupled continuous flow system for the determination of XOD activity in the presence of compounds from a chromatographically separated *P. frutescens* extract was investigated.

The separation was performed isocratically, using only low concentrations of organic solvent in order to maintain a constant enzymatic activity. A temperature gradient was successfully applied to shorten the overall experimental time and to increase the amount of eluting molecules.

The profile of captured extract molecules could be evaluated in detail by calculating the logD of selected compounds. Taking the logDs of known and tentatively identified substances into account, the applied setup mainly provides the possibility to investigate compounds with high to good water solubility. Nevertheless the separation of glucuronidated and glucosylated flavonoids was
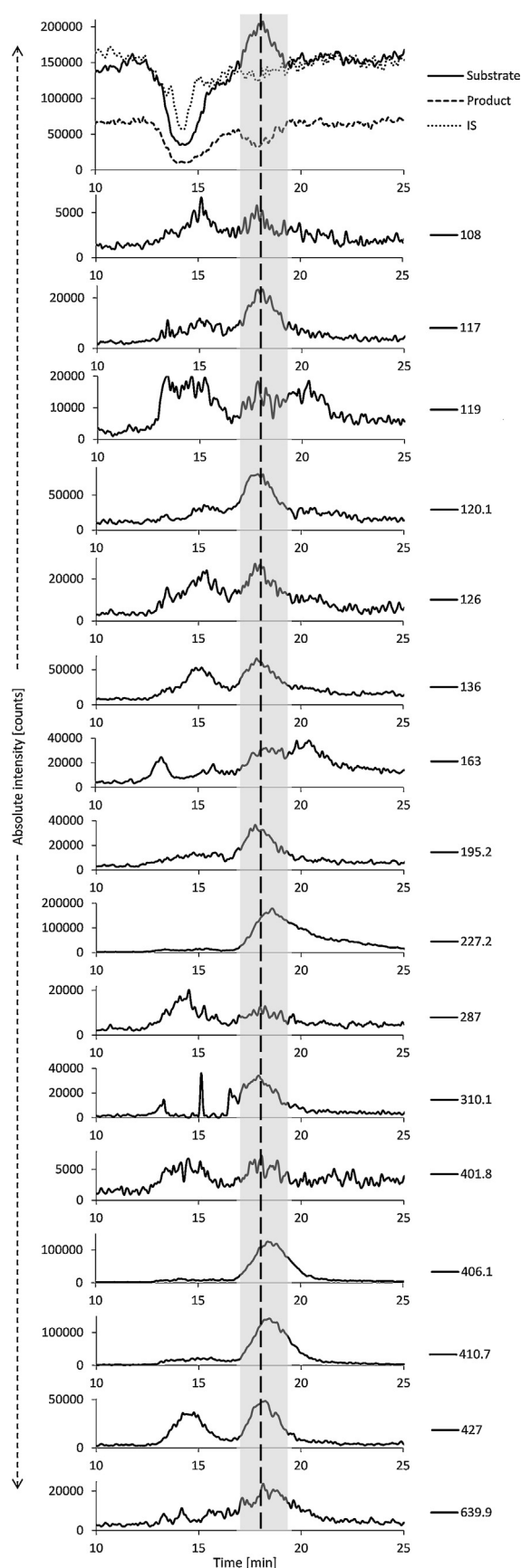
Fig. 6. EICs of potentially regulatory compounds found within the time span of enzymatic inhibition of XOD detected with a single quadrupole MS.

Table 4

m/z found within the range of XOD inhibition ascribed to accurate *m/z* obtained with a ToF-MS (if detected). Molecular formulas calculated from ToF derived *m/z* are listed.

SQ-MS	ToF-MS	Molecular formula(s)	Data base search results
427.1	427.1379	$C_{20}H_{14}N_{10}O_2C_{21}H_{20}N_3O_7C_7H_{22}N_8O_{13}$	No structures found
195.2	195.0987	$C_6H_{14}N_2O_5$ $C_5H_8N_9$ $C_7H_{10}N_6O$	e.g. derivatives of adenine or guanine
120.1	120.0809	C_8H_9N	e.g. derivatives of pyridine or indoline
126	–		–
136	136.0622	$C_7H_7N_2O/C_5H_5N_5$	Adenine
117	117.0692	–	–

found to be satisfactory, even providing a good separation of highly similar compounds like scutellarein 7-O-diglucuronide, luteolin 7-O-diglucuronide and apigenin 7-O-diglucuronide with a mobile phase containing 5% EtOH. Due to their chemical similarity and hence their poor separation, those molecules are likely to remain disregarded in other experimental setups. By changing the organic solvent proportion of the mobile phase, the profile of eluting compounds can be diversified in order to find enzyme regulatory molecules. In this regard an enzymatic regulation was captured with the 5% IPA mobile phase after the injection of 90% MeOH, 0.5% FAc extract. The amount of potentially responsible compounds could be narrowed down by aligning their peaks with the shape of the enzymatic inhibition.

Acknowledgment

Appendix A.   Supplementary data

Supplementary data associated with this article can be found, in the online version, at http://dx.doi.org/10.1016/j.jpba.2016.03.011.

References

[1] S. Masanetz, C. Kaufmann, T. Letzel, M.W. Pfaffl, Effects of pine pollen extracts on the proliferation and mRNA expression of porcine ileal cell cultures, J. Appl. Bot. Food Qual. 83 (2009) 14–18.

[2] J. Muller, M.W. Pfaffl, Synergetic downregulation of 67 kDa laminin receptor by the green tea (*Camellia sinensis*) secondary plant compound epigallocatechin gallate: a new gateway in metastasis prevention? BMC Compl. Altern. Med. 12 (2012) 258.

[3] T. Maier, M. Guell, L. Serrano, Correlation of mRNA and protein in complex biological samples, FEBS Lett. 583 (2009) 3966–3973.

[4] J. Han, M. Ye, H. Guo, M. Yang, B.-r. Wang, D.-a. Guo, Analysis of multiple constituents in a Chinese herbal preparation Shuang-Huang-Lian oral liquid by HPLC-DAD-ESI–MSn, J. Pharm. Biomed. Anal. 44 (2007) 430–438.

[5] J. Grassmann, R.K. Scheerle, T. Letzel, Functional proteomics: application of mass spectrometry to the study of enzymology in complex mixtures, Anal. Bioanal. Chem. 402 (2012) 625–645.

[6] T. Burkhardt, C.M. Kaufmann, T. Letzel, J. Grassmann, Enzymatic assays coupled with mass spectrometry with or without embedded liquid chromatography, Chembiochem 16 (2015) 1985–1992.

[7] A.C. Hogenboom, A.R. de Boer, R.J. Derks, H. Irth, Continuous-flow, on-line monitoring of biospecific interactions using electrospray mass spectrometry, Anal. Chem. 73 (2001) 3816–3823.

[8] C.F. de Jong, R.J.E. Derks, B. Bruyneel, W. Niessen, H. Irth, High-performance liquid chromatography-mass spectrometry-based acetylcholinesterase assay for the screening of inhibitors in natural extracts, J. Chromatogr. A 1112 (2006) 303–310.

[9] A.R. de Boer, J.M. Alcaide-Hidalgo, J.G. Krabbe, J. Kolkman, C.N.V. Boas, W.M.A. Niessen, H. Lingeman, H. Irth, High-temperature liquid chromatography coupled on-line to a continuous-flow biochemical screening assay with electrospray ionization mass spectrometric detection, Anal. Chem. 77 (2005) 7894–7900.

[10] A.R. de Boer, T. Letzel, D.A. van Elswijk, H. Lingeman, W.M. Niessen, H. Irth, On-line coupling of high-performance liquid chromatography to a continuous-flow enzyme assay based on electrospray ionization mass spectrometry, Anal. Chem. 76 (2004) 3155–3161.

[11] K. Ingkaninan, C.M. de Best, R. van der Heijden, A.J.P. Hofte, B. Karabatak, H. Irth, U.R. Tjaden, J. van der Greef, R. Verpoorte, High-performance liquid chromatography with on-line coupled UV, mass spectrometric and biochemical detection for identification of acetylcholinesterase inhibitors from natural products, J. Chromatogr. A 872 (2000) 61–73.

[12] M. Igarashi, Y. Miyazaki, A review on bioactivities of perilla: progress in research on the functions of perilla as medicine and food, evidence-Based complementary, Altern. Med. (2013) (2013), 925342.

[13] C. Sanbongi, H. Takano, N. Osakabe, N. Sasa, M. Natsume, R. Yanagisawa, K. Inoue, K. Sadakane, T. Ichinose, T. Yoshikawa, Rosmarinic acid in perilla extract inhibits allergic inflammation induced by mite allergen, in a mouse model, Clin. Exp. Allergy 34 (2004) 971–977.

[14] E.S. Lin, H.J. Chou, P.L. Kuo, Y.C. Huang, Antioxidant and antiproliferative activities of methanolic extracts of *Perilla frutescens*, J. Med. Plants Res. 4 (2010) 477–483.

[15] Y.K. Yim, H. Lee, K.E. Hong, Y.I. Kim, S.K. Ko, J.E. Kim, S.Y. Lee, K.S. Park, Anti-inflammatory and immune-regulatory effects of subcutaneous perillae fructus extract injections on OVA-induced asthma in mice, evidence-Based complementary, Altern. Med. 7 (2010) 79–86.

[16] Z. Guan, S. Li, Z. Lin, R. Yang, Y. Zhao, J. Liu, S. Yang, A. Chen, Identification and quantitation of phenolic compounds from the seed and pomace of *Perilla frutescens* using HPLC/PDA and HPLC ESI/QTOF/MS/MS, Phytochem. Anal. 25 (2014).

[17] J.H. Lee, K.H. Park, M.H. Lee, H.T. Kim, W.D. Seo, J.Y. Kim, I.Y. Baek, D.S. Jang, T.J. Ha, Identification, characterisation, and quantification of phenolic compounds in the antioxidant activity- containing fraction from the seeds of Korean perilla (*Perilla frutescens*) cultivars, Food Chem. 136 (2013) 843–852.

[18] H.J. Kim, W. Lee, J.M. Yun, Luteolin inhibits hyperglycemia-induced proinflammatory cytokine production and its epigenetic mechanism in human monocytes, Phyther. Res. 28 (2014).

[19] G. Zhao, C. Yao-Yue, G.W. Qin, L.H. Guo, Luteolin from purple perilla mitigates ROS insult particularly in primary neurons, Neurobiol. Aging 33 (2012) 176–186.

[20] J. Yan, G. Zhang, Y. Hu, Y. Ma, Effect of luteolin on xanthine oxidase: inhibition kinetics and interaction mechanism merging with docking simulation, Food Chem. 141 (2013) 3766–3773.

[21] P. Pacher, A. Nivorozhkin, C. Szabo, Therapeutic effects of xanthine oxidase inhibitors: renaissance half a century after the discovery of allopurinol, Pharmacol. Rev. 58 (2006) 87–114.

[22] J. Havlik, R.G. de la Huebra, K. Hejtmankova, J. Fernandez, J. Simonova, M. Melich, V. Rada, Xanthine oxidase inhibitory properties of Czech medicinal plants, J. Ethnopharmacol. 132 (2010) 461–465.

[23] M. Umamaheswari, K. Asokkumar, A.T. Sivashanmugam, A. Remyaraju, V. Subhadradevi, T.K. Ravi, In vitro xanthine oxidase inhibitory activity of the fractions of erythrina stricta roxb, J. Ethnopharmacol. 124 (2009) 646–648.

[24] A.D. Kaufman, P.T. Kissinger, Extra-Column band spreading concerns in post-column photolysis reactors for microbore liquid chromatography, Curr. Sep. 17 (1998) 9–16.

[25] M. Krappmann, C.M. Kaufmann, R.K. Scheerle, J. Grassmann, T. Letzel, Achroma software-high- quality policy in (a-) typical mass spectrometric data handling and applied functional proteomics, J. Proteomics Bioinf. 7 (2014) 264–271.

[26] R.K. Scheerle, J. Grassmann, T. Letzel, Real-time ESI–MS of enzymatic conversion: impact of organic solvents and multiplexing, Anal. Sci. 28 (2012) 607–612.

[27] T. Teutenberg, S. Wiese, P. Wagner, J. Gmehling, High-temperature liquid chromatography. Part III: Determination of the static permittivities of pure solvents and binary solvent mixtures–implications for liquid chromatographic separations, J. Chromatogr. A 1216 (2009) 8480–8487.

[28] T. Letzel, U. Pöschl, E. Rosenberg, M. Grasserbauer, R. Niessner, In-source fragmentation of partially oxidized mono- and polycyclic aromatic hydrocarbons in atmospheric pressure chemical ionization mass

spectrometry coupled to liquid chromatography, Rapid Commun. Mass Spectrom. 13 (1999) 2456–2468.

[29] S. Buchwald-Werner, Investigation of a *Perilla frutescens* special extract—anti-inflammatory and immune-modulatory properties, Agro Food Ind. Hi-Tech 23 (2012) 38–41.

[30] A.A. Aydın, T. Letzel, Simultaneous investigation of sesquiterpenes, pyrrolizidine alkaloids and N- oxides in Butterbur (*Petasites hybridus*) with an offline 2D-combination of HPLC-UV and LC-MMI- ToF-MS, J. Pharm. Biomed. Anal. 85 (2013) 74–82.

[31] J.F. Hsieh, S.H. Wu, Y.L. Yang, K.F. Choong, S.T. Chen, The screening and characterization of 6- aminopurine-based xanthine oxidase inhibitors, Bioorg. Med. Chem. 15 (2007) 3450–3456.

[32] L.N. Huo, W. Wang, C.Y. Zhang, H.B. Shi, Y. Liu, X.H. Liu, B.H. Guo, D.M. Zhao, H. Gao, Bioassay-guided isolation and identification of xanthine oxidase inhibitory constituents from the leaves of *Perilla frutescens*, Molecules 20 (2015) 17848–17859.

[33] P. Cos, L. Ying, M. Calomme, J.P. Hu, K. Cimanga, B. Van Poel, L. Pieters, A.J. Vlietinck, D. Vanden Berghe, Structure-activity relationship and classification of flavonoids as inhibitors of xanthine oxidase and superoxide scavengers, J. Nat. Prod. 61 (1998) 71–76.

[34] D.E.C. Van Hoorn, R.J. Nijveldt, P.A.M. Van Leeuwen, Z. Hofman, L. M'Rabet, D.B.A. De Bont, K. Van Norren, Accurate prediction of xanthine oxidase inhibition based on the structure of flavonoids, Eur. J. Pharmacol. 451 (2002) 111–118.

HPLC method development for the online-coupling of chromatographic *Perilla frutescens* extract separation with xanthine oxidase enzymatic assay

Christine M. Kaufmann, Johanna Grassmann and Thomas Letzel[*]

Chair of Urban Water Systems Engineering, Technical University of Munich, Am Coulombwall, 85748 Garching, Germany

* Corresponding author: Telephone: +49 (0)89 2891 3780; Fax: +49 (0)89 - 289-13718; E-mail: T.Letzel@tum.de

Supplementary material

Experimental

Instrumentation and experimental setup

Real-time online measurement of enzymatic activity in the presence of organic solvent

Xanthine oxidase activity was investigated in the presence of different concentrations of various organic solvents. The substrate degradation as well as product generation was observed in real-time by continuously pumping the assay into the mass spectrometric source. Enzyme concentration was set to 0.004 U/mL with a xanthine substrate concentration of 25 µM in ammonium acetate (NH_4Ac) solution (pH 7.4, 10 mM). Enzyme stock solution was prepared in NH_4Ac (pH 7.4, 10 mM). Substrate was solved in water/NH_3 (0.1 M) (70:30, v/v), due to the poor solubility of xanthine in water. The volume of xanthine added to the assay was therefore kept minor, to preserve the pH value. Besides the detection of enzymatic assays in 100% aqueous solution, enzymatic activity was also tested in the presence of 2%, 5% and 10% methanol (MeOH), ethanol (EtOH), acetonitrile (ACN) or isopropyl alcohol (IPA) (v/v), respectively. Detailed description of the experimental setup can be found in a previous publication [42]. Mass spectrometric data was recorded with a mass range of m/z 100 to 1000, a needle voltage of 3.5 kV, a temperature of 225 °C and a cone voltage of 75 V. Flow rate of the syringe pump was set to 20 µL/min.

Data evaluation

Data were first processed using Xcalibur software 2.1.0.1139 (Thermo Fisher Scientific Inc., Waltham, MA, USA). The extracted ion chromatograms (EIC) of xanthine substrate and uric acid product were obtained by using an m/z range of ±0.5 Da to the respective calculated m/z value. After smoothing the EICs with a Gaussian function using a 15-points function width further processing was conducted with Microsoft Office Excel 2007. After data normalization, a linear trend line was applied to approach the linear range of substrate degradation curves. A y-value of 0.05 was assumed to represent the completion of enzymatic substrate degradation. Calculated x-values, representing the time point of complete substrate depletion, were thereupon compared for assays with different organic solvents in comparison to those without the addition of organic solvent.

Online coupled continuous flow system with 100% aqueous chromatographic separation

The employment of Synergi column (4u Polar-RP, 80A, 2mm ID x 100mm length, Phenomenex, Aschaffenburg, Germany) allowed a 100% aqueous chromatographic separation. Due to the column´s restricted pH range up to pH 7, the isocratic chromatography was performed with NH_4Ac pH 5.5 (10 mM). To regain the physiological of pH 7.4 in RC1, the enzyme was prepared in NH_4Ac pH 8.45 (10 mM) (Figure 1, upper trace), whereas the substrate was solved in NH_4Ac pH 7.4 (10 mM) (Figure 1, bottom trace). Alkaline pH sufficient to neutralize pH 5.5 to pH 7.4 was experimentally determined prior to the online coupled continuous flow system experiments. Chromatographic separation was performed with and without the application of a temperature gradient (Table 1).

Data evaluation

Data were processed using Xcalibur software 2.1.0.1139 (Thermo Fisher Scientific Inc., Waltham, MA, USA) in case of measurements detected with the single quadrupole MS. The EIC were obtained by using an m/z range of ± 0.5Da to the respective calculated m/z value of substrate and product: xanthine with m/z 153, i.e. $[M+H]^+$, uric acid with m/z 169, i.e. $[M+H]^+$ and internal standard histidine with m/z 156, i.e. $[M+H]^+$. Compound peaks originating from the injection of Perilla frutescens extracts were evaluated manually with

Xcalibur software. Assay as wells as extract compound EICs were smoothed with a Gaussian function using a 15 points function width. Further processing was conducted with Microsoft Office Excel 2007. For comparative data evaluation, time point of plant extract injection was set as time point 0.

Results

Enzymatic activity in the presence of organic solvent

Prior to the adaption of xanthine oxidase assay to the online coupled continuous flow system, the enzyme´s tolerance towards different organic solvents was tested as shown before by Scheerle et al [42]. The extent of the solvent effect on substrate degradation was assessed with regard to the employment of organic solvents for the chromatographic separation of Perilla extract in the presence of xanthine oxidase (XOD). The addition of 2% EtOH, IPA or ACN resulted in a similar decrease of enzymatic substrate degradation to a remaining activity of 68%, 74% and 70% respectively, whereas addition of 2% MeOH distinctly affected the enzyme with only 24% activity left compared to the assays in 10 mM NH_4Ac pH 7.4.

5% organic solvent proportion of MeOH resulted in the complete inhibition of enzymatic activity, whereas EtOH and IPA revealed a less pronounced and comparable effect on the enzyme with a remaining activity of 69% and 65% respectively. 10% EtOH and 10% IPA were observed to suppress the enzymatic activity to 48% and 37% respectively, whereas 5% and 10% ACN caused a decrease to 52% and 32%. Hence, the most suitable organic solvents were identified to be EtOH and IPA.

Online coupled continuous flow system

The application of a 100% aqueous eluent altogether prevented the enzymatic activity to be affected by the addition of organic solvent. Expecting more compounds to elute, first experiments with purely aqueous eluent were performed with the injection of polar water extract rather than semi-polar 50% EtOH or non-polar 90% MeOH, 0.5% FAc Perilla extracts. To enhance the solubility of plant compounds and to accelerate the separation, a moderate temperature gradient up to 70°C was applied, thus not conflicting with the column

specifications (Table 1). The chromatographic results were then examined in comparison to results obtained with a constant temperature of 30°C (Table S1).

According to Teutenberg et al. [43] water features a static permittivity at 70°C, which is comparable to an eluent containing approximately 25% MeOH or 20% ACN (mol/mol) at 25°C. Due to the decrease of the aqueous eluent´s permittivity with elevating temperature and the coherent decline in polarity [43], the temperature-related modification of the elution strength resulted in an enhancement of solubility of most compounds and hence in a shift to earlier retention times (Table S1, $\triangle$RT).

Table S1 Retention time of selected compounds with 100% NH_4Ac (pH 7.4, 10 mM) eluent at constant 30°C (RT_{30}) and with the employment of a temperature gradient up to 70°C (RT_{70}) as well as eluent temperature at RTs for measurement with temperature gradient (T_E). Virtual MeOH and ACN concentrations (mol/mol) at 25°C were calculated according to Teutenberg et al. [43]. m/z of compounds are given as obtained by single quadrupol-MS experiments. logD was calculated for known compounds m/z 623.1 and 639.1 (Table 3).

m/z	RT_{30}	RT_{70}	$\triangle$RT	T_E	mol% of organic solvent (mol/mol)		logD
					MeOH	ACN	
325.1	13.7	13.6	-0.1	30.0	0	3	-
179.0	14.3	14.6	0.3	30.6	1	4	-
144.1	16.2	16.1	-0.1	32.1	2	4	-
154.1	29.0	24.9	-4.1	40.9	8	8	-
351.9	32.5	28.5	-4.0	44.5	10	9	-
136.0	39.8	33.5	-6.3	49.5	14	11	-
209.2	54.2	38.4	-15.8	51.7	15	12	-
191.3	54.5	38.3	-16.2	51.6	15	12	-
427.0	66.5	42.2	-24.3	53.6	16	13	-
623.1	-	55.3	-	60.2	21	16	-8.02
639.1	86.7	48.2	-38.5	56.6	19	14	-8.32
		63.2	-	63.6	22	17	-8.23
333.9	-	88.7	-	70	25	20	-

Highly polar, slightly retained or non-retained compounds, which elute between minute 13 and 20, revealed no distinct change of retention time (Table S1, white area, $\triangle$RT). However, the further the progress of experimental time and temperature gradient, the more pronounced alterations in retention times were observed (Table S1, light and dark grey areas).

In this regard a slight shift was detected for those compounds eluting between minute 20 and 40 with 30°C constant temperature (Table S1, light grey area), whereas a rise in temperature to values between 50 and 70°C resulted in a distinct time shift of up to 38.5 minutes (Table S1, dark grey area).

Compounds 623.1 and a second peak for 639.1, both not detectable without the application of a temperature gradient, elute at 60.2 and 63.6°C respectively, which corresponds to an organic

solvent proportion of approximately 21% and 22% MeOH (mol/mol) (Table S1). By employing a ToF-MS in combination with a literature research, features could be identified as Apigenin 7-O-diglucuronide, Luteolin 7-O-diglucuronide and tentatively Scutellarein 7-O-diglucuronide (compare Table 3) [44]. Calculation of their respective logDs revealed distinct negative values (Table S1), which is corresponding to high water solubility.

Although the application of a temperature gradient was proven to be a helpful means to speed up the chromatographic separation, the amount of detectable extract compounds was found to be minor and is composed of mainly highly water soluble compounds with a purely aqueous mobile phase, even with the application of a temperature gradient (Figure S1, upper graph).
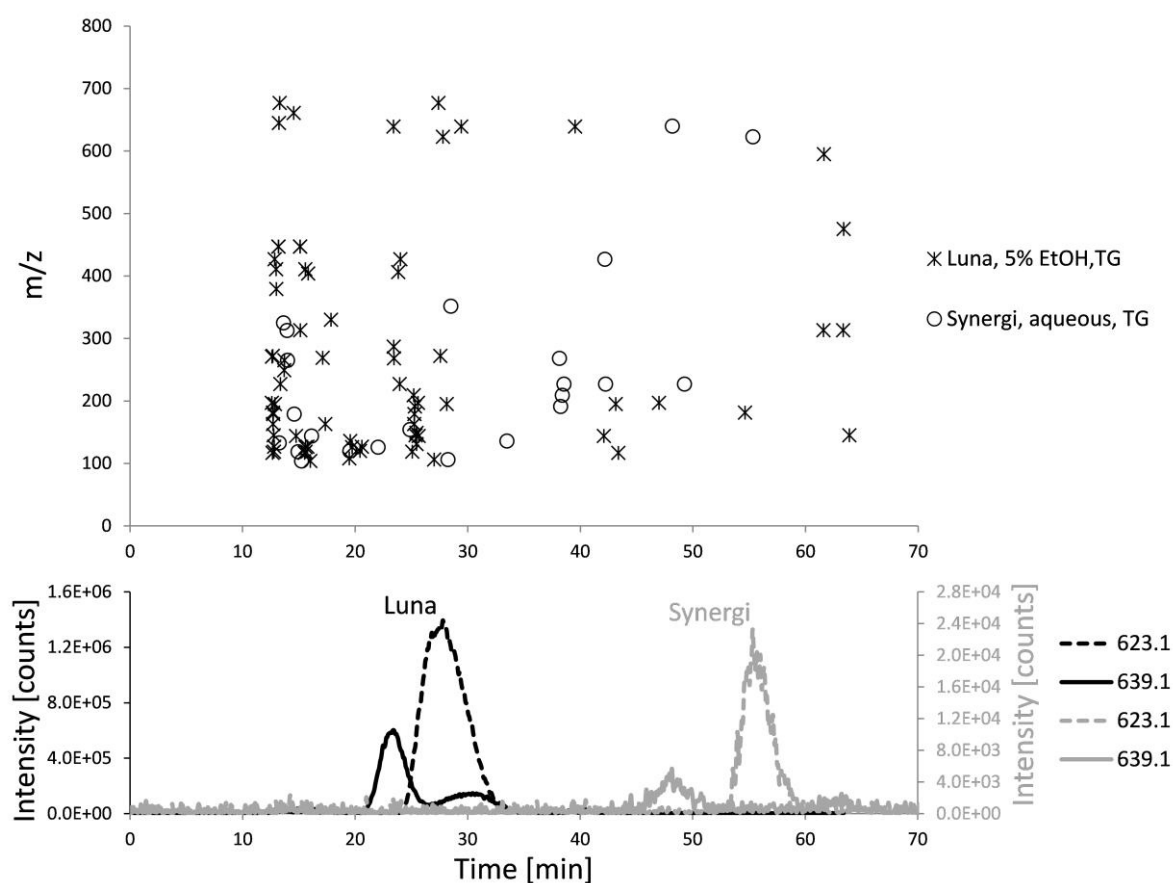
Figure S1 Comparison of Perilla compound elution with Luna column (5% EtOH mobile phase and temperature gradient) and Synergi column (100% aqueous mobile phase and temperature gradient); overview of eluting compounds (upper graph) and differences in retention time and intensity for m/z 623.1 and 639.1 (bottom graph). Due to its inferiority, intensity of m/z 623.1 (light grey EIC) is displayed as secondary y-axis.

Besides the low quantity, peak intensities were observed to be only menial, which might impair or even prevent the detection of low-abundance Perilla compounds (Figure S1, bottom graph). The finding of the late-eluting compounds to possess highly negative logD values (Table S1) furthermore confirms the necessity of organic solvents to extent the spectrum of compound polarities. Due to Synergi column specifications, which limit the pH range

maximum to pH 7.0, the mobile phase pH was set to 5.5 from the first. However, the employment of an acidic pH necessarily involved a neutralization step by consequently preparing the enzymatic solution in an alkaline pH to regain a value of pH 7.4 in RC2 (Figure 1) for the enzymatic substrate degradation. The overall procedure did not prove to be reasonable in terms of practicability and reliability, which led to the employment of another column for further experiments.

Appendix V

Effect of *Perilla frutescens* extracts on porcine jejunal epithelial cells

Christine M. Kaufmann, Thomas Letzel, Johanna Grassmann and Michael W. Pfaffl

The publication characterizes PF extracts with regard to their reducing potential. Moreover the extracts were applied to the porcine jejunal epithelial cell line IPEC-J2 to capture their effects on cell proliferation as well as on the expression of a panel of key genes, amongst others involved in cell growth and apoptosis. Comprehensive control measurements were conducted, which included the assessment of the extract´s cytotoxic effects, the potential generation of H_2O_2 and the stability of PF compounds in cell culture medium. Conduction of RT-qPCR experiments was kindly done by Angela Sachsenhauser. Beyond that, all experiments, data evaluation and the writing were done on my part.

Effect of *Perilla frutescens* Extracts on Porcine Jejunal Epithelial Cells

Christine M. Kaufmann,[1,2]* Thomas Letzel,[1] Johanna Grassmann[1] and Michael W. Pfaffl[2]

[1]Chair of Urban Water Systems Engineering, Technical University of Munich, Am Coulombwall 3, 85748 Garching, Germany
[2]Institute of Animal Physiology and Immunology Weihenstephan, Technical University of Munich, Weihenstephaner Berg 3, 85354 Freising, Germany

Green-leaved *Perilla frutescens* extracts were investigated on their effect on cell proliferation of the porcine jejunal epithelial cell line, IPEC-J2, as well as on the gene expression of cell cycle or cancer-related genes. Some extracted compounds were, however, susceptible to degradation in cell culture medium, whereas others were found to be stable during the entire experimental time. Control experiments also included the assessment of H_2O_2 generation in cell culture medium caused by oxidation of natural extract compounds, which was proved to be absent at low extract concentrations. A fast and significant inhibition of cell growth at low physiological extract concentrations could be observed. This finding, along with an immediate downregulation of 67 kDa laminin receptor and cyclin D1 expression, can be accounted to the presence of *Perilla frutescens* extract. Copyright © 2016 John Wiley & Sons, Ltd.

Keywords: *Perilla frutescens*; cell proliferation; RT-qPCR; 67 kDa laminin receptor; natural compound stability; reactive oxygen species.

INTRODUCTION

Perilla frutescens (PF) is widely used as traditional medicinal plant in large parts of Asia. It has gained interest during the last couple of years, because of its high phenolic content and therefore elevated antioxidative properties (Muller-Waldeck *et al.*, 2010). Besides its protective effect against reactive oxygen species (ROS) (Lee and Han, 2012), individual PF compounds like rosmarinic acid, luteolin or apigenin as well as the whole extract were found to exert a variety of positive effects, ranging from anti-allergic (Chen *et al.*, 2015), antiinflammatory (Jeon *et al.*, 2014) to the inhibition of cancer promotion and progression due to its antiproliferative properties (Kwak and Ju, 2015). To test the specific effects of PF on cell proliferation or apoptosis in the gastrointestinal tract (GIT), the application of a jejunal cell culture model is useful. The knowledge obtained by employing a porcine gastrointestinal cell line may also be considered transferable on the human GIT, because of a highly similar physiology (Guilloteau *et al.*, 2010). To reinforce findings, the influence of PF on the induction of a panel of key genes involved in cell cycle progression and cell survival should be determined. This includes the assessment of cyclin B1 and D1, both of which reported to be overexpressed in various types of cancer (Begnami *et al.*, 2010). Moreover, the expression of 67 kDa laminin receptor (67LR) is of special interest, because of its involvement in the metastasis of tumour cells (Nelson *et al.*, 2008). Besides being elevated in different cancers (de Manzoni *et al.*, 1998), it has been identified as a receptor for the attachment and entry of viruses and bacteria or prion protein into mammalian cells (Morel *et al.*, 2005). In literature, the levels of cyclins and 67LR have been shown to be responsive towards polyphenols. Cyclins have been found to be regulated, for example, by quercetin (Shan *et al.*, 2009), resveratrol (Wolter *et al.*, 2001) or whole pomegranate fruit extract (Malik *et al.*, 2005), whereas 67LR was found to serve as a receptor for the tea polyphenol epigallocatechin gallate (EGCG) (Muller and Pfaffl, 2012). The aim of this study was to investigate the effects of different extracts prepared from a green-leaved PF variety on the proliferation properties in a porcine jejunal epithelial cell line (IPEC-J2) using electric cell-substrate impedance sensing (ECIS). Furthermore, the quantitative mRNA gene expression levels of upper mentioned cell cycle and cancer-related genes were observed after cell treatment with PF extract via quantitative real-time RT-PCR (RT-qPCR). The effect of a plant extract on cell growth and gene expression might, however, be inconclusive without suitable control experiments to take into account artificial effects, which might arise with the conduction of *in vitro* cell culture experiments. Several studies reported the partial degradation of natural compounds like flavonoids in cell culture medium during cultivation , as well as the generation of cell toxic concentrations of H_2O_2 (Long *et al.*, 2010). Therefore, additional experiments were performed herein, to assess the stability of PF extract compounds along with the assessment of H_2O_2 concentration.

EXPERIMENTAL

Preparation of *Perilla frutescens* extracts

Perilla frutescens var. crispa freeze-dried and milled leaves (provided by Vital Solutions GmbH, Langenfeld, Germany, and Amino Up Chemicals Co., Ltd., Sapporo, Japan) were extracted with water (LC-MS

* Correspondence to: Christine Kaufmann, Technical University of Munich, Am Coulombwall 3, 85748 Garching, Germany.
E-mail: c.kaufmann@tum.de

grade, VWR, Darmstadt, Germany), 50% ethanol (EtOH), 100% EtOH (Ethanol absolute, AppliChem, Darmstadt, Germany) or 90% methanol (MeOH) (LC-MS grade, VWR) with 0.5% formic acid (FAc) (Sigma-Aldrich, Steinheim, Germany) ($n = 5$). For this purpose, 500 mg freeze-dried and milled leaves were weighed, followed by the addition of 5 mL extraction solvent. After thoroughly mixing, the PF-solvent mixture was sonicated for 10 min at 4 °C and centrifuged for 20 min at 1500 rpm. The supernatant was transferred to a further tube, and the extraction procedure was repeated twice. The collected supernatant was then evaporated to dryness. The remaining extractable matter (i.e. extraction residue) was stored at -20 °C until use. The extraction residue was determined by weighing the glass tubes prior to extraction and after evaporation. Furthermore, the extraction yield was calculated according to Equation 1.

$$ \text{Extraction yield} = \frac{evaporated\ extractable\ matter\ \ [g]}{freeze-dried\ \ and\ \ milled\ \ leaves\ \ [g]} x100 $$

(1)

'Empty extracts', which served as control, were prepared in the exact same manner as described earlier but without the addition of PF matter.

Extracted PF as well as empty control extracts were redissolved as required, whereby water extract was redissolved in water, 50% EtOH extract in 50% EtOH, 100% EtOH and 90% MeOH, 0.5%FAc extracts in 100% EtOH. A further PF water extract, provided in the form of a powder by Vital solutions GmbH and Amino Up Chemicals Co., Ltd. ('VS water extract'), was redissolved in water. The latter was extracted differently by using hot water extraction as opposed to cold extraction, which was performed here. However, no further information about the detailed method was available.

Determination of extract phenolic contents

The total extract reducing potentials were determined using Folin–Ciocalteau (FC) reagent (Merck Chemicals, Darmstadt, Germany) (Singleton *et al.*, 1999). Three calibration curves were prepared with increasing gallic acid (Acros Organics, Nidderau, Germany) concentrations solved in either water, 50% EtOH or 100% EtOH ($n = 6$); 20 µL of the extract were mixed with 100 µL 10% FC reagent and 100 µL 7% Na_2CO_3 (Acros organics); the assays were incubated for 60 min in the dark (total volume of 220 µL). Absorption was measured at 620 nm. The result is given as gallic acid equivalence (GAE) with $n > 25$.

Assessment of cell proliferation

Cell culture experiments were performed using a porcine jejunal epithelial cell line isolated from neonatal piglet (IPEC-J2). Cells were kindly provided by Dr Karsten Tedin (FU Berlin). Cell culture medium employed consisted of Dulbecco's modified Eagle's medium (DMEM)/Ham's F12 (1:1), 5% Foetal calf serum (FCS), 1mM L-glutamine and 100 U/mL penicillin/streptomycin (Life technologies, Gaithersburg, MD, USA). All reagents to come in contact with

the cells were pre-warmed to 37 °C for all experiments described. Cells were maintained at 37 °C, 5% CO_2 in 25 cm^2 or 75 cm^2 cell culture flasks (Greiner Bio-One, Frickenhausen, Germany), and routine cell passaging procedure was performed every 72 h at 80% to 90% confluence by removing cell culture medium and washing with Phosphate buffered saline (PBS) (Life technologies) twice, followed by cell detachment with trypsin (0.25%) (PAA, Pasching, Austria). Cell proliferation was assessed using ECIS (Applied Biophysics, Troy, NY, USA), employing eight-well slides (#8W10E; Applied Biophysics). Electric cell-substrate impedance sensing wells were pre-incubated with cell culture medium for at least 5 h. The medium was removed, and 10 000 cells/400 µL cell culture medium were transferred randomly into the wells and allowed to adhere for 20 h. Because of the layout of the employed ECIS slides, a total of 16 wells were available per experiment, wherefore neither randomization nor blinding was implemented for the treatment of cells with PF extracts.

Control measurements using redissolved empty control extracts were conducted beforehand to assess possible effects of the redissolution solvents on cell physiology. Cells were treated with redissolved 'VS water extract' corresponding to 4.0, 2.0, 1.6, 1.0 and 0.4 mg freeze-dried and milled PF leaves in a total volume of 400 µL cell culture medium (hereafter referred to as '4.0', '2.0', '1.6', '1.0' and '0.4' mg) ($n \geq 4$). For self-made water, 50% EtOH, 100% EtOH and 90% MeOH, 0.5% FAc extracts solely '4 mg' and '0.4 mg' were applied to the cells ($n = 9$). Proliferation was assessed in comparison to untreated control cells ($n = 12$) in three independent repetitions. In all cases, the final total organic solvent proportion per well, either with empty control or plant extracts, did not exceed 1% of the total well volume.

Assessment of H_2O_2 generation

H_2O_2 generation with '2.0 mg' PF was determined with 'VS water extract', whereas determination of H_2O_2 in the presence of '0.4 mg' PF was measured using both 'VS water extract' as well as self-made extracts ($n \geq 3$). Experiments were performed in the absence of IPEC-J2 cells. Working solution, formulated out of 250 µM $(NH_4)_2Fe(SO_4)_2$ (Merck Chemicals), 100 mM Sorbitol (Sigma-Aldrich), 125 µM Xylenol Orange (Sigma-Aldrich) and 25 mM H_2SO_4 (Merck Chemicals), as well as H_2O_2 stock solutions (Sigma-Aldrich), were freshly prepared each day. Calibration curves were performed by mixing 10 µL of H_2O_2 stock solution with 390 µL cell culture medium containing PF ($n \geq 3$). For the assessment of H_2O_2 generation with PF, '2.0 mg' or '0.4 mg' extract was solved in cell culture medium. At several time points, 30 µL were withdrawn and mixed with 300 µL working solution, incubated for 30 min and measured at 595 nm. Negative controls containing no extract were measured simultaneously.

Perilla frutescens stability in cell culture medium

Stability of PF compounds in cell culture medium (without L-glutamine) was exemplarily investigated using 'VS water extract'. For this purpose, 2.5 mg

powder ($\triangleq$ 12.5 mg freeze-dried and milled PF leaves) was either solved in 200 μL cell culture medium or bidistilled water in triplicate. Samples and controls were then incubated at 37 °C. After 0, 1, 2, 6 and 24 h, the sample was diluted 5:1 with bidest. H$_2$O. The solution was cleaned from proteins, salts and glucose using pre-conditioned Strata C18-E solid phase extraction (SPE) columns (Phenomenex, Aschaffenburg, Germany). Compounds were eluted with MeOH, which was evaporated afterwards (miVac Duo concentrator, GeneVac, Ipswich, England). Residues were redissolved in EtOH/water (50:50) prior to LC-MS (liquid chromatography-mass spectrometry) setup analysis. Details about the employed LC-MS setup and HPLC gradient can be found in the publication of Greco et al. (2013). Each sample was spiked with 20 μM resveratrol (Sigma-Aldrich, ≥99% purity) and 4 μM rutin (Sigma-Aldrich, ≥95% purity) prior to SPE and 10 μM taxifolin (Sigma-Aldrich, >90% purity) and 10 μM galangin (Sigma-Aldrich) prior to LC-MS analysis to enable data correction for loss during Solid phase extraction (SPE) and mass spectrometric signal inconstancies, respectively. Samples and controls were detected with a 'time-of-flight' mass spectrometer (Agilent Technologies, Waldbronn, Germany), equipped with an electrospray ionization source. Samples were detected in positive and negative ionization mode applying the following conditions: gas temperature 325 °C, drying gas 10 L/min, nebulizer gas pressure 45 psig, sheath gas temperature 325 °C, sheath gas flow 7.5 L/min, capillary voltage 3 kV and Fragmentor 100 V. The mass range was set to m/z 60–1700. Data was analysed with Agilent MassHunter Qualitative Analysis B.03.01 (Agilent Technologies) and Microsoft Excel 2010 (Microsoft Inc, Seattle, WA, USA). Peak areas of PF extract compounds were corrected by means of the added spike compounds.

Assessment of gene expression

Per well 40 000 IPEC-J2 cells in 400 μL cell culture medium were seeded randomly using 48-well plates (Greiner Bio-One). After adherence, cells in each well were treated in a non-blinded manner either with '0.4 mg' PF VS water, PF water, PF 50% EtOH, PF 100% EtOH or PF 90% MeOH, 0.5% FAc extract by replacing 1% of the cell culture medium with redissolved PF extract ('0.4 mg'/400 μL total volume). Controls were prepared simultaneously and included non-treated cells, which remained in pure cell culture medium as well as cells treated with 1% PF extract redissolution solvent water, 50% EtOH or 100% EtOH. At time point 0, 6 and 24 h wells containing equally treated cells were randomly pooled by twos and transferred to reaction tubes. RNA of all samples was then extracted according to the manufacturer's guidelines using RNeasy® Plus Mini Kit (Qiagen, Hilden, Germany), and RNA concentration was determined using the NanoDrop ND-1000 spectrophotometer (PEQLab Biotechnologie GmbH, Erlangen, Germany). RNA integrity (RIN) was tested with 2100 Bioanalyzer (Agilent Technologies) using randomly selected samples (Becker *et al.*, 2010). Total RNA samples were stored at −80 °C until use; 300 ng RNA were reversed transcribed in a final volume of 30 μL containing 5× buffer, 0.5 mM deoxyribonucleoside triphosphates (dNTPs) (Life Technologies), 2.5 μM random hexamer primers (Invitrogen, Darmstadt, Germany) and 100 U

Moloney Murine Leukemia Virus (M-MLV) reverse transcriptase (Promega, Mannheim, Germany). Reverse transcription was carried out using the following temperature cycles: 21 °C for 10 min, 48 °C for 50 min and 90 °C for 2 min (Tgradient cycler, Biometra, Goettingen, Germany). RT-PCR was performed using SSoFast Eva Green Kit (Bio-Rad Laboratories, Hercules, CA, USA). The sample volume was 10 μL containing 1 μL cDNA ($\triangleq$ 10 ng), 0.2 μL forward and 0.2 μL reverse primer ($\triangleq$ 0.4 μM) (Table 1), 5 μL SSoFast and DEPC-water. Temperature cycle (CFX 384, Bio-Rad) were as follows: 95 °C for 30 s, 95 °C for 5 s and 60 °C for 20 s (40 cycles), followed by a melting curve analysis. Data evaluation and statistical analysis was performed with Windows Excel 2010 (Microsoft Inc) with $n = 3$ independent repetitions per treatment and control.

To determine the relative mRNA gene expression changes, the previously described ΔΔCq method was applied (Livak and Schmittgen, 2001). For ΔCq, the gene expression data of the target genes were normalized with the arithmetic mean Cq values of all four reference genes (ubiqitin, Glyceraldehyde 3-phosphate dehydrogenase (GAPDH), β-Actin and Histon H3). It was verified that the reference genes were stable and not regulated, by using the Genorm algorithm implemented in GenEx version 5.1 (MultiD, Gothenburg, Sweden) (Logan *et al.*, 2009). To get ΔΔCq relative mRNA expression values, ΔCq values of treatment groups were corrected for the ΔCq values of the respective negative control group treated with the pure extract redissolution solvent. In graphs, the regulative impact of various PE extracts on the gene expression is shown on log2 scale.

Statistics

An unpaired *t*-test was performed for experiments investigating PF compound stability, cell proliferation as well as gene expression assuming equal variances.

Table 1. Forward (fwd) and reverse (rev) primers of reference genes and target genes with respective fragment length

Gene	Primer	Fragment length
Ubiquitin (reference gene)	fwd AGATCCAGGATAAGGAAGGCA rev GCTCCACCTCCAGGGTGAT	198
GAPDH (reference gene)	fwd AGCAATGCCTCCTGTACCAC rev AAGCAGGGATGATGTTCTGG	187
Actin beta (reference gene)	fwd AACTCCATCATGAAGTGTGAC rev GATCCACATCTGCRGGAAGG	234
Histon H3 (reference gene)	fwd ACTGGCTACAAAAGCCGCTC rev ACTTGCCTCCTGCAAAGCAC	232
Caspase 9 (target gene)	fwd CTGACTGCCAAGCAAATGG rev GCCTGACAGCCGTGAGAG	104
Cyclin B1 (target gene)	fwd GGATCACCAGGAACACGAAA rev GCTTCCTTTTTCAGAGGCAGT	187
Cyclin D1 (target gene)	fwd GACGAGCTGCTGCAAATG rev GAAATGAACTTCACGTCTGTGG	188
c-Jun (target gene)	fwd ATGACTGCAAAGATGGAAACG rev TCACGTTCTTGGGGCACA	310
67 kDa laminin receptor (target gene)	fwd AGCGAGCTGTGCTGAAGTTT rev GTGAGCTCCCTTGTTGTTGC	257

In the former case, samples containing extract solved in DMEM were compared with the respective control sample containing extract solved in H_2O. Because of the chemical complexity of a whole plant extract, data correction with spike compounds may necessarily lead to an underestimation or overestimation of some compounds. Level of significance was therefore $p \leq 0.01$.

Gene expression and cell proliferation experiments were assessed by comparing PF treated cells with the control containing the respective PF redissolution solvent. A significant regulation was assumed for $p \leq 0.05$, a highly significant regulation for $p \leq 0.01$ and a non-significant trend towards significance for $0.05 < p \leq 0.1$.

RESULTS

Characterization of *Perilla frutescens* extracts

To encompass a wide range of different compounds, ranging from polar to non-polar, freeze-dried PF leaves were extracted with different organic solvents and solvent contents.

Highest extraction yield for VS water extract (Fig. 1, right dark grey column) is in accordance with a previous publication of Makino *et al.* (2003), whereas yields of self-made extracts were found to range between 16.3% for extraction with water and 2.7% with 100% EtOH. Good extraction efficiency for PF has already been reported with EtOH:water solvent mixtures by Hong *et al.* (2010), because they are more likely to encompass a wide range of different compounds. In this regard, 50% EtOH extract was detected with the second highest phenolic content (GAE equivalence), which was only exceeded by VS water extract.

The latter extract, that is, VS water extract, has been chemically characterized by Buchwald-Werner *et al.* They report the presence of a variety of glucuronidated and glucosylated compounds as well as apigenin,

luteolin, rosmarinic acid and caffeic acid to be present within the extract (Buchwald-Werner, 2012). In our previous study, which focused mainly on the polar fraction of PF extracts, we were able to confirm some of their findings (Kaufmann *et al.*, 2016). All extracts employed here were furthermore characterized using an LC-MS setup, which allowed the simultaneous detection of polar and non-polar compounds (Greco *et al.*, 2013) (data not shown). An elevated abundance of highly polar compounds like hydroxycinnamic acids such as caffeic acid as well as glucuronidated and glucosylated flavonoids such as Apigenin 6,8-di-C-glucoside (Vicenin 2) or Luteolin 7-O-diglucuronide, respectively, were detected in water and 50% EtOH extract compared with less polar extracts 100% EtOH and 90% MeOH. Moderately polar compounds like rosmarinic acid and hydrophobic flavonoids like apigenin or luteolin were increasingly detected in 50% EtOH extract (data not shown).

In general, polar as well as non-polar PF compounds were detected in minor quantities in 100% EtOH and 90% MeOH extract, which consequently results in the observed low phenolic content or reducing capacity (Fig. 1). However, in relation to its extraction yield, 100% EtOH extract reducing capacity is higher than that of 90% MeOH extract. Because the reactivity of FC reagent differs towards various compound classes (Everette *et al.*, 2010), the discrepancy between yield and reducing potential with 90% MeOH extract might be related to an increased extraction efficiency of PF compounds with low reactivity. Similar GAE values as found here have been reported by Hong *et al.*, despite using a purple type of PF. They found the highest amount of reducing compounds for PF extracts obtained with water, followed by 100% MeOH and 100% EtOH (Hong and Kim, 2010), which is comparable with the results presented here. In contrast, Song *et al.* and Mueller-Waldeck *et al.* reported distinctly higher GAE values using a methanolic extraction of purple PF leaves, which are however still comparable with the values obtained here after extraction with water (VS and self-made) and 50% EtOH (Muller-Waldeck *et al.*, 2010). In general, PF water and 50% EtOH extract possess more reducing potential than most vegetables or fruits as detected by Wu *et al.* (2004).

Assessment of cell proliferation

Initial experiments were performed to assess possible effects of the employed extract redissolution solvents on cell proliferation, wherefore redissolved empty control extracts were added to the cells. Data evaluation revealed no significant regulation in comparison to untreated cells in pure cell culture medium.

In the following, cells were treated with increasing concentrations of VS water extract (Fig. 2A). The extract quantities applied to the cells were chosen as to emulate physiologically relevant concentrations. The application of '4.0', '2.0' and '1.6 mg' VS water extract in a total volume of 400 µL cell culture medium caused a drop of signal, which reflects the complete cell death and cell detachment within ~4 h.

The treatment with '1.0' and '0.4 mg' extract resulted in a delayed cell proliferation, with '1.0 mg' revealing a more pronounced effect. Previous studies reported the

Figure 1. *Perilla frutescens* (PF) extraction yield and gallic acid equivalence (GAE), that is, total reducing capacity of PF water, 50% EtOH, 100% EtOH, 90% MeOH, 0.5%FAc and 'VS water extract'. Information about the extraction yield of externally produced VS water extract was provided with an extraction ratio of 20%, (5:1, freeze-dried leaves: extraction residue (w/w)), wherefore no standard deviation is known). Standard deviations for self-prepared extracts shown here were calculated from $n = 5$ (extraction residue, dark grey columns) and $n > 25$ for the calculation of total reducing capacity of PF (GAE, light grey columns).

Figure 2. (A) Effects of different concentrations of 'VS water extract' on IPEC-J2 cell proliferation within 72 h. Time point of treatment = 20 h after seeding. Standard deviations for each treatment concentration were calculated from $n > 3$; (B) H2O2 generation was determined with '0.4' (○) and '2.0 mg' ( ) VS water extract as well as '0.4 mg' water, 50% EtOH, 100% EtOH and 90% MeOH extracts (data not shown) in cell culture medium in the absence of cells. Standard deviations were calculated from $n \geq 3$ for the determination of H_2O_2 generation in the presence of '2.0' and '0.4 mg' VS water extract.

occurrence of H_2O_2 in cell culture medium after the addition of phenolic compounds (Halliwell, 2008). H_2O_2 generation was therefore measured with '2.0' and '0.4 mg' VS water extract (Fig. 2B) as well as '0.4 mg' of all further PF extracts (data not shown) in the absence of cells. A maximum quantity of approximately 110 µM was captured with '2.0 mg' VS water extract (Fig. 2B). In contrast, Long *et al.* detected H_2O_2 levels of more than 500 µM after addition of up to 1 mM of natural compounds like EGCG, quercetin or rosmarinic acid in DMEM within a mere 2 h (Long *et al.*, 2010). Because the addition of F12 and FCS has been observed to distinctly reduce the amount of generated H_2O_2 in the presence of polyphenols (Bellion *et al.*, 2009), the applied medium formulation here may have resulted in the lowered H_2O_2 concentration. Nevertheless, the oxidation of polyphenols does not only cause the generation of H_2O_2 but also generates ROS like O_2^- (Sang *et al.*, 2007) and hydroxyl radicals (OH•), the latter derived from H_2O_2 via fenton reaction (Halliwell *et al.*, 2000). The contribution of H_2O_2, ROS

as well as polyphenol oxidation products like semiquinones and quinones (Awad *et al.*, 2001) to the detected cell death within ~4 h after treatment can be assumed. The amount of PF extract was therefore considerably reduced to '0.4 mg', where only ~5 µM H_2O_2 were constantly detected for VS water extract (Fig. 2B) as well as for all further PF extracts (data not shown). Cells were thereupon treated with '0.4 mg' self-made water, 50% EtOH, 100% EtOH and 90% MeOH extract, respectively, to comparatively assess the effect of different extract polarities on cell growth (Fig. 3A and B).

A distinct decrease of *p*-values, which reflects a decelerated cell proliferation compared with control experiments, was observed within 24 h after application of '0.4 mg' of all extracts to the cells (Fig. 3: "treatment" at 20h). The impact of VS water extract was however the most pronounced with the detection of a significantly reduced cell growth within only ~2 h. Considerable effects on cell proliferation were also found with 50% EtOH extract and self-made water extract in the early stages (Fig. 3A); 100% EtOH and 90% MeOH extract
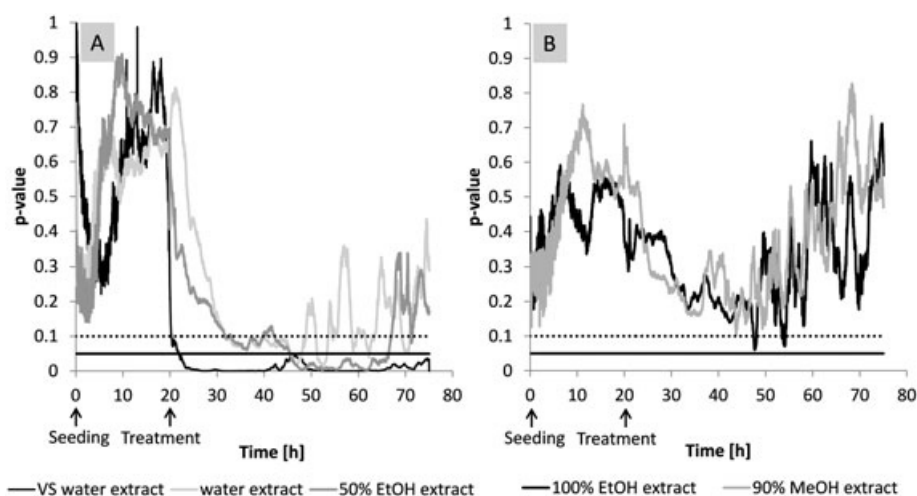
Figure 3. *p*-values of each time point of IPEC-J2 cell proliferation after treatment with '0.4 mg' VS water, self-made water and 50% EtOH extract (A) as well as 100% EtOH and 90% MeOH, 0.5% FAc extracts (B) in comparison to the respective control measurement containing 1% of extract redissolution solvent. Standard deviations are calculated out of $n = 9$ repetitions (not shown for clarity reasons). Significance level is depicted at $p = 0.05$ (horizontal black line) as well as 'non-significant trend towards significance' at $p = 0.1$ (horizontal dashed black line).

were found with a comparable progress of *p*-values, both however showing no significance during the entire measurement (Fig. 3B). While *p*-values increased again with water, 100% EtOH and 90% MeOH extracts after ~48 h, VS water and 50% EtOH extracts maintained a significant deceleration beyond ~48 h. The results are in good accordance to the determined phenolic contents (Fig. 1), with a low reducing potential for 100% EtOH and 90% MeOH extract, which in turn showed a less pronounced regulation of cell growth compared with the applied more polar extracts. Cytotoxic effects of the extract could be excluded to be responsible for the observed effects by the assessment of lactate dehydrogenase (LDH) release, which was detected to be on a constant and minor level within 20 h after treatment with '0.4 mg' of all PF extracts (data not shown).

Gene expression

Perilla frutescens extract was able to inhibit cell proliferation even at low concentrations (Fig. 3). Several studies has already observed an inhibitory effect on cell growth of human cancer cell lines and mouse skin carcinogenesis (Kwak and Ju, 2015) as well as the induction of apoptosis (Kwak *et al.*, 2009), either by individual compounds present in PF or whole PF extract. As already mentioned, cell lysis and LDH release could be excluded to be responsible for the delayed cell proliferation. The absence of notable apoptotic events was furthermore supported by a non-significant regulation of caspase-9 gene expression (data not shown). The decelerated proliferation can therefore be accounted

to the downregulation of cyclin D1 and cyclin B1. The former was observed with an immediate response after treatment at time point 0 h, which is partly maintained up to 6 h (Fig. 4C and D).

Cyclin D1 revealed a downregulation at time points 6 and 24 h after treatment (Fig. 4D). Equally downregulated pro-proliferative protein c-Jun is known to affect a variety of genes involved in cell proliferation and cell survival, including proto-oncogene p53 (Schreiber *et al.*, 1999) and cyclin D1 (Shaulian and Karin, 2001). The observed downregulation of c-Jun at 0 and 6 h is consequently accompanied by a downregulation of cyclin D1 (Schreiber *et al.*, 1999) (Fig. 4B). Moreover, decreasing levels of c-Jun are likely to result in an upregulation of p53 (Schreiber *et al.*, 1999), which in turn has been reported to suppress cyclin B1 (Yu *et al.*, 2002) (Fig. 4C), therewith as well regulating the progression of cell cycle. Most interestingly, cyclin B1, D1 as well as c-Jun have been observed to be overexpressed in tumour cells (Maeda and Karin, 2003). Furthermore, their susceptibility to natural cancer chemopreventive compounds and natural extracts make them potential therapeutic targets for the treatment of cancer (Shan *et al.*, 2009). This also applies to 67LR, which has been discussed to be involved in various steps of cancer development, including tumour-cell migration (Wewer *et al.*, 1987), cancer progression (Ozaki *et al.*, 1998) and angiogenesis (Bernard *et al.*, 2009). The downregulation of 67LR has been reported to be in close association with a variety of different genes involved in cell cycle arrest including a lowered expression of cyclin B1 (Scheiman *et al.*, 2010) as detected here (Fig. 4A and C). In
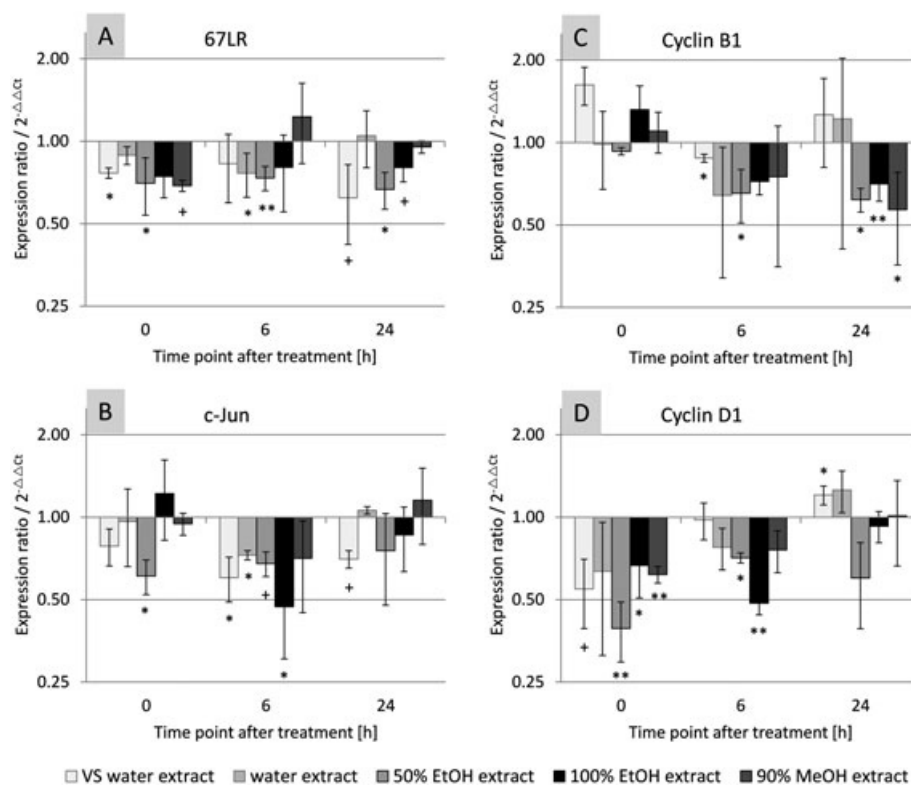
Figure 4. Regulation of 67 kDa laminin receptor (67LR), cyclin B1, c-Jun and cyclin D1 after treatment of IPEC-J2 cells with '0.4 mg' *Perilla frutescens* extracts expressed as "expression ratio/$2^{-\Delta\Delta C_T}$". Significance was calculated compared with the respective controls containing 1% extract redissolution solvents. **for highly significant ($p \leq 0.01$), *for significant ($p \leq 0.05$) and + for non-significant trend towards significance ($0.05 < p \leq 0.1$). Standard deviations were calculated from $n = 3$ independent repetitions.

contrast to recent reports, which describe tea polyphenol ECGC to bind to 67LR and thus exerting its anticancer activity (Umeda *et al.*, 2008), PF extract was found to mediate its effects through 67LR gene regulation (Fig. 4A). Although no general tendency with regard to the most effective PF extract could be observed for the investigated genes, the most consistent results were determined with 50% EtOH extract with significant regulations for cyclin B1 at 0 and 24 h, for cyclin D1 at 0 and 6 h, for 67LR at 0, 6 and 24 h and for c-Jun at 0 h.

Stability of *Perilla frutescens* extracts in cell culture medium

With regard to effects of natural extracts and compounds on physiological parameters, several studies are available that critically discuss the stability of said compounds in cell culture medium, referring to the elevated exposure to oxygen compared with *in vivo* conditions (Long *et al.*, 2010). The occurrence of considerable amounts of H_2O_2 and ROS, which are likely to be generated during the auto-oxidation and

Table 2. Stability of natural *Perilla frutescens* (PF) extract compounds in cell culture medium. Significance was calculated in comparison to PF extract solved in water for each individual time point with $p \leq 0.01$ as level of significance ($n = 3$ independent repetitions)

A
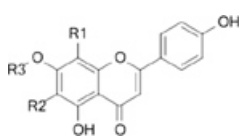
Compound and molecular formula	R1	R2	R3
Apigenin $C_{15}H_{10}O_5$	H	H	H
Apigenin-7-O-glucuronide $C_{21}H_{18}O_{11}$	H	H	Glu
Apigenin-7-O-diglucuronide $C_{27}H_{26}O_{17}$	H	H	Diglu
Apigenin 6,8-di-C-glucoside $C_{27}H_{30}O_{15}$	Glc	Glc	H
Apigenin 7-O-glucoside $C_{21}H_{20}O_{10}$	H	H	Glc
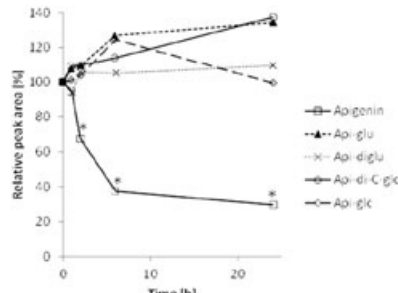
B
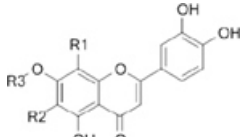
Compound and molecular formula	R1	R2	R3
Luteolin $C_{15}H_{10}O_6$	H	H	H
Luteolin 7-O-glucuronide $C_{21}H_{18}O_{12}$	H	H	Glu
Luteolin 7-O-diglucuronide $C_{27}H_{26}O_{18}$	H	H	Diglu
Luteolin 7-O-glucoside $C_{21}H_{20}O_{11}$	H	H	Glc
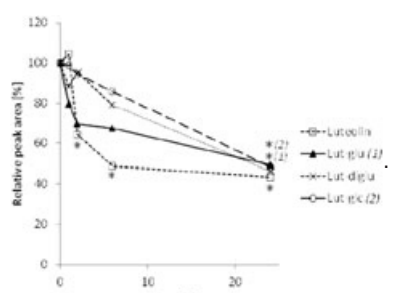
C
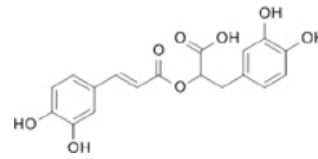
Rosmarinic acid $C_{18}H_{16}O_8$

D
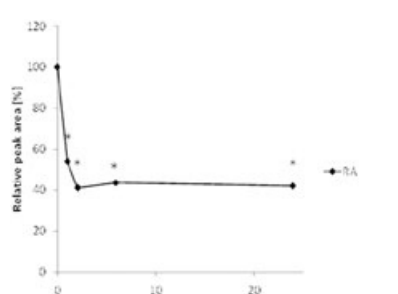
Unknown compounds with increasing peak areas
Molecular weights (with a mass spectrometric accuracy of < 1 ppm)
111.0787 Da
145.0847 Da
288.0856 Da
497.1502 Da
696.2070 Da
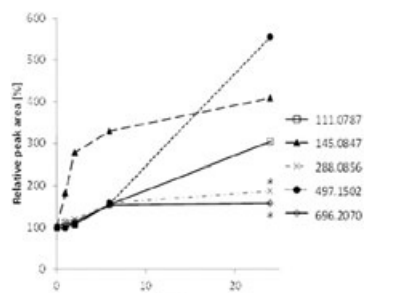
therewith degradation of natural compounds might be responsible for plenty of observed cell growth inhibitions detected throughout the years (Halliwell, 2008). The stability of VS water extract in cell culture medium was therefore investigated by mainly focusing on known PF compounds described in literature (Buchwald-Werner, 2012) (Table 2A–C).

Because of necessary sample preparation procedures and dilution steps, extract concentrations used here were elevated compared with experiments assessing cell and gene expression. Nevertheless, the results may provide insight into the stability of phenolic compounds related to their chemical structure. Apigenin and luteolin were detected with a significant ($p \leq 0.01$) degradation at time points 2, 6 and 24 h. Interestingly, apigenin conjugated either with glucose (Api-glu, Api-di-D-glc) or glucuronide unit(s) (Api-glc, Api-diglc) was found to be stable throughout the observed time range. In contrast, conjugated luteolin (Lut-glu, Lut-diglu, Lut-glc) was detected to decrease, however, not significantly except for Lut-glu and Lut-glc at 24 h. A more likely oxidation and release of H_2O_2 has been observed for polyphenols containing catechol moieties like luteolin (3', 4' ortho hydroxyl groups) (Bellion *et al*., 2009) and rosmarinic acid (Long *et al*., 2010) (Table 2C). Because flavonoid glycosides have already been reported with a comparably lower H_2O_2 release (Bellion *et al*., 2009), the conjugation presumably improves the compounds stability in cell culture medium, which is especially apparent for apigenin conjugates (Table 2A). Apigenin, which lacks the presence of adjacent OH groups, has been reported to be only minorly degraded without an accompanied release of significant amounts of H_2O_2 (Long *et al*., 2010). As opposed to this, a fast and distinct degradation for apigenin was observed here (Table 2A and B). Potential oxidation products like semiquinones, quinones (Bellion *et al*., 2009), dimers (Sang *et al*., 2005) or small phenolic acids (Kern *et al*., 2007) were not detected. This might be partly due to the SPE purification procedure, which results in the loss of highly polar compounds like phenolic acids. Nevertheless, several unidentified masses have been observed to increase, with a significant difference at 24 h for 497.1511 Da and 696.2081 Da compared to the respective controls (Table 2D). Further compounds displayed were also detected with an increase over the time for all experimental repetitions, but were calculated with a non-significant behaviour due to high standard deviations.

DISCUSSION

Perilla frutescens extracts have been investigated on their potential to regulate cell proliferation and gene expression. At a concentration of '0.4 mg'/400 µL medium, only negligible H_2O_2 generation was detected, which might support the conclusion of a sufficient stability of extracted compounds and the absence of ROS and potentially toxic polyphenol oxidation products. At a concentration of '0.4 mg/400 µL medium, PF extracts were demonstrated to inhibit cell proliferation with the most pronounced effect for VS water and 50% EtOH extract, both of which determined to possess high phenolic contents. The cell growth regulation was immediate, which is reflected by the drop of *p*-values directly after cell treatment. The study of relevant genes involved in cell cycle regulation concurrently revealed an immediate downregulation of cyclin D1. The 67LR expression was also observed to decrease at 0 h, but in contrast to cyclin D1, maintains the decrease permanently. Because of the presence of non-degraded polyphenols at 0 h, the observed early alteration of cell cycle progression can be accounted to the extract compounds. Cyclin D1 as well as 67LR are promising targets for the treatment of cancer, whereby the latter also serves as receptor for several viruses and the prion protein (Gauczynski *et al*., 2001). It is therewith directly involved in the development and progression of prion disease.

Because of the preparation of extracts with different solvents in combination with the determination of their respective reducing potentials, conclusion can be drawn on the most effective PF polarity fractions. The employed LC-MS setup (data not shown) furthermore allowed the detection of the overall composition as well as an estimation of the quantity of polar and non-polar compounds contained within the different PF extracts (Greco *et al*., 2013).

Knowledge about the extraction procedure, extraction yield, reducing potential and the phytochemical nature of an extract is essential in order to guarantee comparability as well replicability of experiments. This is also particularly important considering the often contradictory results between different clinical studies (Izzo *et al*., 2016).

However, the conduction of LC-MS analysis does not necessarily result in the identification of individual compounds, but rather provides a general overview of the chemical composition of an extract. With regard to PF, only a portion of compounds have been identified yet, which includes some glucuronidated and glucosylated flavonoids (Kaufmann *et al*., 2016; Buchwald-Werner, 2012). Still, only little research is available with regard to the effects of those compounds on physiological parameters. Despite the observed reduction in stability of some PF compounds in cell culture medium, several have been detected with a constant abundance. Consequently, subsequent research may focus on the most effective PF extract fractions or on single molecules isolated from PF to eventually identify individual compounds, which are able to affect the expression of health-related and disease-related genes as well as the proliferation of cells. This study thus provides first results about promising effects of whole PF extracts on cell physiology in combination with the respective reducing potential of applied extracts as well as a critical assessment of obtained results.

Conflict of interest

The authors have declared no conflict of interest.

REFERENCES

Awad HM, Boersma MG, Boeren S, van Bladeren PJ, Vervoort J, Rietjens IM. 2001. Structure-activity study on the quinone/quinone methide chemistry of flavonoids. *Chem Res Toxicol* **14**(4): 398–408.

Becker C, Hammerle-Fickinger A, Riedmaier I, Pfaffl MW. 2010. mRNA and microRNA quality control for RT-qPCR analysis. *Methods* **50**(4): 237–243.

Begnami MD, Fregnani JH, Nonogaki S, Soares FA. 2010. Evaluation of cell cycle protein expression in gastric cancer: cyclin B1 expression and its prognostic implication. *Hum Pathol* **41**(8): 1120–1127.

Bellion P, Olk M, Will F, *et al.* 2009. Formation of hydrogen peroxide in cell culture media by apple polyphenols and its effect on antioxidant biomarkers in the colon cell line HT-29. *Mol Nutr Food Res* **53**(10): 1226–1236.

Bernard A, Gao-Li J, Franco CA, Bouceba T, Huet A, Li Z. 2009. Laminin receptor involvement in the anti-angiogenic activity of pigment epithelium-derived factor. *J Biol Chem* **284**(16): 10480–10490.

Buchwald-Werner S. 2012. Investigation of a *Perilla frutescens* special extract – anti-inflammatory and immune-modulatory properties. *Agro Food Ind Hi Tech* **23**(5): 38–41.

Chen ML, Wu CH, Hung LS, Lin BF. 2015. Ethanol extract of *Perilla frutescens* suppresses allergen-specific Th2 responses and alleviates airway inflammation and hyperreactivity in ovalbumin-sensitized murine model of asthma. *Evid Based Complement Alternat Med* **2015**: 324265.

de Manzoni G, Guglielmi A, Verlato G, *et al.* 1998. Prognostic significance of 67-kDa laminin receptor expression in advanced gastric cancer. *Oncology* **55**(5): 456–460.

Everette JD, Bryant QM, Green AM, Abbey YA, Wangila GW, Walker RB. 2010. Thorough study of reactivity of various compound classes toward the Folin-Ciocalteu reagent. *J Agric Food Chem* **58**(14): 8139–8144.

Gauczynski S, Peyrin JM, Haik S, *et al.* 2001. The 37-kDa/67-kDa laminin receptor acts as the cell-surface receptor for the cellular prion protein. *Embo J* **20**(21): 5863–5875.

Greco G, Grosse S, Letzel T. 2013. Serial coupling of reversed-phase and zwitterionic hydrophilic interaction LC/MS for the analysis of polar and nonpolar phenols in wine. *J Sep Sci* **36**(8): 1379–1388.

Guilloteau P, Zabielski R, Hammon HM, Metges CC. 2010. Nutritional programming of gastrointestinal tract development. Is the pig a good model for man? *Nutr Res Rev* **23**(1): 4–22.

Halliwell B. 2008. Are polyphenols antioxidants or pro-oxidants? What do we learn from cell culture and in vivo studies? *Arch Biochem Biophys* **476**(2): 107–112.

Halliwell B, Clement MV, Ramalingam J, Long LH. 2000. Hydrogen peroxide. Ubiquitous in cell culture and *in vivo*? *IUBMB Life* **50**(4–5): 251–257.

Hong E, Kim G-H. 2010. Comparison of extraction conditions for phenolic, flavonoid content and determination of rosmarinic acid from Perilla frutescens var. acuta. *Int J Food Sci Technol* **45**(7): 1353–1359.

Izzo AA, Hoon-Kim S, Radhakrishnan R, Williamson EM. 2016. A critical approach to evaluating clinical efficacy, adverse events and drug interactions of herbal remedies. *Phytother Res* **30**(5): 691–700.

Jeon IH, Kim HS, Kang HJ, *et al.* 2014. Anti-inflammatory and antipruritic effects of luteolin from Perilla (*P. frutescens* L.) leaves. *Molecules* **19**(6): 6941–6951.

Kaufmann CM, Grassmann J, Letzel T. 2016. HPLC method development for the online-coupling of chromatographic *Perilla frutescens* extract separation with xanthine oxidase enzymatic assay. *J Pharm Biomed Anal* **124**: 347–357.

Kern M, Fridrich D, Reichert J, *et al.* 2007. Limited stability in cell culture medium and hydrogen peroxide formation affect the growth inhibitory properties of delphinidin and its degradation product gallic acid. *Mol Nutr Food Res* **51**(9): 1163–1172.

Kwak CS, Yeo EJ, Moon SC, Kim YW, Ahn HJ, Park SC. 2009. Perilla leaf, *Perilla frutescens*, induces apoptosis and G1 phase arrest in human leukemia HL-60 cells through the combinations of death receptor-mediated, mitochondrial, and endoplasmic reticulum stress-induced pathways. *J Med Food* **12**(3): 508–517.

Kwak Y, Ju J. 2015. Inhibitory activities of *Perilla frutescens* britton leaf extract against the growth, migration, and adhesion of human cancer cells. *Nutr Res Pract* **9**(1): 11–16.

Lee HA, Han JS. 2012. Anti-inflammatory effect of *Perilla frutescens* (L.) Britton var. frutescens extract in LPS-stimulated RAW 264.7 macrophages. *Prev Nutr Food Sci* **17**(2): 109–115.

Livak KJ, Schmittgen TD. 2001. Analysis of relative gene expression data using real-time quantitative PCR and the 2 (−delta delta C(T)) method. *Methods* **25**(4): 402–408.

Logan J, Edwards KJ, Saunders NA. 2009. Real-time PCR: Current Technology and Applications. Caister Academic Press: Saffron Walden, Essex, UK.

Long LH, Hoi A, Halliwell B. 2010. Instability of, and generation of hydrogen peroxide by, phenolic compounds in cell culture media. *Arch Biochem Biophys* **501**(1): 162–169.

Maeda S, Karin M. 2003. Oncogene at last – c-Jun promotes liver cancer in mice. *Cancer Cell* **3**(2): 102–104.

Makino T, Furuta Y, Wakushima H, Fujii H, Saito K, Kano Y. 2003. Anti-allergic effect of *Perilla frutescens* and its active constituents. *Phytother Res* **17**(3): 240–243.

Malik A, Afaq F, Sarfaraz S, Adhami VM, Syed DN, Mukhtar H. 2005. Pomegranate fruit juice for chemoprevention and chemotherapy of prostate cancer. *Proc Natl Acad Sci U S A* **102**(41): 14813–14818.

Morel E, Andrieu T, Casagrande F, *et al.* 2005. Bovine prion is endocytosed by human enterocytes via the 37 kDa/67 kDa laminin receptor. *Am J Pathol* **167**(4): 1033–1042.

Muller-Waldeck F, Sitzmann J, Schnitzler WH, Grassmann J. 2010. Determination of toxic perilla ketone, secondary plant metabolites and antioxidative capacity in five *Perilla frutescens* L. varieties. *Food Chem Toxicol* **48**(1): 264–270.

Muller J, Pfaffl MW. 2012. Synergetic downregulation of 67 kDa laminin receptor by the green tea (*Camellia sinensis*) secondary plant compound epigallocatechin gallate: a new gateway in metastasis prevention? *BMC Complement Altern Med* **12**: 258.

Nelson J, McFerran NV, Pivato G, *et al.* 2008. The 67 kDa laminin receptor: structure, function and role in disease. *Biosci Rep* **28**(1): 33–48.

Ozaki I, Yamamoto K, Mizuta T, *et al.* 1998. Differential expression of laminin receptors in human hepatocellular carcinoma. *Gut* **43**(6): 837–842.

Sang S, Lee MJ, Hou Z, Ho CT, Yang CS. 2005. Stability of tea polyphenol (−)-epigallocatechin-3-gallate and formation of dimers and epimers under common experimental conditions. *J Agric Food Chem* **53**(24): 9478–9484.

Sang S, Yang I, Buckley B, Ho CT, Yang CS. 2007. Autoxidative quinone formation in vitro and metabolite formation in vivo from tea polyphenol (−)-epigallocatechin-3-gallate: studied by real-time mass spectrometry combined with tandem mass ion mapping. *Free Radic Biol Med* **43**(3): 362–371.

Scheiman J, Tseng JC, Zheng Y, Meruelo D. 2010. Multiple functions of the 37/67-kd laminin receptor make it a suitable target for novel cancer gene therapy. *Mol Ther* **18**(1): 63–74.

Schreiber M, Kolbus A, Piu F, *et al.* 1999. Control of cell cycle progression by c-Jun is p53 dependent. *Genes Dev* **13**(5): 607–619.

Shan BE, Wang MX, Li RQ. 2009. Quercetin inhibit human SW480 colon cancer growth in association with inhibition of cyclin D1 and survivin expression through Wnt/beta-catenin signaling pathway. *Cancer Invest* **27**(6): 604–612.

Shaulian E, Karin M. 2001. AP-1 in cell proliferation and survival. *Oncogene* **20**(19): 2390–2400.

Singleton VL, Orthofer R, Lamuela-Raventós RM. 1999. [14] Analysis of total phenols and other oxidation substrates and antioxidants by means of folin-ciocalteu reagent. In Methods in Enzymology, Lester P (ed). Academic Press; 152–178.

Umeda D, Yano S, Yamada K, Tachibana H. 2008. Involvement of 67-kDa laminin receptor-mediated myosin phosphatase activation in antiproliferative effect of epigallocatechin-3-O-gallate at a physiological concentration on Caco-2 colon cancer cells. *Biochem Biophys Res Commun* **371**(1): 172–176.

Wewer UM, Taraboletti G, Sobel ME, Albrechtsen R, Liotta LA. 1987. Role of laminin receptor in tumor cell migration. *Cancer Res* **47**(21): 5691–5698.

Wolter F, Akoglu B, Clausnitzer A, Stein J. 2001. Downregulation of the cyclin D1/Cdk4 complex occurs during resveratrol-induced cell cycle arrest in colon cancer cell lines. *J Nutr* **131**(8): 2197–2203.

Wu X, Beecher GR, Holden JM, Haytowitz DB, Gebhardt SE, Prior RL. 2004. Lipophilic and hydrophilic antioxidant capacities of common foods in the United States. *J Agric Food Chem* **52**(12): 4026–4037.

Yu M, Zhan Q, Finn OJ. 2002. Immune recognition of cyclin B1 as a tumor antigen is a result of its overexpression in human tumors that is caused by non-functional p53. *Mol Immunol* **38**(12–13): 981–987.